L-squared approximations in atomic scattering theory

Martin Plummer

L-SQUARED APPROXIMATIONS IN ATOMIC SCATTERING THEORY

by

MARTIN PLUMMER M.A.(Cantab.)

A Thesis submitted to The University of Durham in candidature for the Degree of Doctor of Philosophy

May, 1987

ABSTRACT

This thesis is concerned with the use of L-squared or square integrable functions in electron atom scattering at intermediate energies, and tests the success of various L-squared approximations in model problems of electron hydrogen atom scattering. The representation of part or all of the wave and Green's functions by a set of L-squared pseudostates, and the associated occurrence of unphysical pseudoresonances at the pseudostate thresholds is discussed.

The original work of this thesis is in two parts. In the first, a model coupled channel problem is considered in which an L-squared optical potential is used to represent the effect of additional (Q space) channels on the first (P space) channel. A method of Bransden and Stelbovics used successfully for a two channel problem is extended to the case of several channels. Numerical results are presented for the cases of two and three channels and the success of the procedure is assessed. The rest of the research presented here concerns the use of the Schwinger variational method in a restricted model of electron hydrogen atom scattering in which all states are assumed to be spherically symmetric. The method is used successfully to solve coupled channel problems using L-squared pseudostates to represent the s-wave continuum. The origins of the pseudoresonances that occur in these problems are investigated and a method of removing pseudoresonances before T matrix elements are calculated is considered.

The limitations and instabilities of the Schwinger method when applied to the full model problem with different representations of hydrogen states in the trial and Green's functions are investigated, and various modifications are considered in attempts to stabilise results where necessary in these more general cases.

ACKNOWLEDGEMENTS

I would like to thank Professor B.H. Bransden for his excellent supervision of this research, and Dr. D.R. Flower, my original supervisor, for accepting me as a research student at Durham. I would like to thank Professor I.E. McCarthy and Dr. A.T. Stelbovics for the use of their momentum space coupled channels programme and helpful remarks.

For numerous stimulating discussions I would like to thank my colleagues at the Department of Physics, notably Dr. R. Shingal and Dr. G. Danby, and especially my collaborator for the work of chapter five, Mr. R. Hewitt.

I was financed by an SERC quota award.

Finally I would like to thank Mrs. M. Chipchase for undertaking the typing of this thesis.

CONTENTS

CHAPTER ONE

INTRODUCTION AND BACKGROUND THEORY

1.1 Introduction

This thesis is concerned with the study of L-squared methods in electron atom scattering theory at intermediate energies. Intermediate energies are considered to be the range of incident electron energies starting at the threshold for ionisation of the atom and continuing until the first Born approximation (described in section 1.2) is applicable. For the present purposes the lower part of this range, in which simplifying assumptions made at higher energies cannot be applied, is considered, and the discussion is restricted to elastic scattering and excitation to low lying levels. The approximate methods under consideration are tested in simplified model problems, based on electron hydrogen atom scattering, for which exact solutions are known. "L-squared methods" refer to methods making use of L-squared or square integrable functions. For example, an L-squared or Lebesque square integrable function in coordinate space $\phi(\underline{r})$ obeys:

$$\int d^3\underline{r}\, |\phi(\underline{r})|^2 \quad \text{is bounded} \qquad (1.1.1)$$

A finite set of L-squared functions is used to diagonalise an operator L which may model part of or all of an atomic or molecular Hamiltonian

$$\int d^n \underline{r}\ \phi_m L \phi_n = E_n \delta_{mn} \qquad (1.1.2)$$

n = dimension of the space, E_n is an eigenvalue.

In these methods the L-squared functions used are usually real for simplicity, and obey, for example, the atomic boundary conditions at $r \to 0$. The L-squared functions are then used to model the atomic/molecular solutions which do not necessarily vanish as $r \to \infty$, over a finite range of coordinate space.

In the rest of this chapter, the main features of electron hydrogen atom scattering theory are introduced, along with various topics and methods that are referred to in the rest of the thesis. An indication of the extension of the theory to many electron atoms is given. Various low energy methods for calculating scattering data are briefly mentioned as L-squared methods in the guise of pseudo-atomic states and optical potentials are used successfully in this energy region, and extension of these ideas to intermediate energies together with necessary modifications of resulting unphysical behaviour form the motive for the work of this thesis. A review of work published on low energy and higher intermediate energy methods is, however, not attempted.

In chapter two, the L-squared discretisation of electronic continua is discussed in more detail, and the

ideas are applied to a model coupled channel problem in chapter three, using an L-squared optical potential. The rest of the thesis is concerned with the use of the Schwinger variational method in a model problem of electron hydrogen atom scattering, referred to throughout as the "Poet" problem. The model is a restricted one in which all non zero angular momentum terms are ignored: the system is considered to be spherically symmetric and is equivalent to using only s waves in the expansions of the wavefunction and the electron interaction potential. The model was considered by Burke and Mitchell (1973) and solved exactly by Poet (1978). The Schwinger principle is used to solve pseudostate coupled channel problems using purely L-squared trial functions, and its flexibility is used in attempts to remove unphysical structure introduced by the use of (L-squared) pseudostates. The Schwinger variational principle is introduced in chapter four, which also contains a short summary of aspects of the Poet problem not discussed in other contexts. Chapter five details the present work using the Schwinger principle, which was carried out in collaboration with Mr. R. Hewitt. The more general theory described in chapters one and two is discussed in detail as it is applied to the specific model problems considered in chapters three and five. Possible future work is considered in chapter six.

1.2 Electron Atom scattering

1.2A Introductory Theory

We consider electron hydrogen atom scattering, treating the proton as infinitely massive. Relativistic effects are not considered as they are negligible at the energies under consideration. Atomic units are used throughout, the following quantities being unity:

$$\hbar = m_e = e = 1 \qquad (1.2.1)$$

m_e = mass of electron

e = electronic charge ($e = e^*/\sqrt{4\pi\epsilon_0}$; e^* in S.I. units)

a_0 = first Bohr orbit of hydrogen atom.

The fine structure constant $\alpha = (137.0388)^{-1}$

Cross sections in chapters three and five are given in units of πa_0^2.

We consider time independent wavefunctions: time dependence is discussed for example by Bransden (1983). We describe initial and final states of the scattering system for a given total energy E in terms of reaction channels. For example, the initial state may consist of a free electron and a (neutral) hydrogen atom in a 1s state, with

no interaction between them: the 1s channel. After the collision, the final state may be the same, in which case elastic scattering has occurred, or the hydrogen atom may have been excited to a different state, in which case inelastic scattering has occurred, the final channel being labelled by the state of the hydrogen atom. The labelling also describes the final state (direction) of the scattering electron although this is often kept implicit for simplicity of notation. Energetically accessible channels are described as open, the rest as closed. If ionisation occurs the channel labelling is performed as if the two electrons were distinguishable. The work of this thesis does not concern ionisation, but excitation at energies where ionisation is possible. The generalised experimental setup by which this scattering may be realised is described by Bransden (1983) and for example, may consist of a low density collimated electron beam incident on a low density atomic target, the assumptions being that the beam electrons do not interact with themselves, and that only one collision occurs per scattering electron (the actual experimental conditions for electron hydrogen scattering are more complex, but do not concern us here).

The Schrödinger equation for the electronic system is:

$$(H - E)\,\Psi_i^{\pm}(\underline{r}_1, \underline{r}_2) = 0 \qquad (1.2.2)$$

Ψ_i^{+} signifies the outward scattering solution and

corresponds to an incident channel i and outgoing waves in all channels: Ψ_i^+ describes the scattering system and in the time dependent formulation corresponds to the incident channel at times well before the collision. Ψ_i^- corresponds to an incident channel i and incoming waves in all channels: in the time dependent formulation Ψ_i^- corresponds to a final channel i at times long after the collision. The ionisation threshold is at E = 0.

The probability of finding the state j in the state Ψ_i^+ is the scattering matrix element S_{ji} .

$$S_{ji} = \langle \Psi_j^- | \Psi_i^+ \rangle \quad \text{(integration over coordinate space)}$$

$$S_{ji} = \delta_{ji} + 2i\bar{T}_{ji} \qquad (1.2.3)$$

The delta function part of S_{ji} corresponds to no interaction, and the scattering is described by the T matrix:

$$\bar{T}_{ji} = -\pi \delta(E_i - E_j) T_{ji} \qquad (1.2.4)$$

E_i here is the total energy in each channel. The δ function ensures energy conservation and the energy labelling will therefore now be dropped. The reaction partial cross section σ_{ji} may be written:

$$\sigma_{ji} = \frac{1}{4\pi^2} \frac{k_j}{k_i} \int d\Omega_j \, |T_{ji}(E)|^2 \qquad (1.2.5)$$

$\frac{1}{2}k_i^2$ is the energy of the scattered electron in channel i:

$$\frac{1}{2}k_i^2 + \varepsilon_i = \frac{1}{2}k_j^2 + \varepsilon_j = E \qquad (1.2.6)$$

ε_j is the hydrogen atom energy level in channel j.

In terms of the beam experiment, the cross section is the total number of electrons scattered per unit incident flux (the wave function is normalised such that $d\sigma_{ji}/d\Omega_j$ is a particle density). The differential cross section $d\sigma_{ji}/d\Omega_j$ giving the number of electrons scattered at a particular solid angle is proportional to the square of the T matrix element. This emphasizes the fact that the labelling j here includes angular information about the final direction of the scattered electron as well as the quantum numbers of the target atom. Electrons are spin ½ fermions and the system has different spin states: symmetric s = 1 (triplet) and antisymmetric s = 0 (singlet). For an unpolarised beam, cross sections are averaged over initial states and summed over final states:

$$\sigma_{ji} = \frac{1}{4\pi^2}\frac{k_j}{k_i}\int d\Omega_j \left\{ \frac{1}{4}\left| T_{ji}(E, s=0)\right|^2 + \frac{3}{4}\left| T_{ji}(E, s=1)\right|^2 \right\} \qquad (1.2.7)$$

The wave function obeys the relation (1.2.8), as described by Bransden (1983).

$$\Psi^{+*}(-\underline{k}_i, \underline{r}_1, \underline{r}_2) = \Psi^{-}(\underline{k}_i, \underline{r}_1, \underline{r}_2) \qquad (1.2.8)$$

1.2B Structure of The Wave Function

The Hamiltonian H for the system is symmetric

$$H = -\frac{1}{2}\nabla_1^2 - \frac{1}{2}\nabla_2^2 + V_0(r_1) + V_0(r_2) + v(|\underline{r}_1 - \underline{r}_2|) \tag{1.2.9}$$

$V_0(r) = -1/r$: Coulomb interaction between an electron and the proton.

$$v(|\underline{r}_1 - \underline{r}_2|) = \frac{1}{|\underline{r}_1 - \underline{r}_2|} = \frac{1}{r_{12}} = \frac{1}{r_>} \sum_{n=0}^{\infty} \left(\frac{r_<}{r_>}\right)^n P_n(\cos\theta_{12})$$

$v(r_{12})$ is the Coulomb repulsion between the electrons.

$\begin{matrix}(r<)\\(r>)\end{matrix}$ is the $\begin{matrix}(\text{lesser})\\(\text{greater})\end{matrix}$ of r_1 and r_2.

θ_{12} is the angle between $\underline{r}_1$ and $\underline{r}_2$

$P_n(x)$ are Legendre polynomials as described by, for example, Abramowitz and Stegun (1972)

For elastic scattering and excitation, it is useful to rewrite the Hamiltonian as in (1.2.10)

$$H = H_0 + V(\underline{r}_1, \underline{r}_2)$$

$$H_0 = -\frac{1}{2}\nabla_2^2 + V_0(r_2) - \frac{1}{2}\nabla_1^2 \tag{1.2.10}$$

H_0 is the hydrogen atom Hamiltonian for $\underline{r}_2$, together with a free particle Hamiltonian for $\underline{r}_1$.

$V(\underline{r}_1, \underline{r}_2) = V_0(r_1) + v(r_{12})$: a short range potential as $r_1 \to \infty$. For distinguishable particles, this identifies the particle with coordinates $\underline{r}_1$ as the scattering particle. The Hamiltonian may also be written symmetrically in terms of two Coulomb Hamiltonians and a long range interaction potential $v(r_{12})$, as discussed by Peterkop (1977) and Geltman (1969).

$$\left(-\tfrac{1}{2}\nabla^2 + V_0(r) - \varepsilon_n\right) \phi_n(\underline{r}) = 0 \qquad (1.2.11a)$$

$$\sum_n{}' \phi_n(\underline{r}) \phi_n^*(\underline{r}') = \delta^3(\underline{r} - \underline{r}') \qquad (1.2.11b)$$

The ϕ_n are hydrogen functions and the prime on the sum indicates that integration over the positive energy continuum is included. "n" used here is a shorthand way to represent all three quantum numbers n l m for the bound states, and the vector $\underline{k}$ for the continuum states.

$$\langle \phi_n | \phi_{n'} \rangle = \delta^3_{nn'}$$

$$\langle \phi^{\pm}(\underline{k}) | \phi^{\pm}(\underline{k}') \rangle = \delta^3(\underline{k} - \underline{k}') \quad ; \quad \varepsilon_k = \tfrac{1}{2}k^2 \qquad (1.2.11c)$$

In the continuum, $\phi^{\pm}$ are diverging or converging Coulomb functions. The $\phi_n^{(\pm)}$ form a complete set.

Because of the Pauli principle, $\Psi^{\pm}$ must be either symmetric or antisymmetric, according to the total spin of the electrons (since electrons are fermions, the overall wavefunction must be antisymmetric):

$$\Psi_i^{\pm(s)}(\underline{r}_1, \underline{r}_2) = (-1)^s \Psi_i^{\pm(s)}(\underline{r}_2, \underline{r}_1) \qquad (1.2.12)$$

This symmetry/antisymmetry may be included explicitly or implicitly. $\Psi_i^{\pm(s)}$ may be expanded in terms of the $\phi^{\pm}$.

$$\Psi_i^{\pm(s)} = \bar{\chi}_i^{(s)} + \lim_{\epsilon \to 0^+} \sum_n{}' \sum_m{}' \frac{a_{mn}\, \phi_n^{\mp}(\underline{r}_1)\, \phi_m^{\mp}(\underline{r}_2)}{(E \pm i\epsilon - \epsilon_m - \epsilon_n)} \qquad (1.2.13)$$

This is a unique expansion with the a_{mn} determined by the Schrödinger equation (1.2.2). $\bar{\chi}_i^{(s)}$ here corresponds to the initial channel, a bound hydrogen state times a positive Coulomb function then symmetrised/antisymmetrised. The a_{mn} here are symmetric/antisymmetric in m and n. Peterkop (1977) showed that for pure Coulomb interactions the a_{mn} include a logarithmically diverging phase due to the long range potentials. For the present purposes it will be assumed that at large distances the potentials are screened by the other atoms in the target and experimental set up, and the a_{mn} are well behaved. The exact Coulomb case is considered by Peterkop (1977). The expansion (1.2.13) is mainly used for determining the singular properties of other expansions which can be more easily approximated practically. The continuum functions $\phi^{\mp}$ are chosen for $\Psi_i^{\pm(s)}$ as converging waves do not contribute to the asymptotic form of the continuum integral for the scattering amplitudes $f^{\pm}$ (to be defined), as discussed by Bransden (1983) and Peterkop (1977), and vice versa for $\Psi_i^{-(s)}$.

The boundary conditions on $\Psi_i^{\pm(s)}(\underline{r}_1, \underline{r}_2)$ are:

$$\lim_{r_1 \to \infty} \Psi_i^{\pm(s)}(\underline{r}_1, \underline{r}_2) = \phi_i(\underline{r}_2)\, e^{i \underline{k}_i \cdot \underline{r}_1} + \sum_n \phi_n(\underline{r}_2) f_{ni}^{\pm(s)}(\hat{\underline{r}}_1) \frac{e^{\pm i k_n r_1}}{r_1}$$

$$+ \int_{k' \leq k} d^3\underline{k}'\, \phi^{\bar{s}}(\underline{k}', \underline{r}_2) f_{\underline{k}', i}^{\pm(s)}(\hat{\underline{r}}_1) \frac{e^{i(kr_1 + \eta(\underline{k}', r))}}{r_1} \qquad (1.2.14a)$$

There is a similar expression, multiplied by $(-1)^S$, for $r_2 \to \infty$. It is assumed in (1.2.14a) that ionisation is possible. The $f_{ni}^{\pm(s)}(\hat{\underline{r}}_1)$ are scattering amplitudes for excitation into each channel: the spherical waves vanish for closed channels.

$$\frac{d\sigma_{ni}^{(s)}}{d\Omega_1} = \frac{k_n}{k_i} \left| f_{ni}^{\pm(s)}(\hat{\underline{r}}_1) \right|^2 \quad ; \quad T_{ni}^{(s)} = -2\pi f_{ni}^{\pm(s)}(\hat{\underline{r}}_1) \qquad (1.2.14b)$$

There is an additional phase factor in the ionisation channels: in the pure Coulomb case this is logarithmic. In the screened case it does not occur. The first term is the unperturbed incident channel for (1.2.10).

There are three main practical ways of expanding the wave function. In the first, the symmetry/antisymmetry is kept implicit.

$$\Psi_i^{\pm(s)}(\underline{r}_1, \underline{r}_2) = \sum_n{}' \bar{F}_n^{\pm(s)}(\underline{r}_1)\, \phi_n^{\bar{s}}(\underline{r}_2) \qquad (1.2.15)$$

The $\bar{F}_n^{\pm(s)}$ may be expressed in terms of the a_{am} by comparison with (1.2.13). For excitation:

$$\lim_{r_1\to\infty} \bar{F}_n^{\pm(s)}(\underline{r}_1) = \begin{cases} \delta_{ni} e^{i\underline{k}_i\cdot\underline{r}_1} + f_{ni}^{\pm(s)}(\hat{\underline{r}}_1)\dfrac{e^{ik_n r_1}}{r_1} & ; \varepsilon_n < E \\ 0 & ; \varepsilon_n > E \end{cases} \tag{1.2.16}$$

(The boundary conditions are similar for the ionisation channels when E > 0 to give (1.2.14a)).

$$\lim_{r_2\to\infty} \Psi_i^{\pm(s)}(\underline{r}_1,\underline{r}_2) = \int d^3\underline{k}'\, \phi^{\mp}(\underline{k}',\underline{r}_2)\bar{F}^{\pm(s)}(\underline{k}',\underline{r}_1) \tag{1.2.17}$$

The bound state terms vanish as $r_2\to\infty$. The $\bar{F}^{\pm(s)}(\underline{k}',\underline{r}_1)$ contain singularities which combined with the choice of diverging/converging wave preserve the correct boundary conditions. For non-singular $\bar{F}^{\pm(s)}$ the $\phi^{\mp}$ become highly oscillatory as $r_2\to\infty$ and the integral vanishes.

The other two expansions used practically are chosen so that singularities do not so appear and the boundary conditions are included straightforwardly. The first of these finds a solution to (1.2.2) treating the electrons as distinguishable and adds the symmetrised/antisymmetrised solution afterwards: this takes advantage of the symmetry of the Hamiltonian.

$$\Psi_i^{\pm(s)}(\underline{r}_1,\underline{r}_2) = \Psi_i^{\pm}(\underline{r}_1,\underline{r}_2) + (-1)^s \Psi_i^{\pm}(\underline{r}_2,\underline{r}_1)$$

$$(H-E)\Psi_i^{\pm}(\underline{r}_1,\underline{r}_2) = 0 \tag{1.2.18}$$

$$\lim_{r_1\to\infty} \Psi_i^{\pm}(\underline{r}_1,\underline{r}_2) = \phi_i(\underline{r}_2)e^{i\underline{k}_i\cdot\underline{r}_1} + \sum_n \phi_n(r_2)\frac{1}{r_1}e^{ik_n r_1} f_{ni}^{\pm}(\hat{r}_1) + \int_{k'<k} d^3k'\, \phi^{\mp}(k',r_2)\frac{1}{r_1}e^{i(kr_1+\eta)} f_{\underline{k}',i}^{\pm}(\hat{r}_1) \tag{1.2.19a}$$

$$\lim_{r_2\to\infty} \psi_i^{\pm}(\underline{r}_1,\underline{r}_2) = \sum_n \phi_n(r_1)\, g_{ni}^{\pm}(\hat{\underline{r}}_2)\, \frac{1}{r_2}\, e^{ik_n r_2} + \int_{k'<k} d^3k'\, \phi^{\mp}(\underline{k}',\underline{r}_1)\, \frac{1}{r_2}\, e^{i(kr_2+\eta)}\, g_{\underline{k}',i}^{\pm}(\hat{\underline{r}}_2) \qquad (1.2.196)$$

The $g_{ni}^{\pm}$ are exchange scattering amplitudes where the atomic and scattering electrons have swapped over. Rather than use an expansion of the type (1.2.15) for $\psi_i^{\pm}$ and achieve (1.2.19b) through singular terms, an expansion of the form (1.2.20) is used:

$$\psi_i^{\pm}(\underline{r}_1,\underline{r}_2) = \sum_n{}' \left(F_n^{\pm}(\underline{r}_1)\, \phi_n^{\mp}(\underline{r}_2) + G_n^{\pm}(\underline{r}_2)\, \phi_n^{\mp}(\underline{r}_1) \right) \qquad (1.2.20)$$

The $F_n^{\pm}$ and $G_n^{\pm}$ are not uniquely defined by (1.2.20). As described by Peterkop (1977), a unique choice is made by requiring the $F_n^{\pm}$ and $G_n^{\pm}$ to be orthogonal to all states $\phi_n^{\mp}$ of lower energy. In terms of the equivalent equation to (1.2.13), where here the a_{mn} are not symmetric/antisymmetric in m and n

$$F_n^{\pm}(\underline{r}) = \bar{X}_{ni} + \lim_{\varepsilon\to 0^+} \sum_{\substack{m \\ \varepsilon_m \geq \varepsilon_n}}{}' \frac{a_{mn}\, \phi_m^{\mp}(\underline{r})}{(E-\varepsilon_m-\varepsilon_n \pm i\varepsilon)}$$

$$G_n^{\pm}(\underline{r}) = \lim_{\varepsilon\to 0^+} \sum_{\substack{m \\ \varepsilon_m \geq \varepsilon_n}}{}' \frac{a_{nm}\, \phi_m^{\mp}(\underline{r})}{(E-\varepsilon_m-\varepsilon_n \pm i\varepsilon)} \qquad (1.2.21)$$

Thus for continuum energies ε_n discrete singularities do not appear in $F_n^{\pm}(\underline{r})$ or $G_n^{\pm}(\underline{r})$ and asymptotic behaviour of

(1.2.20) is restricted to $F_n^{\pm}(\underline{r}_1)$ as $r_1 \to \infty$ and $G_n^{\pm}(\underline{r}_2)$ as $r_2 \to \infty$.

We then have the boundary conditions for the excitation amplitudes :

$$F_n^{\pm}(\underline{r}_1) \underset{r_1 \to \infty}{\longrightarrow} \begin{cases} \delta_{ni}\, e^{i\underline{k}_i \cdot \underline{r}_1} + f_{ni}^{\pm}(\hat{\underline{r}}_1)\, \dfrac{e^{ik_n r_1}}{r_1} & ; \varepsilon_n < E \\ 0 & ; \varepsilon_n > E \end{cases}$$

(1.2.22a)

$$G_n^{\pm}(\underline{r}_2) \underset{r_2 \to \infty}{\longrightarrow} \begin{cases} g_{ni}^{\pm}(\hat{\underline{r}}_2)\, \dfrac{e^{ik_n r_2}}{r_1} & ; \varepsilon_n < E \\ 0 & ; \varepsilon_n > E \end{cases}$$

(1.2.22b)

Similarly, all the ionisation channel boundary conditions are contained in the $F_{\underline{k}}^{\pm}(\underline{r}_1)$ for $r_1 \to \infty$ and $G_{\underline{k}}^{\pm}(\underline{r}_2)$ for $r_2 \to \infty$. Taking the complete solution $\Psi_i^{\pm(s)}$, we have:

$$\Psi_i^{\pm(s)}(\underline{r}_1, \underline{r}_2) = \sum_n{}' \Big\{ \phi_n^{\mp}(\underline{r}_2)\left(F_n^{\pm}(\underline{r}_1) + (-1)^s G_n^{\pm}(\underline{r}_1)\right) + (-1)^s \phi_n^{\mp}(\underline{r}_1)\left(F_n^{\pm}(\underline{r}_2) + (-1)^s G_n^{\pm}(\underline{r}_1)\right) \Big\}$$

(1.2.23)

The scattering amplitudes are:

$$f_{ni}^{\pm(s)}(\hat{\underline{r}}) = f_{ni}^{\pm}(\hat{\underline{r}}) + (-1)^s g_n^{\pm}(\hat{\underline{r}})$$

(1.2.24)

The third expansion is to include exchange effects explicitly in the problem and define solutions (1.2.25).

$$\Psi_i^{\pm(s)}(\underline{r}_1, \underline{r}_2) = \sum_n{}' \left(F_n^{\pm(s)}(\underline{r}_1)\, \phi_n^{\mp}(\underline{r}_2) + (-1)^s \phi_n^{\mp}(\underline{r}_1)\, F_n^{\pm(s)}(\underline{r}_2)\right)$$

(1.2.25)

$$F_n^{\pm(s)}(\underline{r}) = F_n^{\pm}(\underline{r}) + (-1)^s G_n^{\pm}(\underline{r}) \qquad (1.2.26a)$$

$$F_n^{\pm(s)}(\underline{r}) \underset{r\to\infty}{\longrightarrow} \delta_{ni} e^{i\underline{k}_i\cdot\underline{r}} + f_{ni}^{\pm(s)}(\hat{\underline{r}}) \frac{e^{ik_n r}}{r} \qquad (1.2.26b)$$

Although (1.2.26a) relates the solutions, $F_n^{\pm}$ and $G_n^{\pm}$ are not considered separately in practical calculations. The $F_n^{\pm(s)}(\underline{r})$ should of course, be orthogonal to all states $\phi_m^{\pm}$ of lower energy, so that all asymptotic behaviour is contained in $F_n^{\pm(s)}$. (1.2.25) forms the basis of the approximate expansions used in the work of this thesis as the boundary conditions for $F_n^{\pm(s)}(r)$ are most simply adapted into the Green's function methods used. In chapter three and parts of chapter five the exchange processes are ignored for simplicity while various methods are tested.

1.2C The Lippmann Schwinger Equation

Writing the Hamiltonian as in (1.2.10) we can find unperturbed solutions for H_o:

$$(H_o - E)\,\phi_n(\underline{r}_2)\, e^{i\underline{k}_n\cdot\underline{r}_1} = 0 \qquad (1.2.27a)$$

We define

$$\chi_i(\underline{r}_1,\underline{r}_2) = \phi_i(\underline{r}_2)\, e^{i\underline{k}_i\cdot\underline{r}_1} \qquad (1.2.27b)$$

The Green's function for H_o may be constructed:

$$(E - H_o)\, G_o^{\pm}(\underline{k};\underline{r}_1,\underline{r}_1',\underline{r}_2,\underline{r}_2') = \delta^3(\underline{r}_1-\underline{r}_1')\,\delta^3(\underline{r}_2-\underline{r}_2') \;;\; \tfrac{1}{2}k^2 = E \qquad (1.2.28a)$$

$$G_o^{\pm}(\underline{k},\underline{r}_1,\underline{r}_1',\underline{r}_2,\underline{r}_2') = \frac{2}{(2\pi)^3}\int_0^{\infty} d^3\underline{k}' \sum_m{}' \frac{\phi_m^{\mp}(\underline{r}_2)\,\phi_m^{\mp}(\underline{r}_2')\,e^{\pm i\underline{k}_m\cdot(\underline{r}_1-\underline{r}_1')}}{(2(E-\varepsilon_m)-k'^2 \pm i\varepsilon)}$$

$$= -\frac{2}{4\pi}\sum_m{}' \frac{\phi_m^{\mp}(\underline{r}_2)\,\phi_m^{\mp}(\underline{r}_2')\,e^{\pm i k_m|\underline{r}_1-\underline{r}_1'|}}{|\underline{r}_1-\underline{r}_1'|} \qquad (1.2.29b)$$

In (1.2.28b) and henceforth throughout the limit as $\varepsilon \to 0^+$ is assumed wherever $E \pm i\varepsilon$ occurs. The formal solution for $\psi_i^{\pm(s)}$ is then

$$\psi_i^{\pm(s)}(\underline{r}_1,\underline{r}_2) = \phi_i(\underline{r}_2)\,e^{i\underline{k}_i\cdot\underline{r}_1} + \int_0^{\infty}\!\!\int d^3\underline{r}_1'\,d^3\underline{r}_2'\, G_o^{\pm}(\underline{k},\underline{r}_1,\underline{r}_1',\underline{r}_2,\underline{r}_2') \times V(\underline{r}_1',\underline{r}_2')\,\psi_i^{\pm(s)}(\underline{r}_1',\underline{r}_2') \qquad (1.2.28c)$$

Using the Green's function in operator form

$$|\psi_i^{\pm(s)}\rangle = |\chi_i\rangle + G_o^{\pm} V |\psi_i^{\pm(s)}\rangle \;;\; G_o^{\pm} = \frac{1}{(E\pm i\varepsilon - H_o)} \qquad (1.2.28d)$$

This is the Lippmann Schwinger equation for $\psi_i^{\pm(s)}$. The Lippmann Schwinger equation is the basis for the Schwinger variational method, introduced in chapter four and used extensively in chapter five.

The boundary conditions for $\psi_i^{\pm(s)}$ as $r_1 \to \infty$ are built in, most obviously for excitation:

$$\lim_{\substack{r_1 \to \infty \\ (r_1' \text{ finite})}} \frac{e^{ik_m|\underline{r}_1 - \underline{r}_1'|}}{|\underline{r}_1 - \underline{r}_1'|} = \frac{e^{ik_m(r_1 - r_1'\cos\theta)}}{r_1} \qquad (1.2.29)$$

θ is the angle between $\underline{r}_1$ and $\underline{r}_1'$.

By considering (1.2.28c,d) as $r_1 \to \infty$, the excitation scattering amplitudes are:

$$f_{mi}^{\pm(s)}(\hat{r}_1) = -\frac{2}{4\pi} \iint_0^\infty d^3\underline{r}_1' \, d^3\underline{r}_2' \, \phi_m^*(\underline{r}_2') \, e^{-i\underline{k}_m' \cdot \underline{r}_1'} V_{(\underline{r}_1', \underline{r}_2')} \, \psi_i^{\pm(s)}(\underline{r}_1', \underline{r}_2') \qquad (1.2.30)$$

$\underline{k}_m'$ has magnitude k_m and points in the direction of $\underline{r}_1$.

Geltmann (1969) points out that the integrand of (1.2.30) is a sharply vanishing function of $\underline{r}_1'$ as $r_1' \to \infty$, justifying the use of (1.2.29). For closed channels k_m becomes imaginary and the terms become exponentially vanishing functions of r_1. The ionisation amplitudes appear in a similar way although (1.2.29) is not directly applicable, as described by Geltman (1969). In terms of the T matrix

$$T_{mi}^{\pm(s)} = -2\pi f_{mi}^{\pm(s)} = \langle \chi_m | V | \psi_i^{\pm(s)} \rangle \qquad (1.2.31)$$

Using (1.2.28d) the t operator $t|\chi_i\rangle = V|\psi_i^{\pm(s)}\rangle$ may be defined.

$$T_{mi}^{+(s)} = \langle \chi_m | t | \chi_i \rangle$$

$$t = V + V G_0^+ t$$

$$= V + V G^+ V \quad ; \quad G^+ = \frac{1}{(E + i\varepsilon - H)} \qquad (1.2.32)$$

As $r_2 \to \infty$, the exchange terms in $\Psi_i^{\pm(s)}$ ensure that the boundary conditions are obeyed, as discussed by Geltman (1969), although this is not obvious from inspection. It is necessary to include the continuum terms in the representation of the Green's function, as these are the only terms that do not automatically vanish as $r_2 \to \infty$. In chapter five, a different form of the Lippmann Schwinger equation is used:

$$\Psi_i^{\pm(s)}(\underline{r}_1, \underline{r}_2) = \Phi_i^{\pm(s)}(\underline{r}_1, \underline{r}_2) + (-1)^s \Phi_i^{\pm(s)}(\underline{r}_2, \underline{r}_1)$$

$$\Phi_i^{\pm(s)}(\underline{r}_1, \underline{r}_2) = \sum_m{}' F_m^{\pm(s)}(\underline{r}_1)\, \phi_m^{\bar{}}(\underline{r}_2) \qquad (1.2.33a)$$

$$\Phi_i^{\pm(s)}(\underline{r}_1, \underline{r}_2) = \phi_i(\underline{r}_2)\, e^{i\underline{k}_i \cdot \underline{r}_1} + \iint d^3\underline{r}_1' d^3\underline{r}_2'\; G_0^{\pm}(k, \underline{r}_1, \underline{r}_1', \underline{r}_2, \underline{r}_2') \left\{ \left(V(\underline{r}_1', \underline{r}_2') - (-1)^s (E-H)A \right) \Phi_i^{\pm(s)}(\underline{r}_1', \underline{r}_2') \right\} \qquad (1.2.33b)$$

A interchanges $\underline{r}_1'$ and $\underline{r}_2'$.

$$f_{mi}^{\pm(s)}(\hat{\underline{r}}_1) = -\frac{2}{4\pi} \int_0^{\infty} \iint d^3\underline{r}_1'\, d^3\underline{r}_2'\; \phi_m(\underline{r}_2')\, e^{-i\underline{k}_m \cdot \underline{r}_1'} \times \left\{ \left(V(\underline{r}_1', \underline{r}_2') - (-1)^s (E-H)A \right) \Phi_i^{\pm(s)}(\underline{r}_1', \underline{r}_2') \right\} \qquad (1.2.33c)$$

This is identical to (1.2.30) for exact wavefunctions $\chi_m(\underline{r}_1, \underline{r}_2)$.

$$\lim_{r_2 \to \infty} \Phi_i^{\pm(s)}(\underline{r}_1, \underline{r}_2) = 0 \qquad (1.2.33d)$$

The importance of keeping the continuum terms in the representation of the Green's function is now to improve the

accuracy of the wave function. An alternative Green's function, not discussed here, uses a sum of two Coulomb Hamiltonians as the unperturbed state, and can be useful for discussions of ionisation, although the resultant scattering amplitudes cannot be used to represent elastic scattering, as the contribution to this from electron proton interaction is included in the homogeneous term. As discussed by Geltman (1969), for electron hydrogen atom scattering, in other respects the simplest case of electron atom scattering, (1.2.30) contains an undefined integral over r_i' in the threshold limit $k_m = 0$ due to the degeneracy of hydrogen atom energy levels. This does not occur for more complex atoms or in the case of the Poet model problem considered in chapter five as there is no such degeneracy.

Brief Summary Of The Born Series And Approximation, Following Bransden (1983).

The Lippmann-Schwinger equation may be extended by substitution within itself. (1.2.28d) may be rewritten:

$$|\psi_i^{+(s)}\rangle = |\chi_i\rangle + G_0^+ V|\chi_i\rangle + G_0^+ V G_0^+ V|\psi_i^{+(s)}\rangle \qquad (1.2.34a)$$

$$|\psi_i^{+(s)}\rangle = \{1 + \sum_{j=1}^{n} (G_0^+ V)^j\}|\chi_i\rangle + (G_0^+ V)^{n+1}|\psi_i^{+(s)}\rangle \qquad (1.2.34b)$$

$$= (1 + G^+ V)|\chi_i\rangle$$

$$G^+ = \sum_{j=0}^{\infty} (G_0^+ V)^j G_0^+ = (1 - G_0^+ V)^{-1} G_0^+ = (E + i\epsilon - H)^{-1} \qquad (1.2.34c)\ (1.2.35)$$

(1.2.35) is the Born series for the Green's function $G^{\pm}$, and (1.2.34c) is the Born series for the wave function. The convergence of (1.2.35) is not guaranteed (for bound states of a system for example it diverges). The successive Born approximations are to truncate the Born series at successive terms, starting with $|\psi_i^{\pm(s)}\rangle \approx |\chi_i\rangle$. The results are used in the T matrix elements (1.2.31). the first Born approximation substitutes $|\chi_i\rangle$ for $|\psi_i^{\pm(s)}\rangle$ and is justified at high energies as the second term in the Lippmann Schwinger equation involves integrating over a rapidly oscillating function and tends to vanish.

1.3 Brief Review of Scattering Methods

1.3A Low Energy Methods

The functional I defined by (1.3.1) is stationary about the solutions $\psi_i^{\pm(s)}$ and the errors in the scattering amplitudes are to second order in $\Delta\psi$ if I = 0, provided trial functions with the correct form of boundary conditions (1.3.2) are used, as may be shown to follow from the work of Kohn (1948).

$$I = \langle \psi_i^{+(s)} | H - E | \psi_i^{+(s)} \rangle = 0 \qquad (1.3.1)$$

Trial functions $\psi_{tri}^{(s)} = \psi_i^{\pm(s)} + \Delta\psi$ are used. (1.3.2a)

$$\psi_{tri}^{(s)}(\underline{r}_1, \underline{r}_2) \xrightarrow[r_1 \to \infty]{} e^{i\underline{k}_i \cdot \underline{r}_1} \phi_i(\underline{r}_2) + \sum_n \frac{1}{r_1} e^{ik_n r_1} \phi_n(\underline{r}_2) \bar{f}_{ni}^{(s)}(\hat{r}_1) \qquad (1.3.2b)$$

$(\varepsilon_n < E)$

$$\bar{f}_{ni}^{(s)}(\hat{r}_1) = f_{ni}^{+(s)}(\hat{r}_1) + \Delta f_{ni}(r_1) \qquad (1.3.2c)$$

The trial functions are appropriately symmetrised/antisymmetrised. In (1.3.2b) it is assumed ionisation is not possible for simplicity. For the exact solution when ionisation is possible the ionisation boundary conditions should be included. Setting I = 0 then gives a variational method for the scattering amplitudes. Using an expansion of the form (1.2.25) with unknown functions $\bar{F}_n^{(s)}(r_1)$ reduces (1.3.1) to an infinite set of coupled integro differential equations for the $\bar{F}_n^{(s)}$:

$$\int_0^\infty d^3 r_2 \, \phi_n^*(r_2)(H-E)\,\psi_{tr\,i}^{(s)}(r_1, r_2) = 0 \qquad (1.3.3)$$

(1.3.3) may, of course, be obtained straightforwardly from the Schrödinger equation for the exact solutions. For low energy scattering where only a few channels are open the close coupling method may be applied, or Kohn and Hulthen type variational calculations may be performed on (1.3.1). These variational calculations and the types of trial functions used are described in detail by Nesbet (1980), and a brief description of the Kohn method for single channel scattering is given at the end of this section. A review of variational methods is also given by Callaway (1978). With appropriate trial functions these methods are equivalent to the close coupling methods summarised below.

The close coupling method for low energy electron atom

scattering is based on the fact that $\delta I = 0$ to first order in $\Delta\Psi$ provided conditions (1.3.2) are obeyed. The basic form of the close coupling method uses a truncated expansion of the form (1.2.25) as $\Psi^{(s)}_{tr\,i}$:

$$\Psi^{(s)}_{tr\,i}(\underline{r}_1,\underline{r}_2) = \left(1+(-1)^S A\right)\sum_{n=0}^{N}\phi_n(\underline{r}_2)\,F_n(\underline{r}_1) \qquad (1.3.4)$$

(1.3.3) then becomes

$$\int_0^\infty d^3\underline{r}_2\,\phi_n(\underline{r}_2)(H-E)\Psi^{(s)}_{tr\,i}(\underline{r}_1,\underline{r}_2) = 0 \quad ; n = 0,1,\ldots,N \qquad (1.3.5)$$

Integrating over the angular variables leaves a series of radial equations. The system is in an eigenstate of total orbital angular momentum L and component M, spin S and parity Π. The Hamiltonian and T matrix are diagonal in these quantities. The angular momentum quantum numbers of the target and the scattering electron in channel i are respectively l_i, m_i and L_i, M_i. The angular parts of the expansions (1.3.4) are grouped as in (1.3.6)

$$\Psi^{(s)}_{tr\,i} = \Psi^{S\Pi}_{LM} = \left(1+(-1)^S A\right)\sum_{\substack{n_j,l_j,L_j \\ (j=0,N)}} R_{n_j l_j}(r_2)\,r_1^{-1}\,F^{LS\Pi}_{n_j,l_j,L_j,i}(r_1) \times \mathcal{Y}^{LM}_{l_i,L_i}(\theta_1,\phi_1,\theta_2,\phi_2) \qquad (1.3.6)$$

R_{n_j,l_j} is a radial hydrogen function.

$\mathcal{Y}^{LM}_{l_i,L_i}$ is a simultaneous eigenfunction of the total orbital angular momentum and component, and the orbital angular momentum of the target and scattered electrons.

$$\mathcal{Y}^{LM}_{l_i,L_i} = \sum_{M_i,m_i} \langle L_i, l_i, M_i, m_i \mid L, M\rangle\, Y_{L_i,M_i}(\theta_1,\phi_1)\,Y_{l_i,m_i}(\theta_2,\phi_2) \qquad (1.3.7)$$

Y_{l_i,m_i} are spherical harmonics and the coefficients are Clebsch Gordan coefficients, as described by Bransden (1983) for example.

$$|L - l_i| \leq L_i \leq L + l_i$$

$$\pi = (-1)^{L_i + l_i} \quad \text{is conserved.} \tag{1.3.8}$$

(1.3.8) places restrictions on the L_i. Using the expansion in (1.2.9) for the potential $V(r_{12})$, the equations (1.3.5) become

$$\left(\frac{1}{2}\frac{d^2}{dr^2} - \frac{L_m(L_m+1)}{2r^2} + \frac{1}{2}k_m^2 \right) \bar{F}_{mi}(r) = \sum_{j=0}^{N} \left\{ W_{mj}(r)\,\bar{F}_{ji}(r) + (-1)^s \int_0^\infty dr'\, K_{mj}(r,r')\,\bar{F}_{ji}(r') \right\} \tag{1.3.9}$$

In (1.3.9) $\bar{F}_{mi} \equiv F^{L s \pi}_{n_m, l_m, L_m, i}(r)$. The direct and exchange kernal potentials W_{mj} and K_{mj} are of short range: details are given by Percival and Seaton (1957).

$$\bar{F}_{mi}(r) \underset{r \to 0}{\longrightarrow} 0$$

$$\bar{F}_{mi}(r) \underset{r \to \infty}{\sim} \begin{cases} k_m^{-1/2} \left\{ \delta_{mi} \sin\left(k_i r - \frac{L_i \pi}{2}\right) + T^{L \pi s}_{n_m, l_m, L_m, i} e^{i\left(k_m r - \frac{L_m \pi}{2}\right)} \right\} & ; \varepsilon_m < E \\ 0 & ; \varepsilon_m > E \end{cases} \tag{1.3.10}$$

The radial expansions of unperturbed solutions $e^{i\underline{k}\cdot\underline{r}}$ using Bessel functions and Legendre polynomials are described by Bransden (1983) and Joachain (1983). The boundary conditions are correct to within a constant in each angular momentum channel. The $T^{L \pi s}_{n_m, l_m, L_m, i}$ sum (with

appropriate angular factors) to give the T_{mi}, as described by Percival and Seaton (1957). The individual radial T matrix elements $T^{L\pi S}_{n_m, l_m, l_m, i}$ may be defined using the Lippmann Schwinger equations for the $\bar{F}_{mi}$ in a similar way as described in section 1.2B, to within appropriate factors of k_m, k_i according to the normalisation adopted. This is done for the Poet model problem in chapter five. In many practical calculations, real solutions are defined:

$$\bar{F}_{mi}(r) \underset{r\to\infty}{\sim} \frac{1}{k_m^{1/2}}\left\{\delta_{mi}\sin\left(k_i r - \frac{l_i\pi}{2}\right) + K^{L\pi S}_{mi}\cos\left(k_m r - \frac{l_m\pi}{2}\right)\right\};\ \varepsilon_m < E \qquad (1.3.10b)$$

The $K^{L\pi S}_{mi}$ form the elements of the reaction or K matrix, from which the T matrix and the (unitary by definition) S matrix may be formed (see for example Bransden 1983). Calculations are now all real, but K-matrix elements for all the open channels are needed to form the complex and unitary S matrix. The direct numerical solution of (1.3.9) has been discussed by Burke and Seaton (1971), Crees et al. (1978) and Rowntree et al. (1976). The R matrix method which matches logarithmic derivatives of a trial function of convenient form and the asymptotic function, as discussed by Burke and Robb (1975), or a variational method with algebraic trial function described by Callaway (1978, 1980), can be used.

The most straightforward close coupling calculations use only open channels in the expansion (1.3.4): the "static exchange" model for example includes only the hydrogen ground state for elastic scattering. These are feasible

calculations for low energies when only a few channels are open and are accurate for interactions in which the included channels contribute the bulk of the scattering amplitudes, but can converge slowly as more closed channels are added to (1.3.4). For example, 18% of the hydrogen atom dipole polarisability comes from continuum p states and will not be accounted for as the number of bound states included is increased. The method is improved by the addition of L-squared pseudostates to the expansion to represent the closed channels. These may be non-hydrogenic functions plus additional scattering functions, the target pseudo-functions $\bar{R}_{nl}$ diagonalising the target Hamiltonian:

$$\langle r\bar{R}_{n,l} \left| -\frac{d^2}{dr^2} + \frac{l(l+1)}{2r^2} - \frac{1}{r} \right| r\bar{R}_{n'l} \rangle = \delta_{nn'}\bar{\varepsilon}_{n'l} \qquad (1.3.11)$$

These functions have energies $\bar{\varepsilon}_{nl} \geq \varepsilon_n$ by the Rayleigh Ritz principle, which may be negative or positive. The representation of continuum functions by L-squared functions is discussed in chapter two. A few well chosen pseudostates of this form can improve low energy close coupling results greatly: an example is the work of Burke et al. (1969) on accurate results for the elastic differential cross section for electron hydrogen scattering. The more general form of practical low energy expansion includes the open channels explicitly and uses algebraic L-squared functions to represent the closed channels: details are given by Nesbet (1980).

$$\psi^{(s)}_{tr\ i} = (1 + (-1)^s A) \sum_{n=0}^{N} \phi_n(\underline{r}_2) F_n(\underline{r}_1) + \sum_{i=1}^{M} c_i \Theta_i(\underline{r}_1, \underline{r}_2)$$

(1.3.12)

The Θ_i should be orthogonal to the open channel space or can be made so (Burke and Taylor 1966). Using the Kohn variational principle, as described by Gailitis (1965) and Burke and Taylor (1966), (1.3.1) becomes a mixed set of integro-differential and algebraic equations. A projection operator formalism due to Feshbach (1958, 1962) may be employed to reduce (1.3.1) using (1.3.12) to a finite series of coupled equations, using an optical potential. This is discussed for a model problem in chapter three. The projection operator P projects out the open channel space

$$P \psi^{(s)}_{tr\ i} = (1 + (-1)^s A) \sum_{n=0}^{N} \phi_n(\underline{r}_2) F_n(\underline{r}_1)$$

$$P^2 = P \ ; \ Q = 1 - P$$

(1.3.13a)

For example, for N = 0

$$P_1 \psi^s(\underline{r}_1, \underline{r}_2) = \phi_0(\underline{r}_2) \int d^3\underline{r}_2' \, \phi_0^*(\underline{r}_2') \psi^s(\underline{r}_1, \underline{r}_2')$$

$$P_2 \psi^s(\underline{r}_1, \underline{r}_2) = \phi_0(\underline{r}_1) \int d^3\underline{r}_1' \, \phi_0^*(\underline{r}_1') \psi^s(\underline{r}_1', \underline{r}_2)$$

$$P = P_1 + P_2 - P_1 P_2$$

(1.3.13b)

As shown in chapter three, the Schrödinger equation becomes

$$(PHP + V_p - E) P \psi^s = 0$$

$$V_p = - PHQ \frac{1}{Q(H-E)Q} QHP$$

(1.3.14)

The closed space is represented by the optical potential V_p, and (1.3.9) is solved with additional potential terms due to V_p. V_p is represented approximately by diagonalising the Q space Hamiltonian QHQ on the basis Θ_i, determining the c_i and giving an L-squared representation of the Q space Green's function. This is discussed in chapter two and is valid for low energy scattering where the Q space is all closed. A general survey of these methods and low energy scattering in general has been given by McDowell (1976). As incident energies increase, more and more channels become open, (1.3.9) becomes more cumbersome, and some of the difficulties arising in the intermediate energy region discussed in sections 1.3B appear, although the continuum remains closed.

Kohn Variational Principle (Single Channel), following Bransden (1983).

We define $I[\bar{f}_l] = \int_0^\infty \bar{f}_l(r)\, L\, \bar{f}_l(r)\, dr$ (1.3.15)

$L = \frac{d^2}{dr^2} - \frac{l(l+1)}{r^2} - U(r) + k^2$

$\bar{f}_l(r) = f_l(r) + \Delta f_l(r)$, f_l the true solution.

$\bar{f}_l(r) \underset{r\to\infty}{\sim} \sin(kr - l\frac{\pi}{2}) + \bar{K}_l \cos(kr - l\frac{\pi}{2})$; $\bar{K}_l = K_l + \Delta K_l$

The real K matrix problem is illustrated for a single channel problem. The Kato identity is:

$$I[\bar{f}_l] - I[\Delta f_l] = -k\,\Delta K_l \qquad (1.3.16)$$

Thus $\Delta (I + kK_\ell) = 0$ to first order in Δf_ℓ.

$$\bar{f}_\ell(r) = \sum_{i=1}^{N} c_i Y_i(r) + \sin\left(kr - \tfrac{\ell\pi}{2}\right) + \bar{K}_\ell \cos\left(kr - \tfrac{\ell\pi}{2}\right) \tag{1.3.17}$$

c_i and $\bar{K}_\ell$ are unknown.

The Y_i are L-squared functions which vanish at infinity.

The Kohn variational principle (Kohn 1948) sets:

$$\frac{\partial I}{\partial c_i} = 0 \qquad ; \; i = 1, .., N \tag{1.3.18a}$$

$$\frac{\partial I}{\partial \bar{K}_\ell} = -k \tag{1.3.18b}$$

Applying the Kato identity to the result, an improved approximation to K_ℓ is

$$K_\ell \approx \frac{1}{k}\left(I[\bar{f}_\ell] + \bar{K}_\ell \right) \tag{1.3.19}$$

The Hulthen (Hulthen 1944) principle replaces (1.3.18b) by

$$I[\bar{f}_\ell] = 0 \tag{1.3.20}$$

This also sets $\Delta K_\ell = 0$ to first order. Spurious numerical singularities can occur with the Kohn principle, as the c_i may become infinite for certain values of k^2. The inverse Kohn principle uses the boundary conditions (1.3.21) and may be used if the Kohn principle does not converge.

$$\bar{f}_\ell \sim \cot \bar{\delta}_\ell \sin\left(kr - \tfrac{\ell\pi}{2}\right) + \cos\left(kr - \tfrac{\ell\pi}{2}\right) \tag{1.3.21}$$

Ways of predicting and avoiding spurious singularities have been discussed by Takatsuka and Fueno (1979).

More Complex Atoms

The general methods outlined so far in this chapter can be applied in principle to electron scattering by more complex atoms containing M electrons. However, spatial and spin components of the wave function do not conveniently break up into separate symmetrical/antisymmetrical types. Overall antisymetric sums of products of various spatial/spin functions must be formed. Atomic wave functions (see for example Condon and Odabasi 1980) $\Phi_m(1,2\ldots,M)$, fully antisymetric and including spin terms are used in expansions instead of hydrogen functions for the P space channels, and each combination of a Φ_m and a function $F_m(M+1)$, which includes the spin dependence of the scattering electron, is then fully antisymmetrised. The Q space part of the expansion may be represented by similar sums of closed channels and pseudostates, or by the linear combination (1.3.22).

$$Q\Psi = \sum_{i=1}^{N_c} c_i \Theta_i(1,2,\ldots,M+1) \qquad (1.3.22)$$

The Θ_i are predetermined fully antisymmetrical (M+1) electron wave functions, orthogonal to the P space. They can be expressed as combinations of Slater determinants of one particle orbitals. These "configurations" can then be used to diagonalise the Q-space Hamiltonian, a process also

known as a configuration interaction calculation. A systematic procedure for determining the Θ_i allowing for the distortion of the target due to the perturbing effect of the scattering electron has been described by Mittleman (1966) and further developed by Nesbet (1975, 1980).

1.3B Intermediate Energies

The intermediate energy range is considered to start at the ionisation threshold (E = 0; 0.5 au or 13.605 eV incident electron energy for atomic hydrogen) and continue to energies where the first Born approximation is valid. These energies vary from system to system and cannot be specified quantitatively. Also, the convergence at the Born series to its first term at high energies has not been proved analytically for atomic systems. The Born approximation cannot give inelastic differential cross sections at large angles and elastic differential cross sections in the forward direction.

For the lower end of the intermediate energy range, it is desirable to extend the methods of section 1.3A, with suitable modifications, to calculate elastic and excitation cross sections, as the higher energy approximations mentioned at the end of this section are not valid. The disadvantage, apart from increased complexity of the equations and potentials W_{mn}, K_{mn}, is that not all open channels can be represented explicitly so that the boundary

conditions (1.3.2) guaranteeing first order accuracy are not all fulfilled. Straightforward close coupling results are likely to be poor as no contributions from the continuum (part of which is open) are included. For example, Kingston et al. (1976) calculated 1s-2s-2p close coupling cross sections for electron hydrogen atom scattering at energies up to 300eV. The elastic cross section was given badly as long range contributions from the continuum were missing. However, for higher energies the long range 1s-2p coupling was fully taken into account and 2s-2p terms were also reasonable. For these cross sections results were poor up to 50eV but improved at higher energies, although angular correlation between the scattered electron and subsequently emitted photon after 1s-2p excitation was not well represented (Williams 1981).

The use of pseudostates can, as before, improve results, but judicious choice must be made as convergence with additional pseudostates is not regular. Burke and Webb (1970) carried out close coupling calculations on electron hydrogen atom scattering for incident energies up to 50eV with 1s-2s-2p states and additional 3s, 2p pseudostates with eigenenergies at the ionisation threshold. The pseudostates changed results (improved them) dramatically, but the convergence with respect to choice and additional numbers of pseudostates was not investigated. Burke and Mitchell later investigated this for the "Poet" model problem (see chapter four) and found unphysical structure appeared in the T

matrix elements around each pseudostate threshold. Subsequent work by Callaway et al. (1976) for incident energies up to 54eV with eight pseudostates agreed well with experiment away from the pseudothresholds. Fon and coworkers (1981) calculated elastic scattering cross sections for electron-hydrogen, helium and neon scattering using a pseudostate expansion and the R-matrix method. Pseudoresonances occurred at pseudothresholds, which were removed by a T matrix averaging process of Burke, Berrington and Sukumar (1981) discussed in later chapters. The generalised pseudostate and optical potential methods have similar problems, as part of the Q-space is open, and the discrete L-squared Green's function gives rise to false resonances at the pseudostate eigenvalues.

The investigation of methods of removing false pseudo-structure whether from "pseudo-atomic" states $\bar{R}_{nl}$ or optical potentials diagonalised on an L-squared basis, to allow the systematic but manageable extension of the series expansion techniques to intermediate (up to 54eV) incident energy excitation studies, together with the use of the Schwinger variational method to try and circumvent these problems, makes up the discussion and work of this thesis. Methods discussed in chapter two where the whole wave function rather than just Q-space has been replaced by an L-squared diagonalisation have achieved success for elastic scattering but are numerically unstable for inelastic scattering.

Higher Intermediate Energies

At incident electron energies above 54eV various methods have been used successfully in electron atom scattering. These have been reviewed by Bransden and McDowell (1976) and a few examples are given here. The optical potential method has been used with only channels of interest for excitation retained in P space, and the Q space Green's function expanded in terms of a Born series of free particle Green's functions, only one or two terms being retained. At higher energies, exchange kernals may be neglected (Mittleman and Pu 1962, Bransden and Coleman 1972) and the "second order potential" is simplified. The closure approximation replaces the integral over the continuum in this second order optical potential by an average value, further simplifying the problem. Cross sections have been calculated for elastic scattering of electron by hydrogen and helium by Winters et al. (1973, 1974), comparable with the eikonal-Born series work of Byron and Joachain (1973, 1974, 1977). Other methods used with success for higher intermediate energies include extensions of the first Born approximation, semiclassical methods, and distorted wave methods (in which increasingly sophisticated uncoupled solutions of the elastic scattering equation are used in the equations for inelastic scattering to get aproximate solutions: see for example Bransden 1983). The use of many body theory applied to electron atom scattering has been described by Bransden and McDowell (1976).

CHAPTER TWO

THE L-SQUARED DISCRETISATION OF ELECTRONIC CONTINUA

2.1 Introduction

2.1A General Introduction

L-squared representations of wave functions and associated spectral resolutions have been used to avoid, to differing extents, part or all of the usual specifications of channels and asymptotic forms in scattering problems and photoabsorption studies. In this chapter, theoretical methods of L-squared discretisation and equivalent quadrature are introduced. In section 2.2, certain cases of one particle Hamiltonians for which finite basis approximate L-squared solutions can be directly related to the exact solutions are discussed. Sections 2.3 and 2.4 give examples of how the methods are applied in cases where the exact solutions are not known and the L-squared discretisation is applied numerically, the methods of section 2.3 being directly relevant to the work of this thesis. It should be noted that while the exact cases of section 2.2 treat relatively simple one particle Hamiltonians and use systematic series of well known basis functions to give reasonably straightforward analytic analyses, the general

L-squared wave functions used to discretise many electron atomic and molecular continua in the cases discussed in the latter sections are usually the results of configuration interaction calculations, using Slater determinants composed of atomic/molecular orbitals expanded in the L-squared basis, with additional functions included to represent, where applicable, polarisation and other relevant effects. These more complex cases do not always give single smooth quadratures. Section 2.4 describes one method of extracting physical information in these cases, and in chapter three a method of forming systematic quadratures from the initial discretisation is investigated.

2.1B Theoretical Introduction Following Reinhardt (1979)

The eigenfunctions of an electronic Hamiltonian H form a complete set, allowing H to be expressed in terms of its spectral resolution or eigenfunction expansion (within a subspace defined by a single non-degenerate symmetry):

$$H = \sum_i |\psi_i\rangle E_i \langle\psi_i| + \int_0^\infty dE' \, |\psi(E')\rangle\langle\psi(E')| \qquad (2.1.1)$$

$|\psi_i\rangle$ are orthonormal bound state eigenfunctions and $|\psi(E')\rangle$ are orthonormal continuum eigenfunctions. The continuum is assumed to start at E' = 0 for convenience.

$$H|\psi_i\rangle = E_i|\psi_i\rangle \quad ; \langle\psi_i|\psi_j\rangle = \delta_{ij} \qquad (2.1.2a)$$

$$H|\psi(E)\rangle = E|\psi(E)\rangle \quad ; \langle\psi(E)|\psi(E')\rangle = \delta(E-E') \qquad (2.1.2b)$$

The normalisation is such that

$$\sum_i |\psi_i\rangle\langle\psi_i| + \int_0^\infty dE' \, |\psi(E')\rangle\langle\psi(E')| = 1 \qquad (2.1.2c)$$

The exact wavefunction for a system may be written in terms of the eigenfunctions $|\psi_i\rangle$ and $|\psi(E')\rangle$.

$$(\bar{H} - E)|\bar{\Psi}(E)\rangle = 0$$

$$|\bar{\Psi}(E)\rangle = \sum_i |\psi_i\rangle\langle\psi_i|\bar{\Psi}(E)\rangle + \int_0^\infty dE' \, |\psi(E')\rangle\langle\psi(E')|\bar{\Psi}(E)\rangle \qquad (2.1.3)$$

A finite L-squared calculation with basis ϕ_i, $i = 1,..,N$ diagonalises the matrix representation $\underline{\underline{\hat{H}}}^{(N)}$ of H yielding a set of approximate eigenfunctions $|\psi_i^{(N)}\rangle$ with eigenvalues $E_j^{(N)}$; $j = 1,\ldots,N$

$$\{\underline{\underline{\tilde{H}}}^{(N)}\}_{ij} = \langle \phi_i | H | \phi_j \rangle \quad ; \quad i,j = 1,2,\ldots,N$$

$$|\psi_i^{(N)}\rangle = \sum_{j=1}^{N} \psi_{ij}^{(N)} |\phi_j\rangle \quad ; \quad i = 1,2,\ldots,N$$

$$\underline{\underline{\tilde{H}}}^{(N)} \underline{\psi}_j^{(N)} = E_j^{(N)} \underline{\psi}_j^{(N)} \quad ; \quad \{\underline{\psi}_j^{(N)}\}_i = \psi_{ji}^{(N)}$$

$$\langle \psi_j^{(N)} | \psi_{j'}^{(N)} \rangle = \delta_{jj'} \qquad (2.1.4)$$

Within the subspace defined by the L-squared basis, the spectral resolution of $\hat{H}$ may be written as:

$$\hat{H} = \sum_{E_j^{(N)}<0} |\psi_j^{(N)}\rangle E_j^{(N)} \langle\psi_j^{(N)}| + \sum_{E_j^{(N)}>0} |\psi_j^{(N)}\rangle E_j^{(N)} \langle\psi_j^{(N)}| \qquad (2.1.5)$$

We expect the first sum to correspond to the bound

state sum in (2.1.1) and the second sum to approximate the continuum integral in some way: the continuum is considered to have been discretised by the use of the L-squared basis, hence the term "L-squared discretisation". As the size of the basis is increased to infinity, the representation becomes complete for functions with the correct boundary conditions. The second sum in (2.1.5) is interpreted as a numerical quadrature of the continuum integral. For example, for an arbitrary function $|\chi\rangle$, the matrix element $\langle\chi|H|\chi\rangle$ may be formed:

$$\langle\chi|H|\chi\rangle = \sum_i \langle\chi|\psi_i\rangle E_i \langle\psi_i|\chi\rangle + \langle\chi|\int_0^\infty dE' |\psi(E')\rangle E' \langle\psi(E')|\chi\rangle \qquad (2.1.6)$$

The continuum part of (2.1.6) may be evaluated numerically:

$$\langle\chi|\int_0^\infty dE' |\psi(E')\rangle E' \langle\psi(E')|\chi\rangle \simeq \langle\chi|\sum_j w_j |\psi(E_j)\rangle E_j \langle\psi(E_j)|\chi\rangle \qquad (2.1.7)$$

w_j and E_j are appropriate weights and abscisae. If $|\chi\rangle$ is well represented in the finite L-squared basis, an approximation to the continuum part of (2.1.5) would be

$$\langle\chi|\int_0^\infty dE' |\psi(E')\rangle E' \langle\psi(E')|\chi\rangle \simeq \langle\chi|\sum_{E_j^{(N)}>0} |\psi_j^{(N)}\rangle E_j^{(N)} \langle\psi_j^{(N)}|\chi\rangle \qquad (2.1.8)$$

The use of the L-squared basis can be considered as a numerical "equivalent quadrature" with abscissae $E_j^{(N)}$ and weights $w_j^{(N)}$ (eq) defined such that (2.1.9) is obeyed.

$$|\langle \chi | \psi_j^{(N)} \rangle| = \left(w_j^{(N)}(eq)\right)^{1/2} |\langle \chi | \psi(E_j^{(N)}) \rangle|$$

(2.1.9)

Over a limited range of coordinate space depending on the size and complexity of the basis $|\phi_i\rangle$, we expect (2.1.10) to hold, as exemplified by the work of Hazi and Taylor (1970) for some model potentials, with numerically integrated exact solutions, and Bassichis et al. (1975).

$$|\psi_j^{(N)}\rangle \simeq \left(w_j^{(N)}(eq)\right)^{1/2} |\psi(E_j^{(N)})\rangle$$

(2.1.10)

2.2 The Exact L-squared Treatment

For certain Hamiltonians, detailed comparison between exact continuum scattering solutions and finite L-squared basis approximate solutions is possible. Heller, Yamani, Reinhardt and co-workers (1973, 1974, 1975) used a systematic approach to illustrate the mathematical sense in which the square integrable functions approximate the scattering solutions, and Broad (1978, 1982, 1983) has further developed and refined their methods. Stelbovics and Slim (1986) have also performed a detailed analysis of a model problem involving a separable potential. The crux of the analysis in each case is that an L-squared basis must be found in which the infinite matrix representation of the Hamiltonian H is tridiagonal, leading to an analytically soluble three term recursion relation. Finding such a basis

is tantamount to solving the original Schrödinger equation exactly, and indeed the specific examples for which the analysis has been carried out are all Hamiltonians with known solutions. These Hamiltonians together with the corresponding basis sets and polynomial solutions of the recursion relations are shown in table 2.1. However, the fact that the links between the approximate finite basis solutions and the exact solutions are so direct helps justify and gives confidence in the use of finite L-squared bases in situations where the exact solution is not known. On a slightly different track, the "J matrix" method (to be discussed in section 2.4) of Heller and Yamani (1974), further developed by Broad (1978, 1982), gives exact solutions of model problems that uniformly approximate the physical Hamiltonians under consideration.

The following discussion is generalised and assumes the L-squared basis functions to be orthogonal. This condition may be relaxed in certain cases to tridiagonal overlap, as in the case of the Laguerre/Slater basis used for the kinetic and Coulomb Hamiltonians, and the Stelbovics and Slim (1986) model problem. In these cases, a mapping taking the continuum from $(0,\infty)$ in energy E to $(-1,1)$ in a variable $x(E)$ leads to a recursion relation of the form found more directly below, with off diagonal energy dependence factored out. Appendix 1 summarises the principles of Gaussian quadrature relevant to the discussion, and Appendix 2 reproduces the main points of the analysis for the

TABLE 2.1

Examples of solved Hamiltonians (bases are given to within a normalisation constant).

(a) Radial kinetic energy (Heller and Yamani 1974, Yamani and Fishman 1974)

$$H = -\frac{1}{2}\frac{d^2}{dr^2} + \frac{l(l+1)}{2r^2}$$

(i) $\phi_n = (\lambda r)^{l+1} e^{-\frac{\lambda r}{2}} L_n^{(2l+1)}(\lambda r)$; $n = 0,1,2,\ldots$: Slater / Laguerre basis

The p_n are Gegenbauer polynomials.

(ii) $\phi_n = (\lambda r)^{l+1} e^{-\frac{\lambda^2 r^2}{2}} L_n^{(l+\frac{1}{2})}(\lambda^2 r^2)$; $n = 0,1,2,\ldots$: Oscillator basis

The p_n are Laguerre polynomials.

(b) Coulomb Hamiltonian (Yamani and Fishman 1974, Yamani and Reinhardt 1975)

$$H = -\frac{1}{2}\frac{d^2}{dr^2} + \frac{l(l+1)}{2r^2} + \frac{Z}{r}$$

The Slater / Laguerre basis is used.
The p_n are Pollaczec polynomials ($Z > 0$)
"Extended Pollaczec polynomials" ($Z < 0$)

(c) Radial Harmonic Oscillator (Broad 1982)

$$H = -\frac{1}{2}\frac{d^2}{dr^2} + \frac{l(l+1)}{2r^2} + \frac{Kr^2}{2}$$

The oscillator basis is used.

(d) Morse Oscillator (Broad 1982)

$$H = -\frac{1}{2}\frac{d^2}{dr^2} + Ae^{-2r} + Be^{-r}$$

A Slater / Laguerre basis is used after a coordinate transformation. Broad expressed the p_n for (c) and (d) in terms of hypergeometric functions.

(e) Model With Separable Potential (Stelbovics and Slim 1986)

$$H = -\frac{1}{2}\frac{d^2}{dr^2} + |a\rangle\alpha\langle a| \quad ; \quad \langle r|a\rangle = e^{-\frac{\lambda r}{2}}$$

The Slater / Laguerre basis is used. The p_n are linear combinations of Chebyschev polynomials (all polynomials are described in the references and by Abramowitz and Stegun (1972)).

particular example of the s-wave kinetic Hamiltonian and the Laguerre/Slater basis, as this type of basis is used in later chapters.

2.2A Exact Regular L-squared Solution

An infinite L-squared basis $\{\phi_n\}$ is complete for functions regular at the origin, so the regular solution of the Schrödinger equation (2.2.1) may be expressed in the form (2.2.2).

$$(H - E)\,\psi_R^+(E,r) = 0 \qquad ; \quad \psi_R^+(E,r) \underset{r\to 0}{\longrightarrow} 0 \tag{2.2.1}$$

$$\psi_R^+(E,r) = \sum_{n=0}^{\infty} \psi_n^+(E)\,\phi_n(r) \tag{2.2.2}$$

Equation (2.2.1) is solved as:

$$\int_0^{\infty} dr\, \phi_m(r) \sum_{n=0}^{\infty} (H-E)\,\psi_n^+(E)\,\phi_n(r) = 0 \qquad ; \; m = 0,1,2,\ldots,\infty \tag{2.2.3}$$

Due to the tridiagonal nature of the Hamiltonian matrix (2.2.4), equation (2.2.3) is reduced to the tridiagonal recursion relation (2.2.5)

$$H_{mn} = \int_0^{\infty} dr\, \phi_m(r)\, H\, \phi_n(r) \tag{2.2.4}$$

$$H_{m,m+1}\,\psi_{m+1}^+(E) + (H_{mm} - E)\,\psi_m^+(E) + H_{m,m-1}\,\psi_{m-1}^+(E) = 0 \tag{2.2.5a}$$

$$\psi_{-1}^+(E) = 0 \tag{2.2.5b}$$

Equation (2.2.5b) is the boundary condition choosing the

solution Ψ_R^+. The m dependent parts of the $\Psi_m^+(E)$ are thus the Sturm sequence orthogonal polynomials $p_m(E)$ generated by (2.2.5) as described by Wilkinson (1965) and in Appendix 1.

$$\Psi_m^+(E) = \Psi_0^+(E)\, p_m(E) \tag{2.2.6}$$

$p_{-1}(E) = 0$; $p_0(E)$ = constant, chosen for convenience to be unity.

For Hamiltonians which do not support bound states (for example the radial kinetic energy, the repulsive Coulomb Hamiltonian), the normalisation of $\Psi_R^+(E,r)$ can be defined in terms of the requirement (2.2.7)

$$\int_0^\infty dE\ \Psi_R^+(E,r)\, \Psi_R^{+*}(E,r') = \delta(r-r') \tag{2.2.7}$$

In terms of the infinite basis, this may be rewritten as (2.2.8) which, on taking matrix elements becomes (2.2.9)

$$\sum_{n,n'=0}^{\infty} \phi_n(r)\, \phi_{n'}(r') \int_0^\infty dE\, |\Psi_0^+(E)|^2\, p_n(E)\, p_{n'}(E) = \delta(r-r') \tag{2.2.8}$$

$$\int_0^\infty dE\, |\Psi_0^+(E)|^2\, p_n(E)\, p_{n'}(E) = \delta_{nn'} \tag{2.2.9}$$

The positive weight function $\rho(E)$ for the $p_n(E)$ on the integral $(0,\infty)$ obeying (2.2.9) may thus be related to $\Psi_0^+(E)$, and the normalisation of ρ and the $p_n(E)$ is fixed by (2.2.9)

$$\rho(E) = |\Psi_0^+(E)|^2 \tag{2.2.10}$$

In the Slater/Laguerre case, the interval is $(-1,1)$ and the recursion relation for the ϕ_n must be made use of. (2.2.9) and (2.2.10) are replaced as described in Appendix Two.

If the Hamiltonian supports bound states (for example the attractive Coulomb Hamiltonian) the continuum states can be analysed separately in the same way. Yamani and Reinhardt (1975) have extended the analysis to cover the bound states in the Coulomb case, and Broad (1982, 1983) generalised the method to all attractive tridiagonal Hamiltonians. With bound states $\psi_b(r)$, equation (2.2.7) becomes

$$\sum_b \psi_b(r)\,\psi_b(r') + \int_0^\infty dE\; \psi_a^+(E,r)\,\psi_a^{+*}(E,r) = \delta(r-r')$$

$$\oint dE\; \psi_a^+(E,r)\,\psi_a^{+*}(E,r') = \delta(r-r') \qquad (2.2.11)$$

The terms in the bound state sum are $-2\pi i$ times the residues of the integrand $\psi_a^+(E,r)\,\psi_a^{+*}(E,r')$, which consists of poles at the bound state energies ϵ_b in the negative energy region. In terms of the L-squared expansion, (2.2.11) becomes

$$\oint dE\; \psi_0^+(E)\,\psi_0^{+*}(E)\,\rho_m(E)\,\rho_{m'}(E) = \delta_{mm'} \qquad (2.2.12)$$

(2.2.12) is the replacement for (2.2.9).

The interval has been extended to include the bound state energies, and the extended negative energy weight function consists of poles at these energies. The sign $\oint$ indicates that $-2\pi i$ times the sum of the residues at these poles is taken. As described by Yamani and Reinhardt (1975) and Stelbovics and Slim (1986), in particular cases the coupling strength of the attractive

potential term places restrictions on the magnitude of the otherwise arbitrary L-squared scaling parameter λ when bound states are included, in order for the weight function to remain positive definite.

2.2B Approximate (Finite Basis) Regular Solution

Using an L-squared basis of N terms to represent the wave function ψ_R^+ by a pseudostate $\psi_R^{(N)+}$ corresponds to truncating the Hamiltonian matrix at $H_{N-1,N-1}$.

$$\psi_R^{(N)+}(E,r) = \sum_{n=0}^{N-1} \psi_n^{(N)+}(E)\, \phi_n(r) \qquad (2.2.13)$$

$$\int_0^\infty dr\, \phi_m(r)(H-E)\sum_{n=0}^{N-1} \psi_n^{(N)+}(E)\, \phi_n(r) = 0 \quad ; \; m = 0,1,\ldots,N-1 \qquad (2.2.14a)$$

In a finite basis, limiting the Hamiltonian to tridiagonal form is no great restriction: the standard method of diagonalising a hermitian matrix is to employ a Householder tridiagonalisation as the first step, as described by Wilkinson (1963). (2.2.14a) is an N x N matrix eigenvalue problem:

$$(\underline{\underline{H}}^{(N)} - E\,\underline{\underline{I}})\,\underline{\psi}^{(N)+}(E) = \underline{0} \quad ; \; \{\underline{\psi}^{(N)+}(E)\}_n = \psi_n^{(N)+}(E) \qquad (2.2.14b)$$

The truncation implies the additional boundary condition (2.2.15)

$$(H_{N-1,N-1} - E)\,\psi_{N-1}^{(N)+}(E) + H_{N-1,N-2}\,\psi_{N-2}^{(N)+}(E) = 0 \qquad (2.2.16)$$

The $\psi_n^{(N)+}(E)$ may therefore still be written in terms of the $p_n(E)$ provided (2.2.16) holds:

$$p_N(E) = 0 \tag{2.2.16}$$

Thus the N eigenvalues of the $\underline{\underline{H}}^{(N)}$ are the zeros of the orthogonal polynomial of degree N generated by (2.2.16). For Hamiltonians that do not support bound states, these energies are the abscissae of an N point Gaussian quadrature with weight function $\varrho(E)$ and Gaussian weights $w_j^{(N)}$, $j=1,\ldots,N$. The pseudostates $\psi_R^{(N)+}(E_j^{(N)},r)$ are orthogonal:

$$\psi_n^{(N)+}(E_j^{(N)}) = C(E_j^{(N)})\, p_n(E_j^{(N)}) \tag{2.2.17}$$

$$\int_0^\infty dr\, \psi_R^{(N)+}(E_j^{(N)},r)\, \psi_R^{(N)+*}(E_k^{(N)},r) = C(E_j^{(N)})\, C^*(E_k^{(N)}) \sum_{n=0}^{N-1} p_n(E_j^{(N)})\, p_n(E_k^{(N)})$$

$$= \delta_{jk}\, |C(E_j^{(N)})|^2 (w_j^{(N)})^{-1} \tag{2.2.18}$$

The Christoffel formula, as described by Szegö (1967) was used in (2.2.18). If the pseudostates are normalised to unity, we may write:

$$\psi_n^{(N)+}(E_j^{(N)}) = (w_j^{(N)})^{1/2}\, p_n(E_j^{(N)}) \tag{2.2.19}$$

The equivalent equation to (2.2.7) is the unity operator within the finite L-squared subspace

$$\sum_{j=1}^{N} \psi_R^{(N)+}(E_j^{(N)},r)\, \psi_R^{(N)+}(E_j^{(N)},r')$$

$$= \sum_{n=0}^{N-1} \sum_{n'=0}^{N-1} \phi_n(r)\,\phi_{n'}(r') \left\{ \sum_{j=1}^{N} w_j^{(N)}\, p_n(E_j^{(N)})\, p_{n'}(E_j^{(N)}) \right\}$$

$$= \sum_{n=0}^{N-1} \phi_n(r)\,\phi_n(r') \qquad (2.2.20)$$

((2.2.18) and (2.2.20) are modified in the non-orthogonal case: see Appendix Two).

Broad (1982) has generalised these results for Hamiltonians that support bound states in analogy with Weyl's (1910) theory on the finite interval, also described by Brändas and co-workers (1975). Following the work of Atkinson (1964), he introduces an angular parameter β into the truncation boundary condition and defines a non decreasing weight function $\alpha_\beta^{(N)}(E)$, which may be used over the energy range $(-\infty,\infty)$, in terms of partial sums of the positive Christoffel weights $w_j^{(N)}(\beta)$. Given certain conditions, these weight functions converge with increasing N to a unique β independant weight function (2.2.21), and the negative energy eigenvalues $E_j^{(N)}(\beta)$ and corresponding steps in the $\alpha_\beta^{(N)}(E)$ converge to the bound state eigenvalues ε_b, and steps in the weight function $\alpha(E)$.

$$\alpha(E) = \int^{E} dE'\, \rho(E') \qquad (2.2.21)$$

The step-like $\alpha_\beta^{(N)}(E)$ and negative energy solutions $\underline{\psi}_\beta^{(N)\dagger}(E_j^{(N)}, r)$ provide a representation of the negative energy spectral resolution. The rest of this discussion will assume this occurs for simplicity and will continue to be

based on positive energies, the β specification being suppressed.

The exact continuum solution and the pseudostate solution may be compared.

$$\Psi_R^+(E_j^{(N)}, r) = \sum_{n=0}^{\infty} \Psi_0^+(E_j^{(N)})\, p_n(E_j^{(N)})\, \phi_n(r)$$

$$\Psi_R^{(N)+}(E_j^{(N)}, r) = \sum_{n=0}^{N-1} (w_j^{(N)})^{1/2}\, p_n(E_j^{(N)})\, \phi_n(r)$$

$$\Psi_R^+(E_j^{(N)}, r) = \frac{\Psi_0^+(E_j^{(N)})}{(w_j^{(N)})^{1/2}}\, \Psi_R^{(N)+}(E_j^{(N)}, r) + \sum_{n=N+1}^{\infty} \Psi_0^+(E_j^{(N)})\, p_n(E_j^{(N)})\, \phi_n(r)$$

$$(p_N(E_j^{(N)}) = 0) \qquad (2.2.22)$$

If, as is usually the case, the $\phi_n(r)$ are only large at large r for large n, the pseudostate is equal to the continuum state multiplied by a normalisation constant within a limited range of coordinate space of interest (specifically within the space of the first N $\phi_n(r)$), demonstrating the experience of Hazi and Taylor (1970) and Bassichis et al. (1975). Thus a matrix element M_{fi} may be represented by a spectral decomposition followed by a quadrature representation.

$$M_{fi} = \langle f | O(H) | i \rangle \qquad (2.2.23a)$$

$$= \langle f | \int d\epsilon\, | \Psi_R^+(\epsilon) \rangle\, O(\epsilon)\, \langle \Psi_R^+(\epsilon) |\, | i \rangle \qquad (2.2.23b)$$

$$\approx \langle f | \sum_{j=1}^{N} w_j^{(N)}\, | \Psi_R^+(E_j^{(N)}) \rangle \frac{O(E_j^{(N)})}{\rho(E_j^{(N)})} \langle \Psi_R^+(E_j^{(N)}) |\, | i \rangle \qquad (2.2.23c)$$

(2.2.23c) is exact for $\langle f|\Psi_R^+(E)\rangle O(E)\langle\Psi_R^+(E)|i\rangle/\rho(E)$ is a polynomial in E of degree 2N-1 or less.

$$M_{fi} \approx \langle f|\sum_{n=0}^{N-1}\sum_{m=0}^{N-1}|\phi_n\rangle\sum_{j=1}^{N}\Psi_n^{(N)+}(E_j^{(N)})\Psi_m^{(N)+*}(E_j^{(N)})\,O(E_j^{(N)})\langle\phi_n|i\rangle$$

(2.2.23d)

(2.2.23c) and (2.2.23d) are exactly equal if 1f> and 1i> are expressible entirely in the finite L^2 basis. The equivalent quadrature weights $w_j^{(N)}$ (eq) are given by (2.2.24).

$$W_j^{(N)}(eq) = \frac{W_j^{(N)}}{\rho(E_j^{(N)})}$$

$$\Psi_R^{(N)+}(E_j^{(N)},r)\,\Psi_R^{(N)+*}(E_j^{(N)},r') \approx W_j^{(N)}(eq)\,\Psi_R^{+}(E_j^{(N)},r)\,\Psi_R^{+*}(E_j^{(N)},r')$$

(2.2.24)

(2.2.23), (2.2.24) hold for the tridiagonal Slater/Laguerre basis.

An immediate application of these results is the photoionisation cross section of atomic hydrogen, for a dipole ($\underline{\mu}$) transition between a ground state Ψ_{gr} and a continuum state. (The $\Psi_R^+(E_j^{(N)})$ here are solutions of the Coulomb Hamiltonian)

$$\sigma_{ph} \propto |\langle\Psi_R^+(E_j^{(N)})|\underline{\mu}|\Psi_{gr}\rangle|^2$$

$$\approx \frac{|\langle\Psi_R^{(N)+}(E_j^{(N)})|\underline{\mu}|\Psi_{gr}\rangle|^2}{w_j^{(N)}(eq)}$$

(2.2.25)

Results can be very accurate as $\mu|\psi_{jr}\rangle$ spans a finite range of electron configuration space. Yamani and Reinhardt (1975) produced cross sections correct to 6 significant figures using a 15 state basis.

Thus, for smooth operators O(H) the finite L-squared approximation yields a Gauss quadrature approximation to M_{fi} for $|f\rangle$, $|i\rangle$ contained within the basis, and an approximation to the quadrature for more general functions $|f\rangle$, $|i\rangle$. For scattering purposes, a representation of the Green's function is required. Unfortunately the Green's operator O(z,H) is not smooth. The pseudostate/quadrature representation yields (2.2.26).

$$\langle f|(z-H)^{-1}|i\rangle \approx \langle f|(z-H^{(N)})^{-1}|i\rangle$$

$$= \sum_{j=1}^{N} \frac{\langle f|\psi_\alpha^{(N)+}(E_j^{(N)})\rangle\langle\psi_\alpha^{(N)+}(E_j^{(N)})|i\rangle}{(z-E_j^{(N)})}$$

(2.2.26)

The bound state poles and positive branch cuts have been replaced by a set of N poles, which give unphysical pseudoresonances in, for example, T matrix elements at positive energies z close to the $E_j^{(N)}$. There are various ways of removing the positive energy poles and putting back the continuous structure, and discussion will be deferred until consideration of the soluble exact case has been concluded. It is assumed that if the energy region of

interest contains bound states, the basis is large enough to represent these to the desired accuracy.

2.2C A Second Solution and The Exact Green's function

Since the ϕ_n are regular at the origin, the irregular solution ψ_I^+ to (2.2.1) is not expandable in the basis. Instead, a regular solution of the inhomogeneous equation (2.2.27) is formed.

$$(H-E)\,\bar{\psi}_R^+(E,r) = \gamma\,\bar{\phi}_0(r)$$

$$\langle \bar{\phi}_n \mid \phi_{n'} \rangle = \delta_{nn'} \qquad (2.2.27)$$

For an orthogonal basis $\bar{\phi}_n = \phi_n$. γ is determined by requiring $\bar{\psi}_R^+$ to asymptotically tend to ψ_I^+, using the Green's function (2.2.28).

$$G(E,r,r') = \frac{2\,\psi_R^+(E,r_<)\,\psi_I^+(E,r_>)}{W(\psi_R^+,\psi_I^+)} \qquad (2.2.28)$$

$W(\psi_R^+,\psi_I^+)$ is the Wronskian of the regular and irregular solutions. $r_<^>$ is the $\begin{matrix}\text{(lesser)}\\ \text{(greater)}\end{matrix}$ of r and r'.

$$\bar{\psi}_R(E,r) = -\frac{2\gamma}{W}\left\{\psi_I^+(E,r)\int_0^r dr'\,\psi_R^+(E,r')\,\bar{\phi}_0(r') + \psi_R^+(E,r)\int_r^\infty dr'\,\psi_I^+(E,r')\,\bar{\phi}_0(r')\right\}$$

$$\gamma = -\frac{W}{2\,\psi_0^+(E)} \qquad (2.2.29)$$

In terms of the infinite L-squared basis:

$$\bar{\Psi}_R^+(E,r) = \sum_{n=0}^{\infty} \bar{\Psi}_n^+(E)\,\phi_n(r)$$

(2.2.30)

The $\bar{\Psi}_n^+$ obey the same recursion relation as the Ψ_n^+, with a different boundary condition:

$$H_{m,m+1}\,\bar{\Psi}_{m+1}^+(E) + (H_{mm} - E)\,\bar{\Psi}_m^+(E) + H_{m,m-1}\,\bar{\Psi}_{m-1}^+(E) = 0 \qquad ; m \geq 1$$

(2.2.31a)

$$H_{01}\,\bar{\Psi}_1^+(E) + (H_{00} - E)\,\bar{\Psi}_0^+(E) = \gamma$$

(2.2.31b)

Broad (1978,1982,1983) wrote the m dependent parts $q_m(E)$ of the $\bar{\Psi}_m^+(E)$ in the form (2.2.32)

$$q_m(E) = P \oint dE'\, \frac{\rho(E')\,p_m(E')}{(E'-E)}$$

(2.2.32)

P stands for a principal value integral over the positive energies E'.

He then used the fact that $(p_n(E') - p_n(E))/(E'-E)$ is a polynomial in E' of degree less than n to write $q_n(E)$ in terms of a quadrature:

$$q_n(E) = \oint dE'\, \rho(E')\,\frac{(p_n(E') - p_n(E))}{(E'-E)} + p_n(E)\,P \oint dE'\,\frac{\rho(E')}{(E'-E)}$$

$$= p_n(E)\left(P \oint dE'\,\frac{\rho(E')}{(E'-E)} - \sum_{j=1}^{n} \frac{w_j^{(n)}}{(\epsilon_j^{(n)} - E)} \right)$$

$$= p_n(E)\left(q_0(E) - q_0^{(n)}(E) \right)$$

(2.2.33)

The fact that $p_n(E_j^{(n)}) = 0$ has been used.

The Green's function may be written in terms of the infinite series of L-squared functions:

$$G^+(E,r,r') = \lim_{\varepsilon \to 0^+} \oint dE' \frac{\Psi_n^+(E',r)\,\Psi_n^{+*}(E',r')}{(E + i\varepsilon - E')}$$

$$= \sum_{n=0}^{\infty} \sum_{n'=0}^{\infty} \phi_n(r)\,\phi_{n'}(r') \oint dE' \frac{\Psi_n^+(E')\,\Psi_{n'}^{+*}(E')}{(E + i\varepsilon - E')}$$

$$= \sum_{n=0}^{\infty} \sum_{n'=0}^{\infty} \phi_n(r)\,\phi_{n'}(r')\,G^+(n,n',E) \qquad (2.2.34)$$

The Green's function $G^+(n,n',E)$ may be written in terms of its spectral decomposition as in (2.2.34) or in terms of the Ψ_n^+ and $\bar{\Psi}_n^+$ using a greater than, less than prescription, as described by Heller (1975) and Broad (1978,1982,1983).

$$G^+(n,n',E) = \frac{2}{W}\,\Psi_{n<}^+(E)\left(\bar{\Psi}_{n>}^+(E) + i\,\Psi_{n>}^+(E)\right) \qquad (2.2.35)$$

This form avoids the problems of singularities inherent in a quadrature representation of (2.2.34) and has been used by Heller (1975) to calculate atomic (hydrogen) polarizabilities, for example, the ground state polarizability (2.2.36):

$$\alpha_+ = \langle \phi_{1s} \mid z\,G^+(n,n',E)\,z \mid \phi_{1s} \rangle$$

$$z = r\cos\theta \qquad (2.2.36)$$

The spectral decomposition form of the Green's function does not require knowledge of the Wronskian W and has been given an exact quadrature representation by Broad (1982, 1983)

$$G^+(n,n',E) = \oint dE' \frac{\rho(E')\,p_n(E')\,p_{n'}(E')}{(E + i\varepsilon - E')} \qquad (2.2.37)$$

(2.2.37) is modified by multiplication by a function of E in the non-orthogonal case: see Appendix Two.

The principal part of the integral can be written in terms of a quadrature of degree N where N > n,n'. For continuum energies E, the singularity may be subtracted off leaving a correction term proportional to $\bar{\varphi}_N'(E)$:

$$\mathrm{Re}\ G^{+}(n,n',E) = \int dE'\,\rho(E')\,\frac{(p_n(E')p_{n'}(E') - p_n(E)p_{n'}(E))}{(E-E')} + P\int dE'\,\rho(E')\,p_n(E)\,p_{n'}(E)\,\frac{}{(E-E')}$$

$$= \sum_{j=1}^{N} w_j^{(N)}\,\frac{p_n(E_j^{(N)})\,p_{n'}(E_j^{(N)})}{(E-E_j^{(N)})} + p_n(E)\,p_{n'}(E)\left\{P\int dE'\,\frac{\rho(E')}{(E-E')} - \sum_{j=1}^{N}\frac{w_j^{(N)}}{(E-E_j^{(N)})}\right\}$$

$$= G^{+(N)}(n,n',E) - \frac{p_n(E)\,p_{n'}(E)}{p_N(E)}\left(q_0(E) - q_0^{(N)}(E)\right)$$

$$= G^{+(N)}(n,n',E) - \frac{p_n(E)\,p_{n'}(E)}{p_N(E)}\,q_n(E)$$

The positive energy pseudoresonances in $G^{+(N)}(n,n',E)$ near $E = E_j^{(N)}$ are removed by the subtraction term. At points far away from the $E_j^{(N)}$, the subtraction term is much less important as $q_0(E)$ and $q_0^{(N)}(E)$ become closer. This is the basis of one of the methods of removing false singularities discussed in section 2.3.

The exact Green's function in this form is obviously

most useful in practical calculations in which, by suitable choice of the L-squared basis scaling parameters, only a few terms in the n,n' expansion need be retained, the rest being orthogonal to the states 1f>, 1i> in the matrix elements: Heller's calculations of ground state hydrogen polarizabilities only needed a few terms retained; when he added a polarisation potential a larger number was needed.

In (2.2.38) the number N must be greater than both n and n' for $G^+(n,n',E)$ to be exact. A truncated series for the Green's function may be identified with the finite basis Green's function if the number of terms N retained is used for the quadrature in all the $G^+(n,n'E)$; $0<n,n'<N-1$.

$$\mathrm{Re}\,\langle f|G^+(r,r',E)|i\rangle = P\oint dE' \frac{\langle f|\psi_\kappa^+(\epsilon')\rangle\langle\psi_\kappa^+(\epsilon')|i\rangle}{(E-E')}$$

$$= \oint dE' \langle f| \frac{\{|\psi_\kappa^+(\epsilon')\rangle\langle\psi_\kappa^+(\epsilon')| - \frac{\rho(E')}{\rho(E)}|\psi_\kappa^+(E)\rangle\langle\psi_\kappa^+(E)|\}}{(E-E')} |i\rangle$$

$$+ \frac{\langle f|\psi_\kappa^+(\epsilon)\rangle\langle\psi_\kappa^+(\epsilon)|i\rangle}{\rho(E)} P\oint dE' \frac{\rho(E')}{(\epsilon-E')} \quad ; E>0$$

$$\simeq \sum_{j=1}^{N} \frac{\langle f|\psi_\kappa^{(N)+}(E_j^{(N)})\rangle\langle\psi_\kappa^{(N)+}(E_j^{(N)})|i\rangle}{(E-E_j^{(N)})} - \frac{\langle f|\psi_\kappa^+(E)\rangle\langle\psi_\kappa^+(E)|i\rangle}{\rho(E)} \frac{q_N(E)}{p_N(E)}$$

(2.2.39)

The quadrature is exact for 1f>, 1i> contained within the finite basis. Other subtractions for E>0 are possible, and can be useful in the more general case when the exact

solutions are not known and the finite basis eigenfunctions are found numerically. Two examples are presented.

$$Re\langle f|(E-H)^{-1}|i\rangle = \oint dE' \frac{\langle f|\{|\Psi_R^+(E')\rangle\langle\Psi_R^+(E')| - |\Psi_R^+(E)\rangle\langle\Psi_R^+(E)|\}|i\rangle}{(E-E')}$$

$$+ P\oint dE' \frac{\langle f|\Psi_R^+(E)\rangle\langle\Psi_R^+(E)|i\rangle}{(E-E')}$$

$$\approx \sum_{j=1}^{N} \frac{\langle f|\Psi_R^{(N)+}(E_j^{(N)})\rangle\langle\Psi_R^{(N)+}(E_j^{(N)})|i\rangle}{(E-E_j^{(N)})}$$

$$+ \langle f|\Psi_R^+(E)\rangle\langle\Psi_R^+(E)|i\rangle\left\{P\oint\frac{dE'}{(E-E')} - \sum_{j=1}^{N}\frac{w_j^{(N)}(eq)}{(E-E_j^{(N)})}\right\} \qquad (2.2.40)$$

The principal value integral will require a cutoff. This method has been used by Winick and Reinhardt (1978). A subtraction used by Bransden and Stelbovics (1984) and Bransden and Plummer (1986 and chapter three) leaves an analytic form for the principal value integral.

$$Re\langle f|(E-H)^{-1}|i\rangle \approx \sum_{j=1}^{N} \frac{\langle f|\Psi_R^{(N)+}(E_j^{(N)})\rangle\langle\Psi_R^{(N)+}(E_j^{(N)})|i\rangle - w_j^{(N)}(eq)\left(\frac{E}{E_j^{(N)}}\right)^4\langle f|\Psi_R^+(E)\rangle\langle\Psi_R^+(E)|i\rangle}{(E - E_j^{(N)})}$$

$$+ \langle f|\Psi_R^+(E)\rangle\langle\Psi_R^+(E)|i\rangle P\oint\frac{dx'}{(x^2-x'^2)}$$

$$(x = \sqrt{E}) \qquad (2.2.41)$$

In the cases where the exact solution is not known, it is assumed that the basis is large enough to represent the $|f\rangle$, $|i\rangle$ states, and quantities involving $\Psi_R^+(E, r)$ are calculated by interpolation from the pseudostates $\Psi_R^{(N)+}(E_j^{(N)}, r)$. This requires information about the

(unknown) equivalent weights: methods of finding these weights, of "refining" initial discretisations in complex calculations, and of making use of the unsubtracted Green's function in energy regions where it is valid are considered in the rest of this chapter.

2.3 Exact Solution Not Known I

The direct relationships between the pseudostate and exact solutions in section 2.2, together with the numerical findings of Hazi and Taylor (1970) and Bassichis et al. (1975), are used to justify the application of equivalent quadrature ideas in the general case as described in section 2.1B. Without knowledge of the equivalent weights, however, the discretised spectral resolution of the Hamiltonian is restricted to the approximate evaluation of matrix elements of the form (2.3.1), where 1i> and 1f> are well represented in the finite basis and O(E) is a smooth function of energy.

$$M_{fi} = \langle f | \oint dE \, | \Psi_\alpha^+(E) \rangle \, O(E) \, \langle \Psi_\alpha^+(E) | i \rangle \qquad (2.3.1a)$$

$$M_{fi} \approx \langle f | \sum_{j=1}^{N} \Psi_\alpha^{(N)+}(E_j^{(N)}) \rangle \, O(E_j^{(N)}) \, \langle \Psi_\alpha^{(N)+}(E_j^{(N)}) | i \rangle \qquad (2.3.1b)$$

The accuracy of (2.3.1b) can be tested by checking convergence with increased basis size N, and with varied input parameters in the L-squared functions. In this

section a method of finding the equivalent weights numerically which is used in the next chapter is described, together with extrapolation methods designed to extract useful information from the unsubtracted finite basis L-squared Green's function. In particular, the T-matrix averaging technique of Burke, Berrington and Sukumar (1981) is described : attempts to find systematic alternatives which remove false structure in the formulation of the scattering problem rather than after the on-shell T-matrix elements have been constructed form the bulk of the work of this thesis. In section 2.4, other L-squared techniques are briefly reviewed. The method of moments allows physical data to be extracted from L-squared discretisations of complex many electron Hamiltonians which are not smooth enough for reliable equivalent weights to be found directly, and the J-Matrix method is an extension of the work of section 2.2 allowing additional model potentials to be added to the soluble Hamiltonians. These soluble problems can be extended to multichannel scattering, with separate discretisations in each channel.

Another use of L-squared discretisations not discussed here is the rotated coordinate method (McCurdy and Rescigno 1980), whereby a coordinate rotation into the complex plane shifts the positive pseudostate poles from the real axis, allowing use of the unsubtracted approximate Green's function at real energies. This has been applied to the calculation of bound free (photoabsorbtion) transition

amplitudes by, for example, Johnson and Reinhardt (1983).

2.3A Heller Derivative Method

In his thesis, Heller (1973) suggested that the equivalent weights $w_j^{(N)}(eq) = w_j^{(N)}/\rho(E_j^{(N)})$ for an L-squared discretisation could be directly calculated by considering a function $f^{(N)}(\xi)$ which smoothly interpolates the ordered (increasing) abscissae $E_j^{(N)}$ (or $x_j^{(N)}$ if a coordinate transformation has been made) in the sense (2.3.2).

$$f^{(N)}(\xi)\Big|_{\xi=j} = E_j^{(N)} \qquad (2.3.2)$$

In terms of the $f^{(N)}(\xi)$, Heller's conjecture is:

$$w_j^{(N)}(eq) = \frac{df^{(N)}(\xi)}{d\xi}\Big|_{\xi=j} \qquad (2.3.3)$$

A first orientation to understanding this is gained if we suppose the abscissae $E_j^{(N)}$ are the mesh points of a trapezoidal rule, in which case the corresponding equivalent weights are, apart from the first and last, given by (2.3.4)

$$w_j^{(N)}(eq) = E_{j+1}^{(N)} - E_j^{(N)} = \frac{\Delta E^{(N)}(j+1,j)}{\Delta j} \qquad (2.3.4)$$

The conjecture (2.3.3) may be demonstrated explicitly for the Chebyschev polynomials resulting from the s wave radial kinetic energy diagonalisation (see for example Appendix Two), as they exhibit a simple closed relationship interpolating the abscissae as functions of their number. Yamani and Reinhardt (1975) have demonstrated the validity

of the conjecture numerically for several known weight functions. Broad (1978, 1982) has shown that the rule holds asymptotically at large N for all the classical orthogonal polynomials, and by a reasoned argument proposed a particular functional form for the $\{^{(N)}$ in terms of the functions $p_\lambda(E)$ and $q_\lambda(E)$, Heller's original conjecture not uniquely defining the interpolating function. For cases where the exact solutions are not known, provided the numerically obtained abscissae vary reasonably smoothly, numerical differentiation may be used to find the equivalent weights, which provide the normalisation factors relating the L-squared pseudostates to the unknown continuum solutions over the coordinate space range covered by the L-squared basis. The subtraction terms in the expressions (2.2.40, 2.2.41) for the L-squared Green's function may then be calculated by interpolation. This method is used extensively in the next chapter. Another numerical method for calculating equivalent weights, Stieltjes imaging, is discussed in section 2.4A in the context of the method of moments.

2.3B Extrapolation Methods and T Matrix Averaging

An alternative to making use of exact or inexact knowledge of the quadrature weights to remove unphysical poles in the Green's function is to make use of the fact that at energies away from these poles the unsubtracted

L-squared sum should be a reasonable approximation. Methods making use of this fact were developed by Schlessinger and Schwartz (1966, 1968), and McDonald and Nuttall (1969) and Doolen et al. (1971), for elastic scattering.

$$T_k(E) = \lim_{\varepsilon \to 0^+} \langle k | T(E + i\varepsilon) | k \rangle \qquad (2.3.5a)$$

$$T(E) = \lim_{z \to E} T(z) \; ; \; T(z) = V + V G(z) V \qquad (2.3.5b)$$

$$Re\, G(z) = P \oint dE' \frac{|\Psi_n^+(E')\rangle\langle\Psi_k^+(E')|}{(z - E')} \simeq \sum_{j=1}^{N} \frac{|\Psi_n^{(N)+}(E_j^{(N)})\rangle\langle\Psi_n^{(N)+}(E_j^{(N)})|}{(z - E_j^{(N)})} \qquad (2.3.5c)$$

Here $T_k(E+i\varepsilon)$ is the off shell T matrix element for elastic scattering at energy E. V is the full potential for the scattering system including exchange where relevant. The on shell element is the limit as $E \to \frac{1}{2}k^2$. $|k\rangle$ is the unperturbed state with scattering particle incident energy $\frac{1}{2}k^2$. $|\Psi_n^+(E')\rangle$ are the regular solutions for the whole scattering system, fully discretised to give the approximate pseudostate Green's function, with false poles at continuum energies $E_j^{(N)}$, by the use of versions of the Kohn variational principle. For s wave elastic electron hydrogen scattering (the "Poet" problem), Schlessinger (1968) calculated elements (2.3.5a) below the elastic scattering threshold where there were no false poles and used a square root uniformisation and numerical rational fraction analytic continuation to the appropriate on shell E + iε limit. Schlessinger was unable to calculate amplitudes

above the ionisation threshold because of numerical instabilities in the rational fraction continuation, although more sophisticated techniques have since been proposed by Reinhardt (1973). The McDonald/Nuttall/Doolen method, applied to the equivalent problem in elastic positron hydrogen scattering was to take values of $T_k(z)$ at complex energies z close to the desired scattering energies but far enough away from the spurious poles of the approximate Green's function. Extrapolation to the real axis was then achieved by fitting to a polynomial. S wave elastic scattering amplitudes were successfully calculated by Doolen et al. (1971) but further work by Winick (1976) showed that for higher partial waves the errors introduced by the extrapolation rapidly became larger than the T matrix amplitudes. In each of these cases, separate extrapolations have to be made for each on shell incident energy $\frac{1}{2}k^2$.

Burke, Berrington and Sukumar (1981) introduced an averaging technique for the on shell T matrix element. They performed elastic scattering calculations on a two channel model, both exactly and by representing the effect of the second channel on the first by an optical potential (to be discussed in chapter three) involving an unsubtracted L-squared discretised second channel Green's function. The method used for solution was the R matrix expansion method described for example by Burke and Robb (1975), which allowed scattering solutions at complex energies. The real and imaginary parts of the on shell T matrix elements were

fitted to polynomials at various positive values of $Im(\frac{1}{2}k^2)$, and these "average" curves were extrapolated back to the real axis. The pseudoresonances introduced by the false poles in the Green's function became noticeably smaller and tended to vanish as $Im(\frac{1}{2}k^2)$ was increased, as expected and the fitting process could be unambiguously applied. This averaging technique gave very close results to the exact case, and Burke, Berrington and Sukumar showed that in the limit of the number of L squared functions becoming infinite the complex energy averaging process led directly to the correct real axis on shell T matrix elements. They also found that averaging T matrix values calculated on the real $\frac{1}{2}k^2$ axis gave reliable estimates of the correct values, despite the much greater pseudo-resonant structure and ambiguity in where to fit the polynomials. They then suggested that this real axis averaging could be extended to problems where calculating complex energy on shell T matrix elements is difficult, and presented some calculations for electron scattering from CIII in which channels of interest had been retained and the rest of the continuum had been diagonalised on an L-squared basis. This real axis averaging process provides a blanket method of removing unphysical structure from an on shell T matrix calculation, whatever the cause of the unphysical structure provided where it occurs is known, with only one real and imaginary T matrix fitting for all of the incident energy range. It is somewhat arbitrary in that, if the pseudothresholds

reasonably span the energy range of interest, it assumes that very short energy ranges of the unaveraged T matrix element between pseudostate thresholds, or at either end of a group of them, are accurate enough to fit the averaging polynomial. Burke's, Berrington's and Sukamar's theoretical justification in the limit of infinite L-squared functions also strictly applies to averaging above the real axis. However, their final results were smooth and accurate, and in further applications by Callaway and Oza (1983) it gave smooth and reasonably accurate results. Callaway and Oza solved the s-wave electron hydrogen scattering "Poet" problem, diagonalising the target electron spectrum on a finite basis, and treating the resulting pseudostates as scattering channels. This gave rise in the spin zero case to unphysical pseudoresonances in the on shell T matrix elements at the pseudostate threshold energies. T matrix fitting to polynomials was performed away from these energies. The accuracy of their averaged results depended somewhat on a judicious choice of pseudostates, but overall they achieved accuracy of 3% for elastic scattering and 8% for inelastic (1s-2s) scattering compared to Poet's (1978) exact results, although the wrong choice of basis and averaging polynomials can give worse results. In chapter three, the Heller derivative method is shown to be an efficient and systematic method of removing pseudoresonances in Burke's, Berrington's and Sukumar's two channel model, and extension of the method to more channels is considered.

In chapter five, systematic methods of removing pseudoresonances in the formulation of the pseudostate Poet problem are considered: although subtractions smooth the individual channel Green's functions, the use of pseudostates as scattering channels gives rise to threshold structure which is not so easily removed.

2.4 Exact Solution Not Known II

2.4A The Method of Moments

The method of moments makes use of the fact that L-squared approximations (2.3.1b) to matrix elements of the kind (2.3.1a) may be calculated to a required convergence and then uses these reliable elements to form a new smoother quadrature to which the Heller principle or Stieltjes imaging (discussed below) may be applied to extract new equivalent weights. The method has been successfully applied to the calculation of photoionisation cross sections and photoabsorption dispersion profiles for various atoms and molecules, for example He , $Ne^{\diamond}$, H_2, $Ar_2^{\diamond}$, writing the full electronic wavefunctions in L-squared bases, as reviewed by Reinhardt (1979). All these calculations depend on knowing the oscillator strength distribution (2.4.1).

$$d f(E) = \sum_i f_i \, \delta(E - E_i) + g(E)\, dE$$

$$f_i = 2E_i \, | \langle \phi_{gr} | \underline{\mu} | \psi_i \rangle |^2$$

$$g(E) = 2E \left| \langle \vec{\phi}_{gr} | \underline{\mu} | \Psi_R^+(E) \rangle \right|^2 \qquad (2.4.1)$$

$|\vec{\phi}_{gr}\rangle$ is the ground state and $\underline{\mu}$ is the dipole operator. As $\underline{\mu}|\vec{\phi}_{gr}\rangle$ spans a finite range of configuration space, it can be well represented by an adequate L-squared basis. Moments (2.4.2) of the distribution (2.4.1) are calculated using the finite L-squared distribution (2.4.3).

$$S(-k) = \int d\bar{f}(E)\, E^{-k} \quad ; \; k = 0, 1, 2, \ldots \qquad (2.4.2)$$

$$d\bar{f}(E) = \sum_{j=1}^{N} \bar{f}_j^{(N)} \delta(E - E_j^{(N)})$$

$$\bar{f}_j^{(N)} = 2E_j^{(N)} \left| \langle \bar{\phi}_{gr} | \underline{\mu} | \Psi_j^{(N)+}(E_j^{(N)}) \rangle \right|^2 \qquad (2.4.3)$$

($|\bar{\phi}_{gr}\rangle$ is the approximation to the ground state used.)

Negative moments are taken as only two positive moments exist, although Johnson et al. (1977) proposed a method involving positive moments which may in certain cases be less cumbersome than the present method. The stability of the low order moments can be checked with respect to varying L-squared basis parameters and against various dipole sum rules that can be stated in terms of the moments. For example, $S(-2) = \alpha(0)$, the static dipole polarizability, and $S(0)$ is equal to the number of electrons in the absorbing system. $2n$ moments are extracted, where usually $2n \ll N$, the size of the L-squared basis: if $2n \to N$ the original discretisation is recovered. These are then used to find

the weights $w_j^{(n)}$ and abscissae $E_j^{(n)}$ of a basis independent n point Gauss quadrature exact for polynomials of degree less than (2n-1) in $1/E$, with positive definite weight function $\rho(E) = df(E)/dE$. Langhoff and co-workers (1973, 1974, 1976, 1977) have extensively developed the technique of Stieltjes imaging to extract accurate oscillator strength distributions from the integral (2.4.4)

$$\int d f(E) = \sum_{j=1}^{n} w_j^{(n)} \qquad (2.4.4)$$

Stieltjes imaging uses the boundary property (2.4.5) to interpolate the weight function (2.4.6) from the histogram representation (2.4.4) of S(0).

$$\sum_{j=1}^{n_0} w_j^{(n)} \leq \int^{E} d f(E) \leq \sum_{j=1}^{n_0+1} w_j^{(n)} \quad ; \; E_{n_0}^{(n)} \leq E \leq E_{n_0+1}^{(n)} \qquad (2.4.5)$$

$$\left.\frac{d f(E)}{dE}\right|_{E_{n_0}^{(n)}} \simeq \frac{1}{2} \frac{(w_{n_0+1}^{(n)} + w_{n_0}^{(n)})}{(E_{n_0+1}^{(n)} - E_{n_0}^{(n)})} \qquad (2.4.6)$$

The Stieltjes technique has been refined with the use of continuous (Chebyschev) distributions by Langhoff, Sims et al. (1976) and Langhoff and Corcoran (1976).

Where only small numbers of moments are available, fine resonant structure cannot be built in, as the moment process is a smoothing operation. However resonance widths can be calculated directly using a moment technique, as pointed out by Hazi (1978).

$$\Gamma(E_{RES}) = 2\pi \left| \langle \Psi^{+}_{RES} | H - E | \Psi^{+}_{c} \rangle \right|^{2}_{E = E_{RES}}$$

(2.4.7)

$|\Psi^{+}_{RES}\rangle$ is the L-squared resonant wavefunction and $|\Psi^{+}_{c}\rangle$ is the full scattering solution for the background continuum. Hazi used the fact that good approximations to $|\Psi^{+}_{RES}\rangle$ and E_{RES} may be obtained from stabilisation calculations as described by Hazi and Taylor (1970). Diagonalisation of the projected Hamiltonian with projection operator (2.4.8) yields a set of pseudostates with a width strength distribution (2.4.9).

$$P = I - |\Psi^{+}_{RES}\rangle\langle\Psi^{+}_{RES}|$$

(2.4.8)

$$\Gamma_{n}(E^{(N)}_{n}) = 2\pi \left| \langle \Psi^{+}_{RES} | H - E | \Psi^{(N)+}_{n} \rangle \right|^{2}_{E = E^{(N)}_{n}}$$

(2.4.9)

Moments of this distribution may be taken, and basis independent quadrature weights and abscissae found, the Stieltjes or Heller method then being used to extract the distribution $\Gamma(E)$.

Moment Technique Applied to Scattering

Winick and Reinhardt (1978) have calculated elastic scattering amplitudes for positron hydrogen atom scattering using the moment technique. Rather than use the L-squared unsubtracted Green's function in the expression for the off shell T matrix element (2.3.5), they use the moment technique to extract the positive definite weight function

(2.4.10).

$$T_k(z) = \langle k | V + V G(z) V | k \rangle$$

$$\langle k | V G(z) V | k \rangle = \oint dE \frac{\rho_k(E)}{(z-E)}$$

$$\rho_k(E) = |\langle k | V | \Psi_k^+(E) \rangle|^2$$

(2.4.10)

Aproximate moments of $\rho_k(E)$ were formed using the L-squared basis:

$$\bar{S}(-k) = \sum_{j=1}^{N} \bar{\rho}_k(E_j^{(N)}) (E_j^{(N)})^{-k}$$

$$\bar{\rho}_k(E_j^{(N)}) = |\langle k | V | \Psi_k^{(N)+}(E_j^{(N)}) \rangle|^2$$

(2.4.11)

2n converged moments were used to generate a Gauss quadrature with weights $w_j^{(n)}$ and abscissae $E_j^{(n)}$. In the case of scattering it was found that the cumulative distribution $\sum_{j=1}^{n} w_j^{(n)}$ varied by several orders of magnitude over a small range of energy, and the Stieltjes technique was not reliable. The Heller method was successfully used to extract $\rho(E_j^{(n)})$ (the abscissae are by definition evenly spaced in the interpolation variable j and were found to be reasonably smooth). The new basis independent quadrature was used to represent the Green's function, knowledge of the equivalent weights allowing singularities to be subtracted off, by interpolation of the $\rho(E_j^{(n)})$

$$Re\ T_k(E+i\varepsilon) = \langle k | V | k \rangle + \sum_{j=1}^{n} \frac{w_j^{(n)}}{(E-E_j^{(n)})} + \rho_k(E) \left\{ P \oint \frac{dE'}{(E-E')} - \sum_{i=1}^{n} \frac{w_i^{(n)(eq)}}{(E-E_i^{(n)})} \right\}$$

(2.4.12a)

$$\mathrm{Im}\, T_k(E+i\epsilon) = -\pi \rho_k(E)$$

(2.4.126)

The principal value integral was taken to a cutoff E_{MAX}. Calculations of s,p,d,f partial cross sections in the intermediate energy range up to 34eV were made, giving a converged elastic cross section, although the total cross section was less well converged. For each partial wave, Winick and Reinhardt made calculations with between 40 and 100 basis functions, from which ~ 16 moments were extracted. The disadvantage of the method of moments applied to scattering is that the $w_i^{(n)}$ and $E_i^{(n)}$ are dependent on the on shell energy $\frac{1}{2}k^2$, so that for every scattering calculation a new set of moments needs to be constructed and analysed, which is a time consuming procedure. For applications to inelastic scattering, the positive definiteness of the weight function $\rho(E)$ is not guaranteed.

2.4B The J-Matrix Method and Multichannel Scattering

The J-Matrix method was introduced by Heller and Yamani (1974) to extend their exact L-squared representation of the kinetic Hamiltonian to include model potentials, extended by Yamani and Fishman (1974) to cope with angular momentum and Coulomb scattering, and may be used to extend all soluble Hamiltonians. Starting from the solved Hamiltonian H_o,

successive approximations to a Hamiltonian H are obtained by solving for the model Hamiltonian H^N:

$$H = H_0 + V$$

$$H^N = H_0 + V^N$$

$$V^N = \sum_{n,n'=0}^{N-1} |\bar{\phi}_n\rangle\langle\phi_n|V|\phi_{n'}\rangle\langle\bar{\phi}_{n'}| \qquad (2.4.13)$$

The model problem can be shown to have a real solution of the general form (2.4.14):

$$\Psi_N(E,r) = \sum_{n=0}^{N-1} a_n(E)\,\phi_n(r) + \sum_{n=N}^{\infty} \Psi_n^+(E)\,\phi_n(r) + t\sum_{n=N}^{\infty} \bar{\Psi}_n^+(E)\,\phi_n(r) \qquad (2.4.14)$$

The problem becomes an (N+1)x(N+1) matrix equation for the unknowns a_n, t, which in some way uniformly approaches the exact problem as N is increased. Heller (1975) and Broad (1978) have found Green's functions and quadratures for the solution of the H^N problem. Broad (1982) has also noted that the L-squared matrix of H^N can be brought into infinite tridiagonal form (for finite N) by applying a Householder reduction, described by Wilkinson (1965), in reverse order, so that the results of section 2.2 apply. He also noted that information about the phaseshift due to the model potential may be extracted from finite basis representations of H^N using his spacing functions for Heller's derivative rule.

The infinite L-squared basis method can be extended to the treatment of multichannel close coupling problems, as considered by Heller and Yamani (1974) and Broad and

Reinhardt (1976). Formally, the wave function in the scattering coordinate is written in terms of an L-squared sum for each target channel. Heller and Yamani used the same type of L-squared basis for diagonalising the target Hamiltonian and for the scattering function expansions in an electron hydrogen scattering calculation, the finite number of channels and target pseudostates N defining the truncation limit for the channel potentials. Pseudoresonances appeared at the target pseudostate thresholds, but became smaller as N was increased. Broad and Reinhardt (1976) extended these schemes to the general LS coupled electron atom collision problem using configuration interaction numerical diagonalisations for the target pseudostates, and calculated H^- photodetachment cross sections. The Laguerre/Slater one particle Coulomb Hamiltonian equivalent quadrature was used to give an approximation to the electron photodetachment cross section. Broad (1985) has applied this quadrature to calculations of two photon ionisation of hydrogen, extrapolating finite basis calculations to the complete basis limit. All these calculations involve using either an infinite basis or an equivalent quadrature representation for each channel. The possibilities of extending equivalent quadrature ideas to cover more than one channel are considered in the next chapter.

CHAPTER THREE

OPTICAL POTENTIALS IN AN L-SQUARED APPROACH TO THE SOLUTION OF COUPLED CHANNEL SCATTERING EQUATIONS

3.1 Introduction

The use of an optical potential is a means of including the effect of ignored channels in a coupled channel scattering calculation. Following Feshbach (1958, 1962), a projection operator P is introduced to project out the channels of interest from the full wave function Ψ. P and the associated operator Q are defined such that (3.1.1.) holds:

$$P^2 = P$$

$$Q = 1 - P \quad ; \quad QP = PQ = 0 \qquad (3.1.1)$$

In practical calculations where the wave function is expanded in terms of a truncated set of target states multiplied by scattering functions and a set of L-squared pseudostates, and P projects onto the target state/scattering function expansion, these conditions may still be imposed, as described by Burke and Taylor (1966).

The Schrödinger equation (3.1.2) may be written in the form (3.1.3):

$$(H - E)(P + Q)\Psi = 0 \qquad (3.1.2)$$

$$P(H-E)P\Psi = -P(H-E)Q\Psi = -PHQ\Psi$$
$$Q(H-E)Q\Psi = -Q(H-E)P\Psi = -QHP\Psi$$

(3.1.3a)

$$P\left[H - PHQ\frac{1}{Q(H-E)Q}QHP - E\right]P\Psi = 0$$

(3.1.3b)

The problem is reduced to one in the projected space with the optical potential (3.1.4) representing the rest of the space

$$V_{opt} = -PHQ\frac{1}{Q(H-E)Q}QHP$$

$$= PHQ\,G^{+Q}\,QHP$$

(3.1.4)

G^{+Q} is the Q-space Green's function.

$$G^{+Q} = \oint dE' \frac{|\phi^Q(E')\rangle\langle\phi^Q(E')|}{(E+i\varepsilon-E')}$$

$$(QHQ-E')|\phi^Q(E')\rangle = 0$$

(3.1.5)

The $|\phi^Q(E')\rangle$ are within the Q space and are normalised to a Kronecker delta or a Dirac delta function according to whether they are bound or continuum states. To find an expression for G^{+Q}, the Q space Hamiltonian may be diagonalised in terms of a set of L-squared functions. The initial representation of the Green's function is then

$$\bar{G}^{+Q} = \sum_{j=1}^{N} \frac{|\Theta_j^{(N)}\rangle\langle\Theta_j^{(N)}|}{(E-E_j^{(N)})}$$

(3.1.6a)

$$\langle \Theta_{j'}^{(N)} | \not{\emptyset} H Q - E_j^{(N)} | \Theta_j^{(N)} \rangle = 0$$

$$\langle \Theta_{j'}^{(N)} | \Theta_j^{(N)} \rangle = \delta_{jj'} \qquad ; j,j' = 1,2,\ldots,N$$

(3.1.6b)

Following from the discussion of the previous chapter, $\bar{G}^{+\mathcal{A}}$ may be interpreted as a quadrature representation of $G^{+\mathcal{A}}$ if all the continuum Q space channels are closed. If some of the Q space continuum channels are open, spurious poles must be removed (it is assumed that any bound states within the energy region of interest are well represented by the L-squared pseudostates). The fundamental reason for employing an optical potential formalism is that a substantial part of the cross section is due to direct coupling between the channels of interest. It follows that the Green's function representing the Q subspace need be calculated to a lower degree of accuracy than would be the case if the total space were being approximated by an L-squared expansion or otherwise. Burke, Berrington and Sukumar (1981) introduced their T matrix averaging technique described in section 2.3B to deal with Q space poles. This chapter describes an alternative approach which is not based on calculation of elements away from the real axis, and attempts to use the equivalent quadrature ideas of chapter two to remove poles directly from the Q space Green's function. Section 3.2 contains a resumé of the work of Bransden and Stelbovics (1984) on Burke's, Berrington's and Sukumar's two channel model and details further

investigation by myself of equivalent quadrature techniques applied to this model. Section 3.3 considers the case where the Q space involves more than one channel, and the initial diagonalisation of its Hamiltonian does not, as noted in chapter two, lead to a straightforward smooth quadrature.

3.2 The Two Channel Model Problem

3.2A Theory, and the Work of Bransden and Stelbovics (1984)

The problem posed by Burke et al. (1981) is that of two coupled s-channels in which the first channel is treated explicitly (P-space) and the second (Q-space) channel is described by an optical potential represented on an L^2 basis. The channel functions $F_i(r)$ satisfy (3.2.1)

$$\left(\frac{d^2}{dr^2} - V_{11}(r) + k_1^2 \right) F_1(r) = V_{12}(r) F_2(r) \qquad (3.2.1a)$$

$$\left(\frac{d^2}{dr^2} - V_{22}(r) + k_2^2 \right) F_2(r) = V_{21}(r) F_1(r) \qquad (3.2.1b)$$

The notation of Burke et al. (1981) is used and the equations are written in configuration space. However in specific numerical calculations the corresponding momentum-space formalism (see for example, Bransden 1983) was employed and the coupled-channel or single-channel T-matrix equations were solved using the programme package developed by McCarthy and Stelbovics (1983).

In this package the momentum space Lippmann Schwinger equations for the t operator (described in section 1.2C) are converted into matrix equations by representing the integrals as numerical quadratures, and the on shell values of the T matrix elements are taken after solution, as detailed by McCarthy and Stelbovics (1983).

The potentials V_{ij} are of short range and $V_{12} = V_{21}$. The inelastic threshold is taken to be at $k_1^2 = \Delta$, so that

$$k_2^2 = k_1^2 - \Delta \tag{3.2.2}$$

Representing the effect of the second channel on the first through the optical potential W(r,r'), we find $F_1(r)$ satisfies

$$\left(\frac{d^2}{dr^2} - V_{11}(r) + k_1^2 \right) F_1(r) = \int_0^\infty dr' \, W(r,r') \, F_1(r') \tag{3.2.3}$$

with the boundary condition

$$F_1(r) \sim \sin k_1 r + f(k_1) e^{ik_1 r} \tag{3.2.4}$$

and both the elastic and inelastic cross sections can be obtained from the amplitude $f(k_1)$ as indicated in chapter one. The optical potential can be expressed in terms of the Green's function G^a, by

$$W(r,r') = V_{12}(r) \, G^a(k_1^2; r, r') \, V_{21}(r') \tag{3.2.5a}$$

$$G^{\oplus}(k_1^2; r, r') = \sum_n \frac{\phi_n(r)\,\phi_n(r')}{(k_2^2 + s_n^2)} + \lim_{\varepsilon \to 0^+} \int_0^\infty ds^2 \frac{\phi(s,r)\,\phi(s,r')}{(k_2^2 - s^2 + i\varepsilon)} \qquad (3.2.5b)$$

k_2^2 is expressed in terms of k_1^2 through (3.2.2). The functions $\phi_n(r)$ and $\phi(s,r)$ are bound state and continuum solutions, respectively, of the homogeneous equation, obtained from (3.2.1b) by setting the right-hand side zero:-

$$\left(\frac{d^2}{dr^2} - V_{22}(r) + s^2\right) \phi(s,r) = 0 \qquad (3.2.6)$$

with, for $s^2 > 0$,

$$\phi(s,r) \underset{r \to \infty}{\sim} (\pi s)^{-1/2} \sin(sr + \delta_2) \qquad (3.2.7)$$

The normalisation is:

$$\langle \phi(s) | \phi(s') \rangle = \delta(s^2 - s'^2)$$

$$G^{\oplus} = \frac{1}{(k_2^2 + \frac{d^2}{dr^2} - V_{22} + i\varepsilon)} \qquad (3.2.8)$$

The bound state functions ϕ_n, corresponding to eigenenergies $-s_n^2$ vanish at large values of r, exponentially. For convenience in what follows, potentials V_{22} which do not support a bound state are considered, but no problems are encountered if bound states ϕ_n exist. In the absence of bound states the Green's function $G^{\oplus}$ becomes:

$$\text{Im } G^{Q}(k_1^2; r, r') = -\pi \phi(k_2, r)\phi(k_2, r') \quad ; k_2^2 > 0$$

$$= 0 \quad ; k_2^2 < 0$$

(3.2.9a)

$$\text{Re } G^{Q}(k_1^2; r, r') = P\int_0^\infty ds^2 \frac{\phi(s, r)\phi(s, r')}{(k_2^2 - s^2)}$$

(3.2.9b)

The identity

$$P\int_0^\infty ds^2 \frac{1}{(k_2^2 - s^2)} = 0$$

(3.2.10)

is used to write Re G^{Q} as, for $k_1^2 > \Delta$, $k_2^2 > 0$

$$\text{Re } G^{Q}(k_1^2; r, r') = \int_0^\infty ds^2 \frac{\phi(s, r)\phi(s, r') - \frac{k_2}{s}\phi(k_2, r)\phi(k_2, r')}{(k_1^2 - s^2)}$$

(3.2.11)

while for $k_1^2 < \Delta$, $k_2^2 < 0$, we retain Re G^{Q} in the unsubtracted form (3.2.9b).

The numerical evalution of the exact expression (3.2.9b) for $k_1^2 < \Delta$, or (3.2.11) for $k_1^2 > \Delta$ proceeds by the introduction of mesh points s_i^2 and corresponding integration weights w_i^{eq}, so that with N points and weights the unsubtracted form (3.2.9b) becomes

$$\text{Re } G^{Q}(k_1^2; r, r') = \sum_{i=1}^{N} w_i^{eq} \frac{\phi(s_i, r)\phi(s_i, r')}{(k_2^2 - s_i^2)} \quad ; k_2^2 < 0$$

(3.2.12a)

The subtracted form (3.2.11) becomes

$$\text{Re } G^{Q}(k_1^2; r, r') = \sum_{i=1}^{N} w_i^{eq} \frac{\phi(s_i, r)\phi(s_i, r') - \frac{k_2}{s_i}\phi(k_2, r)\phi(k_2, r')}{(k_2^2 - s_i^2)}$$

(3.2.12b)

The function $\emptyset(s,r)$ is approximated over a finite region of r by linear combinations of N normalisable functions (for example Slater functions, Gaussian functions and so on) $U_i(r)$. Taking the linear combinations

$$\Theta_j(r) = \sum_{i=1}^{N} c_{ji} U_i(r) \quad ; \quad j = 1,2,\ldots,N \tag{3.2.13}$$

the coefficients c_{ji} can be found by requiring that the Hamiltonian

$$H_{22} = \frac{d^2}{dr^2} - V_{22}(r) \tag{3.2.14}$$

is diagonal on the finite basis of functions

$$\int_0^\infty dr\, \Theta_j(r)\, H_{22}\, \Theta_i(r) = -\bar{s}_i^2\, \delta_{ij} \tag{3.2.15}$$

We order the eigenvalues so that $\bar{s}_{i+1} > \bar{s}_i$, all i. The normalisation of the functions $\Theta_i(r)$ is

$$\int_0^\infty dr\, \Theta_j(r)\, \Theta_i(r) = \delta_{ji} \tag{3.2.16}$$

For a sufficiently large set of functions U_i, the function Θ_i represents the function $\emptyset(s,r)$ over a finite range of r, in the sense that

$$\emptyset(\bar{s}_i, r) \simeq N_i(\bar{s}_i)\, \Theta_i(r) \tag{3.2.17}$$

where N is a normalisation factor, (Bassichis et al. 1975, 1978; Hazi and Taylor 1970).

Since only one channel has been diagonalised in the L-squared basis, it is assumed that the equivalent

quadrature ideas can be applied directly to the problem, and that the $\bar{s}_i^2$ vary smoothly with i so that the Heller derivative method can be used to give the equivalent weights w_i^{eq}. We set

$$\bar{s}_i^2 = s_i^2$$

$$\Theta_i(r) \simeq (w_i^{eq})^{1/2} \phi(s_i, r)$$

$$N_i \simeq (w_i^{eq})^{1/2} \qquad (3.2.18)$$

The spectral resolution of Re G^Q on the finite basis of the N functions Θ_i is then

$$Re\, G^Q(k_1^2; r, r') \simeq \sum_{i=1}^{N} \frac{\Theta_i(r)\,\Theta_i(r')}{(k_2^2 - s_i^2)} \qquad (3.2.19)$$

To calculate Im G^Q from (3.2.9a) and Re G^Q from (3.2.11) the function $\phi(k_2, r)$ is required. This is calculated approximately by interpolation from the set of quantities $\phi_A = (1/\sqrt{w_i^{eq}})\Theta_i$ which are known at the points s_i. Thus (3.2.11) becomes

$$Re\, G^Q(k_1^2; r, r') \simeq \sum_{i=1}^{N} \frac{\Theta_i(r)\,\Theta_i(r') - w_i^{eq} \frac{k_2}{s_i} \phi_A(k_2, r)\,\phi_A(k_1, r')}{(k_2^2 - s_i^2)} \quad ; k_2^2 > 0 \qquad (3.2.20a)$$

and (3.2.9a) becomes

$$Im\, G^Q(k_1^2; r, r') = -\pi\, \phi_A(k_2, r)\,\phi_A(k_2, r') \quad ; k_2^2 > 0 \qquad (3.2.20b)$$

The w_i^{eq} are calculated numerically, treating i as a smooth variable:

$$w_i^{eq} = \frac{\partial s_i^2}{\partial i} = 2 s_i \frac{\partial s_i}{\partial i} \qquad (3.2.21)$$

The calcuated Green's functions are smooth and contain no poles.

Bransden and Stelbovics (1984) presented cross sections for this model calculated exactly and in the L-squared formulation. They used various non-orthogonal bases for the $U_j(r)$, and found no particular advantage attached to any of them. They presented results for a Slater basis (3.2.22), optimising the exponential parameter below the inelastic threshold where the phase shifts obey a minimum principle, as described by Bransden (1983), although the variation with this parameter was not great.

$$U_j(r) = r^j e^{-\alpha r} \qquad (3.2.22)$$

They found that the elastic (P-space) results were given to good accuracy by the L-squared method, as expected since the optical potential is only contributing to a small proportion of the cross section. The reaction cross sections for transitions from P space to Q space, the totality of which are derived from the optical potential, were of lesser but reasonable accuracy. The results converged slowly with basis size, and the Heller prescription removed pseudoresonances.

3.2B Further Investigation of The Two Channel Model

My initial task was to repeat the work of Bransden and Stelbovics (1984) using an orthogonal basis. This simplifies the numerical diagonalisation of the Hamiltonian from the form (3.2.23a) to the form (3.2.23b).

$$\underline{\underline{H}}\,\underline{c}_i = \lambda_i \underline{\underline{S}}\,\underline{c}_i \qquad (3.2.23a)$$

$$\underline{\underline{H}}\,\underline{c}_i = \lambda_i \underline{c}_i \qquad (3.2.23b)$$

$$\{\underline{\underline{H}}\}_{nn'} = \langle U_n | H_{zz} | U_{n'} \rangle$$

$$\{\underline{\underline{S}}\}_{nn'} = \langle U_n | U_{n'} \rangle$$

$\underline{c}$ is the ith eigenvector of basis function coefficients. The basis chosen was the Slater/Laguerre basis (3.2.24)

$$U_j(r) = \left(\frac{\alpha}{j(j+1)}\right)^{1/2} \alpha r\, e^{-\frac{\alpha r}{2}} L^{(2)}_{j-1}(\alpha r) \quad ; \quad j = 1, 2, \ldots, N \qquad (3.2.24a)$$

$L^{(2)}_{j-1}(x)$ is an associated Laguerre polynomial as described in Appendix Two and by Abramowitz and Stegun (1972).

$$\int_0^\infty dr\, U_j(r)\, U_{j'}(r) = \delta_{jj'} \qquad (3.2.24b)$$

This basis is a linear combination of Slater terms and should result in identical eigenvectors to those found by Bransden and Stelbovics (1984) after diagonalisation of the Hamiltonian. The numerical work involved construction of the Hamiltonian matrix in the basis (the kinetic part is done analytically : see Appendix Two) and subsequent diagonalisation to form eigenvalues and vectors, and construction of Heller weights and (analytic) momentum space matrix elements of the P-space and optical potentials to run in a version of the McCarthy and Stelbovics (1983) coupled channel programme. The weights w_i^{α} were calculated using both prescriptions in (3.2.21), the latter form proving the most stable. The potentials examined are shown in equation (3.2.25)

$$V_{11}(r) = V_{22}(r) = -1.5\,e^{-r}/r$$

$$V_{12}(r) = V_{21}(r) = -0.25\,e^{-r} \qquad (3.2.25)$$

The parameter α was optimised below the inelastic threshold at a value $\alpha = 2$ and results for the L-squared method are shown in table 3.1. As expected, they are the same as those of Bransden and Stelbovics (1984). Convergence with increased basis size was slow, as eigenvalues tended to cluster below the inelastic threshold and high above it, with very few eigenvalues in the intermediate energy range of interest; samples of eigenvalues are given in table 3.2.

A refinement to the method above the inelastic threshold was then considered. The Green's integral

TABLE 3.1

Elastic (E) and reaction (R) cross sections computed from Equations (3.2.1). The models employed are defined in the text.

K**2	Exact Results		L-Squared Method					
			N = 5		N = 10		N = 15	
	E	R*	E	R*	E	R*	E	R*
0.2	13.87	-	13.87	-	13.87	-	13.87	-
0.4	6.271	-	6.271	-	6.271	-	6.271	-
0.6	3.875	-	3.875	-	3.875	-	3.875	-
0.8	2.534	1.441	2.515	1.587	2.522	1.453	2.522	1.457
1.0	1.925	0.609	1.929	0.634	1.926	0.625	1.926	0.615
1.2	1.527	0.384	1.527	0.435	1.528	0.397	1.928	0.390
1.4	1.250	0.272	1.248	0.231	1.251	0.282	1.251	0.276
1.6	1.049	0.204	1.047	0.231	1.050	0.212	1.050	0.209
1.8	0.8969	0.160	0.8966	0.169	0.8981	0.169	0.8979	0.164
2.0	0.7787	0.129	0.7796	0.129	0.7797	0.136	0.7795	0.133
2.2	0.6844	0.107	0.6861	0.103	0.6856	0.110	0.6851	0.108
2.4	0.6079	0.091	0.6099	0.087	0.6087	0.099	0.6086	0.095
2.6	0.5448	0.077	0.5467	0.077	0.5457	0.083	0.5454	0.080
2.8	0.4919	0.066	0.4934	0.069	0.4927	0.074	0.4924	0.069
3.0	0.4471	0.058	0.4482	0.063	0.4476	0.065	0.4476	0.060
3.2	0.4086	0.051	0.4095	0.057	0.4090	0.057	0.4091	0.053
3.4	0.3754	0.045	0.3761	0.052	0.3758	0.049	0.3759	0.048
3.6	0.3464	0.041	0.3470	0.047	0.3469	0.043	0.3468	0.044
3.8	0.3210	0.037	0.3214	0.043	0.3216	0.038	0.3213	0.039
4.0	0.2985	0.033	0.2988	0.039	0.2992	0.034	0.2987	0.036

R* : Reaction cross sections are *10

Atomic units (detailed in chapter 1) are used throughout.

TABLE 3.2

Eigenvalues s_i^2 for the Green's function (3.2.19/20)

N = 5	N = 10	N = 15
0.0335	0.0113	0.0059
		0.0283
	0.0599	0.0726
	0.1631	0.1433
0.2259	0.3426	0.2470
		0.3947
0.7584	0.6428	0.6042
		0.9057
	1.1589	1.3523
2.2325	2.1187	2.0451
	4.1764	3.1942
		5.2979
10.6225	9.9615	9.7982
	41.504	22.573
		92.579

Units are as in table 3.1. Eigenvalues are given to four decimal places. The models and parameters used are given in the text.

(3.2.11, 3.2.20a) was transformed using a variable x:

$$x = \frac{(k^2 - \lambda^2)}{(k^2 + \lambda^2)} \quad ; \quad k^2 = \lambda^2 \frac{(1+x)}{(1-x)} \quad ; \quad -1 \leq x \leq 1$$

(3.2.26)

With respect to x the new eigenfunctions are:

$$\bar{\phi}(x,r) = \phi(k,r)\left(\frac{dk^2}{dx}\right)^{1/2} \quad ; \quad \int_{-1}^{1} dx\, \bar{\phi}(x,r)\,\bar{\phi}(x,r') = \delta(r-r')$$

(3.2.27a)

$$\Theta_i(r) \approx (\bar{w}_i^{eq})^{1/2}\, \bar{\phi}(x_i,r)$$

(3.2.27b)

$$x_i^2 = \frac{(s_i^2 - \lambda^2)}{(s_i^2 + \lambda^2)} \quad ; \quad \bar{w}_i^{eq} = \frac{\partial x_i}{\partial i}$$

(3.2.27c)

Formally there is no difference between the two methods, but suitable choice of the parameter λ^2 might allow for more stable numerical differentiation and interpolation. Equation (3.2.21) may then be rewritten as

$$Re\ G^{Q}(k_1^2; r, r') = \sum_{i=1}^{N} \frac{(1-x_i)\left(\Theta_i(r)\,\Theta_i(r') - \bar{w}_i^{eq}\,\frac{k_2}{\lambda}\,\frac{(1-x_i)^{1/2}}{(1+x_i)^{1/4}}\,\frac{2\lambda^2}{(1-x_i)^2}\,\phi(k_2,r)\,\phi(k_2,r')\right)}{\left(k_2^2 - \lambda^2 - x_i(k_2^2 + \lambda^2)\right)}$$

$$Im\ G^{Q}(k_1^2; r, r') = -\pi\,\phi(k_2,r)\,\phi(k_2,r') \quad ; k_2^2 > 0$$

(3.2.28)

The momentum space matrix elements of Im G^{Q} and the subtraction term are interpolated as:

$$\phi(k_2,r)\,\phi(k_1,r') \simeq \left(\frac{\theta(x(i),r)\,\theta(x(i),r')\,(1-(x(i))^2)}{2\lambda^2\,\bar{w}^{eq}(i)} \right)\Bigg|_{x(i)\to x_2}$$

$$x_2 = \frac{(k_2^2-\lambda^2)}{(k_2^2+\lambda^2)} \qquad (3.2.29)$$

Representative results are shown in table 3.3 for the case $\lambda^2 = k_2^2$. This has the advantage of placing $\phi(k_2,r)$ in the middle of the interpolation range, although a different value of λ^2 should be used to calculate cross sections at energies just above threshold where $k_1^2 \to 0$. Results are as good as before, and slightly better in the range $k_1^2 = 2.0 - 4.0$. Calculated weights $\bar{w}_i^{eq} \cdot 2k_2^2/(1-x_i^2)$ were slightly different to those calculated as w_i^{eq}, showing the limitations of the numerical differentiation, but remained constant as k_2^2 varied.

A final test was to use the values of elements of $\bar{\phi}(x_i,r)$ with a standard numerical integration programme. This method in effect tests the smoothness of the equivalent quadrature as further interpolation is required for values of $\bar{\phi}(x,r)$ at the points needed by the routine. No particular advantage arose, the number of points and interpolations required making the programme longer to run than using the direct L-squared sum. Some representative results are shown in table 3.4.

3.3 More Than One Q-Space Channel

The work of this section has been published by Bransden and Plummer (1986). There is no difficulty in

TABLE 3.3

Elastic (E) and reaction (R) cross sections computed from equations (3.2.1). The models employed are defined in the text.

K**2	Exact Results		L-Squared Method					
			N = 5		N = 10		N = 15	
	E	R*	E	R*	E	R*	E	R*
0.2	13.87	-	13.87	-	13.87	-	13.87	-
0.4	6.271	-	6.271	-	6.271	-	6.271	-
0.6	3.875	-	3.875	-	3.875	-	3.875	-
0.8	2.534	1.441	2.492	1.659	2.536	1.512	2.526	1.407
1.0	1.925	0.609	1.931	0.651	1.924	0.609	1.926	0.593
1.2	1.527	0.384	1.523	0.423	1.527	0.383	1.528	0.374
1.4	1.250	0.272	1.248	0.295	1.250	0.272	1.250	0.270
1.6	1.049	0.204	1.047	0.209	1.049	0.206	1.049	0.204
1.8	0.8969	0.160	0.8973	0.150	0.8973	0.161	0.8970	0.160
2.0	0.7787	0.129	0.7803	0.119	0.7790	0.130	0.7791	0.128
2.2	0.6844	0.107	0.6865	0.098	0.6851	0.105	0.6848	0.106
2.4	0.6079	0.091	0.6098	0.084	0.6086	0.088	0.6081	0.090
2.6	0.5448	0.077	0.5462	0.074	0.5453	0.076	0.5448	0.076
2.8	0.4919	0.066	0.4928	0.067	0.4923	0.065	0.4921	0.065
3.0	0.4471	0.058	0.4473	0.061	0.4472	0.056	0.4472	0.057
3.2	0.4086	0.051	0.4084	0.055	0.4088	0.048	0.4087	0.050
3.4	0.3754	0.045	0.3750	0.049	0.3756	0.044	0.3755	0.045
3.6	0.3464	0.041	0.3459	0.043	0.3468	0.035	0.3465	0.040
3.8	0.3210	0.037	0.3205	0.038	0.3214	0.033	0.3210	0.036
4.0	0.2985	0.033	0.2980	0.034	0.2984	0.030	0.2985	0.033

R* : Reaction cross sections are *10

Units are as in Table 3.1

TABLE 3.4

Elastic (E) and reaction (R) cross sections computed from Equations (3.2.1). The models employed are defined in the text.

K**2	Exact Results		L-Squared Method			
			N = 10		N = 15	
	E	R*	E	R*	E	R*
0.2	13.87	-	13.92	-	13.87	-
0.4	6.271	-	6.295	-	6.273	-
0.6	3.875	-	3.893	-	3.876	-
0.8	2.534	1.441	2.542	1.486	2.536	1.440
1.0	1.925	0.609	1.932	0.636	1.929	0.599
1.2	1.527	0.384	1.534	0.397	1.528	0.388
1.4	1.250	0.272	1.257	0.279	1.252	0.270
1.6	1.049	0.204	1.056	0.209	1.050	0.207
1.8	0.8969	0.160	0.9041	0.161	0.8981	0.160
2.0	0.7787	0.129	0.7861	0.128	0.7799	0.129
2.2	0.6844	0.107	0.6918	0.105	0.6852	0.109
2.4	0.6079	0.091	0.6150	0.090	0.6088	0.092
2.6	0.5448	0.077	0.5516	0.077	0.5454	0.078
2.8	0.4919	0.066	0.4981	0.067	0.4928	0.066
3.0	0.4471	0.058	0.4530	0.059	0.4480	0.057
3.2	0.4086	0.051	0.4140	0.048	0.4096	0.051
3.4	0.3754	0.045	0.3806	0.040	0.3765	0.045
3.6	0.3464	0.041	0.3516	0.036	0.3475	0.040
3.8	0.3210	0.037	0.3256	0.034	0.3221	0.038
4.0	0.2985	0.033	0.3025	0.031	0.2990	0.036

R* : Reaction cross sections are *10

Units are as in Table 3.1

extending the L-squared method to the case in which (N-1) coupled channels are treated explicitly and the N^{th} channel is taken into account by a matrix optical potential, but considerable difficulties arise if it is desired to account for more than one channel implicitly through the optical potential. We now describe these difficulties and explore an example in which two channels contribute to the optical potential acting in a third channel.

3.3A The theoretical model

The optical potential

We consider the system of coupled channel equations (3.3.20) for the case N > 2.

$$\left(\frac{d^2}{dr^2} + k_i^2\right) F_i(r) = \sum_{j=1}^{N} V_{ij}(r) F_j(r) \qquad ; \; j = 1, 2, \ldots, N \tag{3.3.1}$$

The potentials V_{ij} are again of short range with $V_{ij} = V_{ji}$. The inelastic thresholds are at $k_1^2 = \Delta_1, \Delta_2, \ldots, \Delta_{N-1}$, with $\Delta_{i+1} > \Delta_i$, so that:

$$k_i^2 = k_1^2 - \Delta_{i-1} \qquad ; \quad i > 1 \tag{3.3.2}$$

The optical potential W(r,r') which represents in channel 1 the effect of the remaining (N-1) channels can be represented as

$$W(r,r') = \sum_{i=2}^{N}\sum_{j=2}^{N} V_{1i}(r)\, G^{Q}_{ij}(k_1^2; r,r')\, V_{j1}(r') \qquad (3.3.3)$$

where $\underline{\underline{G}}^{Q}$ is the outgoing Green's function for the Hamiltonian $\underline{\underline{H}}^{Q}$, with elements

$$H^{Q}_{ij} = \left(\frac{d^2}{dr^2} - \Delta_{i-1}\right)\delta_{ij} - V_{ij}(r) \quad ; \quad i,j = 2,\ldots,N \qquad (3.3.4)$$

The channel function $F_1(r)$ is determined from the optical potential as the solution of the equation

$$\left(\frac{d^2}{dr^2} + k_1^2 - V_{11}(r)\right) F_1(r) = \int_0^\infty W(r,r')\, F_1(r')\, dr' \qquad (3.3.5)$$

subject to the boundary condition

$$F_1(r) \sim \sin k_1 r + f(k_1)\, e^{i k_1 r} \qquad (3.3.6)$$

The Green's function $\underline{\underline{G}}^{Q}$ can be constructed from the solutions of the Q space Schrödinger equation

$$\sum_{j=2}^{N} \left(H^{Q}_{ij} + s^2\right) \phi_j(s,r) = 0 \qquad (3.3.7)$$

These solutions can be classified as follows with respect to the energy, s^2:

(a) $s^2 < \Delta_1$

All channels $j \geq 2$ are closed. Bounded solutions $\phi_j(s_n, r)$ may exist at energies $s^2 = s_n^2$.

(b) $\Delta_2 > s^2 > \Delta_1$

Channel 2 is open and the remainder are closed.

There is a unique regular solution such that

$$\phi_2(s,r) \sim \frac{1}{\sqrt{\pi s_2}} \sin(s_2 r + \delta) \quad , \quad \phi_j(s,r) \sim 0 \; ; \; j \geq 3$$

(3.3.8)

where

$$s_j^2 \equiv s^2 - \Delta_{j-1} \qquad ; \; j \geq 2$$

(3.3.9)

with the normalisation

$$\sum_{j\geq 2}^{N} \int_0^\infty \phi_j(s,r)\, \phi_j(s',r)\, dr = \delta(s^2 - s'^2)$$

(3.3.10)

(c) $\Delta_{J+1} > s^2 > \Delta_J$

In this energy interval the J channels from j = 2 to j = J + 1 are open, correspondingly there are J independent regular solutions $\phi_j^{Jn}(s,r)$ of equations (3.3.7) with n = 1,2...J. The boundary conditions can be conveniently specified in terms of eigenphaseshifts δ_n, n = 1,2,...J and a real orthogonal J x J matrix $R_{nm}(s)$, as follows:

$$\phi_j^{Jn}(s,r) \sim R_{nj} \frac{1}{\sqrt{\pi s_j}} \sin(s_j r + \delta_n) \quad ; \; j = 2,3,\ldots,J+1$$

$$\phi_j^{Jn}(s,r) \sim 0 \qquad ; \; j > J+1$$

(3.3.11)

Writing the independent solutions $\phi_j^{Jn}(s,r)$ as column vectors, $\underline{\phi}^{Jn}(s,r)$ and using the orthogonality relations

$$\underline{\underline{R}}^T \underline{\underline{R}} = \underline{\underline{R}}\, \underline{\underline{R}}^T = \underline{\underline{I}}$$

(3.3.12)

where $\underline{\underline{R}}^T$ is the transpose of $\underline{\underline{R}}$, the normalisation conditions

are found to be

$$\int_0^\infty dr \left(\underline{\phi}^{J_n}(s',r) \right)^T \underline{\phi}^{J_m}(s,r) = \delta_{nm} \delta(s^2 - s'^2)$$

(3.3.13)

The solutions $\underline{\phi}^{J_n}$ are, of course, orthogonal to the bounded solutions and the solutions in each of the other energy intervals.

The Green's function G^{Θ}_{ij} is then easily written down in terms of these solutions. We have

$$G^{\Theta}_{ij}(k_1^2; r, r') = \sum_m \frac{\phi_i^m(r)\,\phi_j^m(r')}{(k_1^2 - s_m^2)} + \lim_{\varepsilon \to 0} \int_{\Delta_1}^{\Delta_2} ds^2 \frac{\phi_i(s,r)\,\phi_j(s,r')}{(k_1^2 + i\varepsilon - s^2)}$$

$$+ \lim_{\varepsilon \to 0} \int_{\Delta_2}^{\Delta_3} ds^2 \sum_{n=1}^{2} \frac{\phi_i^{2n}(s,r)\,\phi_j^{2n}(s,r')}{(k_1^2 + i\varepsilon - s^2)} + \cdots + + - + \cdots$$

$$+ \lim_{\varepsilon \to 0} \int_{\Delta_{N-1}}^{\infty} ds^2 \sum_{n=1}^{N-1} \frac{\phi_i^{(N-1)n}(s,r)\,\phi_j^{(N-1)n}(s,r')}{(k_1^2 + i\varepsilon - s^2)}$$

(3.3.14)

This expression is the generalisation of equation (3.2.5b). The imaginary part of $\underline{\underline{G}}^{\Theta}$ at an energy between the thresholds at Δ_J and Δ_{J+1} is of the form

$$\mathrm{Im}\, G^{\Theta}_{ij}(k_1^2; r, r') = -\pi \sum_{n=1}^{J} \phi_i^{J_n}(k_1, r)\,\phi_j^{J_n}(k_1, r')$$

(3.3.15)

and contains a contribution from each of the J degenerate solutions.

The L^2 representation of G

To illustrate the problems that arise in attempting to represent $\underline{\underline{G}}^Q$ in a finite basis of L^2 functions, it is sufficient to consider two Q space channels and to employ potentials which do not support Q space bound states, in which case

$$\mathrm{Re}\ G^Q_{ij}(k_1^2;r,r') = P\int_{\Delta_1}^{\Delta_2} ds^2\ \frac{\phi_i(s,r)\,\phi_j(s,r')}{(k_1^2-s^2)} + P\sum_{n=1}^{2}\int_{\Delta_2}^{\infty} ds^2\ \frac{\phi_i^n(s,r)\,\phi_j^n(s,r')}{(k_1^2-s^2)} \qquad (3.3.16)$$

$$\mathrm{Im}\ G^Q_{ij}(k_1^2;r,r') = 0 \quad ; \ k_1^2 < \Delta_1$$
$$= -\pi\,\phi_i(k_1,r)\,\phi_j(k_1,r') \quad ; \ \Delta_1 < k_1^2 < \Delta_2$$
$$= -\pi\sum_{n=1}^{2}\phi_i^n(k_1,r)\,\phi_j^n(k_1,r') \quad ; \ \Delta_2 < k_1^2 \qquad (3.3.17)$$

In evaluating the real part of the $\underline{\underline{G}}^Q$ numerically subtractions can be made to avoid the singularities. For example if $\Delta_1 < k_1^2 < \Delta_2$ the first integral on the right hand side of (3.3.16) can be expressed as

$$\int_{\Delta_1}^{\Delta_2} ds^2 \frac{\phi_i(s,r)\,\phi_j(s,r') - \frac{k_1}{s}\phi_i(k_1,r)\,\phi_j(k_1,r')}{(k_1^2 - s^2)}$$

$$+ \phi_i(k_1,r)\,\phi_j(k_1,r') \ln\left(\left|\frac{(k_1+\sqrt{\Delta_1})(k_1-\sqrt{\Delta_2})}{(k_1-\sqrt{\Delta_1})(k_1+\sqrt{\Delta_2})}\right|\right)$$

(3.3.18)

and when $k_1^2 > \Delta_2$ the second integral in (3.3.16) can be treated in a similar way.

As in section 3.2 the Q space Hamiltonian can be diagonalised on a finite basis of functions, $\underline{\theta}_n$. In the present case these functions have two components $\theta_{n,j}(r)$; j = 2,3 and

$$\sum_{i,j=2}^{3} \int_0^\infty dr\; \theta_{n,j}(r)\, H^Q_{ji}\, \theta_{m,i}(r) = -s_n^2 \delta_{nm} \quad ; \; n,m = 1,2,\ldots,N$$

(3.3.19)

The discrete eigenvalues s_n^2 are non-degenerate and the (unsubtracted) real part of the Green's function is approximated by

$$\mathrm{Re}\, G^Q_{ij}(k_1^2; r, r') = \sum_{n=1}^{N} \frac{\theta_{n,i}(r)\,\theta_{n,j}(r')}{(k_1^2 - s_n^2)}$$

(3.3.20)

In the single channel case, the eigenvalues s_n^2 formed a smooth sequence in terms of n.

In the two channel case, they no longer form this smooth sequence. The reason for this can be seen as

follows. We introduce a parameter λ by replacing V_{ij} in (3.3.4) by

$$V_{ij}(\lambda, r) = V_{ij}(r)\,\delta_{ij} + (1-\delta_{ij})\,\lambda\, V_{ij}(r) \tag{3.3.21}$$

When $\lambda = 0$ the coupling between the channels in (3.3.4) is removed. In this case, each of the Q space channels contributes independently to the optical potential (3.3.3), and each contribution can be calculated as in section 2.2. This means that (for $\lambda = 0$) the sequence of eigenvalues s_n in the two channel case splits into two, each of which is a smooth function of n. The first sequence $s_n^{(1)}$ spans the interval starting at the lower inelastic threshold, $\Delta_1 < s^2 < \infty$ while the second sequence $s_n^{(2)}$ starts at the second threshold and spans the interval $\Delta_2 < s^2 < \infty$. The corresponding eigenfunctions $\Theta_{n,j}^{(1)}$ and $\Theta_{n,j}^{(2)}$ approximate the elastic scattering wave functions in the two Q space channels, and each has one component: $\Theta_{n,2}^{(1)} \neq 0$, $\Theta_{n,3}^{(1)} = 0$, $\Theta_{n,2}^{(2)} = 0$, $\Theta_{n,3}^{(2)} \neq 0$.

The association of the sequences of eigenvalues with one or other of the inelastic cuts along the real axis persists as λ is increased from zero, provided λ is small enough so that λV_{ij} $(i \neq j)$ can be treated as a small perturbation. In fact the eigenvalues $s_n^{(\mu)}$, $\mu = 1,2$ vary smoothly with λ and for finite λ each sequence $s_n^{(1)}$ and $s_n^{(2)}$ remains a smoothly varying function of the index n. This suggests that, for not too large λ, one sequence can be

associated with the integration along the cut from Δ_1 to ∞ and the other with the integration along that from Δ_2 to ∞, with corresponding approximate weights $w_n^{(\mu)} = 2s_n^{(\mu)} \partial(s_n^{(\mu)})/\partial n$. If this is the case, the Green's function can be approximated by

$$Re\ G_{ij}^{Q}(k_1^2; r_1, r_1') = \sum_n \sum_{\mu=1}^{2} \frac{\theta_{n,i}^{(\mu)}(r)\,\theta_{n,j}^{(\mu)}(r') - w_n^{(\mu)} \frac{(k_1^2-\Delta_\mu)^{1/2}}{(s_n^{(\mu)2}-\Delta_\mu)^{1/2}} \phi_i^{A,(\mu)}(k_1, r)\,\phi_i^{A,(\mu)}(k_1, r')\,\varepsilon_\mu(k_1)}{(k_1^2 - s_n^{(\mu)2})} \qquad (3.3.22a)$$

$$Im\ G_{ij}^{Q}(k_1^2; r_1, r_1') = -\pi \sum_{\mu=1}^{2} \phi_i^{A,(\mu)}(k_1, r)\,\phi_j^{A,(\mu)}(k_1, r')\,\varepsilon_\mu(k_1) \qquad (3.3.22b)$$

where $\varepsilon_\mu(k_1) = 1$, $k_1^2 > \Delta_\mu$; $\varepsilon_\mu(k_1) = 0$ otherwise, and where $\phi_i^{A,(\mu)}(k_1, r)$ is interpolated from the set of functions $\phi_i^{\mu}(s_n^{(\mu)}, r) = N_n(s_n^{(\mu)})\,\theta_{n,i}^{(\mu)}(r)$, where the renormalisation factor N_n is given by

$$N_n(s_n^{(\mu)}) = (w_n^{(\mu)})^{-1/2} \qquad (3.3.23)$$

The expressions (3.3.21) and (3.3.23) reduce exactly to the approximation of section 3.2 when $\lambda = 0$, and should be accurate for sufficiently small λ. As in the single channel case the subtractions ensure that no spurious resonances are encountered, without having to continue into the complex energy plane.

3.3B Numerical Examples

As a numerical example, the potentials in three

coupled channels were taken to be

$$V_{11} = -2.0\ e^{-r}/r;\ V_{12} = V_{21} = -0.25\ e^{-r};$$
$$V_{13} = V_{31} = -0.125\ e^{-r}$$
$$V_{22} = -1.5e^{-r}/r;\ V_{33} = -1.0\ e^{-1.5r}/r$$
$$V_{23} = V_{32} = -\lambda\, 1.5\ e^{-0.5r},\ 0 \leq \lambda \leq 1$$

(3.3.24)

The thresholds were chosen to be $\Delta_1 = 0.75$ and $\Delta_2 = 1.0$. There is nothing significant in the particular strengths and ranges chosen; similar results are obtained with different strengths and ranges.

To form the discrete basis of functions the functions $\theta_{n,i}(r)$ were represented as

$$\theta_{n,i}(r) = \sum_{q=1}^{q_m} c^{q}_{n,i}\, U_{i,q}(r)$$

(3.3.25)

with

$$U_{i,q}(r) = \left(\frac{\alpha_i}{q(q+1)}\right)^{1/2} (\alpha_i r)\, e^{-\alpha_i r/2}\, L^{(2)}_{q-1}(\alpha_i r)$$

(3.3.26)

and

$$\langle U_{i,q} \mid U_{i,q'} \rangle = \delta_{qq'}$$

(3.3.27)

The scale parameters α_i were chosen, so that on diagonalising $\underline{\underline{H}}^{\mathcal{Q}}$ the eigenvalues spanned the energy interval of interest, which was taken to be $0.2 < k_1^2 < 4.0$.

In principle, the size of the basis set should be increased until convergence is obtained. In practice we

employed bases of 10,15 or 20 functions, which we know to be adequate for the uncoupled Q space problem with $\lambda = 0$.

A great many numerical experiments were carried out, varying the scale parameters α_i and testing various methods of numerical interpolation to obtain the functions $\phi_i^{\lambda\mu}$ and $w_n^{(\mu)}$. The results are illustrated in tables 3.5 to 3.7, where a comparison is made with the direct numerical solution of the equations using the programme of McCarthy and Stelbovics (1983).

In table 3.5 we show the results of the uncoupled Q space problem ($\lambda = 0$). As expected from section 3.2, accurate results were obtained for the elastic scattering cross section and for the reaction cross section. In tables 3.6 and 3.7 λ has been increased to 0.3 and to 1.0 respectively. It is seen that even for $\lambda = 1$ the results are good over all of the energy range for elastic scattering, but the more sensitive reaction cross section is given poorly near to $k_1^2 = 1.0$ and also near to $k_1^2 = 1.6$.

Although these results are encouraging, the chief defect of the procedure is a certain lack of stability against varying the scale parameter. This can be seen by comparing the results of tables 3.7 and 3.8. The results of table 3.8 differ from those of table 3.7 in that two scale parameters were used, one in each channel, chosen so that the sets of eigenvalues $s_n^{(1)}$ and $s_n^{(2)}$ overlapped as little as possible. The resulting reaction cross section is given well for energies up to the threshold Δ_2, but poorly for

TABLE 3.5

Elastic (E) and reaction (R) cross sections computed from Equations (3.3.1). The models employed are defined in the text.

($\lambda = 0.0$, $\alpha = 3.0$) Basis of 15 vectors

K1**2	Exact Results		L-Squared Method	
	E	R*	E	R*
0.2	19.97	-	19.97	-
0.4	9.479	-	9.480	-
0.6	5.950	-	5.951	-
0.9	3.536	0.568	3.535	0.566
1.1	2.766	0.354	2.766	0.355
1.2	2.480	0.301	2.480	0.303
1.4	2.040	0.227	2.040	0.232
1.6	1.718	0.177	1.718	0.180
1.8	1.474	0.145	1.475	0.146
2.0	1.283	0.122	1.284	0.123
2.2	1.131	0.100	1.132	0.106
2.4	1.007	0.086	1.007	0.092
2.6	0.9042	0.075	0.9049	0.078
2.8	0.8177	0.067	0.8187	0.068
3.0	0.7445	0.060	0.7452	0.062

R* : Reaction cross sections are *10

Units are as in Table 3.1

TABLE 3.6

Elastic (E) and reaction (R) cross sections computed from Equations (3.3.1), The models employed are defined in the text.

(λ = 0.3, α = 3.0) Basis of 15 vectors

K1**2	Exact Results		L-Squared Method	
	E	R*	E	R*
0.2	19.98	-	19.98	-
0.4	9.498	-	9.498	-
0.6	5.981	-	5.980	-
0.7	5.047	-	5.045	
0.9	3.505	0.666	3.514	0.673
1.0	3.099	0.461	3.108	0.459
1.1	2.754	0.400	2.767	0.365
1.2	2.470	0.338	2.480	0.325
1.4	2.033	0.252	2.033	0.286
1.6	1.713	0.195	1.713	0.213
1.8	1.471	0.157	1.475	0.152
2.0	1.281	0.129	1.283	0.136
2.2	1.129	0.109	1.130	0.117
2.4	1.005	0.094	1.008	0.097
2.6	0.9031	0.081	0.9045	0.084
2.8	0.8171	0.070	0.8180	0.075
3.0	0.7440	0.061	0.7444	0.068
3.2	0.6812	0.055	0.6814	0.060
3.4	0.6269	0.049	0.6270	0.052
3.6	0.5793	0.044	0.5796	0.046
3.8	0.5375	0.040	0.5379	0.040
4.0	0.5005	0.037	0.5010	0.036

R* : Reaction cross sections are *10

Units are as in Table 3.1

TABLE 3.7

Elastic (E) and reaction (R) cross sections computed from Equations (3.3.1). The models employed are defined in the text.

(λ = 1.0, α = 2.7) Basis of 15 vectors

K1**2	Exact Results		L-Squared Method	
	E	R*	E	R*
0.2	20.00	-	20.00	-
0.4	9.829	-	9.829	-
0.6	5.741	-	5.742	-
0.7	4.861	-	4.862	
0.8	4.097	0.456	4.085	0.498
0.9	3.523	0.521	3.522	0.515
1.0	3.080	0.510	3.112	0.324
1.1	2.742	0.398	2.771	0.405
1.2	2.460	0.342	2.467	0.288
1.4	2.025	0.260	2.019	0.274
1.6	1.707	0.203	1.717	0.140
1.8	1.465	0.166	1.466	0.165
2.0	1.276	0.139	1.280	0.127
2.2	1.126	0.114	1.128	0.113
2.4	1.003	0.097	1.003	0.102
2.6	0.9005	0.084	0.9013	0.087
2.8	0.8147	0.075	0.8158	0.075
3.0	0.7419	0.067	0.7427	0.067
3.2	0.6796	0.057	0.6803	0.058
3.4	0.6254	0.051	0.6262	0.051
3.6	0.5781	0.046	0.5788	0.046
3.8	0.5364	0.042	0.5369	0.043
4.0	0.4995	0.038	0.4997	0.040

R* : Reaction cross sections are *10

Units are as in Table 3.1

TABLE 3.8

Elastic (E) and reaction (R) cross sections computed from Equations (3.3.1). The models employed are defined in the text.

($\lambda = 1.0$, $\alpha_2 = 1.0$, $\alpha_3 = 2.4$) Basis of 15 vectors

K1**2	Exact Results		L-squared Method	
	E	R*	E	R*
0.7566	4.435	0.208	4.433	0.205
0.7688	4.337	0.319	4.335	0.319
0.7857	4.198	0.413	4.198	0.411
0.8123	4.016	0.480	4.019	0.476
0.8504	3.785	0.518	3.791	0.509
0.9049	3.499	0.520	3.508	0.519
0.9773	3.175	0.503	3.212	0.385
1.025	2.991	0.460	3.051	0.598
1.057	2.880	0.430	2.864	0.598
1.122	2.677	0.384	2.652	0.538
1.181	2.508	0.352	2.474	0.526
1.260	2.314	0.315	2.308	0.319
1.376	2.069	0.270	2.087	0.285
1.478	1.890	0.234	1.877	0.363
1.656	1.632	0.191	1.636	0.177
1.829	1.435	0.162	1.454	0.188
2.019	1.261	0.136	1.257	0.184
2.396	1.005	0.098	1.010	0.092

R* : Reaction cross sections are *10

Units are as in Table 3.1

higher energies. In principle, whatever the scale parameters (in reason) the basis set could be increased to obtain convergence. However, numerical problems were encountered in diagonalising $\underline{\underline{H}}^{\alpha}$ for much larger sets and although, no doubt, these numerical problems could be overcome, the method loses its simplicity, and makes an extension to realistic problems more difficult.

CHAPTER FOUR

THE SCHWINGER VARIATIONAL METHOD AND THE POET MODEL PROBLEM

4.1 The Schwinger Variational Method

This section introduces the Schwinger variational method in terms of one particle radial single channel scattering, for simplicity. The method depends on the use of the Lippmann Schwinger equation (see section 1.2C) to provide different expressions for T matrix elements, and formally may be generalised straightforwardly to many coordinate problems where target coordinate(s) and angular momentum have not been integrated over, using adequately complex trial functions and full enough representation of the required Green's functions. The work of chapter five on the use of the method for the Poet model problem and its coupled channel approximations exemplifies these generalisations. The Schwinger variational method is discussed by Joachain (1983), Bransden (1983) and in more detail by Nesbet (1980). We consider a Hamiltonian H(r) made up of an unperturbed Hamiltonian $H_o(r)$ with known solutions, and a short range potential V(r), which may include implied integration over a symmetric exchange kernel. The regular solutions ψ^+ and ψ^- obey the Lippman Schwinger equations (4.1.1)

$$|\psi^{\pm}(E)\rangle = |\phi(E)\rangle + G_o^{\pm} V |\psi^{\pm}(E)\rangle$$

(4.1.1)

The asymptotic boundary conditions for outward (+) and inward (-) scattering are included in the Green's functions as described in section 1.2C. The regular unperturbed radial solutions $\phi(E)$ are real.

$$H|\psi^{\pm}(E)\rangle = E|\psi^{\pm}(E)\rangle$$

$$H_o|\phi(E)\rangle = E|\phi(E)\rangle$$

(4.1.2a)

$$(E - H_o)\, G_o^{\pm}(E,r,r') = \delta(r-r')$$

(4.1.2b)

$$G_o^{+}(E,r,r') = (G_o^{-}(E,r,r'))^{*}$$

(4.1.2c)

$$G_o^{+}(E,r,r') = \frac{2}{W(\phi,\phi_I)}\phi(E,r_<)\{\phi_I(E,r_>) + i\,\phi(E,r_>)\}$$

(4.1.2d)

$\phi_I(E,r)$ is the irregular solution of the unperturbed Schrödinger equation. W is the Wronskian of ϕ and ϕ_I. The ϕ, ϕ_I may be normalised such that W = -1 for convenience. The T matrix element may be written

$$\tfrac{1}{2}T = -\langle \phi(E)|V|\psi^{+}(E)\rangle = -R$$

(4.1.3a)

Using (4.1.1) and (4.1.2c) the T matrix element may be

rewritten as in (4.1.3b,c)

$$\tfrac{1}{2}T = \langle \psi^{-}(E) | -V + V G_0^{+} V | \psi^{+}(E) \rangle = \overline{T} \qquad (4.1.3b)$$

$$= -\langle \psi^{-}(E) | V | \phi(E) \rangle = -S \qquad (4.1.3c)$$

The expressions (4.1.3) are hermitian. They imply

$$\psi^{+}(E) \xrightarrow[r\to\infty]{} \phi(E,r) + T\left(\phi_3(E,r) + i\,\phi(E,r)\right) \qquad (4.1.4)$$

The Schwinger variational principle in its bilinear form is written

$$\tfrac{1}{2}T = -\langle \phi(E) | V | \psi^{+}(E) \rangle - \langle \psi^{-}(E) | V | \phi(E) \rangle - \langle \psi^{-}(E) | -V + V G_0^{+} V | \psi^{+}(E) \rangle \qquad (4.1.5)$$

Variation of $|\psi^{+}\rangle$ and $\langle\psi^{-}|$ about the exact values leads to the expression (4.1.6) to first order in $\delta\psi^{+}$.

$$\delta(\tfrac{1}{2}T) = -\langle \phi | V | \delta\psi^{+} \rangle - \langle \delta\psi^{-} | V | \phi \rangle - \langle \psi^{-} | -V + V G_0^{+} V | \delta\psi^{+} \rangle - \langle \delta\psi^{-} | -V + V G_0^{+} V | \psi^{+} \rangle$$

$$= -\langle \delta\psi^{-} | V \{ | \phi \rangle - (1 - G_0^{+} V) | \psi^{+} \rangle \} - \{ \langle \phi | - \langle \psi^{-} | (V - V G_0^{+}) \} V | \delta\psi^{+} \rangle$$

$$= 0 \qquad (4.1.6)$$

The Lippmann Schwinger equation is reproduced and $\delta(\frac{1}{2}T) = 0$ for variation about the exact wave functions $|\psi^{\pm}\rangle$. The

Schwinger variational principle may also be stated in fractional form:

$$\frac{1}{2}T = \frac{\langle \psi^- | V | \phi \rangle \langle \phi | V | \psi^+ \rangle}{\langle \psi^- | -V + V G_0^+ V | \psi^+ \rangle} \qquad (4.1.7)$$

This form may be achieved by replacing $|\psi^\pm\rangle \rightarrow A^\pm |\psi^\pm\rangle$ in (4.1.5) and varying with respect to the $A^\pm$. It may also be seen to be stationary by varying $|\psi^\pm\rangle$ in (4.1.7).

There are various advantages in using the Schwinger principle rather than, for instance, the Kohn principle. The asymptotic boundary conditions for the problem are built into the Green's function G_0^+, and the trial wave functions $|\psi_{tr}\rangle$ need not include them: the trial functions always occur matched against the short range potential V, and may be expressed in terms of L-squared functions which adequately represent the $|\psi^\pm\rangle$ over the range of V once the stationary value has been found. The fractional form (4.1.7) is also independent of the normalisation of the trial function. We now illustrate the method used in chapter five for finding the stationary value. We write:

$$|\psi_{tr}^+\rangle = \sum_{i=1}^{N} c_i |\psi_i\rangle$$

$$\langle \psi_{tr}^- | = \sum_{i=1}^{N} c_i \langle \psi_i | \qquad (4.1.8)$$

$|\psi_i\rangle$ are real L-squared functions.

In this single channel radial case $\psi^{-*}(E,r) = \psi^{+}(E,r)$. In more general problems variation of $|\psi^{+}_{\alpha}\rangle$ and $|\psi^{-}_{\alpha}\rangle$ is performed separately. For multichannel problems the c_i are also labelled by channel as will be described in section 5.2.

$$\tfrac{1}{2}T \leftrightarrow F = \frac{R(\underline{c})\,S(\underline{c})}{\bar{T}(\underline{c})} \qquad ; \{\underline{c}\}_i = c_i \tag{4.1.9}$$

$$\frac{\partial F}{\partial c_i} = \frac{S(\underline{c})}{\bar{T}(\underline{c})}\frac{\partial R(\underline{c})}{\partial c_i} + \frac{R(\underline{c})}{\bar{T}(\underline{c})}\frac{\partial S(\underline{c})}{\partial c_i} - \frac{R(\underline{c})\,S(\underline{c})}{(\bar{T}(\underline{c}))^2}\frac{\partial \bar{T}(\underline{c})}{\partial c_i} = 0 \; ; \; i = 1,2,\ldots,N \tag{4.1.10}$$

Since the normalisation of $|\psi^{\pm}_{\alpha}\rangle$ is arbitrary we may impose a limitation on (4.1.10). We may require

$$-R = -S = \bar{T} \tag{4.1.11}$$

$$\Rightarrow \frac{\partial R}{\partial c_i} + \frac{\partial S}{\partial c_i} - \frac{\partial \bar{T}}{\partial c_i} = 0 \quad ; \; i = 1,2,\ldots,N \tag{4.1.12a}$$

(4.1.12a) may be rewritten:

$$\left\{ \langle \phi | V | \psi_i \rangle + \sum_{j=1}^{N} c_j \langle \psi_j | -V + V G_0^{+} V | \psi_i \rangle \right\}$$

$$+ \left\{ \langle \psi_i | V | \phi \rangle + \sum_{j=1}^{N} c_j \langle \psi_i | -V + V G_0^{+} V | \psi_j \rangle \right\}$$

$$= 0 \qquad ; \; i = 1,2,\ldots,N \tag{4.1.12b}$$

The two halves of this expression are identical (in the more general case (4.1.12b) splits into two separate equations for the two sets of constants $\underline{c}^{\pm}$). In matrix form, we have (4.1.12c).

$$\underline{R} + \underline{\underline{D}}\,\underline{c} = \underline{0} \tag{4.1.12c}$$

$$\{\underline{R}\}_i = \langle \psi_i | V | \phi \rangle$$

$$\{\underline{\underline{D}}\}_{ij} = \langle \psi_i | -V + VG_o^+ V | \psi_j \rangle = \{\underline{\underline{D}}\}_{ji}$$

The matrix problem (4.1.12c) is soluble for non singular $\underline{\underline{D}}$

$$\underline{c} = -\underline{\underline{D}}^{-1}\underline{R} \tag{4.1.13}$$

$$F = \underline{R}^+ \underline{\underline{D}}^{-1} \underline{R}$$

$$= \sum_{ij} \langle \phi | V | \psi_i \rangle \{\underline{\underline{D}}^{-1}\}_{ij} \langle \psi_j | V | \phi \rangle \tag{4.1.14}$$

For the more general case, the equivalent results are

$$\underline{R}_a + \underline{\underline{D}}\,\underline{c}_a = \underline{0} \quad ; \quad \underline{R}_b^\dagger + (\underline{c}_b^*)^\dagger \underline{\underline{D}} = \underline{0}^\dagger$$

$$F_{ba} = \underline{R}_b^\dagger \underline{\underline{D}}^{-1} \underline{R}_a$$

$$\{\underline{R}_a\}_j = \langle \psi_j | V | \phi_a \rangle \tag{4.1.15}$$

a and b label the channels and the $\dagger$ process includes complex conjugation.

Not imposing (4.1.11) is equivalent to choosing the value of one of the c_i. For example (4.1.12c) becomes

$$\underline{R} - \alpha(\underline{c})\,\underline{\underline{D}}\,\underline{c} = \underline{0} \quad ; \quad \alpha(\underline{c}) = \frac{\underline{R}\cdot\underline{c}}{\underline{c}^\dagger \underline{\underline{D}}\,\underline{c}}$$

$$\alpha(\underline{c})\,\underline{c} = \underline{\underline{D}}^{-1}\underline{R} \tag{4.1.16}$$

Choosing a value of c_1 fixes $\alpha(\underline{c})$ and the factor $1/\alpha$ appears in the expressions for the c_i. This then cancels

out in the expression (4.1.9) which reduces to (4.1.14) as the approximation to $\frac{1}{2}T$. The linear method chooses $\alpha = -1$ and is more straightforward to use as $F = -R = -\hat{S} = -T$ after the matrix inversion has been accomplished.

The stationary value found using $|\psi_\alpha^+\rangle$ is equivalent to finding the exact T matrix element for a Hamiltonian $\bar{H} = H_0 + \bar{V}$, as described for example by Adhikari and Sloan (1975).

$$\bar{V} = \sum_{ij} V|\psi_i\rangle \{\underline{\underline{d}}^{-1}\}_{ij} \langle\psi_j|V$$

$$\{\underline{\underline{d}}\}_{ij} = \langle\psi_i|V|\psi_j\rangle \qquad (4.1.17)$$

This may be seen as the t operator for F may be written:

$$F = -\langle\phi|t|\phi\rangle$$

$$t = -\sum_{ij} V|\psi_i\rangle \{\underline{\underline{D}}^{-1}\}_{ij} \langle\psi_j|V \qquad (4.1.18a)$$

t obeys (4.1.18b) which is the exact t operator equation for the Hamiltonian $\bar{H}$

$$t = \bar{V} + \bar{V} G_0^+ t \qquad (4.1.18b)$$

$$\bar{V} + \bar{V} G_0^+ t = \bar{V} - \sum_{ijkl} V|\psi_i\rangle \{\underline{\underline{d}}^{-1}\}_{ij} \langle\psi_j|V G_0^+ V|\psi_k\rangle \{\underline{\underline{D}}^{-1}\}_{kl} \langle\psi_l|V$$

$$= \bar{V} - \sum_{ijkl} V|\psi_i\rangle \{\underline{\underline{d}}^{-1}\}_{ij} \{\underline{\underline{D}} + \underline{\underline{d}}\}_{jk} \{\underline{\underline{D}}^{-1}\}_{kl} \langle\psi_l|V$$

$$= t \qquad (4.1.18c)$$

We also have $\bar{V}|\psi_i\rangle = V|\psi_i\rangle$. As the basis extends to

completeness $\bar{V} \rightarrow V$. In various tests of one dimensional problems solved approximately in a restricted space using a finite set of L-squared basis functions, either expanding the full Green's function or the potential in the basis, Schneider (1985) found the Schwinger method (i.e. solving for a model separable potential $\bar{V}$) to be the most reliable giving results closest to the exact solution.

The disadvantages of the Schwinger variational principle are that it is not a minimum principle (although neither for example, is the Kohn principle) and that the method requires calculation of Green's function matrix elements, which can be time consuming. For physical problems, this is especially problematical as continuum states need to be included in the Green's function. This is investigated in terms of the Poet model problem in chapter five. For single channel scattering, Takatsuka, Luchesse and McKoy (1981) have related the Schwinger variational principle to the Kohn variational principle when the same trial function is used in both: the Schwinger principle gives a more accurate result corresponding to the Kohn principle combining the basic trial function with the higher order function resulting from one iteration of the Lippmann Schwinger equation. The Schwinger principle also appears ostensibly more flexible as the choice of trial function does not imply a particular approximation to the Green's function for the problem, although complications arise which are discussed in chapter five.

Relationship With The Second Born Approximation

If the unperturbed wave function ϕ is used as a trial function the expression for the T matrix element is

$$\frac{1}{2}T \simeq \frac{\langle \phi|V|\phi\rangle\langle\phi|V|\phi\rangle}{\langle \phi|-V+VG_0^+V|\phi\rangle} \qquad (4.1.19a)$$

$$\frac{1}{2}T \simeq -\langle\phi|V|\phi\rangle\left(1+\frac{\langle\phi|VG_0^+V|\phi\rangle}{\langle\phi|V|\phi\rangle}+\ldots\right) \qquad (4.1.19b)$$

Thus the Schwinger principle is equivalent to the second Born approximation at this level of accuracy. (4.1.19a) in general is often more accurate than the second Born approximation though this is not guaranteed. Altshuler (1953) performed tests of the Schwinger method for the static s-wave hydrogen potential (i.e. no exchange), using the full method in one dimension and (4.1.19b) in three dimensions, finding (4.1.19b) superior to the second Born approximation. Moiseivitsch (1973) for example, has related the Schwinger principle to the theory of Padé approximants.

Applications Of The Schwinger Principle

Maleki and Macek (1980) formulated the Schwinger

principle for electron ion scattering and applied it successfully to a single channel model problem involving a Yukawa potential (the wave functions for which have been used as trial functions in configuration interaction calculations incorporating screened potentials). A great deal of work has been performed by McKoy (M), Watson (W), Luchesse (Lu), Takatsuka (T), Lee (Le), Marco (Ma), Gibson (G), Lima (Li), and Rescigno (R). The Schwinger method has been applied with success to low energy electron-atom, ion and molecule scattering in the static exchange approximation (W M 1979, W Lu M R 1980, Lu M 1979, 1980, Lu W M 1980, Maleki 1984) and, using a modified form of the Schwinger principle discussed in section 5.6, electron-atom and molecule scattering beyond the static exchange approximation but still at low energies as all open channels need to be included in the Green's function for the problem (T M 1981, 1984, Li G T M 1984, G Li Ma T M 1984).

Luchesse, Takatsuka and McKoy (1986) have presented a review detailing their use of the Schwinger principle and various variational principles derived from it in electron molecule collisions and molecular photoionisation. L W M (1980) presented an iterative approach in which the basis set in the Schwinger trial function was augmented by the solutions to the model problem $\bar{H}$, producing a higher order model t operator for which solutions were found. This process could be continued until convergence was achieved, but was somewhat time consuming, involving a variational

stationary value calculation for each iteration. T M (1980) and Li T M (1981), presented a series of variational functionals ("C" functionals) related to the Schwinger principle, some of which had also been suggested by Kolsrud (1958) and Moe and Saxon (1958), which were also applied to the static exchange approximation for electron molecule scattering. Moiseiwitsch (1982, 1983) has related the Schwinger variational principle to a linear algebraic equations method developed by Eisner and Seaton (1972): the Green's integral in the Lippmann Schwinger equation is written as a numerical quadrature, resulting in a set of linear equations, equivalent to using the Schwinger variational principle with an appropriate trial function. The method was applied to static exchange and 1s - 2s close coupling cross sections for electron hydrogen atom scattering. Luchesse (1986) compared a Kohn type variational method with the Schwinger and "C" functional methods in a coupled channel model problem due to Huck (1957) and modified by Fels and Hazi (1972). The model involves two distinguishable particles, one moving in an infinite square well, and the other free, interacting with separable potentials in two or three channels, with only s-wave scattering included. Other channels were represented by an L-squared optical potential and the testing energy was kept low enough for these channels to be closed. The Schwinger type methods gave faster convergence than the Kohn type method, with little to choose between the Schwinger and

"C" functional methods. The tests did not include indistinguishability. Finally Brendle et al. (1983) have applied the Schwinger method to heavy particle scattering. All these applications involve a limited number of exact open channels and calculations at low energies. In chapter five the Schwinger method is applied to excitation above the ionisation threshold in the Poet model problem.

4.2 The Poet Problem

The Poet problem was introduced in chapter one and is considered theoretically in the next chapter. The model ignores angular momentum and the degeneracy of the hydrogen atom energy levels, but retains an infinite series of discrete bound states and an ionisation continuum. Thus, ways of modelling continuum effects for intermediate scattering energies may be investigated in this less complex case, in particular the use of pseudostates.

Poet's Aproach

The approach used by Poet (1978) is radically different to the methods considered so far, and is similar to that of Temkin (1965). The restriction to s states replaces the electron interaction potential with the first term in its Legendre polynomial expansion, and Poet solved the resulting separable partial differential equations using sums (and

integrals) over known free particle and Coulomb functions.

$$\left(\frac{d^2}{dr_1^2} + \frac{d^2}{dr_2^2} + \frac{2}{r_2} - E \right) \psi^{(s)}(r_1, r_2) = 0 \quad ; \; r_1 \geq r_2$$

$$\left(\frac{d^2}{dr_2^2} + \frac{d^2}{dr_1^2} + \frac{2}{r_1} - E \right) \psi^{(s)}(r_1, r_2) = 0 \quad ; \; r_2 \geq r_1$$

$$\psi^{(s)}(r_1, r_2) = (-1)^s \psi^{(s)}(r_2, r_1)$$

(4.2.1)

The boundary conditions as r_1 , $r_2 \to \{ \begin{smallmatrix} 0 \\ \infty \end{smallmatrix} \}$ and those defined by the symmetry/antisymmetry of $\psi^{(s)}$ at $r_1 = r_2$ allow the coefficients in the sums to be calculated using an interpolation method. Essentially exact results for elastic and 1s - 2s scattering were presented for low and intermediate incident energies up to $\sim$ 30eV.

The generalisation of this approach to more complex systems (for example, including angular momentum states, complex atoms) was considered by Poet (1980) who attempted to solve the same model problem using a coupled partial differential equations approach, as a starting point to include angular momentum. The method produced results close to the exact ones but as the size of the problem increases with each electron the method is limited to cases with up to two or at most three active electrons. Further work by Poet (1981) on the same model, using a coupled channel approach in which continuum functions were treated numerically over a finite region of configuration space where exchange is important, and solutions were matched to asymptotic

(exchange free) solutions, gave rise to pseudoresonances at the discretised "continuum" energies.

Callaway and Oza (1984) extended Poet's (1978) method to calculate the total cross section for the model, and approximate ionisation cross sections calculated from pseudostate calculations compared favourably with bounds given by the exact method.

Pseudostates and The Poet Problem

Burke and Mitchell (1973) added pseudostates $\overline{3}s$, $\overline{4}s$, $\overline{5}s$ to a 1s-2s basis and produced elastic and 1s-2s singlet scattering cross section in the incident energy range 10 - 30eV. Pseudoresonances appeared at each pseudothreshold, fairly broad especially for inelastic scattering, with structure below and above the threshold. Burke and Mitchell noted that away from the pseudoresonances the results converged quickly with added pseudostates, and that cross sections averaged over the pseudothresholds exhibited an oscillatory convergence. On later comparison with Poet's results, the pseudostate calculations were seen to be a good improvement on 1s-2s-3s close coupling calculations away from pseudoresonances: for elastic cross sections where pseudoresonances were less pronounced the calculations with positive pseudostates were very close to the exact results away from the thresholds. The further work of Callaway and Oza (1983), using the algebraic variatonal method (Callaway

1978) to solve the coupled equations has been described in the discussion of T matrix averaging in chapter two. Their conclusions are considered in the next chapter. Increasing the basis size (Oza 1984) narrowed the pseudoresonances and gave converging results, although a judicious choice of pseudostates, to represent short range behaviour, and the averaging polynomial had the most effect in improving accuracy. In the next chapter we attempt, using the Schwinger principle, to remove pseudoresonant behaviour in a systematic way before the calculation of T matrix elements.

CHAPTER FIVE

The Schwinger Variational Method Applied to The "Poet" Model Problem

5.1 Introduction

The problem considered is a restricted model of electron hydrogen atom scattering in which it is assumed that the coordinate wavefunction is spherically symmetric with respect to both projectile and target electron positions. Thus all non zero angular momentum terms are ignored: the target electron occupies "s" states only, and the Coulomb interaction between the electrons is replaced by the leading term in its Legendre polynomial expansion. We may write the Schrödinger equation for the system as

$$\hat{H}\,\Psi_i^{(+)s}(r_1, r_2) = 0 \qquad (5.1.1)$$

where

$$\hat{H} = E + \tfrac{1}{2}\frac{d^2}{dr_1^2} + \tfrac{1}{2}\frac{d^2}{dr_2^2} - V_0(r_1) - V_0(r_2) - v_0(r_1, r_2)$$

E is the energy of the system

$$V_0(r) = -\frac{1}{r}$$

$v_0(r_1, r_2) = \frac{1}{r_>}$, $r_{>}^{<}$ is the $\begin{matrix}\text{greater}\\ \text{lesser}\end{matrix}$ of r_1 and r_2.

i denotes the incident channel and s denotes the total

electron spin.

We include the spatial symmetry/antisymmetry of the solution explicitly and write

$$\Psi_i^{(+)S}(r_1,r_2) = \Phi_i^{(+)S}(r_1,r_2) + (-1)^S \Phi_i^{(+)S}(r_2,r_1)$$

(5.1.2a)

$$\Phi_i^{(+)S}(r_1,r_2) = \sum_m{}' \phi_m(r_2) f_{mi}^{(+)S}(r_1)$$

(5.1.2b)

The ϕ_m are hydrogenic states ($\phi_m(r) = r \times R_{m0}(r)$) with associated energies ε_m, and the prime denotes that the sum includes integration over the continuum. The scattering solutions $f_{mi}^{(+)S}$ have boundary conditions:

$$f_{mi}^{(+)S}(r) \xrightarrow[r\to 0]{} 0$$

$$f_{mi}^{(+)S}(r) \xrightarrow[r\to\infty]{} \begin{cases} k_i^{-1} \sin k_i r \cdot \delta_{im} + T_{mi}^S e^{ik_m r} & ; E > \varepsilon_m \\ 0 & ; E < \varepsilon_m \end{cases}$$

$$k_i = \sqrt{2(E-\varepsilon_i)}$$

(5.1.3)

The $f_{mi}^{(+)S}$ should also obey certain orthogonality conditions as considered by Peterkop (1977) and in chapter one to give a unique solution.

In practical calculations it is usually assumed that the trial functions are flexible enough for these conditions to be modelled by the variational procedure and arise "automatically" in the determination of the wave function coefficients. The matter is considered and tested in

section 5.5A.

The problem may now be rewritten as

$$\hat{H}_o \, \phi_i^{(+)s}(r_1, r_2) = \left(V(r_1, r_2) - (-1)^s \hat{H} A \right) \phi_i^{(+)s}(r_1, r_2) \tag{5.1.4}$$

where

$$\hat{H}_o = E + \frac{1}{2}\frac{d^2}{dr_1^2} + \frac{1}{2}\frac{d^2}{dr_2^2} - V_o(r_2)$$

$$V(r_1, r_2) = V_o(r_1) + V_o(r_1, r_2)$$

A interchanges r_1 and r_2.

Equation (5.1.4) has a formal solution:

$$\phi_i^{(+)s}(r_1, r_2) = \chi_i(r_1, r_2) + \int_0^\infty \int dr_1' dr_2' \, G_o^{(+)}(E; r_1, r_1', r_2, r_2') \times \left\{ \left(V(r_1', r_2') - (-1)^s \hat{H} A \right) \phi_i^{(+)s}(r_1', r_2') \right\} \tag{5.1.5}$$

$\chi_i(r_1, r_2) = \phi_i(r_2) \frac{1}{k_i} \sin k_i r_1$, the unperturbed solution.

$G_o^{(+)}$ is the Green's function for the unperturbed Hamiltonian H_o

$$G_o^{(+)}(E; r_1, r_1', r_2, r_2') = \sum_m{}' \phi_m(r_2) \phi_m^*(r_2') \, g_{om}^{(+)}(E; r_1, r_1') \tag{5.1.7a}$$

$$g_{om}^{(+)}(E, r_1, r_1') = \frac{4}{\pi} \int_0^\infty dk' \frac{\sin k' r_1 \sin k' r_1'}{(2(E - \varepsilon_m) + i\epsilon - k'^2)}$$

$$= -\frac{2}{k_m} \sin k_m r_< \, e^{i k_m r_>} \tag{5.1.7b}$$

$$\hat{H}_o \, G_o^{(+)}(E; r_1, r_1', r_2, r_2') = \delta(r_1 - r_1') \, \delta(r_2 - r_2') \tag{5.1.8}$$

Substituting (5.1.7) into (5.1.6), letting $r_1 \to \infty$ and comparing with (5.1.2b) and (5.1.3), we see that the T-matrix element T^s_{mi} may be written:

$$T^s_{mi} = -2 \int_0^\infty\!\!\int dr_1\, dr_2\, \chi_m(r_1,r_2)\left(V(r_1,r_2) - (-1)^s \hat{H}A\right) \Phi_i^{(+)s}(r_1,r_2)$$

$$= -2 \langle \chi_m \mid V - (-1)^s HA \mid \Phi_i^{(+)s} \rangle$$

$$= -R_{mi} \qquad (5.1.9a)$$

Using (5.1.5) and the fact that $G_0^{(+)} = (G_0^{(-)})^*$ we may also express T^s_{mi} as:

$$T^s_{mi} = -2\{ \langle \Phi_m^{(-)s} \mid V-(-1)^s \hat{H}A \mid \Phi_i^{(+)s} \rangle$$

$$- \langle \Phi_m^{(-)s} \mid (V-(-1)^s \hat{H}A)\, G_0^{(+)} (V-(-1)^s \hat{H}A) \mid \Phi_i^{(+)s} \rangle \}$$

$$= T_{mi} \qquad (5.1.9b)$$

$$T^s_{mi} = -2 \langle \Phi_m^{(-)s} \mid V-(-1)^s \hat{H}A \mid \chi_i \rangle$$

$$= -S_{mi} \qquad (5.1.9c)$$

The expression $T^s_{mi} = \dfrac{R_{mi}\, S_{mi}}{T_{mi}}$ (5.1.10)

gives the Schwinger variational functional for T^s_{mi} when

$\Phi_i^{(+)S}(r_1, r_2)$ is replaced by an L squared trial function and the stationary value found.

With the definition of the T matrix (5.1.3), the cross section (without spin factor $\frac{1}{4}$ or $\frac{3}{4}$) is

$$\sigma_{mi}^{(S)} = 4 \frac{k_m}{k_i} \left| T_{mi}^{(S)} \right|^2 \qquad (5.1.11)$$

Using an alternate real K matrix formulation, (5.1.3) becomes

$$f_{mi}^{(+)S}(r) \underset{r \to 0}{\longrightarrow} 0$$

$$f_{mi}^{(+)S}(r) \underset{r \to \infty}{\longrightarrow} \begin{cases} k_i^{-1} \sin k_i r \, \delta_{im} + K_{mi}^{S} \cos k_i r & ; E > \varepsilon_m \\ 0 & ; E < \varepsilon_m \end{cases} \qquad (5.1.12)$$

Schwinger expressions may be found for K_{mi}^{S} using the principle value Green's function $G_o^P = R_o G_o^{(+)}$. Over a matrix of open channels

$$\underline{\underline{T}} = i \underline{\underline{k}}^{-1} \left(\underline{\underline{K}} + i \underline{\underline{k}}^{-1} \right)^{-1} \underline{\underline{K}} \quad ; \left\{ \underline{\underline{k}}^{-1} \right\}_{mn} = \delta_{mn} k_m^{-1} \qquad (5.1.13)$$

Our investigation concerns the use of different trial functions and approximations to the Green's function $G_o^{(+)}$ in the Schwinger principle. Section 5.2 details our successful use of the principle to solve the coupled channel problems with pseudostates of Burke and Mitchell (1973) and Callaway and Oza (1983). Section 5.3 describes our attempts to remove the pseudoresonances inherent in these problems by modification of the Green's function, and how the success of

this procedure is masked by the instabilities encountered when the Schwinger principle is applied to the full Poet problem without explicit full representation of the continuum. The latter sections describe our investigations of these instabilities and our attempts to remove them by various modifications of the principle.

5.2 The Pseudostate Coupled Channel Problem

5.2.A Theory

In this further restricted model the infinite number of bound and continuum hydrogenic states of the target electron is replaced by a finite set of L-squared functions, after the manner described in chapters one and two. A set of target pseudostates may be found by selecting M component Slater functions η_j and constructing

$$R_n(r) = \sum_{j=1}^{M} \eta_j(r)\, a_{jn}$$

$$\eta_j(r) = r^{l_j} e^{-\beta_j r} \quad ; \quad l_j \geq 1 \,, \; \beta_j > 0 \qquad (5.2.1)$$

The a_{jn} are determined by the requirements

$$\int_0^\infty dr\; R_n(r) \left(-\frac{d^2}{2dr^2} + V_0(r) \right) R_{n'}(r) = \delta_{nn'} \bar{E}_{n'} \qquad (5.2.2a)$$

$$\int_0^\infty dr\; R_n(r) R_{n'}(r) = \delta_{nn'} \qquad (5.2.2b)$$

The first N of these functions may be chosen as the target basis. Proper choice of the $\eta_j(r)$ allows the lowest hydrogen eigenstates to be included exactly, while the positive energy states represent the continuum as considered in chapter two and by Hazi and Taylor (1970) and Bassichis et al. (1975).

The coupled channel wavefunction is then defined as

$$\bar{\Phi}_i^{(+)S}(r_1,r_2) = \sum_{m=1}^{N} R_m(r_2)\,\bar{f}_{mi}^{(+)S}(r_1) \qquad (5.2.3)$$

$$\bar{f}_{mi}^{(+)S}(r) \underset{r\to 0}{\to} 0$$

$$\bar{f}_{mi}^{(+)S}(r) \underset{r\to\infty}{\to} \begin{cases} \bar{k}_i^{-1}\sin\bar{k}_i r\,\delta_{im} + \bar{T}_{mi}^{S} e^{i\bar{k}_m r} & ; E > \bar{\varepsilon}_m \\ 0 & ; E < \bar{\varepsilon}_m \end{cases}$$

$$\bar{k}_m = \sqrt{2(E-\bar{\varepsilon}_m)} \qquad (5.2.4)$$

The incident channel i should be included in the pseudostate sum. $\bar{\Phi}_i^{(+)S}$ must obey the equations

$$\int_0^\infty dr_2\, R_m(r_2)\left(\hat{H} + (-1)^S \hat{H}\hat{A}\right)\bar{\Phi}_i^{(+)S}(r_1,r_2) = 0 \qquad ; m = 1,2,..,N \qquad (5.2.5a)$$

Equations (5.2.5) are a set of coupled equations for the $\bar{f}_{mi}^{(+)S}(r_1)$:

$$\left(E + \tfrac{1}{2}\frac{d^2}{dr_1^2} - \bar{\varepsilon}_n\right)\bar{f}_{ni}^{(+)S}(r_1) = \sum_{m=1}^{N}\int_0^\infty dr_2\, R_n(r_2)\left\{\left(V(r_1,r_2) + (-1)^S\hat{H}\hat{A}\right)R_m(r_2)\,\bar{f}_{mi}^{(+)S}(r_1)\right\}$$

$$; n = 1,2,\ldots,N \qquad (5.2.5b)$$

They may be solved using the Green's functions

$$\bar{g}_{on}^{(+)}(E;r,r') = \frac{4}{\pi}\int_0^\infty dk' \frac{\sin k'r \sin k'r'}{(2(E-\bar{\varepsilon}_n)+i\epsilon - k'^2)}$$

$$= -\frac{2}{\bar{k}_n}\sin \bar{k}_n r_< e^{i\bar{k}_n r_>}$$

(5.2.6)

$$\left(E + \frac{1}{2}\frac{d^2}{dr^2} - \bar{\varepsilon}_n\right)\bar{g}_{on}^{(+)}(E;r,r') = \delta(r-r')$$

(5.2.7)

Formally

$$\bar{f}_{ni}^{(+)s}(r_1) = \delta_{ni}\sin \bar{k}_i r_1 + \int_0^\infty dr_1'\, \bar{g}_{on}^{(+)}(E;r_1,r_1')\sum_{m=1}^{N}\int_0^\infty dr_2' R_n(r_2')$$

$$\times\left\{\left(V(r_1',r_2') - (-1)^s\hat{H}A\right)R_m(r_2')\,\bar{f}_{mi}^{(+)s}(r_1')\right\}$$

$$; \; n = 1, 2, \ldots, N$$

(5.2.8)

In terms of $\bar{\Phi}_i^{(+)s}$,

$$\bar{\Phi}_i^{(+)s}(r_1,r_2) = \chi_i(r_1,r_2) + \int_0^\infty\int dr_1' dr_2'\, \bar{G}_o^{(+)}(E;r_1,r_1',r_2,r_2')\left(V(r_1',r_1') - (-1)^s\hat{H}A\right)\bar{\Phi}_i^{(+)s}(r_1',r_2')$$

(5.2.9)

$$\bar{G}_o^{(+)}(E;r_1,r_1',r_2,r_2') = \sum_{n=1}^{N} R_n(r_2)R_n(r_2')\,\bar{g}_{on}^{(+)}(E;r_1,r_1')$$

(5.2.10)

The coupled channel T matrix element $\bar{T}_{mi}^{s}$ may thus be written

$$\bar{T}_{mi}^{s} = -2\langle \chi_m | V - (-1)^s\hat{H}A | \bar{\Phi}_i^{(+)s}\rangle$$

(5.2.11)

$\bar{T}^{s}_{mi}$ only has physical meaning as an approximation to T^{s}_{mi} when the target states in channels m and i are exact hydrogen functions, and as discussed by Burke and Mitchell (1973) and Callaway and Oza (1983), away from the pseudothresholds. As in the general Poet case, a Schwinger variational principle for $\bar{T}^{s}_{mi}$ may be formed using equations (5.2.11) and (5.2.9). This principle is a restricted form of the general principle (5.1.10) in which $G^{(+)}_{o}$ is replaced by $\bar{G}^{(+)}_{o}$ in the denominator, and the trial function is of the form

$$\Phi^{(+)}_{i\,tr}(r_1, r_2) = \sum_{m=1}^{N} \sum_{j=1}^{NTR} R_m(r_2)\, C_{jm}\, \Theta_{jm}(r_1)$$

(5.2.12)

The NTR scattering trial functions Θ_{jm} in each channel represent the $\bar{f}^{(+)s}_{mi}$. As discussed in chapter four, one advantage of the Schwinger principle is that they may be L-squared functions and need not obey the long distance boundary condition for the $\bar{f}^{(+)s}_{mi}$.

The method requires construction of the following matrix elements:

$$\frac{1}{k_m} \langle R_i(r_2)\, \Theta_{ji}(r_1) \mid V - (-1)^s \hat{H} A \mid R_m(r_2) \sin k_m r_1 \rangle$$

: numerator elements

(5.2.13a)

$$\langle R_i(r_2)\, \Theta_{ji}(r_1) \mid V - (-1)^s \hat{H} A \mid R_{i'}(r_2)\, \Theta_{ji'}(r_1) \rangle$$

: non Green's denominator elements

(5.2.13b)

$$-\sum \alpha_m \frac{2}{\bar{k}_m} \langle R_i(r_1)\,\Theta_{ji}(r_1)\,|V-I|^s \hat{H}A\,|R_m(r_2)\sin\bar{k}_m r_2\rangle\langle R_m(r_2)\sin\bar{k}_m r_2\,|V-I|^s \hat{H}A\,|R_{i'}(r_2)\,\Theta_{j'i'}(r_1)\rangle$$

$$\alpha_m = \begin{cases} 1 & : E > \bar{\varepsilon}_m \\ 0 & : E < \bar{\varepsilon}_m \end{cases}$$

: imaginary Green's matrix elements

(5.2.13c)

The real Green's elements are most easily constructed using the spectral form of the Green's function $\bar{g}^{(+)}_{on}$:

$$\sum_{m=1}^{N} \frac{4}{\pi} P\int_0^\infty \frac{dk'}{(\bar{k}_m^2 - k'^2)} \langle R_i(r_2)\,\Theta_{ji}(r_1)\,|V-I|^s \hat{H}A\,|R_m(r_2)\sin k' r_1\rangle\langle R_m(r_2)\sin k' r_1\,|V-I|^s \hat{H}A\,|R_{i'}(r_2)\,\Theta_{j'i'}(r_1)\rangle$$

(5.2.13d)

(P represents a principal value integral.)

As well as using the Schwinger variational principle to solve for the complex T matrix elements, we also solved for the real K matrix elements by ignoring the imaginary terms. A T matrix was then constructed from the K matrix of open channels (including elements $\bar{K}_{mi}$ for unphysical open channels). In the coupled channel problem the two methods gave identical results. An S matrix of open channels formed using the complex method was always unitary to within 4-5 decimal places.

5.2.B Initial Investigations : 1s-2s-3s Close Coupling

We initially considered the 1s-1s static exchange case discussed by Moiseiwitsch (1983) and the 1s-2s and 1s-2s-3s coupled channel results of Burke and Mitchell (1973) in order to test the basic method and also different ways of

representing the Green's functions $\bar{g}^{+}_{on}$. Matrix elements (5.2.13) were formed analytically apart from the energy integral in each Green's function which was performed using standard Gaussian quadrature rules and also by the use of an L-squared equivalent quadrature on the Slater-Laguerre basis described in chapter two and Appendix Two. The principal value integrals for the open channels were effected by a subtraction of the kind discussed in chapter three.

(i) Numerical Method

For open channels:

$$\mathrm{Re}\ \bar{g}^{+}_{on}(E;r,r') = \frac{4}{\pi}\int_0^{\infty} dk\, \frac{(\sin kr \sin kr' - \sin \bar{k}_n r \sin \bar{k}_n r')}{(\bar{k}_n^2 - k^2)} \quad ; \ \bar{k}_n^2 > 0 \qquad (5.2.14a)$$

This may be rewritten:

$$\mathrm{Re}\ \bar{g}^{+}_{on}(E;r,r') = \frac{4}{\pi} \times \frac{\bar{k}_n}{2}\int_{-1}^{1} dx\, \frac{(\sin k(x) r \sin k(x) r' - \sin \bar{k}_n r \sin \bar{k}_n r')}{(\bar{k}_n^2 - k^2(x))}$$

$$+ \frac{4}{\pi} \times 2\bar{k}_n \int_{-1}^{1} \frac{dx}{(1-x)^2}\, \frac{(\sin k'(x) r \sin k'(x) r' - \sin \bar{k}_n r \sin \bar{k}_n r')}{(\bar{k}_n^2 - k'^2(x))} \qquad (5.2.14b)$$

The integral is split into two, from $(0, \bar{k}_n)$ and from $(\bar{k}_n, \infty)$, and the following transformations used:

$$k(x) = \tfrac{1}{2}\bar{k}_n(1+x) \quad : \quad 0 \le k \le \bar{k}_n$$

$$k'(x) = \frac{2\bar{k}_n}{(1-x)} \quad : \quad \bar{k}_n \le k' \le \infty$$

$$-1 \le x \le 1 \qquad (5.2.15)$$

A Gauss Legendre quadrature is then used for the integrals. An advantage of this method is that, taken on

its own, the subtraction part of the integral sums exactly to zero if the same rule is used for both integrals, since Gauss Legendre quadrature ab scissae are evenly distributed and the corresponding weights are symmetric about x = 0.

$$0 = \frac{4}{\pi} P \int_0^\infty \frac{dk}{(\bar{k}_n^2 - k^2)} = \frac{2\bar{k}_n}{\pi} P \int_{-1}^{1} dx \frac{1}{\bar{k}_n^2 \left(1 - \frac{1}{4}(1+x)^2\right)} + \frac{8\bar{k}_n}{\pi} P \int_{-1}^{1} \frac{dx}{(1-x)^2} \frac{1}{\bar{k}_n^2 \left(1 - \frac{4}{(1-x)^2}\right)}$$

$$= \frac{8}{\pi \bar{k}_n} P \int_{-1}^{1} \frac{dx\, 4x}{(9-x^2)(1-x^2)} \qquad (5.2.16)$$

For closed channels ($\bar{k}_n^2 < 0$) the subtraction is not required. A channel independent transformation for the whole range was used, and a Gauss Legendre quadrature performed .

$$k = \frac{\lambda(1+x)}{(1-x)} \quad ; \quad 0 \leq k \leq \infty \quad , \quad -1 \leq x \leq 1 \qquad (5.2.17)$$

λ was chosen to give a reasonable range of k values: a maximum Gaussian k value of k = 77.5 ($\frac{1}{2}k^2$ = 3000) was generally used.

(ii) L-squared Method

As detailed in chapter two and Appendix Two, the kinetic Hamiltonian is exactly soluble in an infinite series of Slater-Laguerre functions, and the equivalent quadrature representation with a finite basis has known weights/normalisation constants. The Green's function $\bar{g}_{nn}^{(+)}$ was represented by such a sum of N_L basis functions, the

subtraction terms in the open channels being interpolated from the matrix elements equivalent to (5.2.13) of the L-squared eigenfunctions $\phi_\lambda(r)$ (these functions should not be confused with the hydrogenic functions $\phi_m(r)$).

$$\mathrm{Re}\ \bar{g}_{on}^{(+)}(E;r,r') \simeq \sum_{\lambda=1}^{N_L} \frac{\phi_\lambda(r)\,\phi_\lambda(r')}{(\bar{k}_n^2 - k_\lambda^2)} \quad ; \ \bar{k}_n^2 < 0$$

$$\mathrm{Re}\ \bar{g}_{on}^{(+)}(E;r,r') \simeq \sum_{\lambda=1}^{N_L} \frac{\phi_\lambda(r)\,\phi_\lambda(r') - w_\lambda \frac{\bar{k}_n}{k_\lambda}\left[\frac{\phi(\mu,r)\,\phi(\mu,r')}{w(\mu)}\right]_{E(\mu)=\frac{1}{2}k_\lambda^2}}{(\bar{k}_n^2 - k_\lambda^2)} \quad ; \ \bar{k}_n^2 > 0 \qquad (5.2.18)$$

(iii) Comparison

In comparing the results for static exchange, 1s-2s, and 1s-2s-3s scattering using the two representations of the Green's function, the numerical method was most stable. Examining Green's matrix elements (5.12.13d), convergent results were obtained using 40-60 points in the Gauss quadrature for each integral. For the equivalent quadrature method to give comparable results a greater number of L-squared functions were required and no advantage was gained. It was initially hoped that the number of L-squared functions required would be relatively small, so that this method would be more efficient. For the infinite series with eigenvalue k (see Appendix Two for precise definitions):

$$\sin kr = N(k) \sum_{m=1}^{\infty} c_m(k)\, \chi_m(r) \qquad (5.2.19_a)$$

$X_m(r)$ is a Slater-Laguerre basis function.

For the finite series:

$$\frac{1}{\sqrt{w_\lambda}} \phi_\lambda(r) = N(k_\lambda) \sum_{m=1}^{N_L} c_m(k_\lambda) X_m(r) \simeq \sin k_\lambda r \quad , r < r_0 \qquad (5.2.19b)$$

The higher order functions $X_m(r)$ are only large for large r. Depending on the potential parameters (determining how fast the potentials decayed) and the scaling parameter in the Slater-Laguerre functions, different large numbers (between 50-150) of L-squared functions were needed to give convergent Green's matrix elements, and the L-squared method was dropped in favour of the numerical method.

Using the numerical method, the Moiseiwitsch (1983) static exchange, and 1s-2s and 1s-2s-3s coupled channel results of Burke and Mitchell (1973) were reproduced. Diagonalisations were carried out using a complex eigenproblem routine in the NAG library. We achieved converged cross sections using trial functions of the form

$$\theta_{ji}(r) = \theta_j(r) = r^{n_j} e^{-\lambda_j r} \quad ; \; n_j \geq 1 \; , \; \lambda_j > 0 \; , \; j = 1, 2, \ldots NTR \qquad (5.2.20)$$

and NTR > 10. Table 5.1 compares our converged 1s-2s-3s results with those of Burke and Mitchell. We then investigated the use of the Schwinger method for the coupled channel approximation to the Poet problem with positive pseudostates, as considered by Callaway and Oza (1983).

TABLE 5.1

1S-2S-3S CLOSE COUPLING

CROSS SECTIONS (SINGLET S=0)

ENERGY	1S-1S		1S-2S		1S-3S	
	BM	SCH	BM	SCH	BM	SCH
0.5	0.3052	0.3068	0.0419	0.0419	0.0146	0.0146
0.605	0.2034	0.2035	0.0584	0.0585	0.0184	0.0184
0.72	0.1432	0.1442	0.0511	0.0513	0.0151	0.0151
0.85	0.1133	0.1137	0.0396	0.0398	0.0114	0.0114
1.0	0.0959	0.0964	0.0297	0.0297	0.0084	0.0084
1.125	0.0873	0.0877	0.0238	0.0237	0.0066	0.0066

BM : Burke & Mitchell (1973)

SCH : Present Work

Atomic units (as described in chapter one) are used in all tables. Cross sections include the appropriate statistical spin factor. Energies shown are incident electron energies.

5.2.C The Positive Energy Pseudostate Problem

The form and pseudostate energies of two bases of Callaway and Oza (1983) that we examined are shown in table 5.2. Basis B includes the 1s and 2s states exactly, and two further short range orbitals are added. This basis gave Callaway and Oza the most accurate 1s-1s and 1s-2s cross sections of those they considered, after T-matrix fitting. The unfitted results contain a pseudoresonance approximately in the middle of the incident energy range we are considering, making it useful for further investigation. Basis D contains the 1s, 2s and 3s states exactly, and has also been previously used by Huck (1957). Also shown in table 5.2 is an eleven state basis used in section 5.5.

It was found that the Slater functions Θ_j were not sufficiently flexible to give converged results in this problem: the large numbers (NTR $\sim$ 20) required meant that the resulting $N^2 \times NTR^2$ matrix was too large to be accurately diagonalised. The addition to the expansion in the open channels of asymptotic terms (5.2.21) improved the results considerably.

$$j = NTR+1 \quad : \quad \Theta_{ji}(r) = \sin \bar{k}_i r$$

$$j = NTR+2 \quad : \quad \Theta_{ji}(r) = (1 - e^{-\gamma_i r}) \cos \bar{k}_i r \quad ; \quad \gamma_i > 0 \qquad (5.2.21)$$

Converged results with NTR $\sim$ 13, or 15 trial functions per open channel were found. Since the Schwinger principle does not require the trial function to have the correct

TABLE 5.2

PARAMETERS AND ENERGIES OF THREE PSEUDOSTATE BASIS SETS

BASIS SET	j	l_j	ζ_j	$\bar{e}_j$	$(\bar{e}_j + 0.5)$
B	1	1	1.0	-0.5000	0.0000
	2	1	0.5	-0.1250	0.3750
	3	2	0.5	-0.0261	0.4739
	4	2	1.0	0.3405	0.8405
	5	1	1.5	3.1337	3.5337
D	1	1	1.0	-0.5000	0.0000
	2	1	0.5	-0.1250	0.3750
	3	2	0.5	-0.0556	0.4444
	4	1	1/3	-0.0312	0.4688
	5	2	1/3	-0.0086	0.4914
	6	3	1/3	0.0979	0.5979
	7	1	0.2	1.0198	1.5198
G	1	1	1.0	-0.5000	0.0000
(M = 12)	2	1	0.5	-0.1250	0.3750
(N = 11)	3	2	0.5	-0.0556	0.4444
	4	1	1/3	-0.0312	0.4688
	5	2	1/3	-0.0197	0.4803
	6	3	1/3	-0.0122	0.4878
	7	1	1.5	0.0210	0.5210
	8	2	1.5	0.1213	0.6213
	9	3	1.5	0.3800	0.8800
	10	4	1.5	1.0562	1.5562
	11	1	0.1	3.1989	3.6989
	12	2	0.1	(15.76)	

Units and symbols are as described in table 5.1 and in the text. Energies were calculated accurately to eight significant figures and are shown to four decimal places for convenience. The last column shows the pseudothresholds in terms of the incident electron energy, for reference to later figures.

asymptotic form, it was decided that the improvement was due to the use of oscillatory functions. More flexible trial functions (5.2.22) were introduced, all matrix elements still being formed analytically with the exception of the Green's integral.

$$\Theta_{ji}(r) = r^{n_{ji}} g_{ji}(r) e^{-\lambda_{ji} r} \quad ; \quad j = 1,2,\ldots,NTk$$

$$n_{ji} \geq 1 \quad ; \quad \lambda_{ji} > 0$$

$$g_{ji}(r) = \begin{cases} \sin(\alpha_{ji} |\bar{k}_i| r) \\ \cos(\alpha_{ji} |\bar{k}_i| r) \end{cases}$$

(5.2.22)

It was found that Callaway and Oza's results were reproduced using 10-12 or more such functions per channel over a wide choice of input parameters.

For solving the coupled channel problem this would seem satisfactory, but for our further investigation into possible removal of pseudoresonances before construction of the T matrix, the explicit inclusion of pseudochannel energy dependence in the Θ_{ji} resulting in matrix elements (5.2.13) that are intrinsically not smooth over the pseudoenergies with respect to incident electron energy, is self defeating. Further investigation showed that efficiently converged results were possible as long as oscillatory functions were used in the physical channels. Since we are concerned with excitation in the intermediate energy region, we kept the

oscillating functions for the negative energy channels and used Slater trial functions for the positive pseudostates, choosing cosine functions for the g_{ji} with $\alpha_{ji} = 0$. Results were not affected by further suppression of pseudochannel dependence of input parameters, resulting in the form (5.2.23):

$$\Theta_{ji}(r) = \begin{cases} r^{n_j} \begin{matrix} \sin \\ \cos \end{matrix} (\alpha_j |\bar{k}_i| r) e^{-\lambda_j r} & ; \bar{\varepsilon}_i < 0 \\ r^{m_j} e^{-\mu_j r} & ; \bar{\varepsilon}_i > 0 \end{cases}$$

$$n_j, m_j \geq 1 \; ; \; \lambda_j, \mu_j > 0 \qquad (5.2.23)$$

11-14 such functions per channel produced converged results. Table 5.3 compares our results with Callaway's and Oza's, and figure 5.1 shows elastic and 1s-2s cross sections before and after T matrix fitting for basis B in the spin zero case. As described by Callaway and Oza, the coupled channel method gives results indistiguishable from Poet's (1978) in the spin one case, but gives rise to visible pseudoresonances in the spin zero case.

The triplet case may be expected to be simpler to solve than the singlet case, as the antisymmetry of the spatial wave function restricts the strength of the interaction between the electrons, and associated distortion and excitation processes, as they are kept apart by the Pauli principle. After T-matrix fitting, all of the Callaway and Oza bases gave elastic cross sections correct to within 3% and 1s-2s cross sections correct to within 8% of Poet's

TABLE 5.3

(i) S = 1 Data (Basis D)

Cross Sections

Energy	1s-1s		1s-2s (*10E-1)	
	CO	SCH	CO	SCH
0.605	2.3005	2.3005	0.035	0.035
0.72	1.8336	1.8336	0.048	0.048
0.85	1.4607	1.4607	0.055	0.055
1.0	1.1587	1.1587	0.058	0.058
1.125	0.9750	0.9750	0.057	0.057
1.25	0.8330	0.8331	0.056	0.055
1.5	0.6310	0.6310	0.051	0.051
1.75	0.4972	0.4972	0.046	0.046
2.0	0.4037	0.4037	0.041	0.041

Energy	1s-3s (*10E-2)		2s-3s	
	CO	SCH	CO	SCH
0.605	0.024	0.024	0.134	0.134
0.72	0.052	0.052	0.102	0.102
0.85	0.076	0.076	0.073	0.073
1.0	0.092	0.090	0.052	0.052
1.125	0.098	0.099	0.041	0.041
1.25	0.101	0.098	0.033	0.032
1.5	0.100	0.099	0.022	0.022
1.75	0.093	0.093	0.016	0.016
2.0	0.084	0.084	0.013	0.013

CO : Callaway and Oza (1984)

SCH : Present Work

Units are as in table 5.1.
Where indicated, cross sections should be multiplied by the appropriate factor of 10.

TABLE 5.3

(ii) S = 0 Data (Basis B)

Cross Sections

ENERGY	1s-1s		1s-2s (*10E-1)	
	CO	SCH	CO	SCH
0.605	0.2501	0.2501	-	0.307
0.63	-	0.2320	0.247	0.247
0.72	0.1926	0.1926	-	0.307
0.85	0.1724	0.1724	0.149	0.149
1.0	0.1340	0.1340	0.147	0.147
1.125	0.1131	0.1131	-	0.140
1.25	-	0.1001	0.123	0.123
1.5	0.0866	0.0866	0.083	0.084
1.75	0.0772	0.0776	0.055	0.055

CO : Callaway and Oza (1984)

SCH : Present Work

Units are as in table 5.1.
Where indicated, cross sections should be multiplied by the appropriate factor of 10.

FIGURE 5.1

CROSS SECTIONS AGAINST INCIDENT ELECTRON ENERGY FOR BASIS B.

Models are as described in the text. Units are as described in Table 5.1.

(i) 1S - 1S Cross Sections

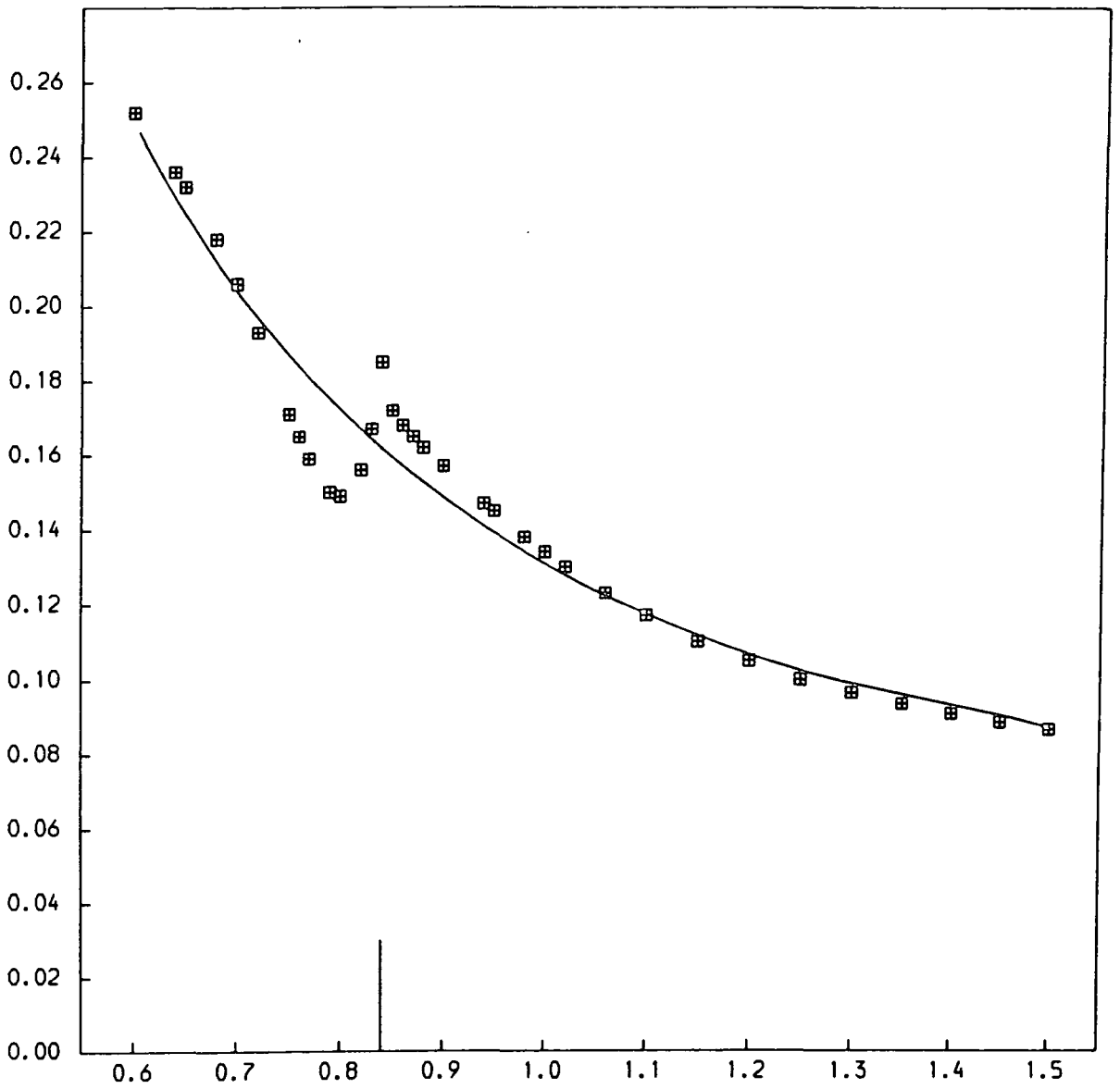

S = 0 The points are unaveraged results. The lines are the averaged results. Trial / Green's function positive pseudostate thresholds in the range are marked (see Table 5.2).

FIGURE 5.1

CROSS SECTIONS AGAINST INCIDENT ELECTRON ENERGY FOR BASIS B.

Models are as described in the text. Units are as described in Table 5.1.

(ii) 1S - 2S Cross Sections

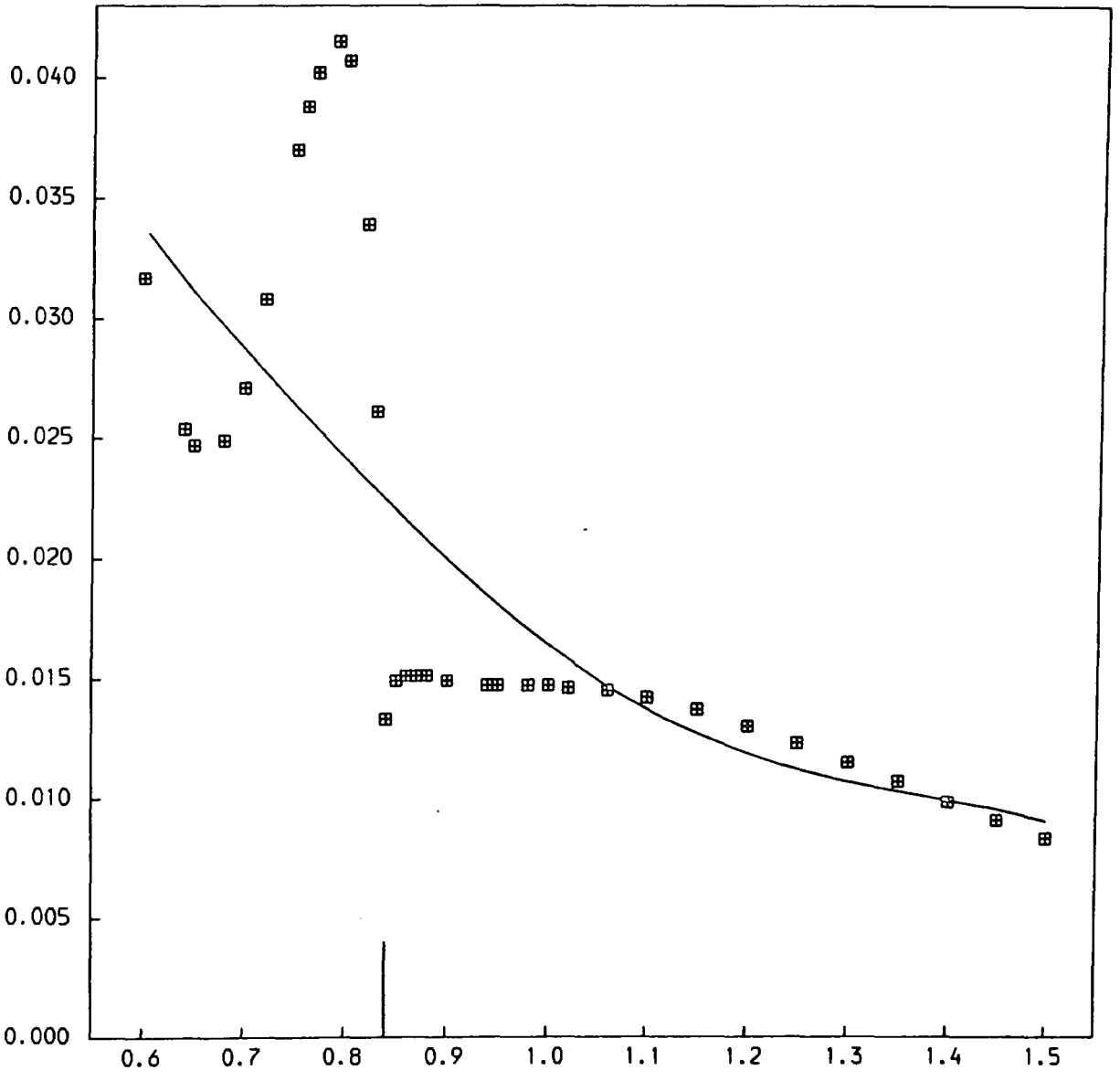

S = 0 The points are unaveraged results. The lines are the averaged results. Trial / Green's function positive pseudostate thresholds in the range are marked (see Table 5.2).

results for the singlet case, although basis B gave better results, the elastic cross section being indistinguishable from Poet's and the 1s-2s cross section being good to within 3%. As noted by Oza (1984), the pseudothreshold structure gets narrower as more positive pseudostates are used in the basis. Having found the Schwinger method a good one for the coupled channel problem, our further work concerns the attempted elimination of pseudoresonances for the singlet case.

5.3 Beyond The Coupled Equations : Elimination of Pseudoresonances

We can consider the coupled channel problems as Schwinger variational principles for the Poet problem in which the pseudostates used in the trial function and the approximation to the Green's function $G_o^{(+)}$ coincide : our original aim in using the principle was to expand the representation of the Green's function and investigate the origin of the pseudoresonances. We hoped to remove pseudoresonances by smoothing out the matrix elements (5.2.13) with respect to incident electron energy before solving for the T-matrix elements. Since our choice of trial function ensured that in the energy region of interest the numerator and non Green's denominator elements were smooth as required, this involved smoothing the Green's elements: although the Green's function $\bar{G}_o^{(+)}$ is continuous

with respect to incident energy as it passes across a threshold, its derivatives are not, as detailed in figure 5.2. This is to be contrasted with the smooth behaviour of $G_o^{(+)}$. One possibility that was considered was to apply a fitting procedure to the matrix elements (5.2.13d) away from the thresholds, and comparison tests between matrix elements containing $\overline{G}_o^{(+)}$ and $G_o^{(+)}$ are detailed below. Investigation of the effect on the cross sections of this approach was hampered by an unexpected phenomenon that has severely limited our use of the Schwinger principle beyond the coupled channel problem. The resulting T-matrix elements contain false resonances that are not related to the Green's function but occur numerically in the solution of the stationary value problem. These resonances appear and disappear as different trial functions are used, and badly affect the convergence of the T matrix. They seem to occur in more complicated problems: there are no false resonances in the coupled channel case which is essentially a one coordinate problem with all target electron information supplied, and in the more general problems they do not occur if electron exchange is ignored except in a few very complex cases. In the exchange case, these resonances do not appear if the trial function target expansion contains all of the states used in the Green's function. Illustrative results appear below and in section 5.4.

In the rest of this chapter, the results displayed were obtained by the complex T matrix method unless explicitly

FIGURE 5.2

Behaviour Of Coupled Channel Green's Function $\bar{\bar{G}}_0^+$

At A Threshold.

$$\bar{\bar{G}}_0^+ = \sum_{m=1}^{N} R_m(r_2)\, R_m(r_2')\, \bar{g}_{0m}^+(E; r_1, r_1')$$

We consider the incident energy crossing the positive threshold n. $\bar{k}_n^2$ passes through zero and becomes positive.
The terms $m \neq n$ in $\bar{\bar{G}}_0^+$ vary smoothly.

$$\mathrm{Im}\ \bar{g}_{0n}^+(E; r, r') = \begin{cases} 0 & ; \bar{k}_n^2 < 0 \\ -\frac{2}{\bar{k}_n} \sin \bar{k}_n r \sin \bar{k}_n r' & ; \bar{k}_n^2 > 0 \end{cases}$$

$$\frac{d}{d\bar{k}_n^2}\left(\mathrm{Im}\ \bar{g}_{0n}^+(E; r, r')\right) = X$$

$$X = \begin{cases} 0 & ; \bar{k}_n^2 < 0 \\ \frac{1}{\bar{k}_n^2}\left(\sin \bar{k}_n r \left(\frac{1}{\bar{k}_n} \sin \bar{k}_n r' - r' \cos \bar{k}_n r'\right) - r \cos \bar{k}_n r \sin \bar{k}_n r'\right) & ; \bar{k}_n^2 > 0 \end{cases}$$

$$\lim_{\bar{k}_n^2 \to 0^+} X = -\frac{r r'}{\bar{k}_n}$$

$$\mathrm{Re}\ \bar{g}_{0n}^+(E; r, r') = \begin{cases} -\frac{2}{\bar{K}_n} \sinh \bar{K}_n r_< \, e^{-\bar{K}_n r_>} & ; \bar{k}_n^2 < 0 \\ -\frac{2}{\bar{k}_n} \sin \bar{k}_n r_< \cos \bar{k}_n r_> & ; \bar{k}_n^2 > 0 \end{cases}$$

$$(\bar{k}_n^2 = -\bar{K}_n^2,\ \bar{k}_n^2 < 0)$$

FIGURE 5.2

$$\frac{d}{d\bar{k}_n^2}\left(\mathrm{Re}\,\bar{g}_{on}^{+}(E;r,r')\right) = Y$$

$$Y = \begin{cases} -\dfrac{e^{-\bar{K}_n r_>}}{\bar{K}_n^2}\left(\left(\dfrac{1}{\bar{k}_n}\sinh\bar{K}_n r_< - r_< \cosh\bar{K}_n r_<\right) + r_> \sinh\bar{K}_n r_<\right) & ; \bar{k}_n^2 < 0 \\ \dfrac{1}{\bar{k}_n^2}\left(\left(\dfrac{1}{\bar{k}_n}\sin\bar{k}_n r_< - r_< \cos\bar{k}_n r_<\right)\cos\bar{k}_n r_> + r_> \sin\bar{k}_n r_< \sin\bar{k}_n r_>\right) & ; \bar{k}_n^2 > 0 \end{cases}$$

$$\lim_{\bar{k}_n^2 \to 0^-} Y = -\frac{r_< r_>}{\bar{K}_n} \quad ; \quad \lim_{\bar{k}_n^2 \to 0^+} Y = r_<\left(\tfrac{1}{3}r_<^2 + r_>^2\right)$$

The continuum Green's function G^{+} varies smoothly. The behaviour of $\bar{G}_o^{+}$ does not match that of G_o^{+} close to the thresholds, as shown by the broad pseudoresonant structure of the T matrix elements around them.

described as otherwise. The K matrix method was always more unstable, containing false resonances in virtually all cases, and giving unconverged results whether a matrix of open trial function channels or of channels common to both the trial function and Green's function was used. This might be expected as T matrix elements formed using the K matrix method require solution of the stationary value problem for several channel combinations, and numerical errors are compounded. Similarly the open channel S matrix formed using the complex method was generally only unitary to within about a factor of ten in these more general problems.

A. Illustration of false resonances

Our first tests beyond the coupled channel problem involved using different pseudostate expansions in the Green's function and trial function, in the hope that pseudoresonances would be suppressed. It was found that results did not quickly converge, as false resonances were introduced. This is illustrated in figure 5.3 where the elastic cross section for a basis B trial function and basis D Green's function is shown for various values of NTR. Basis D pseudoresonances appear just outside the range of energies shown. A false resonance with NTR = 10 vanishes for NTR = 12 and a smooth cross section results. However, increasing NTR to 14 brings in further false resonances

FIGURE 5.3

CROSS SECTIONS AGAINST INCIDENT ELECTRON ENERGY

TRIAL FUNCTION BASIS B, GREEN'S FUNCTION BASIS D ELASTIC CROSS SECTIONS

Models and symbols are as described in the text. Units are as described in Table 5.1.

(i) NTR = 10

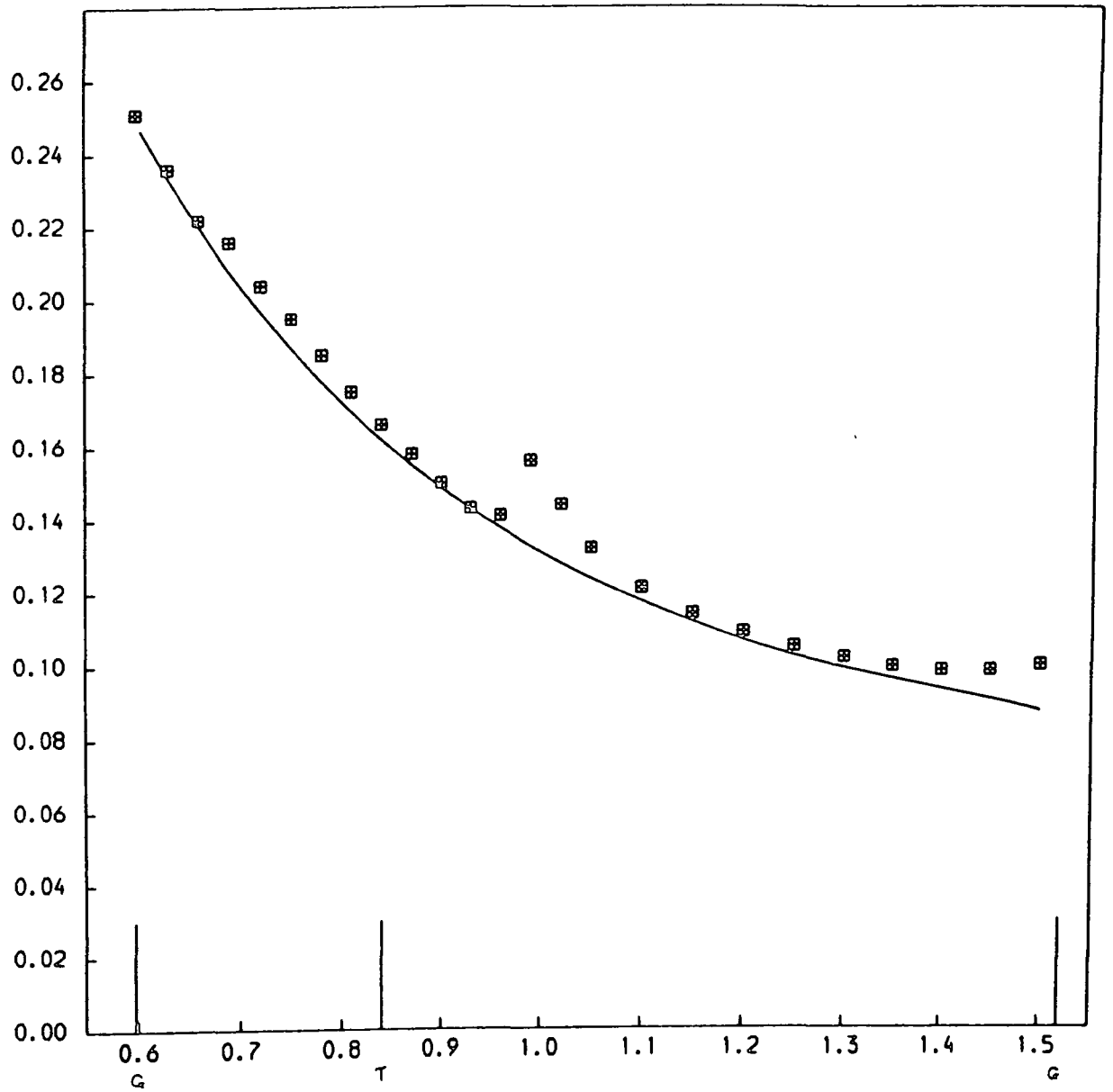

The line shows the exact results. Trial (T) and Green's (G) function positive pseudostate thresholds in the range are marked (see Table 5.2).

FIGURE 5.3

CROSS SECTIONS AGAINST INCIDENT ELECTRON ENERGY

TRIAL FUNCTION BASIS B, GREEN'S FUNCTION BASIS D ELASTIC CROSS SECTIONS

Models and symbols are as described in the text. Units are as described in Table 5.1.

(ii) NTR = 12

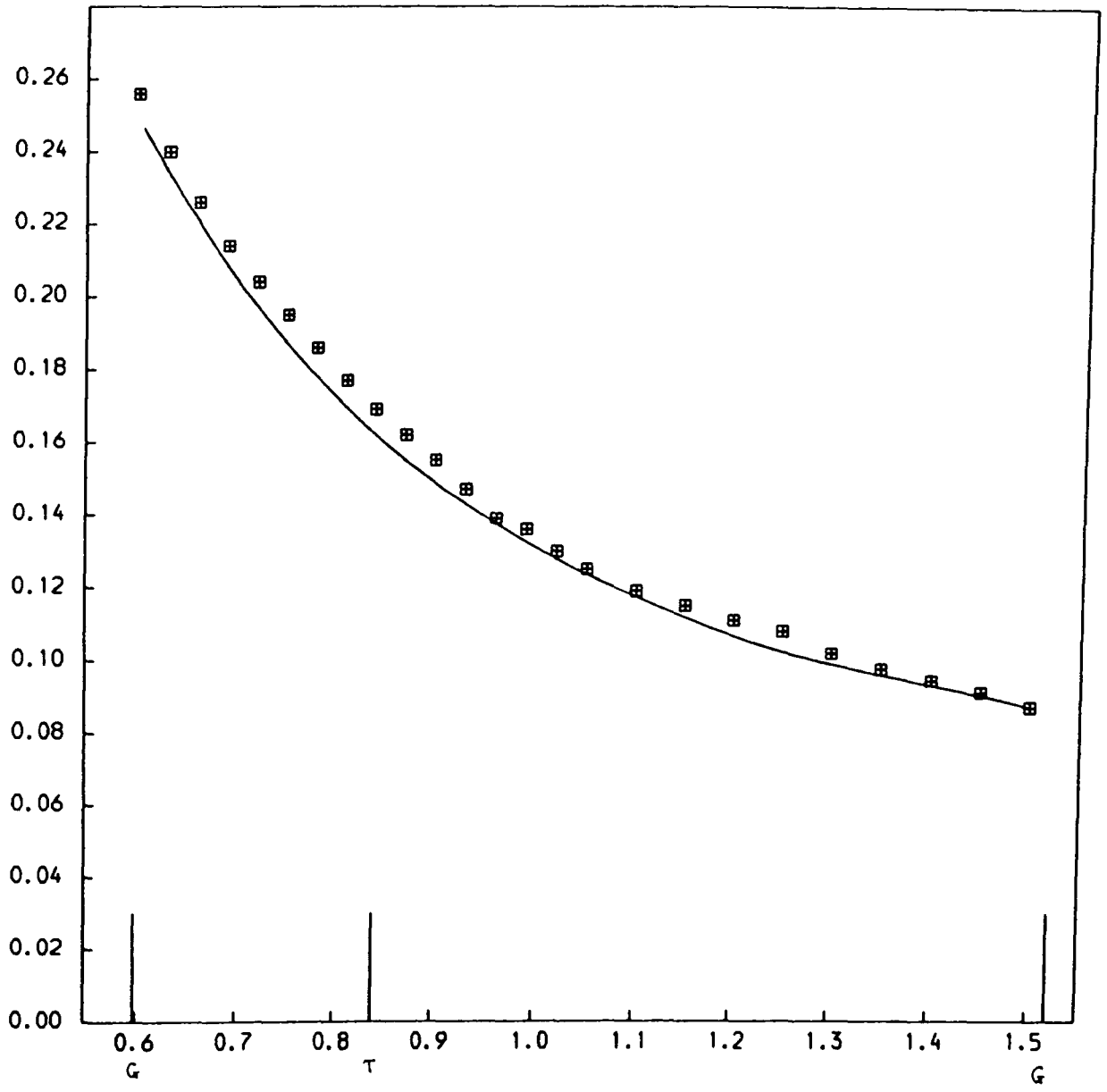

The line shows the exact results. Trial (T) and Green's (G) function positive pseudostate thresholds in the range are marked (see Table 5.2).

FIGURE 5.3

CROSS SECTIONS AGAINST INCIDENT ELECTRON ENERGY

TRIAL FUNCTION BASIS B, GREEN'S FUNCTION BASIS D ELASTIC CROSS SECTIONS

Models and symbols are as described in the text. Units are as described in Table 5.1.

(iii) NTR = 14

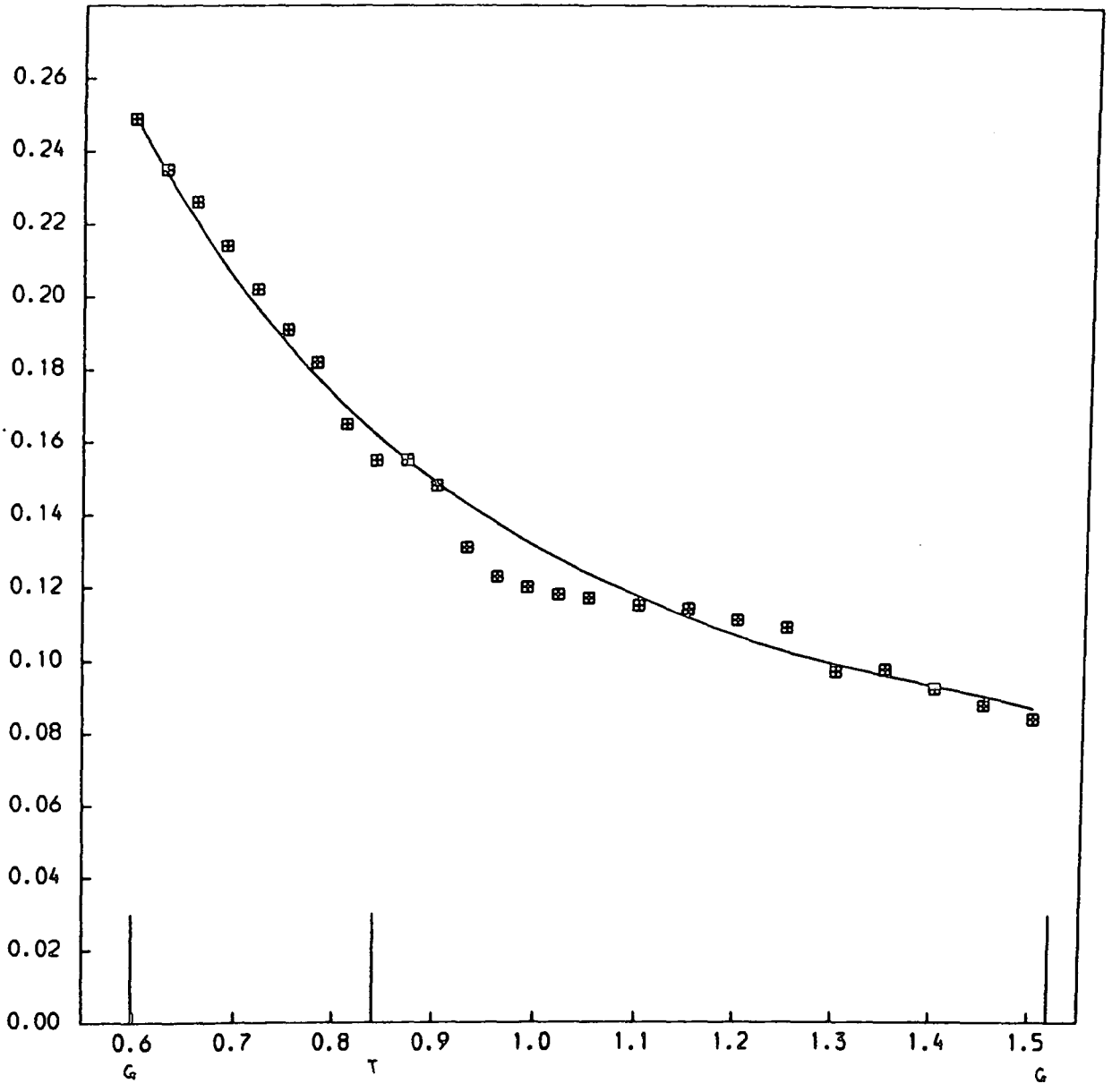

The line shows the exact results. Trial (T) and Green's (G) function positive pseudostate thresholds in the range are marked (see Table 5.2).

which upset the convergence. Further increase and variation of input parameters did not recover the smooth curve which would appear to be due to a fortuitous choice of trial function. The 1s-2s cross section remained unstable and unphysical for all values of NTR. Other tests with a basis B Green's function and basis D trial function gave unconverged inelastic cross sections and elastic cross sections with false resonances although there was a vague resemblance to the basis B close coupling results. The false resonances did not occur in the non exchange case where results were convergent. Figure 5.4 shows cross sections without exchange for basis B close coupling and for a basis D trial, basis B Green's function. The similarity between the two sets of results suggests if the trial function approximately "contains" the Green's function, then additional terms are "ignored" by the method and the close coupling results are reproduced. This is investigated further in section 5.4 and also appears true for the exchange case when the Green's function is exactly contained in the trial function. The case of a basis B trial function and basis D Green's function without exchange also produced convergent results, with basis D pseudoresonances still present, but smaller in size.

FIGURE 5.4

CROSS SECTIONS AGAINST INCIDENT ELECTRON ENERGY : NO EXCHANGE

Models and bases employed are as described in the text. Units are as in Table 5.1.

(i) 1S - 1S Cross Sections

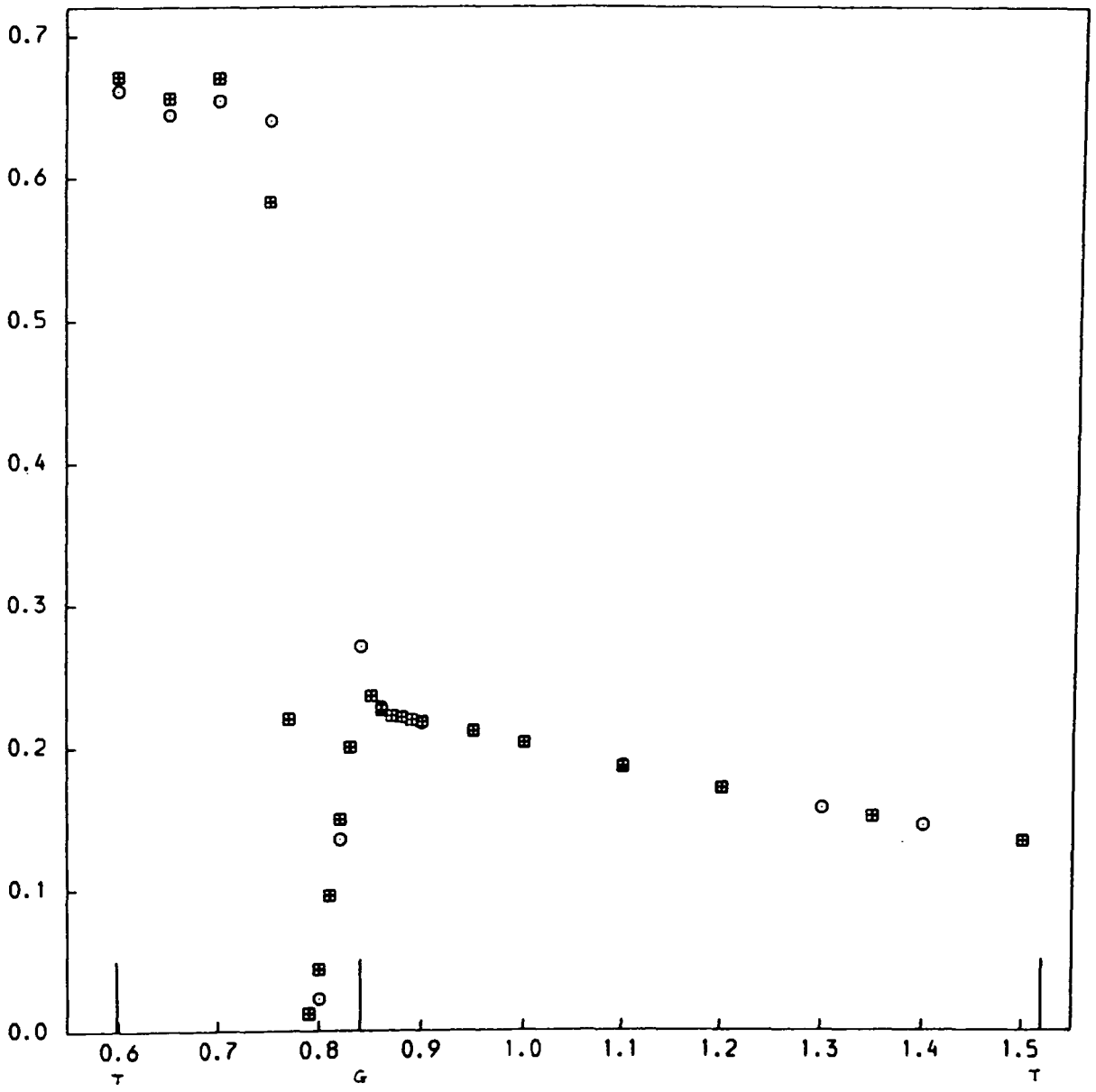

⊞ : Coupled channel results

⊙ : D trial function, B Green's function results

Trial (T) and Green's (G) function positive pseudostate thresholds in the range are marked (see Table 5.2).

FIGURE 5.4

CROSS SECTIONS AGAINST INCIDENT ELECTRON ENERGY : NO EXCHANGE

Models and bases employed are as described in the text. Units are as in Table 5.1.

(ii) 1S - 2S Cross Sections

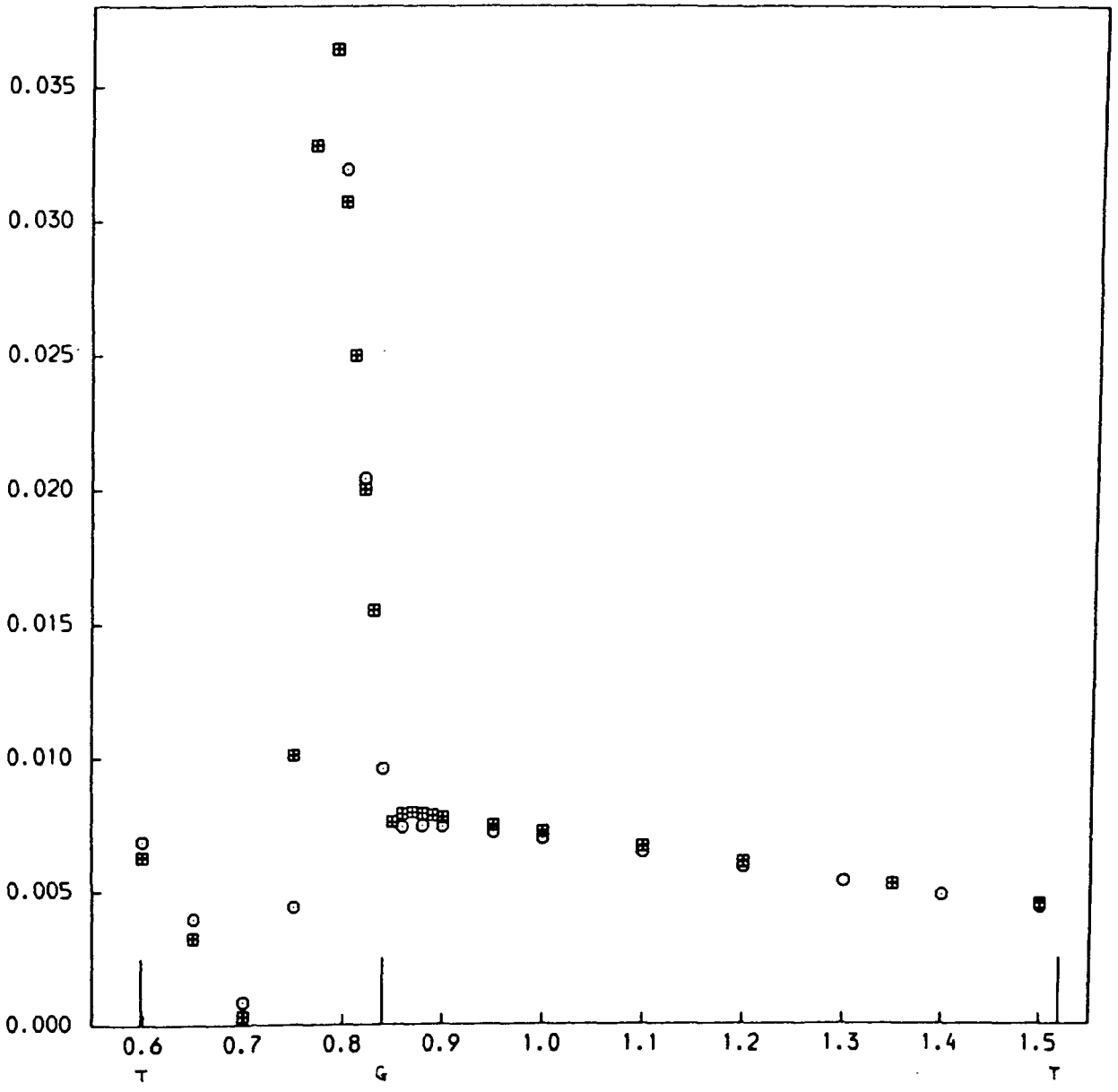

⊞ : Coupled channel results

⊙ : D trial function, B Green's function results

Trial (T) and Green's (G) function positive pseudostate thresholds in the range are marked (see Table 5.2).

B. Removal of Pseudoresonances : Use of Exact Green's Function

The rest of this section considers the removal of pseudothreshold structure from matrix elements (5.2.13d) of the basis B coupled channel problem. The subsequent automatic removal of pseudoresonances from the resulting cross sections is displayed in terms of the non-exchange case, which is in general not susceptible to the appearance of false resonances as exemplified above.

(i) Matrix Elements

Our first test was to replace the imaginary part of the Green's function $\bar{G}_o^{(+)}$ with the imaginary part of G_o^+.

$$\mathrm{Im}\,\bar{G}_o^{(+)} = -\sum_{i=1}^{N_o} 2\bar{k}_i^{-1} R_i(r_1) R_i(r_1') \sin \bar{k}_i r_1 \sin \bar{k}_i r_1' \quad ; \bar{\varepsilon}_{N_o} < E < \bar{\varepsilon}_{N_o+1}$$

$$\mathrm{Im}\,G_o^+ = -\frac{4}{\pi} \oint_0^k dK\, F(K, r_2) F(K, r_2') \frac{1}{\sqrt{(k^2-K^2)}} \sin\sqrt{(k^2-K^2)}\, r_1 \sin\sqrt{(k^2-K^2)}\, r_1' \qquad (5.3.1)$$

(E is assumed positive, $F(K, r_2)$ are standard Coulomb functions.)

Above the ionisation threshold, a smooth change in the Green's function $G_o^{(+)}$ with increasing incident electron energy is replaced in $\bar{G}_o^{(+)}$ by a series of continuous but not smooth steps as each positive channel becomes open. For $\mathrm{Im}\,G_o^{(+)}$ we used seven negative energy hydrogen states and

performed the continuum integral numerically using a 40 point Gauss quadrature and a routine of Bardin et al. (1972) for the Coulomb functions. A selection of sample matrix elements of the form (5.2.13d) for both cases are shown in figure 5.5. Although the two sets of matrix elements are similar away from the pseudoresonance, they are not in a uniform manner that is easily modelled. This means that a fitting process applied to the pseudostate matrix elements away from threshold would seem to be at least as arbitrary as one applied to the T-matrix elements, and probably more so, as the fitting has to be done for a large number of matrix elements which cannot all be examined graphically to achieve the best fit.

We then considered matrix elements for a 1s-2s-3s trial function and the "complete" Green's function $G_o^{(+)}$, taken to be made up of seven negative energy s states and a numerically integrated 36 point continuum with a cutoff above the range of incident energies of interest. Open channel $\bar{g}_{on}^{(+)}$ integrals were performed as a series of quadratures between the continuum integration points, with up to 90 points in total. Closed channel $\bar{g}_{on}^{(+)}$ integrals were performed as before. Sample elements for the non exchange case are shown in figure 5.6, with similar conclusions to be drawn about the possibilities of a fitting process. However, as noted by Oza (1984) as the number of positive pseudostates increases the pseudoresonances become narrower, and a fitting procedure might seem more appropriate with a larger

FIGURE 5.5

MATRIX ELEMENTS (5.2.13D) AGAINST INCIDENT ELECTRON ENERGY

Models, symbols and bases used are as described in the text. Units are as in Table 5.1.

Basis B sample imaginary elements: i,j,i',j' = n,1,n,1 ; n = 1,-,5

(i) n = 1

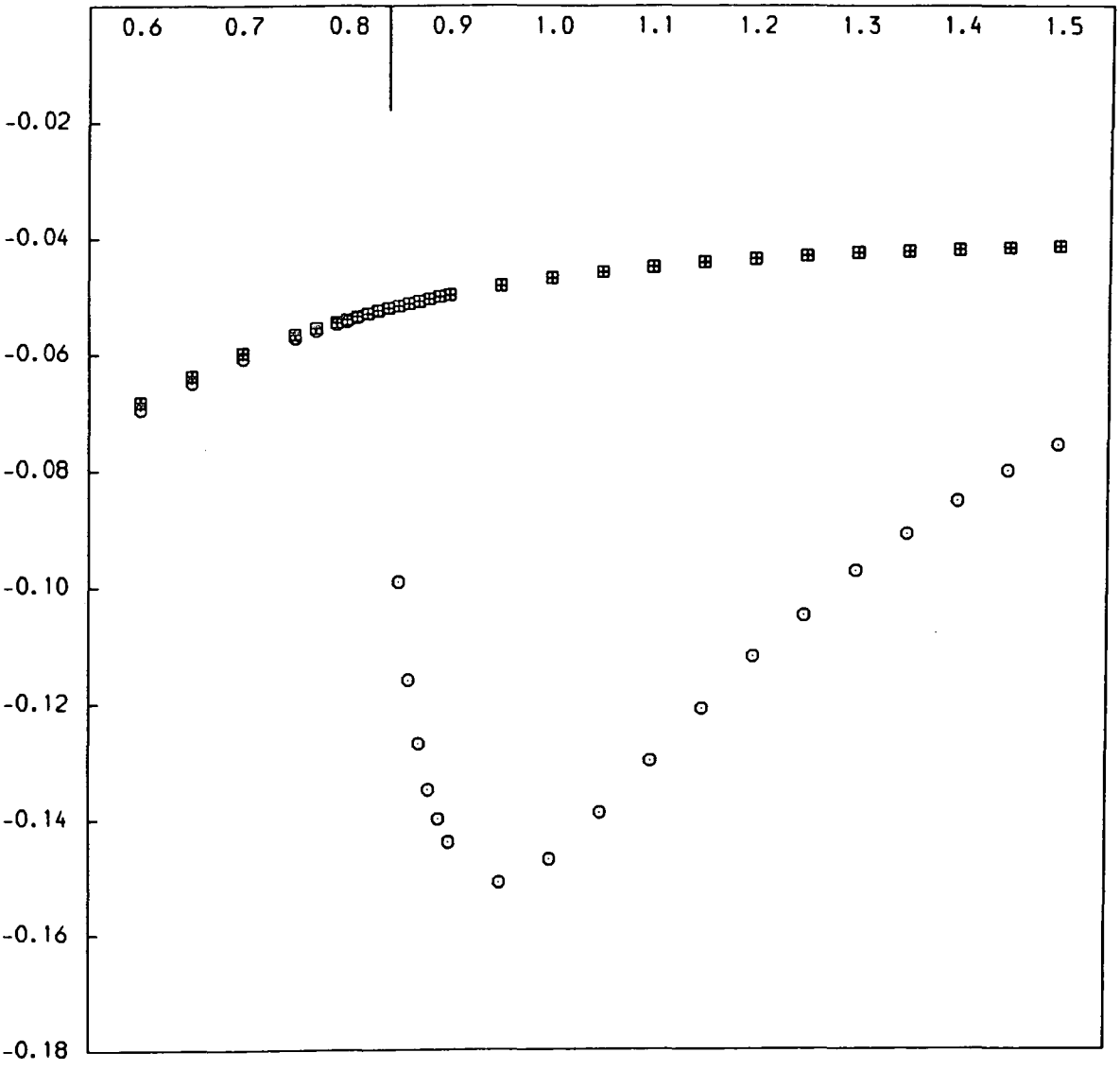

⊙ : pseudoststates

⊞ : full imaginary Green's function

Trial / Green's function positive pseudostate thresholds in the range are marked (see Table 5.2).

FIGURE 5.5

MATRIX ELEMENTS (5.2.13D) AGAINST INCIDENT ELECTRON ENERGY

Models, symbols and bases used are as described in the text. Units are as in Table 5.1.

Basis B sample imaginary elements: i,j,i',j' = n,1,n,1 ; n = 1,-,5

(ii) n = 2

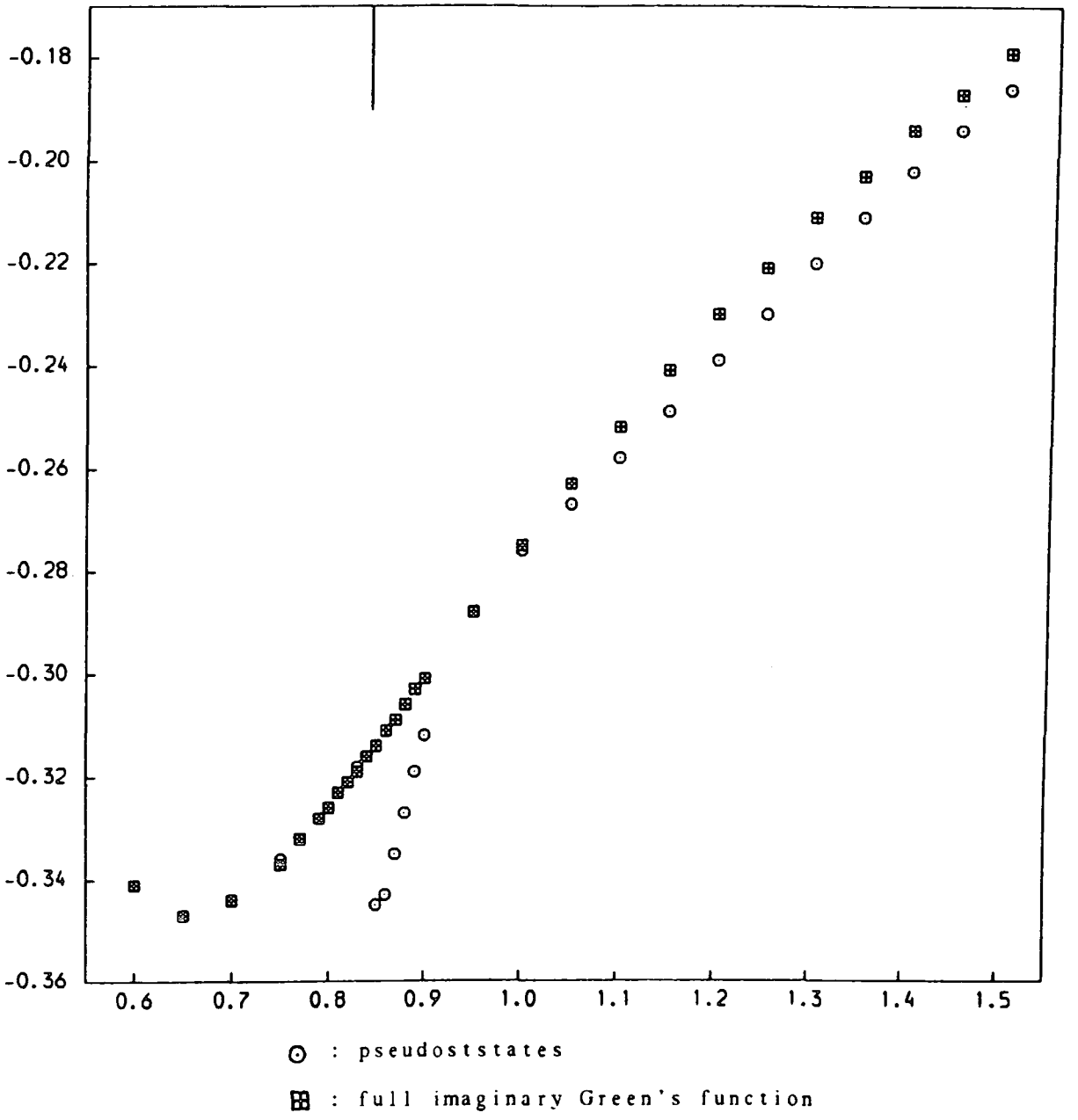

Trial / Green's function positive pseudostate thresholds in the range are marked (see Table 5.2).

FIGURE 5.5

MATRIX ELEMENTS (5.2.13D) AGAINST INCIDENT ELECTRON ENERGY

Models, symbols and bases used are as described in the text. Units are as in Table 5.1.

Basis B sample imaginary elements: i,j,i',j' = n,1,n,1 ; n = 1,-,5

(iii) n = 3

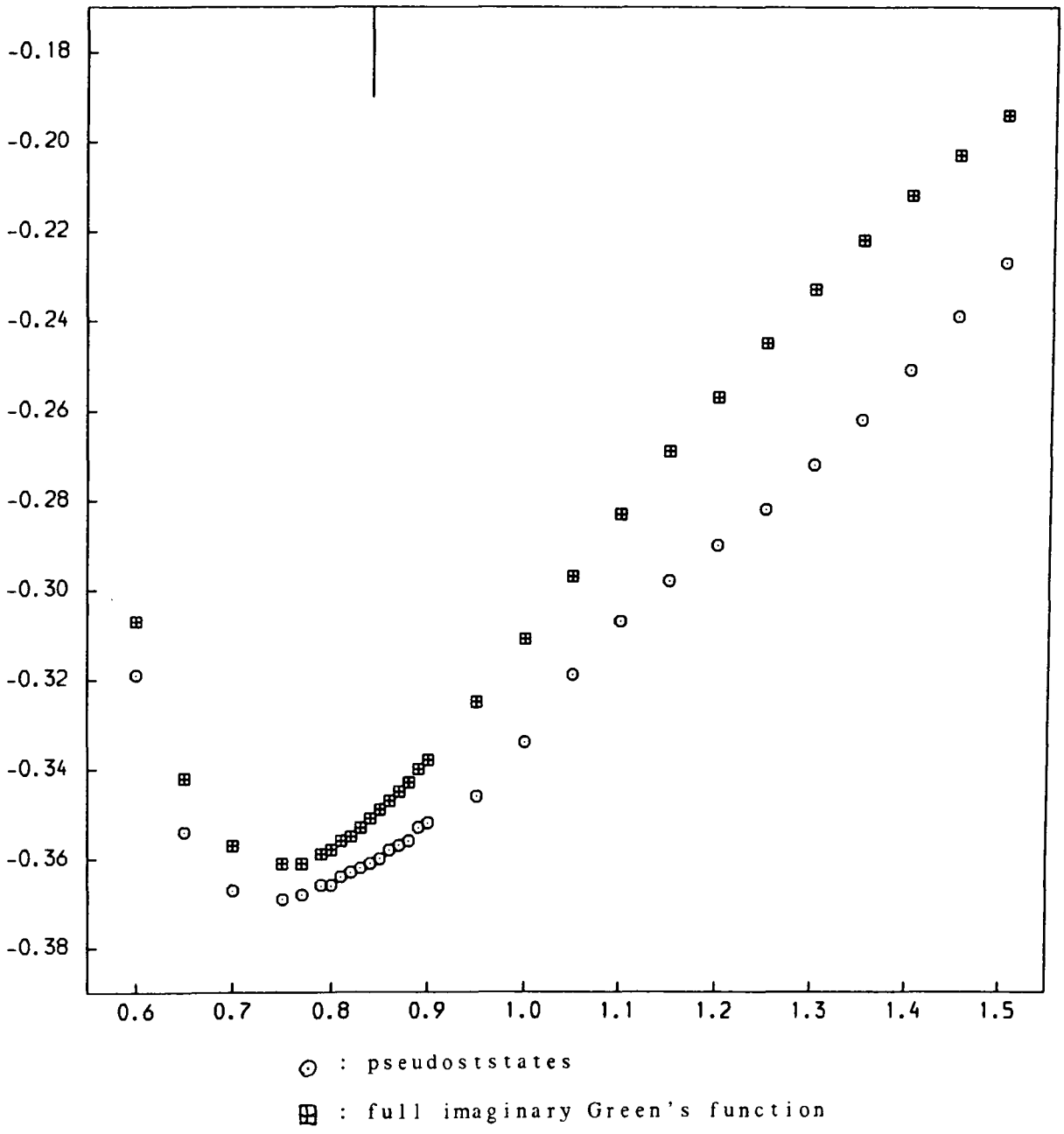

Trial / Green's function positive pseudostate thresholds in the range are marked (see Table 5.2).

FIGURE 5.5

MATRIX ELEMENTS (5.2.13D) AGAINST INCIDENT ELECTRON ENERGY

Models, symbols and bases used are as described in the text. Units are as in Table 5.1.

Basis B sample imaginary elements: i,j,i',j' = n,1,n,1 ; n = 1,-,5

(iv) n = 4

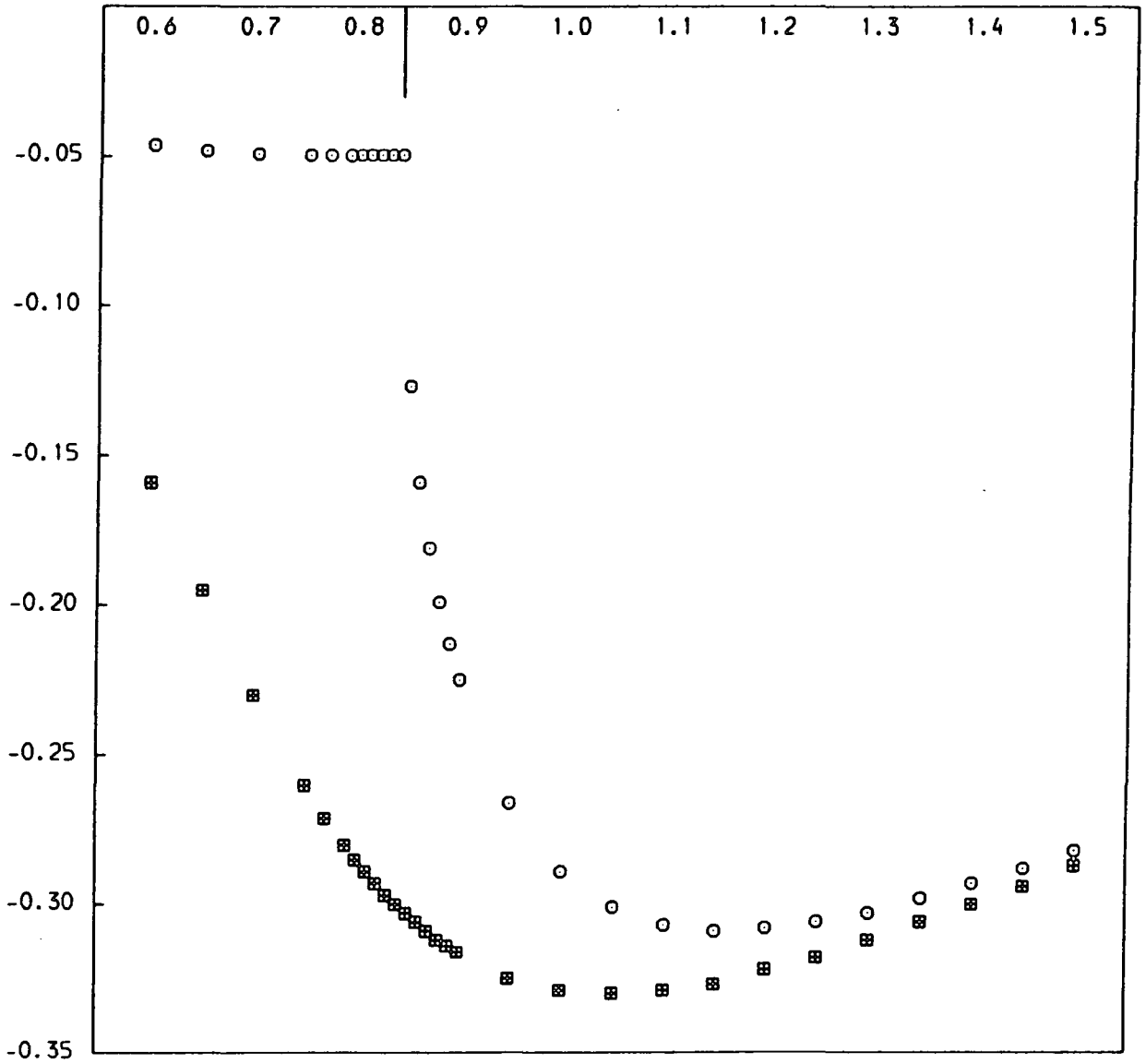

⊙ : pseudoststates

⊞ : full imaginary Green's function

Trial / Green's function positive pseudostate thresholds in the range are marked (see Table 5.2).

FIGURE 5.5

MATRIX ELEMENTS (5.2.13D) AGAINST INCIDENT ELECTRON ENERGY

Models, symbols and bases used are as described in the text. Units are as in Table 5.1.

Basis B sample imaginary elements: i,j,i',j' = n,1,n,1 ; n = 1,-,5

(v) n = 5

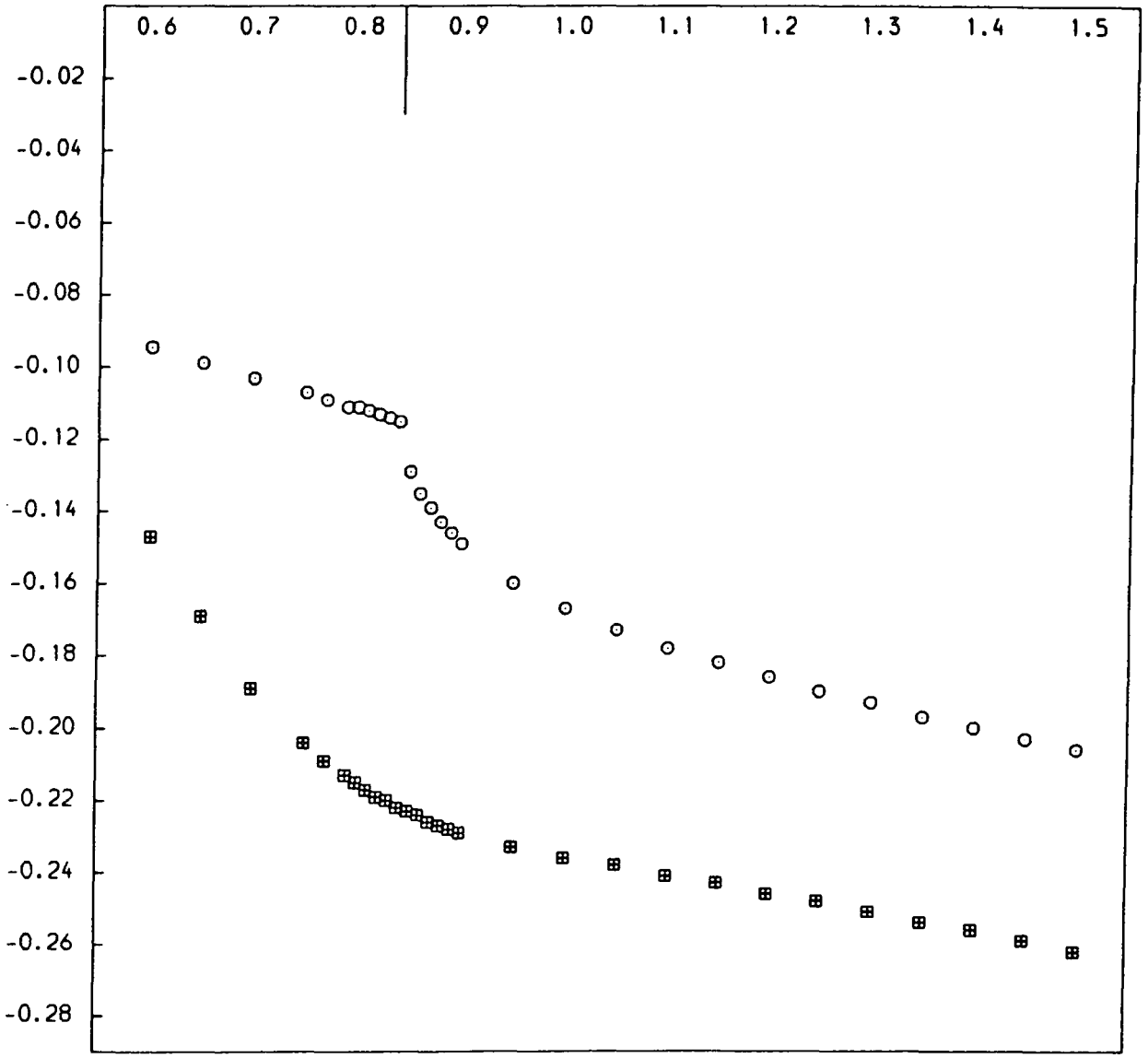

⊙ : pseudoststates

⊞ : full imaginary Green's function

Trial / Green's function positive pseudostate thresholds in the range are marked (see Table 5.2).

FIGURE 5.6

MATRIX ELEMENTS (5.2.13D) AGAINST INCIDENT ELECTRON ENERGY

Models, symbols and bases used are as described in the text. Units are as in Table 5.1.

1s-2s-3s trial function, full / B Green's function (the positive basis B pseudothreshold in the range is marked).

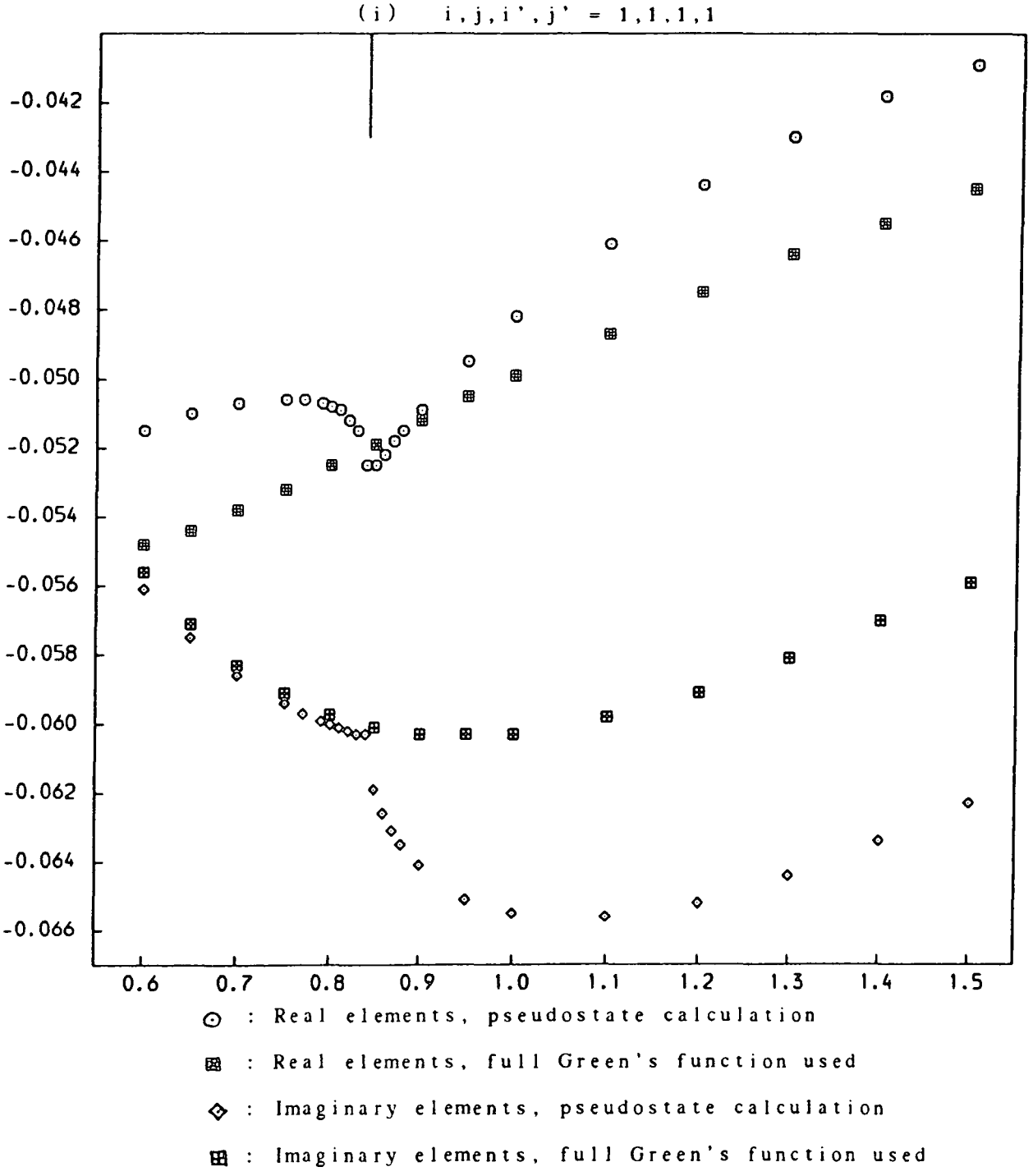

FIGURE 5.6

MATRIX ELEMENTS (5.2.13D) AGAINST INCIDENT ELECTRON ENERGY

Models, symbols and bases used are as described in the text. Units are as in Table 5.1.

1s-2s-3s trial function, full / B Green's function (the positive basis B pseudothreshold in the range is marked).

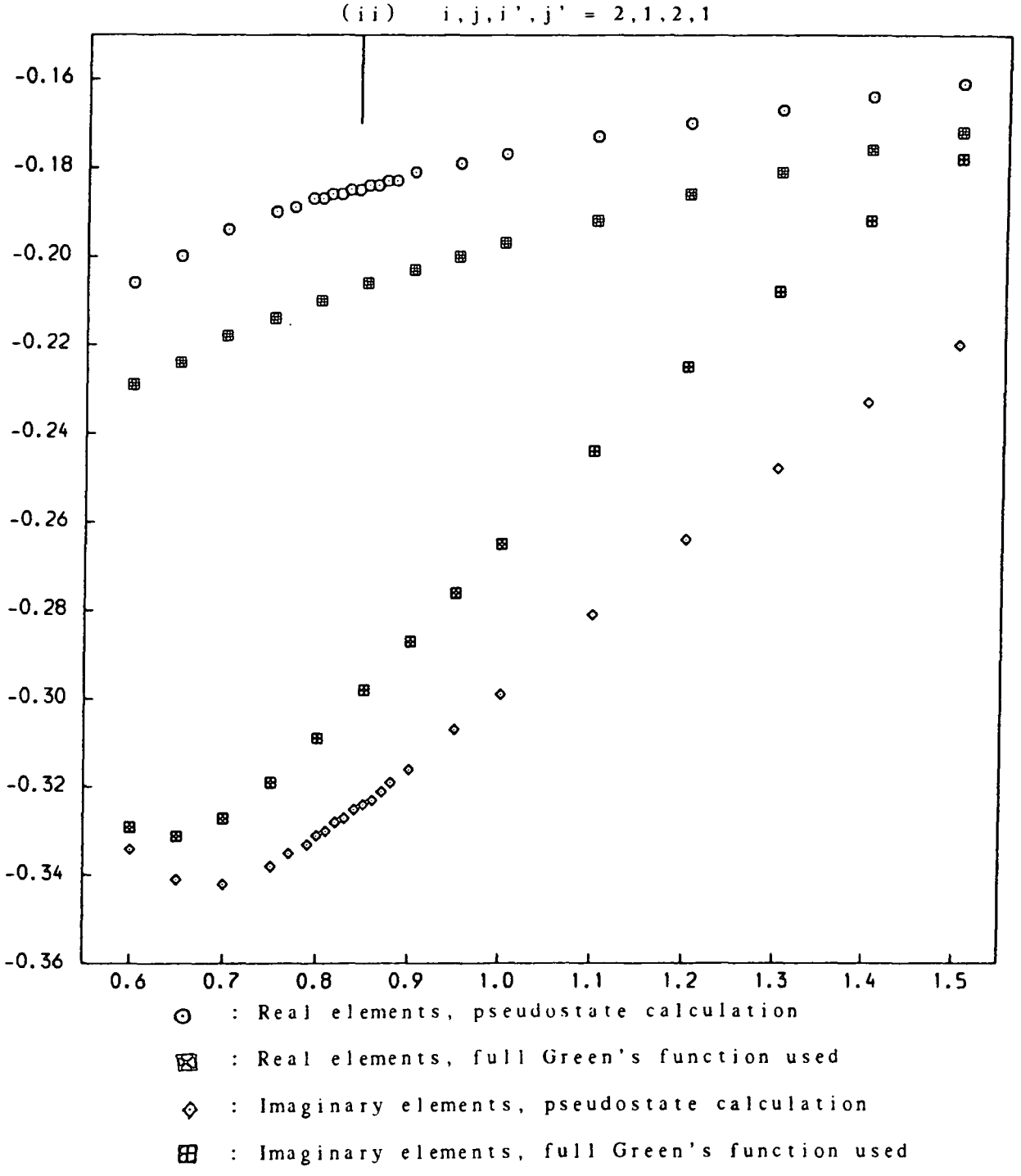

FIGURE 5.6

MATRIX ELEMENTS (5.2.13D) AGAINST INCIDENT ELECTRON ENERGY

Models, symbols and bases used are as described in the text. Units are as in Table 5.1.

1s-2s-3s trial function, full / B Green's function (the positive basis B pseudothreshold in the range is marked).

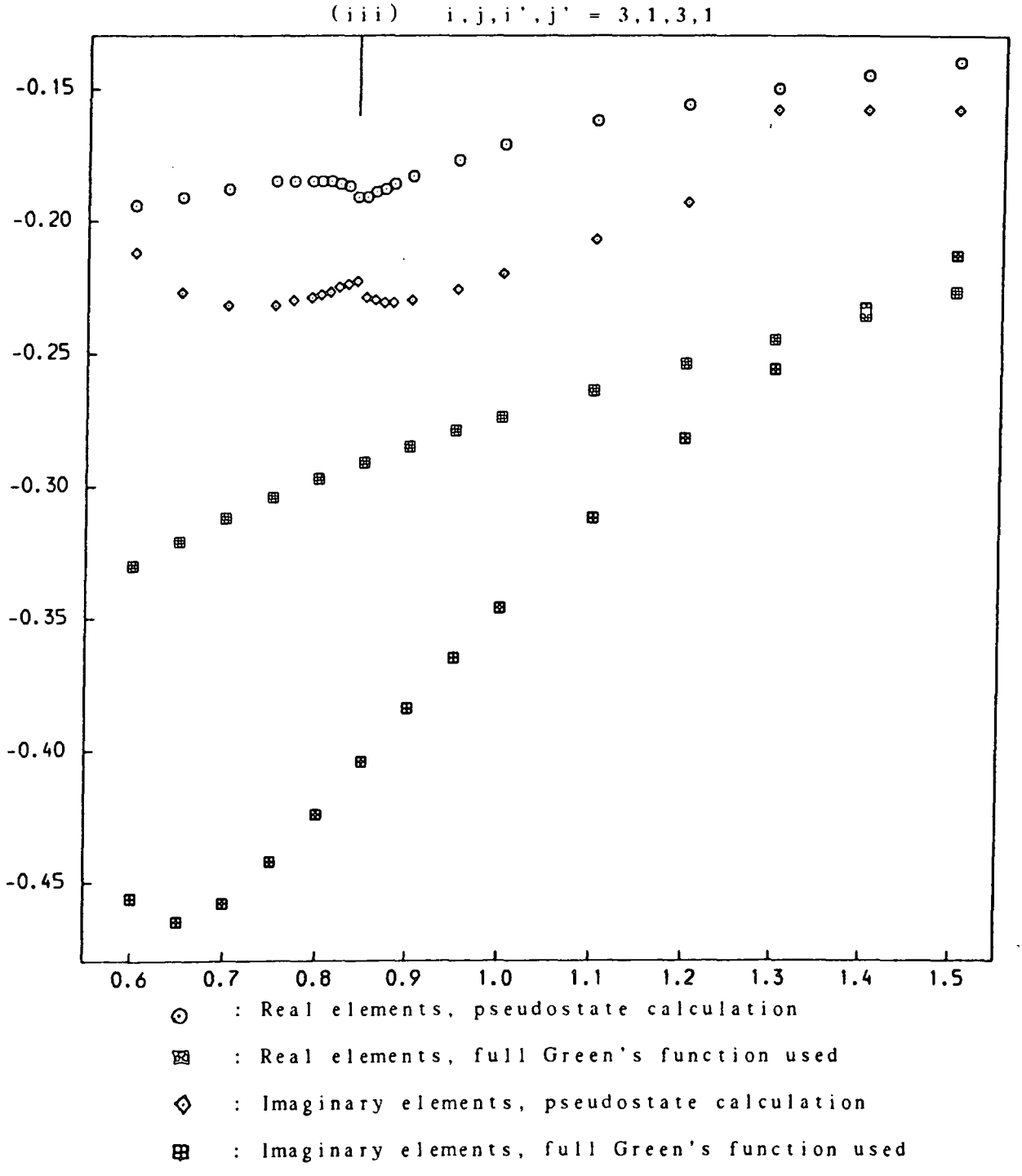

basis (the full Green's function used here is in effect equivalent to a pseudostate basis too large for practical application, and gives smooth results), although conversely more matrix elements would need to be averaged. We did not pursue this matter as our attention was diverted by the problem of false resonances, but the cross sections for the non exchange case discussed below show that the use of a smoothed Green's function removes pseudoresonances in principle. At the time of writing, McCarthy, Hewitt and Bransden are applying these ideas to adapt a coupled channels with distorted waves momentum space method of McCarthy, Mitroy and Stelbovics (1986) solving the Lippmann-Schwinger integral equation for the Poet problem.

(ii) Cross sections

In figures 5.7 and 5.8 we present results without exchange. Figure 5.7 shows the effect on the basis B coupled channel cross sections of using the full imaginary Green's function. Figure 5.8 shows a calculation using a 1s-2s-3s trial basis and the full Green's function $G_o^{(+)}$, together with a calculation using the same trial function and a basis B Green's function $\overline{G}_o^{(+)}$. Here the cross sections are completely smooth, and the idea of a smoothing process seems justified. Unfortunately, Poet did not provide exact non-exchange cross sections for comparison. Table 5.4 indicates variation with increased numbers of scattering trial functions Θ_{ji} for this case.

Although these results show that smoothing the Green's

FIGURE 5.7

CROSS SECTIONS AGAINST INCIDENT ELECTRON ENERGY : NO EXCHANGE

Models and bases used are as described in the text. Units are as in Table 5.1.

(i) 1S - 1S Cross Sections

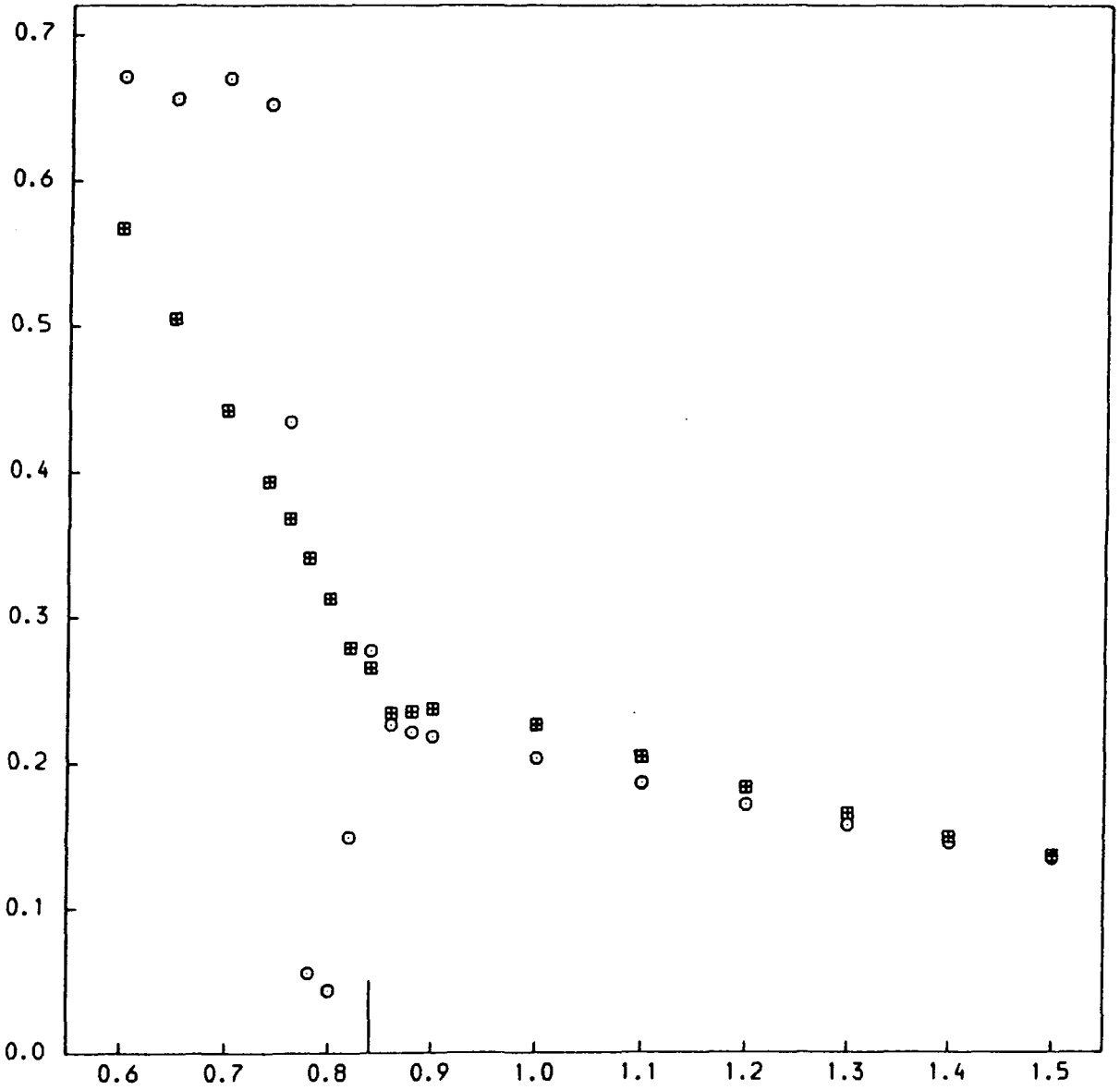

⊙ : close coupling results

⊞ : full imaginary Green's function

Trial / Green's function positive pseudostate thresholds in the range are marked (see Table 5.2).

FIGURE 5.7

CROSS SECTIONS AGAINST INCIDENT ELECTRON ENERGY : NO EXCHANGE

Models and bases used are as described in the text. Units are as in Table 5.1.

(ii) 1S - 2S Cross Sections

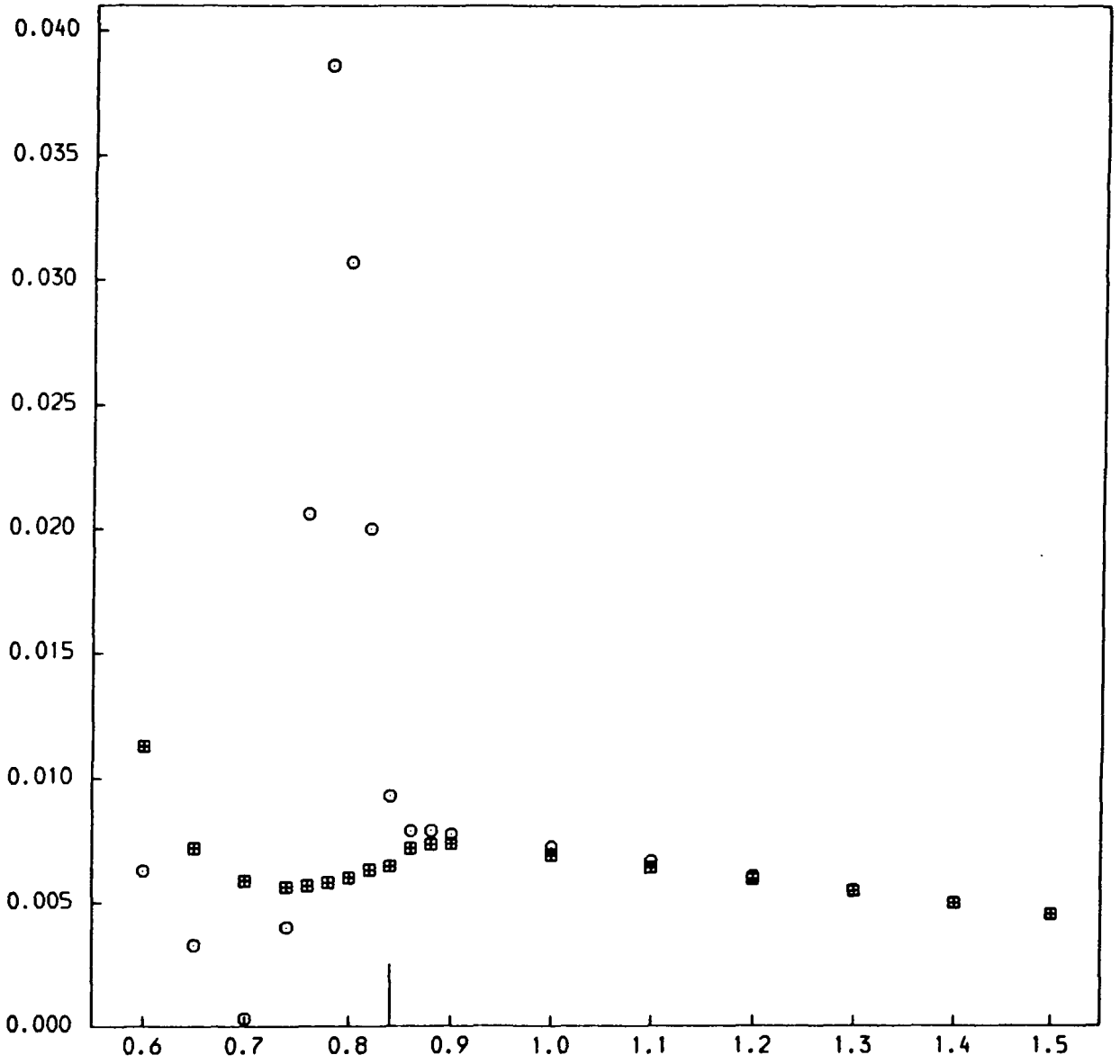

⊙ : close coupling results

⊞ : full imaginary Green's function

Trial / Green's function positive pseudostate thresholds in the range are marked (see Table 5.2).

FIGURE 5.8

CROSS SECTIONS AGAINST INCIDENT ELECTRON ENERGY : NO EXCHANGE

Models and bases used are as described in the text. Units are as in Table 5.1.

(i) 1S - 1S Cross Sections

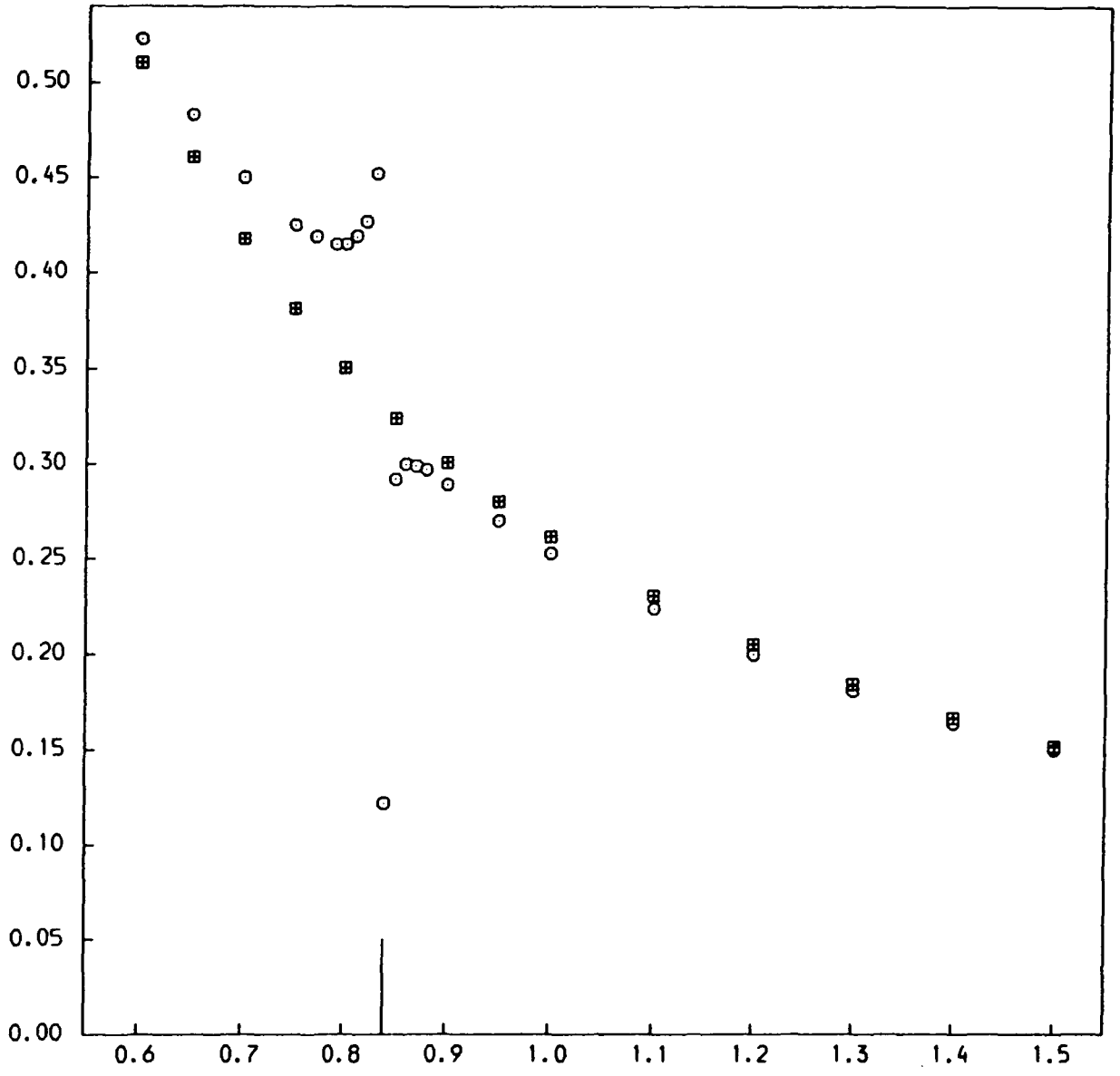

⊙ : 1s-2s-3s trial function, B Green's function

⊞ : 1s-2s-3s trial function, full Green's function

Green's function positive pseudostate thresholds in the range are marked (see Table 5.2).

FIGURE 5.8

CROSS SECTIONS AGAINST INCIDENT ELECTRON ENERGY : NO EXCHANGE

Models and bases used are as described in the text. Units are as in Table 5.1.

(ii) 1S - 2S Cross Sections

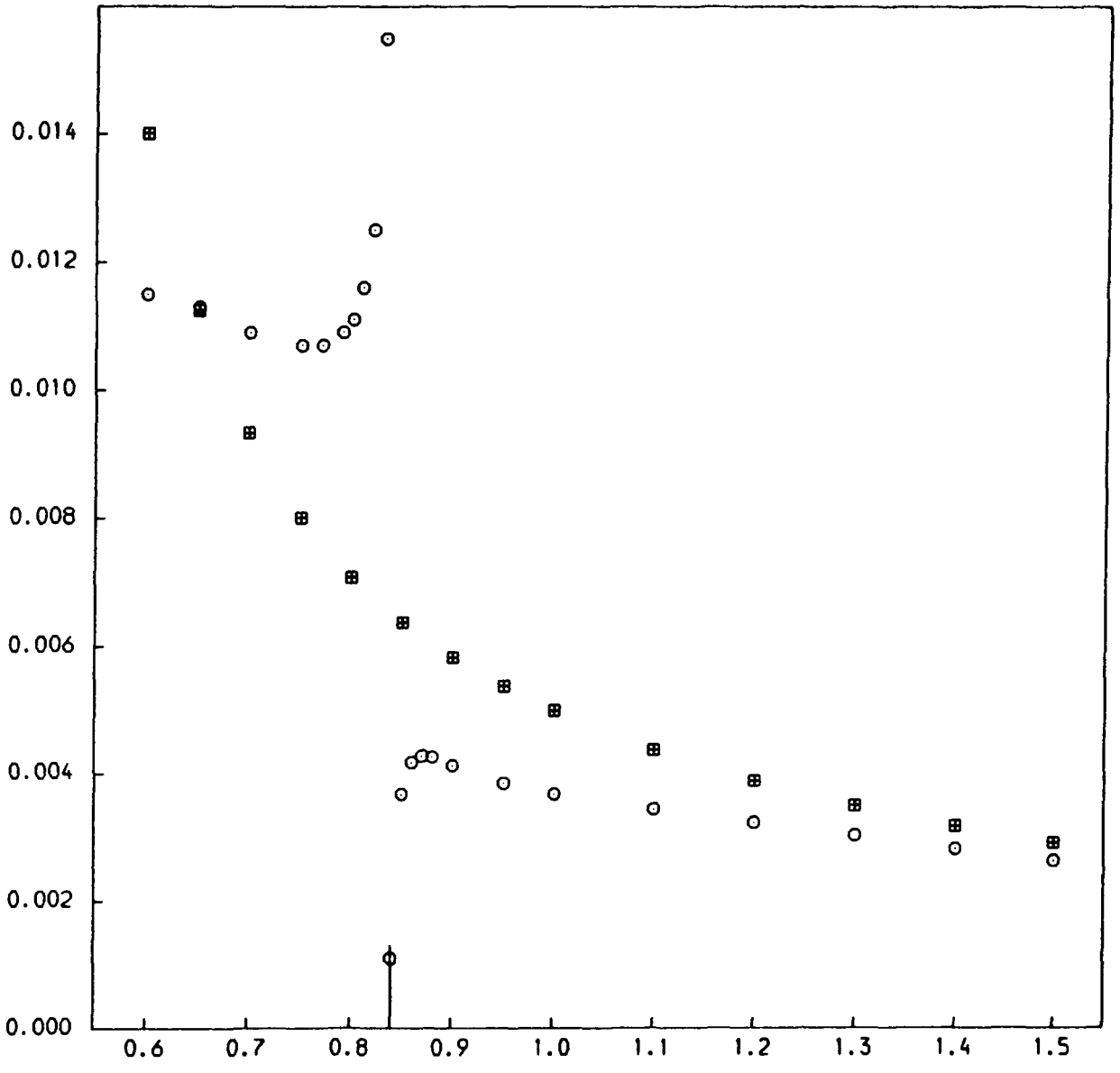

⊙ : 1s-2s-3s trial function, B Green's function

⊞ : 1s-2s-3s trial function, full Green's function

Green's function positive pseudostate thresholds in the range are marked (see Table 5.2).

TABLE 5.4

CONVERGENCE TESTS: 1S-2S-3S TRIAL BASIS WITH "FULL" NUMERICAL GREEN'S FUNCTION (EXCHANGE IS NOT INCLUDED IN THE CALCULATION)

ENERGY = 0.7

	CROSS SECTIONS	
NTR	1S-1S	1S-2S (*10E-1)
10	0.4145	0.0978
11	0.4177	0.0935
12	0.4186	0.0941
13	0.4184	0.0937
14	0.4186	0.0936
15	0.4184	0.0933
16	0.4178	0.0933

ENERGY = 1.3

	CROSS SECTIONS	
NTR	1S-1S	1S-2S (*10E-1)
10	0.1836	0.0353
11	0.1843	0.0350
12	0.1843	0.0350
14	0.1843	0.0350
16	0.1843	0.0350

(Units and symbols are as described in table 5.1 and in the text. Where indicated, cross sections should be multiplied by the appropriate factor of 10.)

FIGURE 5.9

CROSS SECTIONS AND MATRIX ELEMENTS (5.2.13D) AGAINST INCIDENT ENERGY

Models, matrix elements and symbols are as described in the text. Units are as in Table 5.1.

1s Trial basis, full Green's function with exchange.

(i) 1S - 1S Cross Sections

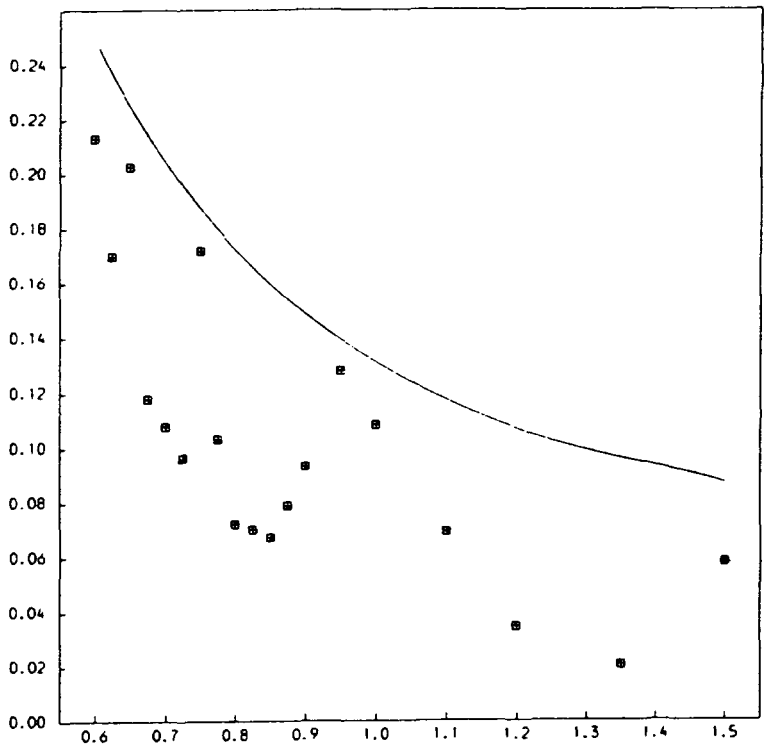

(ii) Matrix Elements (5.2.13cd)for i,j,i',j' = 1,1,1,1

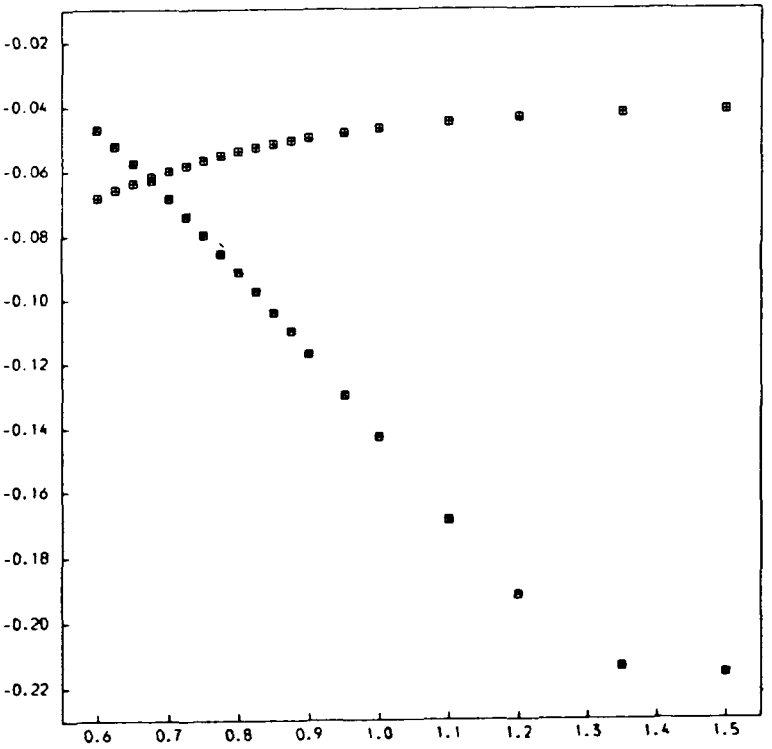

function removes pseudoresonances, it is not a practical process in conjunction with the Schwinger method, due to the problem of false resonances. Using a basis B trial function complicates the problem enough to introduce false resonances and non-convergence in the non-exchange case, and in the exchange case false resonances obscure the smoothing process entirely. Figure 5.9 shows sample results with exchange for the full Green's function and a single channel ls trial function.

In this and other exchange cases, smooth matrix elements do not lead to smooth cross sections. The false resonance structure varied with the number and input parameters of the Θ_{ji} used.

5.4 Investigation of False Resonances

5.4A Occurrence of False Resonances and some limitations of the Schwinger Method

In order to avoid confusion with pseudoresonances, several tests were made of the Schwinger method with a Green's function containing exact negative hydrogen functions; 1s-2s ... ns, $n \leq 7$, and various trial bases. Without exchange, smoothly decaying cross sections were

found. With exchange, the following rule emerged: false resonances occurred if the Green's function basis contained more information than or different information from the trial function basis. If the trial function contained all the states included in the Green's function, the results converged on the coupled channel results for that Green's function, as suggested in section 5.3A. An example shown in figure 5.10a is for a 1s-2s-3s Green's function with a basis D trial function, superimposed on 1s-2s-3s close coupling results. Also shown are two cases of false resonance. Figure 5.10b shows the combination of a single channel 1s trial function and a 1s-2s Green's function, and figure 5.10c shows sample results for a 7 state Green's function and a 1s-2s-3s trial function. In each case the position of the false resonance varied with the number and input parameters of functions Θ_{ji} used. Sample matrix elements of the form (5.2.13) were smooth in all cases .

On a different track, investigations (performed by R. Hewitt) of close coupling Schwinger calculations using up to seven s states gave results that converged at values close to the 1s-2s-3s results (section 5.2B, Burke and Mitchell 1973). This shows the importance of representing the continuum states, as these results are not close to the exact results (Poet 1978), and also indicates that seven s states are adequate to represent the negative energy part of the Green's function $G_o^{(+)}$ as in section 5.3. Also, some investigation by R. Hewitt at low incident energies showed

FIGURE 5.10A

CROSS SECTIONS AGAINST INCIDENT ELECTRON ENERGY

Models and bases employed are as described in the text. Units are as in Table 5.1.

(i) 1S - 1S Cross Sections

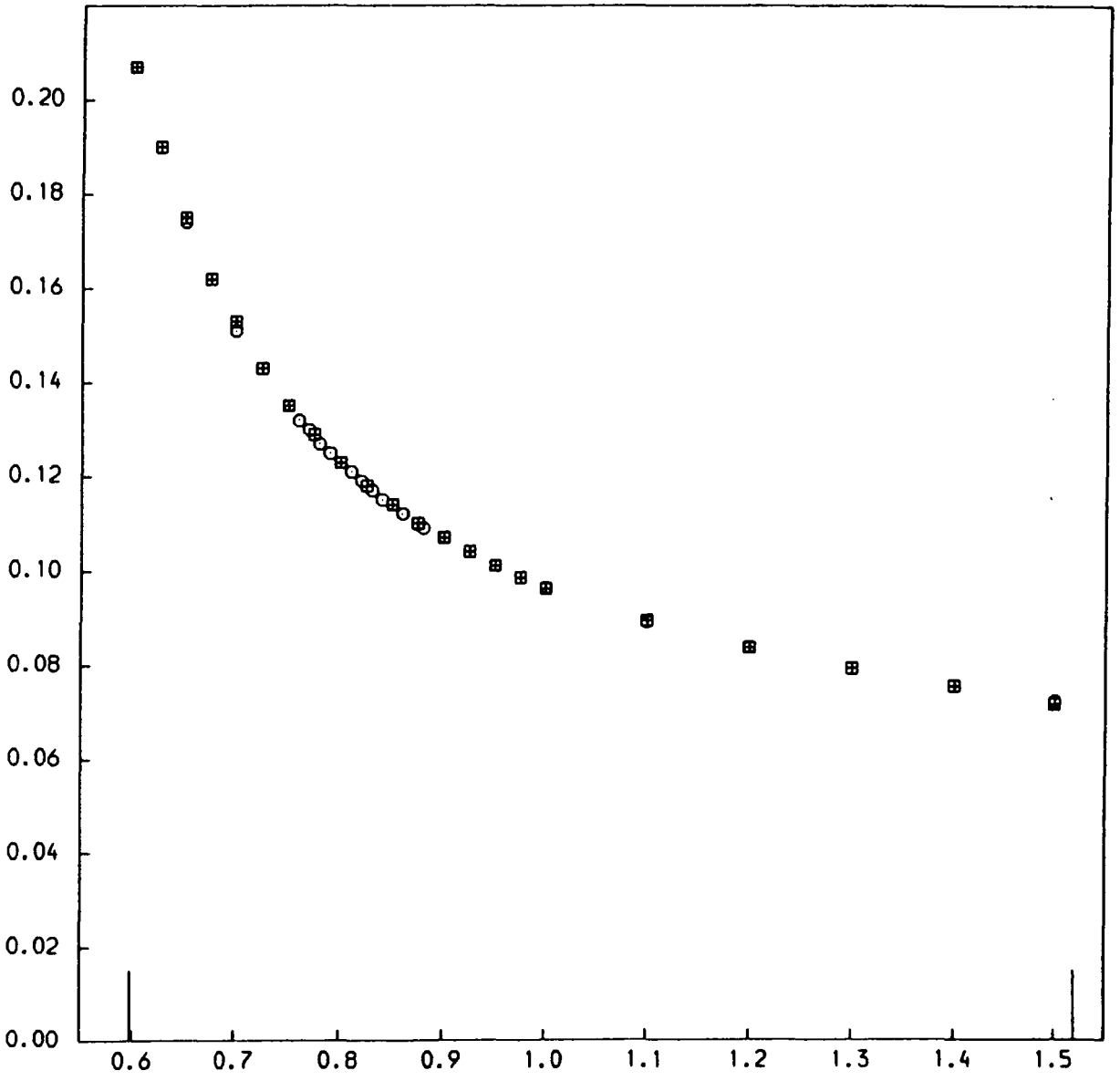

⊙ : 1s-2s-3s close coupling

⊞ : D trial function, 1s-2s-3s Green's function

Trial function positive pseudostate thresholds in the range are marked (see Table 5.2).

FIGURE 5.10A

CROSS SECTIONS AGAINST INCIDENT ELECTRON ENERGY

Models and bases employed are as described in the text. Units are as in Table 5.1.

(ii) 1S - 2S Cross Sections

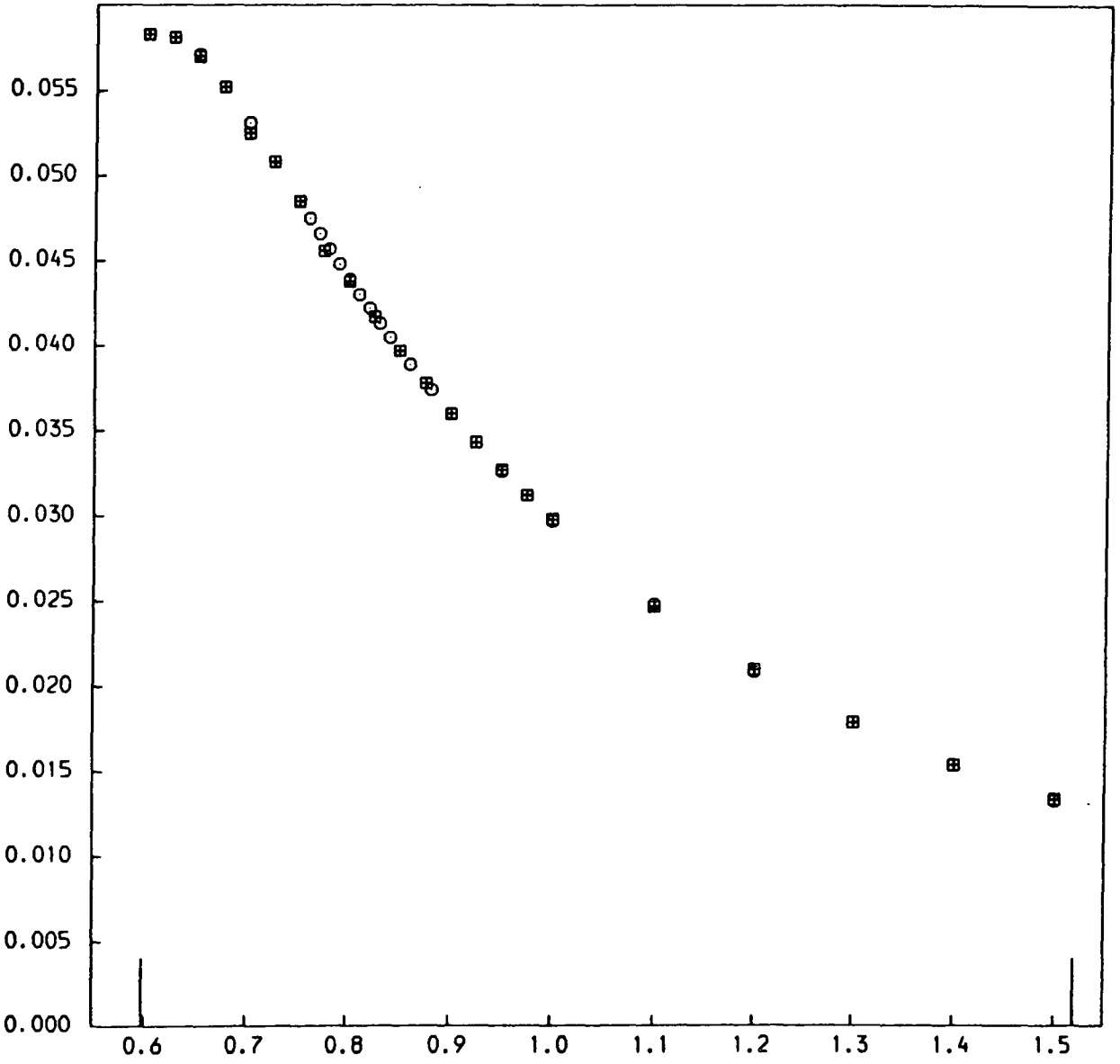

⊙ : 1s-2s-3s close coupling

⊞ : D trial function, 1s-2s-3s Green's function

Trial function positive pseudostate thresholds in the range are marked (see Table 5.2).

FIGURE 5.10B

CROSS SECTIONS AGAINST INCIDENT ELECTRON ENERGY

Models and symbols are as described in the text.
Units are as in Table 5.1.

Elastic Cross Sections: 1s trial basis, 1s-2s Green's function.

(i) NTR = 12

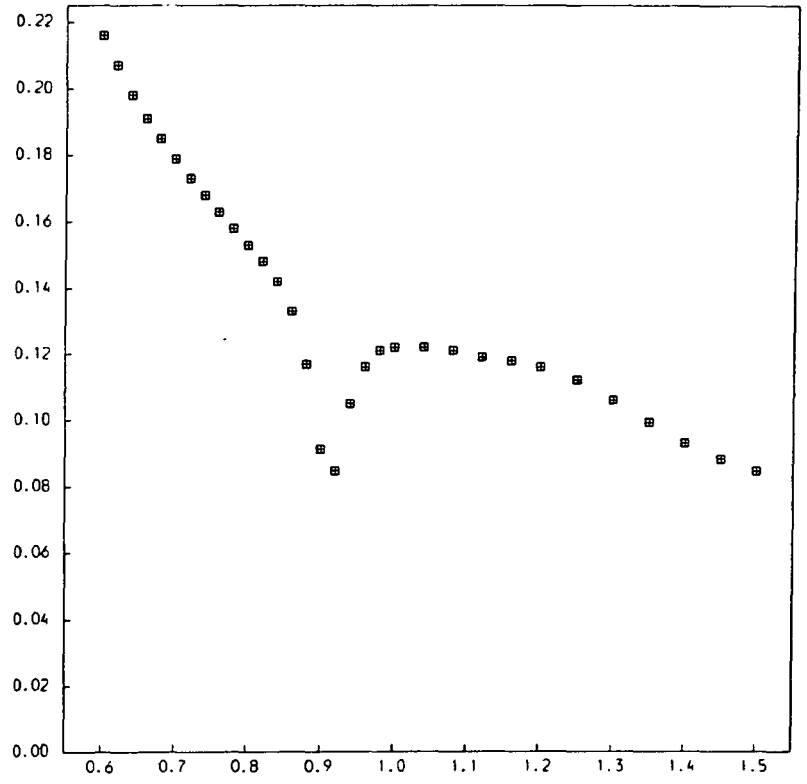

(ii) NTR = 14

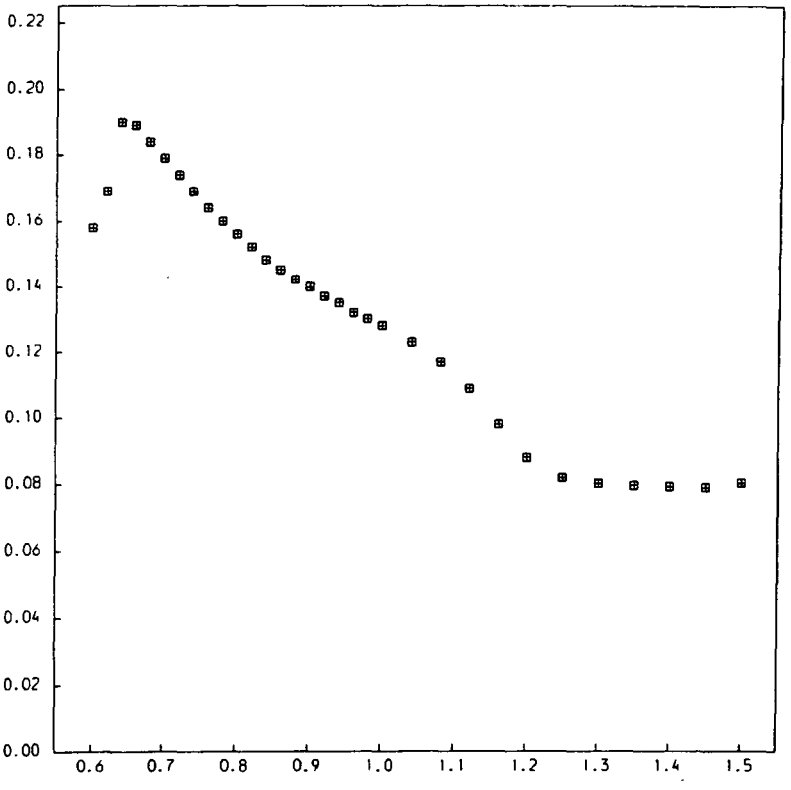

FIGURE 5.10C

CROSS SECTIONS AGAINST INCIDENT ELECTRON ENERGY

Models and symbols are as described in the text.
Units are as in Table 5.1.

Elastic Cross Sections: 1s--3s trial basis, 1s--7s Green's function.

(i) NTR = 12

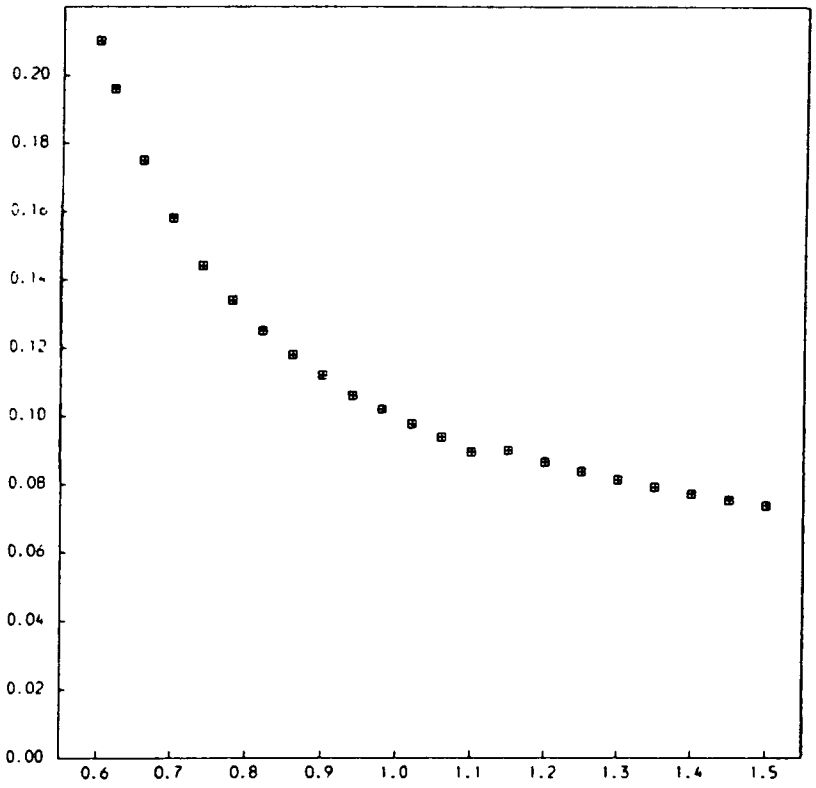

(ii) NTR = 14

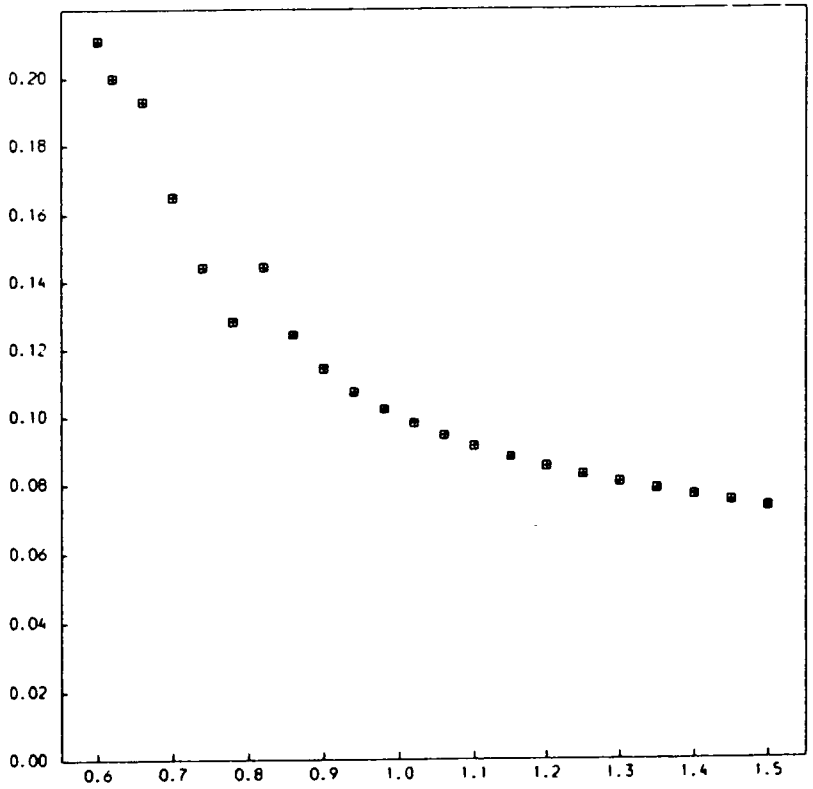

FIGURE 5.10C

CROSS SECTIONS AGAINST INCIDENT ENERGY

Models and symbols are as described in the text.
Units are as in Table 5.1.

1s-2s Cross Sections: 1s--3s trial basis, 1s--7s Green's function.

(i) NTR = 12

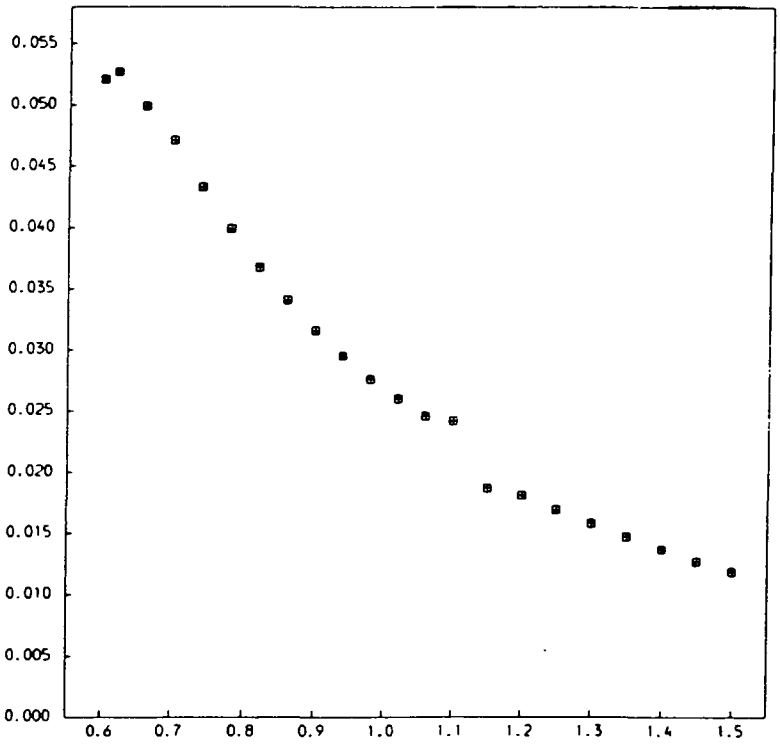

(ii) NTR = 14

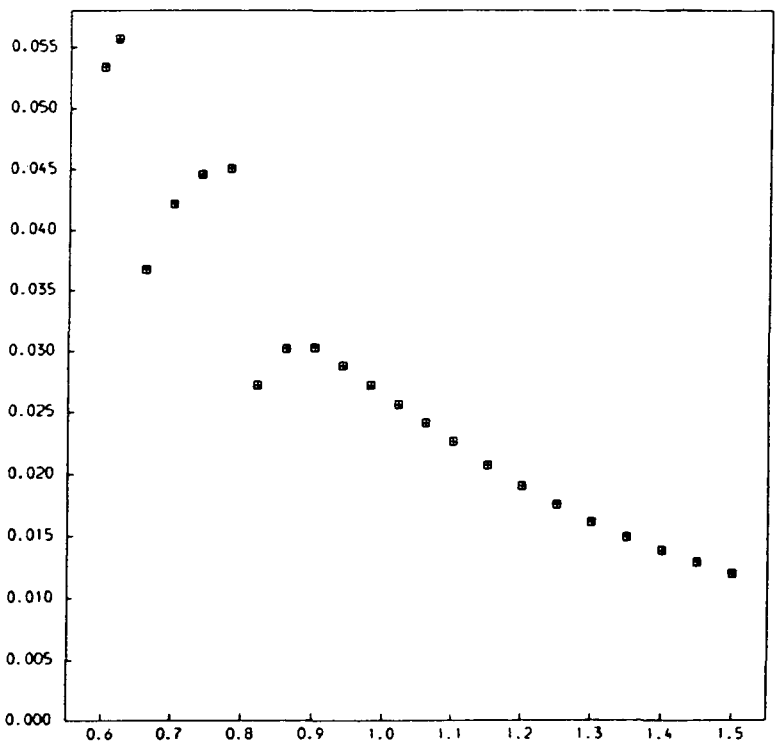

that false resonances did not seem to occur below the inelastic threshold, and that the K matrix method gave the same results as the T matrix method in this region, although this behaviour was not investigated fully as we were concerned with the intermediate energy range. The rest of this section concerns our analysis of a possible method of removing false structure.

5.4B "t" Variational Principle

In an attempt to remove the false resonant structure from the T matrix, we considered a method proposed by Takatsuka and McKoy (1981) which was claimed to remove spurious poles from Schwinger-type principles. In our principle the final approximation to the T matrix element $\frac{1}{2}T^{S}_{ba}$ may be written:

$$F_{ba} = \sum_{ij} \langle \chi_b | \bar{V} | \psi_i \rangle (\underline{\underline{D}}^{-1})_{ij} \langle \psi_j | \bar{V} | \chi_a \rangle \qquad (5.4.1)$$

$$\bar{V} = V - (-1)^{S} \hat{H} A$$

$|\psi_i\rangle$ represents the trial function $R_m(r_2)\,\Theta_{mn}(r_1)$, i running over both indices m and n

$$\{\underline{\underline{D}}\}_{ij} = \langle \psi_i | -\bar{V} + \bar{V} G_0^{(+)} \bar{V} | \psi_j \rangle$$

$G_0^{(+)}$ stands here for either the Poet Green's function or the approximation used for it.

Following Takatsuka and McKoy, we introduced a

parameter t and found the stationary value for the functional (5.4.2) requiring equality of the three terms at the stationary value.

$$\frac{\langle \bar{\Phi}^{-}_{tr\,b}(t) | \bar{V} | \chi_a \rangle \langle \chi_b | \bar{V} | \Phi^{+}_{tr\,a}(t) \rangle}{\langle \bar{\Phi}^{-}_{tr\,b}(t) | \{ -\bar{V} + \bar{V} G_o^{+} \bar{V} + t \bar{V} | \chi_a \rangle \langle \chi_b | \bar{V} \} | \Phi^{+}_{tr\,a}(t) \rangle}$$

(5.4.2)

The exact wave function $|\Phi_a^{(+)s}(t)\rangle$ obeys equations (5.4.3) and differs from the Poet wave function $|\Phi_a^{(+)s}\rangle$ by a constant factor x_t:

$$|\Phi_a^{(+)s}(t)\rangle = |\chi_a\rangle + \{ \bar{V} G_o^{(+)} \bar{V} + t \bar{V} | \chi_a \rangle \langle \chi_b | \bar{V} \} | \Phi_a^{(+)s}(t) \rangle$$

(5.4.3a)

$$|\Phi_a^{(+)s}(t)\rangle = |\Phi_a^{(+)s}\rangle \left(1 - t \langle \chi_b | \bar{V} | \Phi_a^{(+)s} \rangle \right)^{-1}$$

(5.4.3b)

$$x_t = \left(1 - t \langle \chi_b | \bar{V} | \Phi_a^{(+)s} \rangle \right)^{-1}$$

(5.4.3c)

We note also:

$$|\Phi_a^{(+)s}\rangle = |\Phi_a^{(+)s}(t)\rangle \left(1 + t \langle \chi_b | \bar{V} | \Phi_a^{(+)s}(t) \rangle \right)^{-1}$$

(5.4.3d)

$$x_t = 1 + t \langle \chi_b | \bar{V} | \Phi_a^{(+)s}(t) \rangle$$

(5.4.3e)

In the original "t" principle, the T matrix element is rewritten in terms of the new stationary value

$$\tfrac{1}{2} T^{S}_{ba} = -\langle \chi_b | \bar{V} | \hat{\phi}^{(+)S}_{a} \rangle$$

$$= -\frac{\langle \chi_b | \bar{V} | \hat{\phi}^{(+)S}_{a}(t) \rangle}{(1 + t\langle \chi_b | \bar{V} | \hat{\phi}^{(+)S}_{a}(t) \rangle)}$$

$$\approx \frac{\bar{F}_{ba}}{(1 - t\bar{F}_{ba})} \qquad (5.4.4)$$

$$\bar{F}_{ba} = \sum_{ij} \langle \chi_b | \bar{V} | \psi_i \rangle (\underline{\underline{\bar{D}}}^{-1}_{ba})_{ij} \langle \psi_j | \bar{V} | \chi_a \rangle$$

$$\underline{\underline{\bar{D}}}_{ba} = \underline{\underline{D}} + t\,\underline{R}_a \underline{R}^{\dagger}_b \quad ; \quad \{\underline{R}_a\}_i = \langle \psi_i | \bar{V} | \chi_a \rangle \qquad (5.4.5)$$

Takatsuka and McKoy also presented a generalised "t" method in which $\underline{\underline{\bar{D}}}$ was channel independent. The following arguments also apply to this model (details are in Appendix Three). Our tests showed that the t-method gave exactly the same results as the basic Schwinger method, and mathematically we find the two expressions for the T matrix to be identical. Further consultation of the literature showed that the same conclusions had already been drawn by Abdel-Raouf (1984), but the following analysis was performed independently.

We wish to show that:

$$X(t) = \frac{\bar{F}_{ba}}{(1 - t\bar{F}_{ba})} = X(0) = F_{ba} \quad ; \quad \bar{F}_{ba} \neq 1/t \qquad (5.4.6)$$

$$\frac{d\underline{X}(t)}{dt} = \frac{1}{(1-t\bar{F}_{ba})^2}\left[(1-t\bar{F}_{ba})\frac{d\bar{\underline{F}}_{ba}}{dt} + \bar{F}_{ba}\left(\bar{\underline{F}}_{ba} + t\frac{d\bar{\underline{F}}_{ba}}{dt}\right)\right]$$

$$= \frac{1}{(1-t\bar{F}_{ba})^2}\left(\frac{d\bar{F}_{ba}}{dt} + \bar{F}_{ba}^2\right)$$

(5.4.7)

$$\frac{d\bar{\underline{F}}_{ba}}{dt} = \frac{d}{dt}\left(\underline{R}_b^+ \bar{\underline{\underline{D}}}_{ba}^{-1} \underline{R}_a\right) = \underline{R}_b^+\left(\frac{d}{dt}\bar{\underline{\underline{D}}}_{ba}^{-1}\right)\underline{R}_a$$

(5.4.8)

Since $\bar{\underline{\underline{D}}}_{ba}\,\bar{\underline{\underline{D}}}_{ba}^{-1} = \underline{\underline{I}}$

(5.4.9)

$$\frac{d}{dt}\bar{\underline{\underline{D}}}_{ba}^{-1} = -\bar{\underline{\underline{D}}}_{ba}^{-1}\left(\frac{d}{dt}\bar{\underline{\underline{D}}}_{ba}\right)\bar{\underline{\underline{D}}}_{ba}^{-1}$$

$$= -\bar{\underline{\underline{D}}}_{ba}^{-1}\,\underline{R}_a\,\underline{R}_b^+\,\bar{\underline{\underline{D}}}_{ba}^{-1}$$

(5.4.10)

(5.4.8) becomes

$$\frac{d\bar{\underline{F}}_{ba}}{dt} = -\underline{R}_b^+\,\bar{\underline{\underline{D}}}_{ba}^{-1}\,\underline{R}_a\,\underline{R}_b^+\,\bar{\underline{\underline{D}}}_{ba}^{-1}\,\underline{R}_a = -\bar{F}_{ba}^2$$

(5.4.11)

Thus for $\bar{F}_{ba} \neq 1/t$,

$$X(t) = X(0) = F_{ba}$$

(5.4.12)

The case $\bar{F}_{ba} = 1/t$ corresponds to $F_{ba} \to \infty$, and applies when singularities appear in the calculated T matrix elements. These may be genuine resonances, or, as argued by Abdel-Raouf (1984), spurious singularities related to those obtained by the corresponding Kohn variational principle. Our false resonances are not singular and their structure is

in any case preserved in the "t"-method as our analysis shows.

In their reply to Abdel-Raouf, Takatsuka and McKoy (1984) suggest an alternative expression for x_t which, due to the inexactness of the variational method, may not be zero at $\bar{F}_{ba} = 1/t$, and thus may eliminate some spurious singularities. This does not help our work as our false resonances are not singular, and once again the expression for the T matrix elements remains independent of t away from the singularities. In terms of the Schwinger method, we may write:

$$\bar{V}|\chi_a\rangle = \{\bar{V} - \bar{V}G_o^{(+)}\bar{V} - t\bar{V}|\chi_a\rangle\langle\chi_b|\bar{V}\}|\phi_a^{(+)s}(t)\rangle \tag{5.4.13}$$

$$\langle\chi_b|\bar{V} - \bar{V}G_o^{(+)}\bar{V}|\phi_a^{(+)s}(t)\rangle = \langle\chi_b|\bar{V}|\chi_a\rangle(1 + t\langle\chi_b|\bar{V}|\phi_a^{(+)s}(t)\rangle) \tag{5.4.14}$$

$$x_t = \frac{\langle\chi_b|\bar{V} - \bar{V}G_o^{+}\bar{V}|\phi_a^{(+)s}(t)\rangle}{\langle\chi_b|\bar{V}|\chi_a\rangle} \tag{5.4.15}$$

The alternative approximation to the T-matrix element is

$$\frac{1}{2}T_{ba}^{s} \simeq X_2(t) = \frac{\bar{F}_{ba}S_{ba}}{\underline{G}_b^{\dagger}\underline{\bar{D}}_{ba}^{-1}\underline{R}_a} \tag{5.4.16}$$

$$S_{ba} = \langle\chi_b|\bar{V}|\chi_a\rangle$$

$$\{\underline{G}_a\}_i = \langle\psi_i|\bar{V} - \bar{V}G_o^{(+)}\bar{V}|\chi_a\rangle$$

Again,

$$\frac{d}{dt} X_2(t) = \frac{S_{ba}}{(\underline{G}_b^+ \underline{\underline{D}}_{ba}^{-1} \underline{R}_a)^2} \left[\underline{G}_b^+ \underline{\underline{D}}_{ba}^{-1} \underline{R}_a \frac{d\bar{F}_{ba}}{dt} - \bar{F}_{ba} \underline{G}_b^+ \left(\frac{d}{dt} \underline{\underline{D}}_{ba}^{-1} \right) \underline{R}_a \right]$$

$$= \frac{S_{ba}}{(\underline{G}_b^+ \underline{\underline{D}}_{ba}^{-1} \underline{R}_a)^2} \left[\frac{d\bar{F}_{ba}}{dt} + \bar{F}_{ba} \underline{R}_b^+ \underline{\underline{D}}_{ba}^{-1} \underline{R}_a \right]$$

$$= 0 \quad ; \quad \underline{G}_b^+ \underline{\underline{D}}_{ba}^{-1} \underline{R}_a \neq 0 \qquad (5.4.17)$$

The two t methods only differ from the t = 0 cases at singularities in X(t) and $X_2(t)$. Thus they are not useful in removing false structure in X(0) and $X_2(0)$, as the only different results they can give are singularities.

The use of (5.4.18) as an expression for $\frac{1}{2} T^s_{ba}$ was tested as (5.4.19) only holds formally for the exact wavefunction $| \Phi_a^{(+)s} \rangle$.

$$X_2(0) = \frac{F_{ba} S_{ba}}{\underline{G}_b^+ \underline{\underline{D}}^{-1} \underline{R}_a} \qquad (5.4.18)$$

$$\langle \chi_b | \bar{V} | \chi_a \rangle = \langle \chi_b | \bar{V} - \bar{V} G_o^{(+)} \bar{V} | \Phi_a^{(+)s} \rangle \qquad (5.4.19)$$

However, in all tests using the T matrix method, the expression $U_{ba} = S_{ba} / (\underline{G}_b^+ \underline{\underline{D}}^{-1} \underline{R}_a)$ was very close (within three to four figures in both real and imaginary parts) to unity for the 1s-1s and 1s-2s T matrix elements over all the energy range, and did not affect the cross sections. For the higher channels, agreement was not always so good, and

TABLE 5.5

SAMPLE VALUES OF U_{ba}

BASIS B CLOSE COUPLING (NTR = 14)

ENERGY	b	a	$Re(U_{ba})$	$\overline{Im(U_{ba})}$
0.6	1	1	1.0 : 7	10E-8
0.6	2	1	1.0 : 6	10E-6
0.85	1	1	1.0 : 5	10E-5
0.85	2	1	1.0 : 4	10E-3
1.3	1	1	1.0 : 5	10E-6
1.3	2	1	1.0 : 5	10E-5

BASIS B TRIAL, BASIS D GREENS (NTR = 14)

ENERGY	b	a	$Re(U_{ba})$	$\overline{Im(U_{ba})}$
0.6	1	1	1.0 : 4	10E-5
0.6	2	1	1.0 : 3	10E-3
0.96	1	1	1.0 : 4	10E-6
0.96*	2	1	1.0 : 4	10E-3
1.25*	1	1	1.0 : 4	10E-4
1.25	2	1	1.0 : 3	10E-4

$Re(U_{ba})$: The number of decimal places to which the value is exactly 1.0 is shown.

$\overline{Im(U_{ba})}$: The modulus of the value rounded up to the next power of 10 is shown.

* : A false resonance occurs at this energy with the basis functions used.

Energies are shown as described in table 5.1. Other units are dimensionless. Symbols are as described in the text.

the K matrix method for the coupled channel problem was slightly destabilised here. Tests were made on the coupled channel problem, the 1s trial, 1s-2s Green's problem of figure 5.10b, and on problems using combinations of bases B and D for trial bases and the Green's function. Some sample values of $U_{b\alpha}$ for the T matrix method are shown in table 5.5.

5.5 Modifications of the Schwinger Method

The rest of this chapter concerns various modifications we made to the Schwinger principle in order to try and improve on results beyond the coupled channel problem. In this section, two methods of limited success are detailed. Section 5.6 applies a variational principle used with success at low energies to the present intermediate energy problem.

5.5A Use of an Orthogonalised Trial Function

The trial functions $\phi^{(+)s}_{b\alpha}(r_1, r_2)$ we have used so far retain a degree of non-uniqueness, as there is the possibility of them containing the rearranged system which we include explicitly in the exchange terms. As described by Peterkop (1977) and in chapter one, double counting may be avoided by making the scattering functions $f^{(+)s}_{ni}$ orthogonal to all hydrogen functions ϕ_n with energy $\varepsilon_n < \varepsilon_m$. In the

case of our method, we have so far assumed that this would occur "automatically" as the coefficients c_{ji} were determined, provided a reasonable variety of trial functions were used, and in the coupled equations case convergent results were obtained. As the more general case was not so convergent, owing to the false resonances, we thought it worthwhile approximating the orthogonality condition more explicitly. We changed the form of the scattering trial functions so that they were orthogonal to all the trial function target pseudostates of lower energy.

$$\Theta_{ji}(r) \rightarrow \Theta_{ji}(r) - \sum_{m<i} \langle R_m | \theta_{ji} \rangle R_m(r) \qquad (5.5.1)$$

$R_m(r)$ = trial function hydrogen/pseudo state.

This would not eliminate false resonance entirely, as shown by the most simple case of a single channel 1s trial function and a 1s-2s Green's function, which would be unaffected by the process.

In practice, we found that energy independent sine and cosine type trial functions were required in the positive pseudochannels, as purely S.T.O. based trial functions were reduced to zero by the subtraction process. The close coupled results were not seriously affected by the change, and some comparisons of convergence for basis B are shown in table 5.6. More general tests showed that false resonances were not eliminated by this procedure, which made little

TABLE 5.6

CONVERGENCE COMPARISON: STANDARD METHOD 5.2 (S) AND METHOD 5.5A (P) FOR BASIS B CLOSE COUPLING

ENERGY = 0.7

NTR	CROSS SECTIONS 1S-1S		1S-2S	
	S	P	S (*10E-1)	P (*10E-1)
7	0.207	0.195	0.259	0.277
8	0.206	0.188	0.271	0.258
9	0.206	0.206	0.272	0.266
10	0.206	0.206	0.271	0.271
11	0.206	0.206	0.272	0.272
12	0.206	0.206	0.272	0.272

ENERGY = 1.3

NTR	CROSS SECTIONS 1S-1S		1S-2S	
	S (*10E-1)	P (*10E-1)	S (*10E-1)	P (*10E-1)
7	0.972	0.805	0.103	0.107
8	0.959	0.913	0.117	0.106
9	0.961	0.960	0.115	0.119
10	0.960	0.961	0.116	0.119
11	0.968	0.965	0.114	0.115
12	0.964	0.965	0.115	0.115
13	0.964	0.965	0.115	0.115
14	0.965	0.965	0.115	0.115

(Units and symbols are as described in table 5.1 and in the text. Where indicated, cross sections should be multiplied by the appropriate factor of 10.)

difference to the results, but were sometimes narrowed or appeared in different places. Shown in figure 5.11 are cross sections with and without orthogonalisation for a 1s-2s-3s Green's function and a 1s-2s trial function. Convergence was not affected, being good away from false resonances but unreliable owing to the possibility of them appearing. Also shown in figure 5.11 are results using a basis B trial function and a 1s-2s-3s Green's function using both methods. The results are smooth apart from a very narrow false resonance, and follow fairly closely the 1s-2s close coupling results. Further tests, with $m \lesssim i$ in (5.5.1) gave unstable results for NTR $\lesssim$ 16 as if too much information had been removed from the trial function.

5.5B Method of R. Hewitt

This method attempts to relate the positive channel pseudostates $R_n(r)$ ($\bar{\varepsilon}_n > 0$) to the Coulomb functions $F(K,r)$ and modify the Green's function $\bar{G}_0^{(+)}$ to relate it to the Poet Green's function $G_0^{(+)}$, hopefully removing pseudoresonances in the process. Following the discussion of chapter two, we may write, over a limited range of coordinate space:

$$F(K_m, r) \simeq N_m R_m(r) \quad ; \quad \tfrac{1}{2} K_m^2 = \bar{\varepsilon}_m \ , \ N_m \text{ a constant.}$$

This method supposes that the real continuum part of the Green's function $G_0^{(+)}$

$$\mathrm{Re}\, G_{0>}^{(+)} = \frac{8}{\pi^2} \int_0^\infty dK\, F(K,r_2) F(K,r_2') \, P\int_0^\infty dq \frac{\sin qr_1 \sin qr_1'}{(2(E-\frac{1}{2}K^2) - q^2)} \qquad (5.5.3a)$$

FIGURE 5.11A

CROSS SECTIONS AGAINST INCIDENT ELECTRON ENERGY

Models and bases employed are as described in the text. Units are as in Table 5.1.

1s-2s trial basis, 1s-2s-3s Green's function.

(i) 1S - 1S Cross Sections

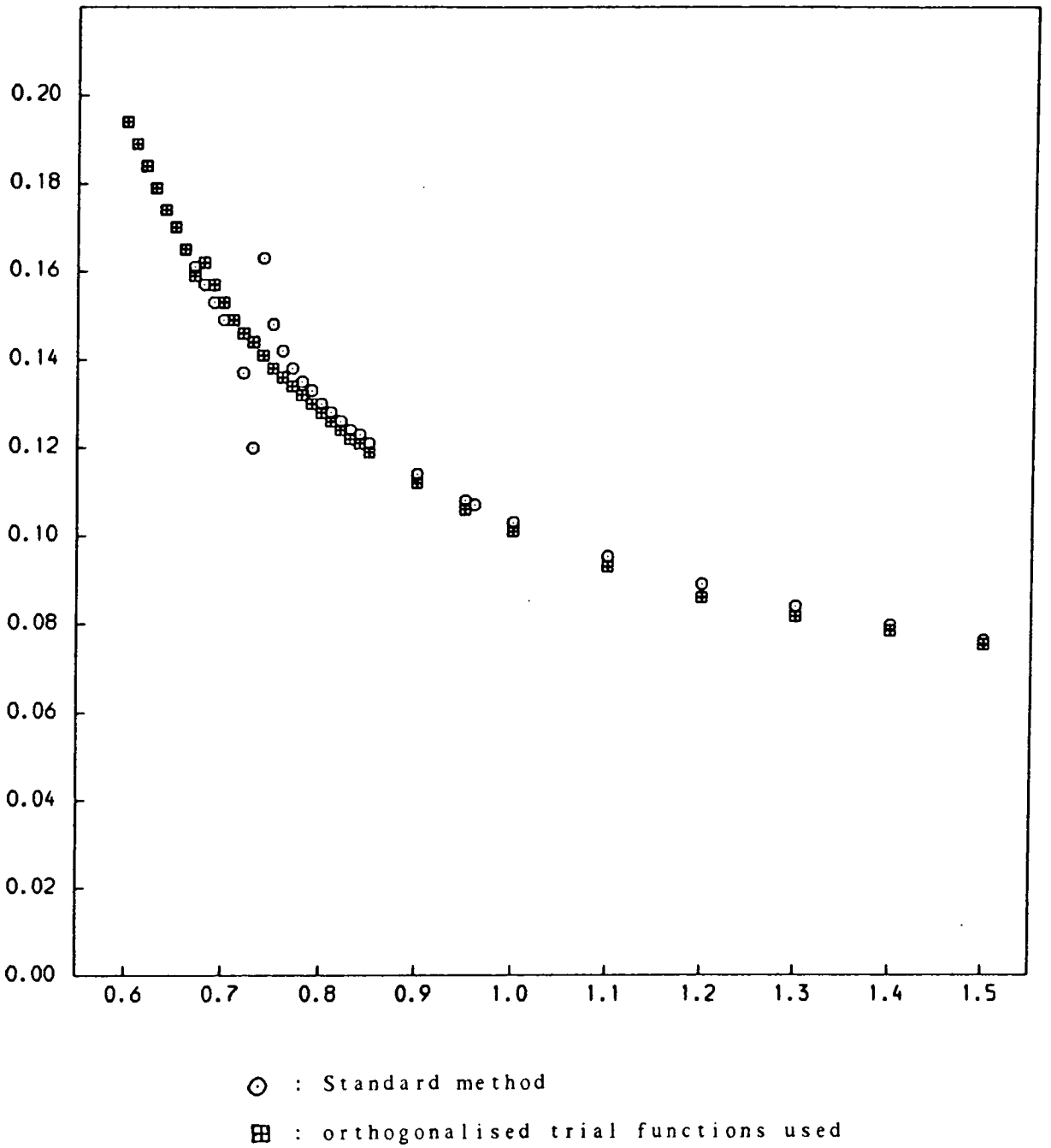

⊙ : Standard method

⊞ : orthogonalised trial functions used

FIGURE 5.11A

CROSS SECTIONS AGAINST INCIDENT ELECTRON ENERGY

Models and bases employed are as described in the text. Units are as in Table 5.1.

1s-2s trial basis, 1s-2s-3s Green's function.

(ii) 1S - 2S Cross Sections

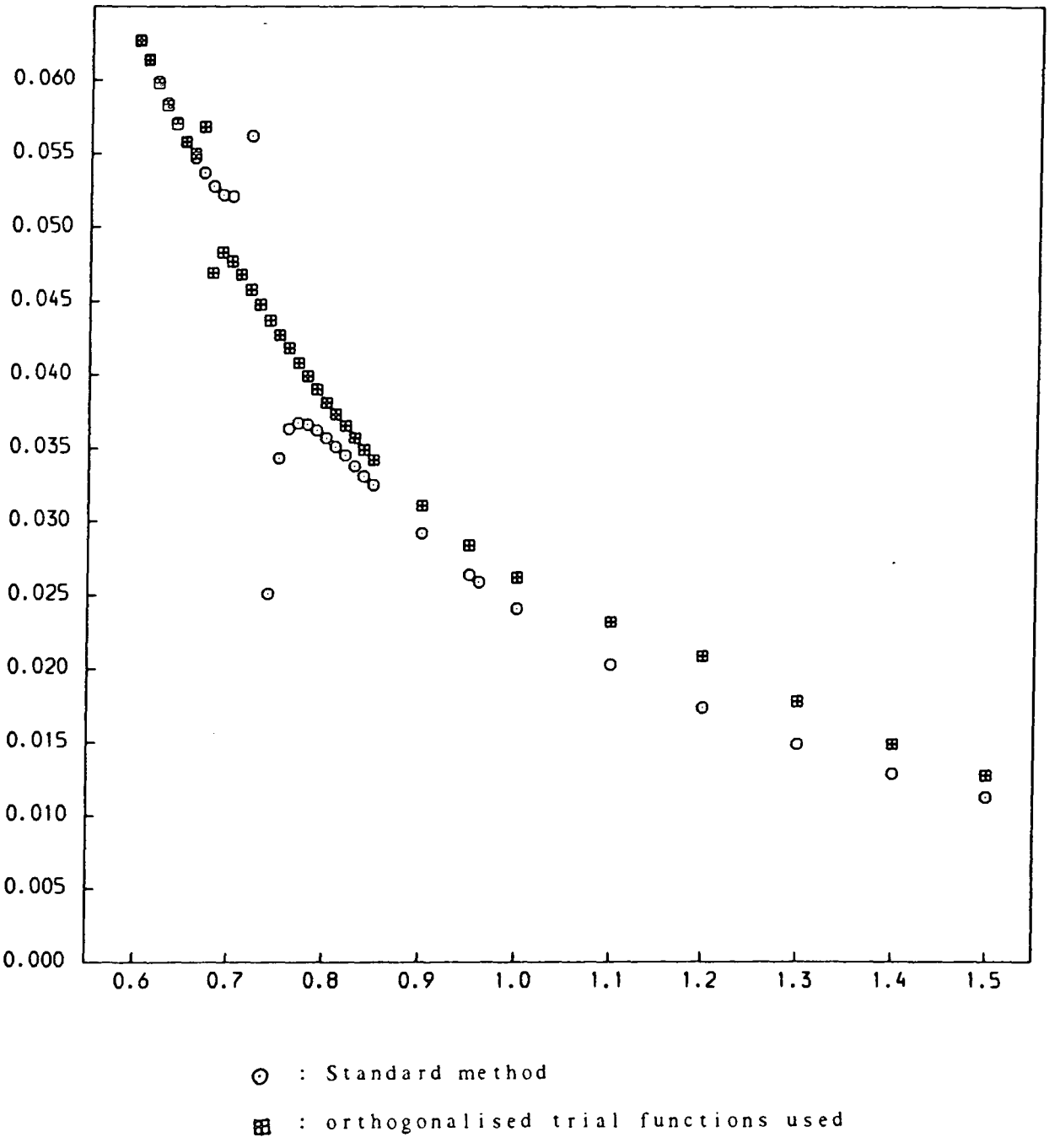

FIGURE 5.11B

CROSS SECTIONS AGAINST INCIDENT ELECTRON ENERGY

Models and bases employed are as described in the text. Units are as in Table 5.1.

B trial basis (positive pseudostate threshold in range marked), 1s-2s-3s Green's function.

(i) 1S - 1S Cross Sections

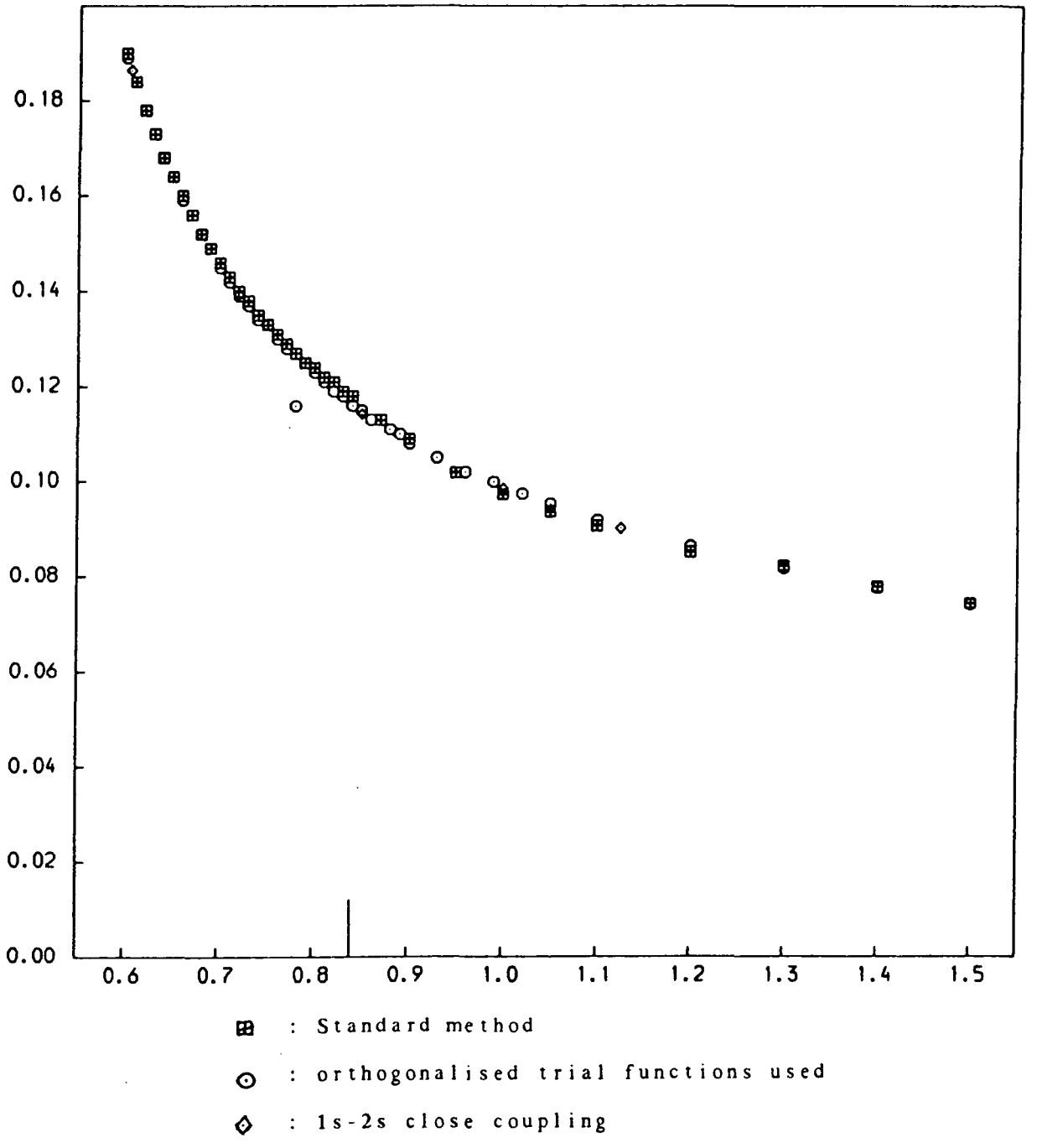

FIGURE 5.11B

CROSS SECTIONS AGAINST INCIDENT ELECTRON ENERGY

Models and bases employed are as described in the text. Units are as in Table 5.1.

B trial basis (positive pseudostate threshold in range marked), 1s-2s-3s Green's function.

(ii) 1S - 2S Cross Sections

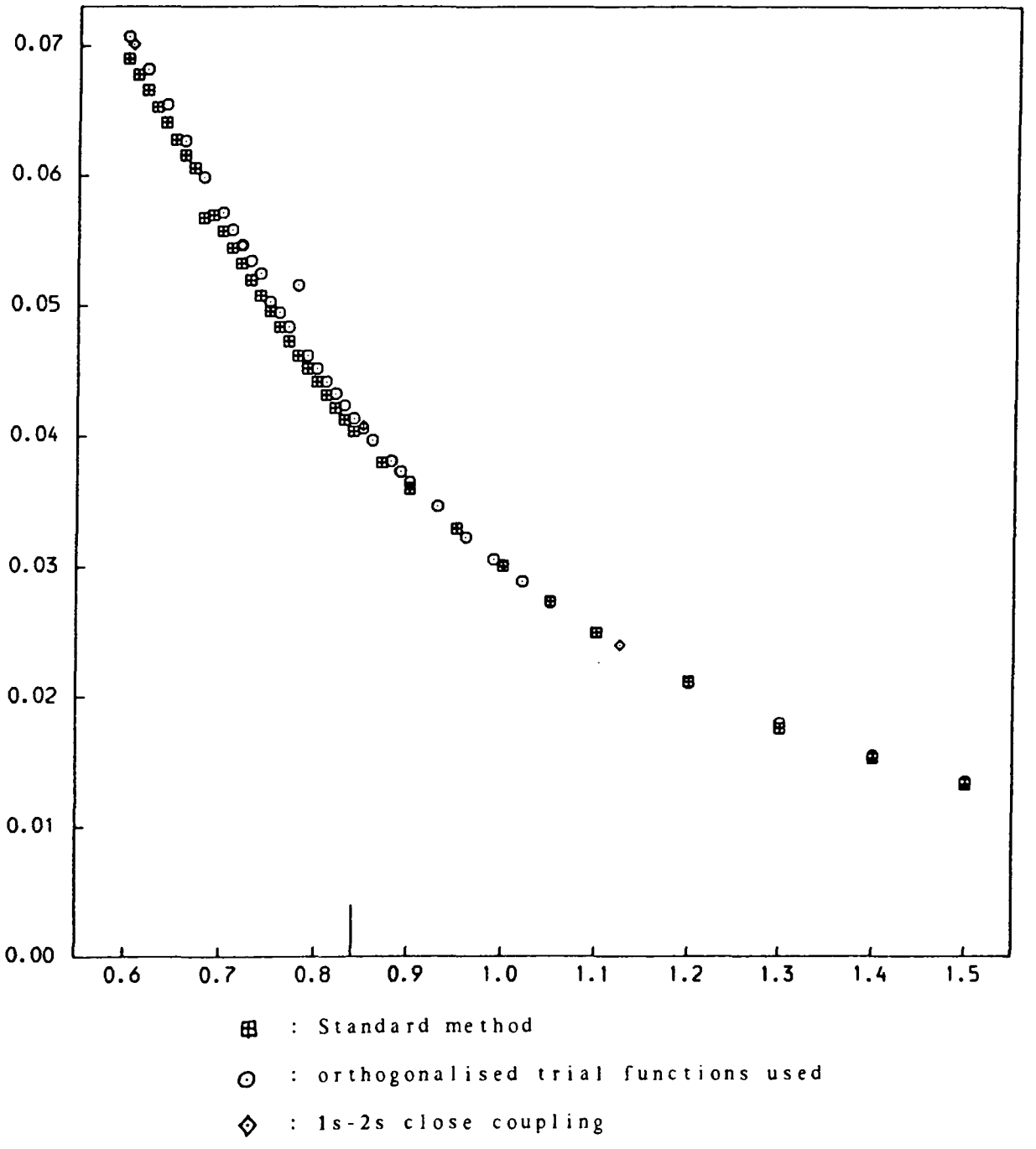

may be written as

$$\mathrm{Re}\, G^{(+)}_{o,} \lesssim \sum_m \frac{8}{\pi^2} \int_{K_a - \frac{\Delta_a}{2}}^{K_a + \frac{\Delta_m}{2}} dK\; F(K, r_2) F(K, r_2') P \int_0^\infty dq \frac{\sin qr \sin qr'}{2(E - \frac{1}{2}K^2) - q^2} \; ; \bar{\varepsilon}_m > 0$$

$$\lesssim \sum_m \frac{8}{\pi^2} N_m^2 R_m(r_2) R_m(r_2') \int_0^\infty dq \sin qr \sin qr' S_m(E, q) \; ; \bar{\varepsilon}_m > 0 \qquad (5.5.3b)$$

P represents a principal value ingegral. We have assumed F(K,r) does not vary greatly over the range Δ_m.

$$S_m(E, q) = P \int_{K_a - \frac{\Delta_a}{2}}^{K_a + \frac{\Delta_a}{2}} dK \frac{1}{(2E - q^2) - K^2}$$

$$= \begin{cases} \dfrac{1}{(q^2 - 2E)^{1/2}} \left[\tan^{-1}\left(\dfrac{K_m - \frac{\Delta_m}{2}}{(q^2 - 2E)^{1/2}} \right) - \tan^{-1}\left(\dfrac{K_m + \frac{\Delta_m}{2}}{(q^2 - 2E)^{1/2}} \right) \right]; & 2E < q^2 \\ \dfrac{1}{(K_m + \frac{\Delta_m}{2})} - \dfrac{1}{(K_m - \frac{\Delta_m}{2})} & ; 2E = q^2 \\ \dfrac{1}{(2E - q^2)^{1/2}} \ln \left| \dfrac{((2E - q^2)^{1/2} + \frac{\Delta_m}{2})^2 - K_m^2}{((2E - q^2)^{1/2} - \frac{\Delta_m}{2})^2 - K_m^2} \right| & ; 2E > q^2 \end{cases} \qquad (5.5.4)$$

The integral over q is then performed numerically using a single Gaussian quadrature transformation of the form (5.2.17). Δ_m is found as follows. In our pseudostate "target" expansion, we have replaced the continuous spectrum (5.5.5a) with the sum (5.5.5b)

$$\int_0^\infty \frac{2}{\pi K} |F(K)\rangle\langle F(K)| \, d\left(\tfrac{1}{2}K^2\right) \qquad (5.5.5a)$$

$$\sum_m |R_m\rangle\langle R_m| \qquad (5.5.5b)$$

Thus we may require in the present method:

$$\sum_m \int_{K_m-\frac{\Delta_m}{2}}^{K_m+\frac{\Delta_m}{2}} dK \, \frac{2}{\pi} |F(K)\rangle\langle F(K)|$$

$$\simeq \sum_m \frac{2}{\pi} N_m^2 |R_m\rangle\langle R_m| \int_{K_m-\frac{\Delta_m}{2}}^{K_m+\frac{\Delta_m}{2}} dK$$

$$= \sum_m |R_m\rangle\langle R_m| \qquad ; \varepsilon_m > 0 \qquad (5.5.6a)$$

i.e.

$$1/\Delta_m = \frac{2N_m^2}{\pi} \qquad (5.5.6b)$$

We found N_m numerically using the Coulomb function generator routine mentioned in section 5.3 and requiring:

$$N_m \int_0^\infty dr \, R_m(r) F(K_m, r) = \int_0^\infty dr \, \left(F(K_m, r)\right)^2 \qquad (5.5.7a)$$

Similar numerical equalities, for example (5.5.7b), gave consistent results.

$$N_m \int_0^\infty dr \, \frac{R_m(r) F(K_m, r)}{r} = \int_0^\infty dr \, \frac{\left(F(K_m, r)\right)^2}{r} \qquad (5.5.7b)$$

The positive imaginary part of the Green's function is

treated in a similar manner to the positive real part:

$$\mathrm{Im}\, G_{o,}^{(+)} = -\frac{4}{\pi}\int_0^k dK\, \frac{F(K,r_2)\,F(K,r_2')}{\sqrt{(k^2-K^2)}} \sin\sqrt{(k^2-K^2)}\,r_1 \sin\sqrt{(k^2-K^2)}\,r_1' \quad ; \tfrac{1}{2}k^2 = E$$

$$\simeq -\frac{4}{\pi}\sum_{m'}\int_{K_{m'}-\frac{\Delta_{m'}}{2}}^{K_{m'}+\frac{\bar{\Delta}_{m'}}{2}} dK\, \frac{F(K,r_2)\,F(K,r_2')}{\sqrt{(k^2-K^2)}} \sin\sqrt{(k^2-K^2)}\,r_1 \sin\sqrt{(k^2-K^2)}\,r_1'$$

$$\simeq -\frac{4}{\pi}\sum_{m'} N_{m'}^2\, R_{m'}(r_2)\, R_{m'}(r_2')\, \sin \bar{k}_{m'} r_1\, \sin \bar{k}_{m'} r_1'\, Q_{m'}(E)$$

$$; \quad 0 \le \bar{E}_{m'} \le E \qquad (5.5.8)$$

$$Q_m(E) = \int_{K_m-\frac{\Delta_m}{2}}^{K_m+\frac{\bar{\Delta}_m}{2}} dK\, \frac{1}{\sqrt{(k^2-K^2)}}$$

$$= \sin^{-1}\left(\frac{K_m+\frac{\bar{\Delta}_m}{2}}{k}\right) - \sin^{-1}\left(\frac{K_m-\frac{\Delta_m}{2}}{k}\right) \qquad (5.5.9)$$

The bar over Δ_m is there because in the uppermost imaginary pseudochannel ($K_m + \Delta_m/2$) is replaced by k if ($K_m + \Delta_m/2$) > k. The final result is to replace $(\bar{k}_m)^{-1}$ with $\Delta_m^{-1} Q(E)$ in the positive channels in the expression for Im $G_o^{(+)}$. The negative energy Green's channels remain the same as in $\bar{G}_o^{(+)}$ for both real and imaginary parts.

Results for the method were disappointing. Sample matrix elements were still found to have discontinuous derivatives with respect to incident electron energy at the pseudostate thresholds, and pseudoresonances still appeared in the cross sections despite being "hidden" in the formalism. With exchange, false resonances appeared in all

cases and distorted the curves further. Shown in figure 5.12 are cross sections without exchange using a basis B trial and Green's function. Also shown are cross sections found using an eleven pseudostate Green's function basis G (see table 5.2) and a 1s-2s-3s trial function, where pseudoresonances are much smaller and narrower. This agrees with the findings of Oza (1984) and our own work in section 5.3 that pseudoresonances become less apparent as the number of pseudostates in the Green's function increases.

5.6 Method of Luchesse and McKoy

The major drawbacks in applying the Schwinger principle to the Poet problem are that firstly, the continuum states of the hydrogen atom need to be represented in the Green's function, and secondly, false resonances obscure the results if the Green's function contains more information than the trial function. Luchesse and McKoy (1979) and Takatsuka and McKoy (1984) in their work on low energy electron atom scattering and electron molecule scattering, proposed a new principle which avoided this problem at low energies. This principle can be adapted into our formalism to be tested at intermediate energies, both in the general case and in the pseudostate coupled channel problem where it can be applied exactly.

A projection operator (different in form to the Feshbach projection operators mentioned in chapter three) is

FIGURE 5.12A

CROSS SECTIONS AGAINST INCIDENT ELECTRON ENERGY: NO EXCHANGE

Models and symbols as described in the text. Units as in Table 5.1.

Basis B trial and Green's function (the positive pseudothreshold in the range is marked).

(i) 1S - 1S Cross Sections

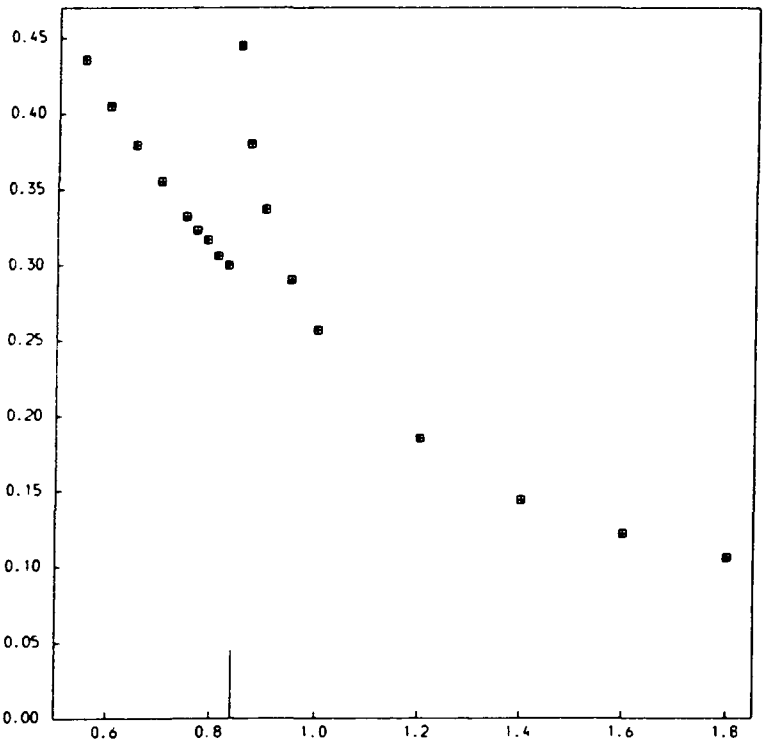

(ii) 1S - 2S Cross sections

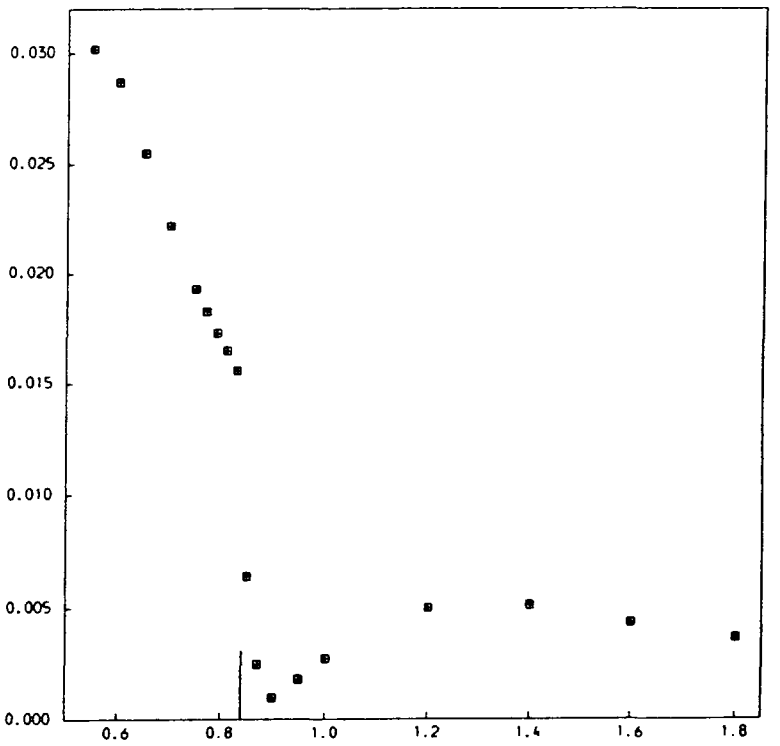

FIGURE 5.12B

CROSS SECTIONS AGAINST INCIDENT ELECTRON ENERGY: NO EXCHANGE

Models and symbols as described in the text. Units as in Table 5.1.

1s-2s-3s trial basis, basis G Green's function (positive pseudothresholds in the range are marked).

(i) 1S - 1S Cross Sections

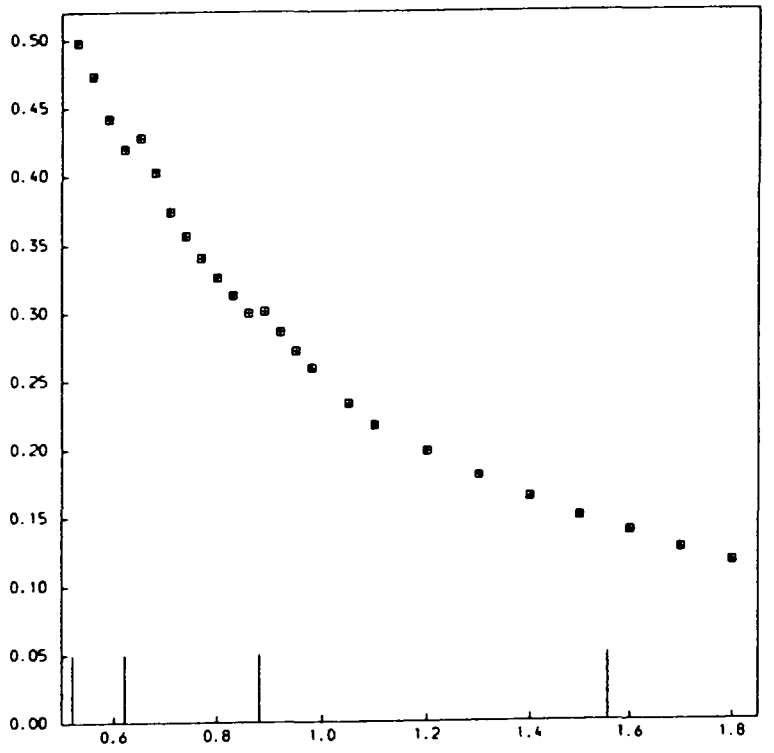

(ii) 1S - 2S Cross sections

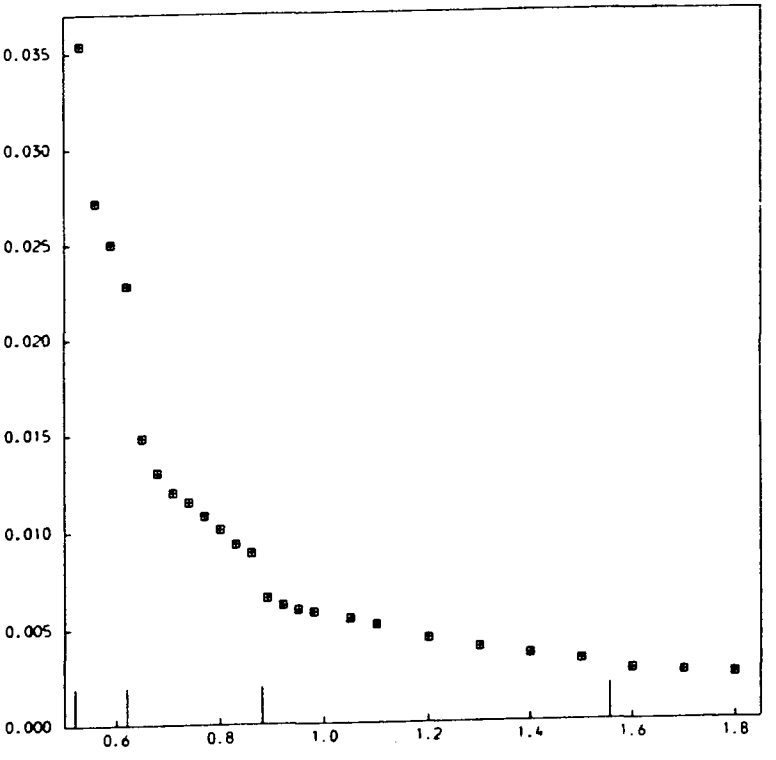

defined as

$$P = \sum_{m=1}^{N_o} |\phi_m\rangle\langle\phi_m| \quad ; P^N = P \tag{5.6.1}$$

P projects onto the target coordinate (r_2) and contains the incident channel.

We operate with P on the Lippmann Schwinger equation (5.6.2)

$$|\phi_i^{(+)s}\rangle = |\chi_i\rangle + G_o^{(+)}(V - (-1)^s \hat{H}A)|\phi_i^{(+)s}\rangle \tag{5.6.2}$$

$$P|\phi_i^{(+)s}\rangle = |\chi_i\rangle + G_o^{(+)P}(V - (-1)^s \hat{H}A)|\phi_i^{(+)s}\rangle \tag{5.6.3}$$

$$G_o^{(+)P} = \sum_{m=1}^{N_o} |\phi_m\rangle g_{om}^{(+)} \langle\phi_m| \tag{5.6.4}$$

(5.6.3) implies the T matrix elements may be rewritten:

$$-\tfrac{1}{2} T_{fi}^s = \langle \phi_f^{(-)s} | V - (-1)^s \hat{H}A | \chi_i \rangle$$

$$= \langle \phi_f^{(-)s} | (V - (-1)^s \hat{H}A) P | \phi_i^{(+)s} \rangle$$

$$- \langle \phi_f^{(-)s} | (V - (-1)^s \hat{H}A) G_o^{(+)P} (V - (-1)^s \hat{H}A) | \phi_i^{(+)s} \rangle \tag{5.6.5}$$

As it stands, this term cannot replace (5.1.9b) in the Schwinger principle as the first term is not hermitian, and variation of $\phi_i^{(+)s}$ does not recover the projected Lippmann-Schwinger equation. To recover the unprojected part of $G_o^{(+)}$, the following Schrödinger equations are considered.

$$P\hat{H}P\,|\,\phi_i^{(+)s}\rangle = P(V-(-1)^s\hat{H}A)\,|\,\phi_i^{(+)s}\rangle - PVP\,|\,\phi_i^{(+)s}\rangle$$

(5.6.6)

$$(1-aP)(\hat{H}+(-1)^s\hat{H}A)(1-aP)\,|\,\phi_i^{(+)s}\rangle = -a(1-aP)(\hat{H}+(-1)^s\hat{H}A)P\,|\,\phi_i^{(+)s}\rangle$$

(5.6.7)

(5.6.7) may be rewritten:

$$\left[\hat{H}+(-1)^s\hat{H}A - a\{P(\hat{H}+(-1)^s\hat{H}A)+(\hat{H}+(-1)^s\hat{H}A)P\}\right]|\,\phi_i^{(+)s}\rangle$$

$$= -a(\hat{H}+(-1)^s\hat{H}A)P\,|\,\phi_i^{(+)s}\rangle$$

$$= a(V-(-1)^s\hat{H}A)P\,|\,\phi_i^{(+)s}\rangle - a\hat{H}_0P\,|\,\phi_i^{(+)s}\rangle$$

$$= a(V-(-1)^s\hat{H}A)P\,|\,\phi_i^{(+)s}\rangle - aP(V-(-1)^s\hat{H}A)\,|\,\phi_i^{(+)s}\rangle$$

(5.6.8)

The identity $P\hat{H}_0 = \hat{H}_0P$ has been used.

(5.6.9)

Using (5.6.8), the T matrix element may be written:

$$-\tfrac{1}{2}T^s_{fi} = \langle\phi_f^{(-)s}\,|\,\tfrac{1}{2}\{(V-(-1)^s\hat{H}A)P + P(V-(-1)^s\hat{H}A)\}$$

$$-\tfrac{1}{2}\{P(\hat{H}+(-1)^s\hat{H}A)+(\hat{H}+(-1)^s\hat{H}A)P\}$$

$$+\tfrac{1}{2a}(\hat{H}+(-1)^s\hat{H}A)-(V-(-1)^s\hat{H}A)G_0^{(+)P}(V-(-1)^s\hat{H}A)\,|\,\phi_i^{(+)s}\rangle$$

(5.6.10)

Choosing the parameter a = ½ recovers the original functional when P = 1, and (5.6.10) may be used as the denominator in a Schwinger type variational principle.

This method was tested using the Schwinger principle for the coupled channel problem, with (5.6.1) replaced by

$$P = \sum_{m=1}^{N_o} |R_m\rangle\langle R_m| \qquad (5.6.11)$$

$G_o^{(+)}$ is replaced by $\bar{G}_o^{(+)}$, and trial functions of the form (5.2.12) are used. Equation (5.6.9) is replaced by (5.6.12):

$$\langle R_n | P \hat{H}_o | R_{n'} \rangle = \langle R_n | \hat{H}_o P | R_{n'} \rangle \qquad (5.6.12)$$

It should be noted that in manipulating the equivalent of equations (5.6.6-8) multiplication on the left by a function $\langle R_n|$ is implicit. It was found that as long as P contained all the open channels for the problem, the new principle gave correct converged results. That is to say, for a particular N_o, the Luchesse-McKoy principle gave correct results, including "below threshold threshold structure", for incident energies up to the threshold for the $(N_o + 1)$ channel. Above this energy (i.e. not all open channels are included in P) the results did not converge and were inaccurate. Sample results for basis B are shown in figure 5.13 and table 5.7. The first three states are included in P. Both T matrix and K matrix (using a matrix of channels common to the trial function and $\bar{G}_o^{(+)P}$) methods give the same results. Table 5.7 shows that convergence below the threshold is slightly faster in the full Schwinger method, and that above threshold the new method does not converge.

FIGURE 5.13

CROSS SECTIONS AGAINST INCIDENT ELECTRON ENERGY FOR BASIS B.

Models are as described in the text. Units are as described in Table 5.1.

(i) 1S - 1S Cross Sections

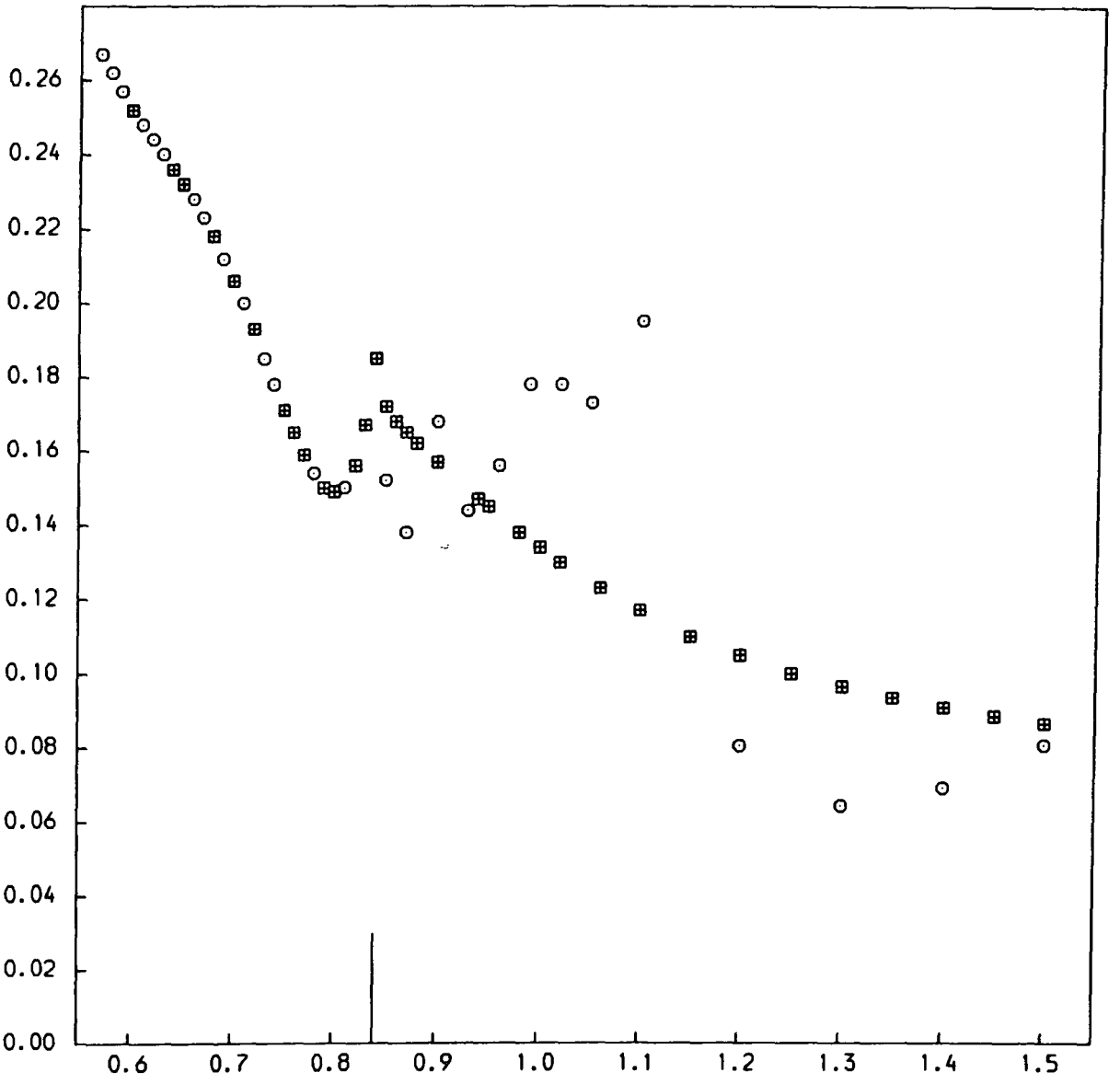

⊞ : Standard coupled channel results

⊙ : Projection operator method

Trial / Green's function positive pseudostate thresholds in the range are marked (see Table 5.2).

FIGURE 5.13

CROSS SECTIONS AGAINST INCIDENT ELECTRON ENERGY FOR BASIS B.

Models are as described in the text. Units are as described in Table 5.1.

(ii) 1S - 2S Cross Sections

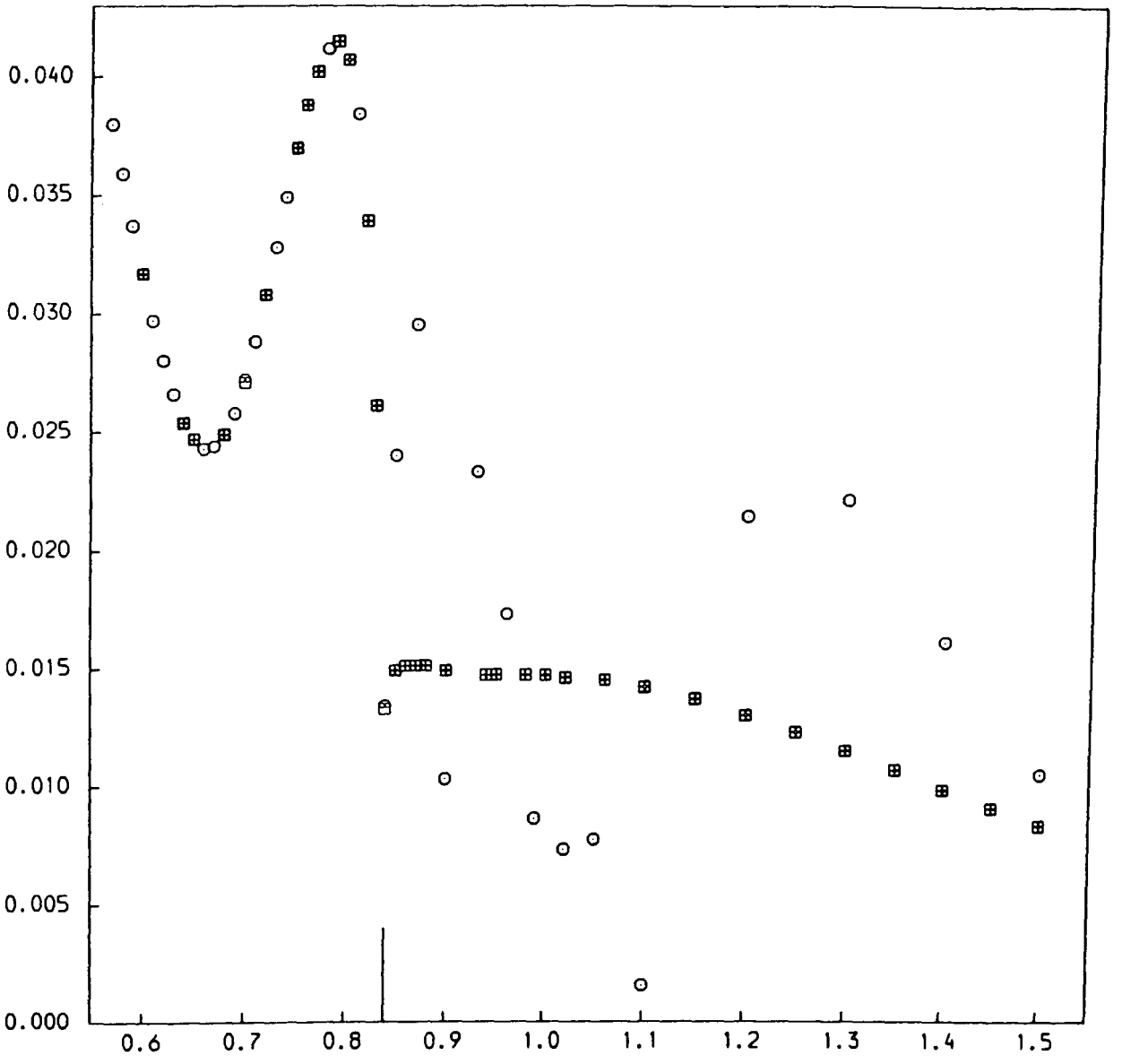

⊞ : Standard coupled channel results

⊙ : Projection operator method

Trial / Green's function positive pseudostate thresholds in the range are marked (see Table 5.2).

TABLE 5.7

CONVERGENCE COMPARISON: STANDARD METHOD 5.2 (S) AND METHOD 5.6 (M) FOR BASIS B CLOSE COUPLING

ENERGY = 0.7

NTR	CROSS SECTIONS 1S-1S		1S-2S	
	S	M	S	M
			(*10E-1)	
7	0.207	0.224	0.259	0.130
8	0.206	0.204	0.271	0.281
9	0.206	0.207	0.272	0.264
10	0.206	0.206	0.271	0.271
11	0.206	0.206	0.272	0.271
12	0.206	0.206	0.272	0.271

ENERGY = 1.3

NTR	CROSS SECTIONS 1S-1S		1S-2S	
	S	M	S	M
	(*10E-1)		(*10E-1)	
7	0.972	0.695	0.103	0.279
8	0.959	1.18	0.117	0.098
9	0.961	0.879	0.115	0.150
10	0.960	0.888	0.116	0.145
11	0.968	0.819	0.114	0.160
12	0.964	0.786	0.115	0.169
13	0.964	0.809	0.115	0.163
14	0.965	0.694	0.115	0.193

(Units and symbols are as described in table 5.1 and in the text. Where indicated, cross sections should be multiplied by the appropriate factor of 10.)

This is perhaps to be expected, as if not all the open channels are contained in $\bar{G}_o^{(+)P}$, a complex term is being replaced by a real term and information is lost. As a check on this, we tried including the full imaginary part of $\bar{G}_o^{(+)}$ above the fourth threshold. This also gave unstable results, equivalent to the K matrix method when a matrix of the four open channels was formed. This matrix is inherently wrong, as the modified Lippmann Schwinger equation from which the elements are formed does not include the fourth channel. However, for energies below the (N_o+1) threshold, the method is a good one, and also time saving, as fewer matrix elements (5.2.13d) need to be calculated and, as shown in figure 5.14, several of the matrix elements equivalent to (5.2.13c) vanish. This is obviously useful if the basis has some high energy pseudostates, like for example, the fifth state of basis B, which is above the energy range of interest.

We also performed tests on this method for the full Poet problem, using a projected Green's function of up to seven exact s states. The above results suggested the method was likely to be unstable in the intermediate energy range where some continuum channels are open, and this proved to be the case for the inelastic cross section and the K-matrix method generally. Judicious choice of the combination of trial function and N_o did give reasonable results for the elastic cross section at lower energies using the T matrix method. Figure 5.15 shows the elastic

FIGURE 5.14

Matrix Elements For The Method of Section 5.6

Notation is as in the text.

We consider matrix elements:

$$\langle R_m(r_2)\,\theta_{jm}(r_1) \,|\, \tfrac{1}{2}\{(V-(-1)^s\hat{H}A)P + P(V-(-1)^s\hat{H}A) - P(\hat{H}+(-1)^s\hat{H}A) - (\hat{H}+(-1)^s\hat{H}A)P\} + \hat{H}+(-1)^s\hat{H}A \,|\, R_{m'}(r_2)\,\theta_{j'm'}(r_1)\rangle$$

$$= \langle R_m(r_2)\,\theta_{jm}(r_1) \,|\, \hat{H}_0 - \tfrac{1}{2}(P\hat{H}_0+\hat{H}_0P) - V + (PV+VP) + (-1)^s(\hat{H}A - P\hat{H}A - \hat{H}AP) \,|\, R_{m'}(r_2)\,\theta_{j'm'}(r_1)\rangle$$

(a) If $m, m' \leq N_0$, $P = 1$ and the original matrix element is recovered.

(b) If $m \leq N_0$, $m' > N_0$, then $\langle R_m|P = \langle R_m|\,;\ P|R_{m'}\rangle = 0$

The element is:

$$\langle R_m(r_2)\,\theta_{jm}(r_1) \,|\, \tfrac{1}{2}\hat{H}_0 \,|\, R_{m'}(r_2)\,\theta_{j'm'}(r_1)\rangle$$

$$= \langle \theta_{jm} \,|\, \tfrac{1}{2}\left(E - \bar{\varepsilon}_m + \frac{d^2}{2dr^2}\right) |\, \theta_{j'm'}\rangle\, \delta_{mm'}$$

$$= 0 \qquad \text{since } m \neq m'.$$

(c) If $m, m' > N_0$, then $P = 0$

We have:

$$\langle R_m(r_2)\,\theta_{jm}(r_1) \,|\, \hat{H}_0 \,|\, R_{m'}(r_2)\,\theta_{j'm'}(r_1)\rangle - \langle R_m(r_2)\,\theta_{jm}(r_1) \,|\, V-(-1)^s\hat{H}A \,|\, R_{m'}(r_2)\,\theta_{j'm'}(r_1)\rangle$$

$$= \langle \theta_{jm} \,|\, \left(E - \bar{\varepsilon}_m + \frac{d^2}{2dr^2}\right) |\, \theta_{j'm'}\rangle\, \delta_{mm'} - \langle R_m(r_2)\,\theta_{jm}(r_1) \,|\, V-(-1)^s\hat{H}A \,|\, R_{m'}(r_2)\,\theta_{j'm'}(r_1)\rangle$$

cross section found using a basis B trial function and N_o = 4. The convergence at lower energies, though not as good as in the coupled channel case, is to two figures. However, given a particular trial function, the number N_o must be large enough to give reasonable results above the ionisation threshold but not so large that the "projected" Green's function contains much more information than the trial function; for example, with a basis B trial function, N_o = 3 and N_o = 7 gave unphysical, unconverged results throughout. Basis D with N_o = 6 and 7 gave reasonable elastic cross sections up to an incident electron energy of 0.75 a.u. We conclude that the method would be a useful one at low energies when only a few channels are open, as found by Luchesse, Takatsuka and McKoy, but has limited applicability in the intermediate energy range as too much information is lost from the Green's function and not replaced.

FIGURE 5.15

CROSS SECTIONS AGAINST INCIDENT ELECTRON ENERGY

Models and symbols as in the text, units as in Table 5.1.

Elastic Cross Sections: the points are results for the projection operator method, the lines are the exact results

(i) NTR = 10

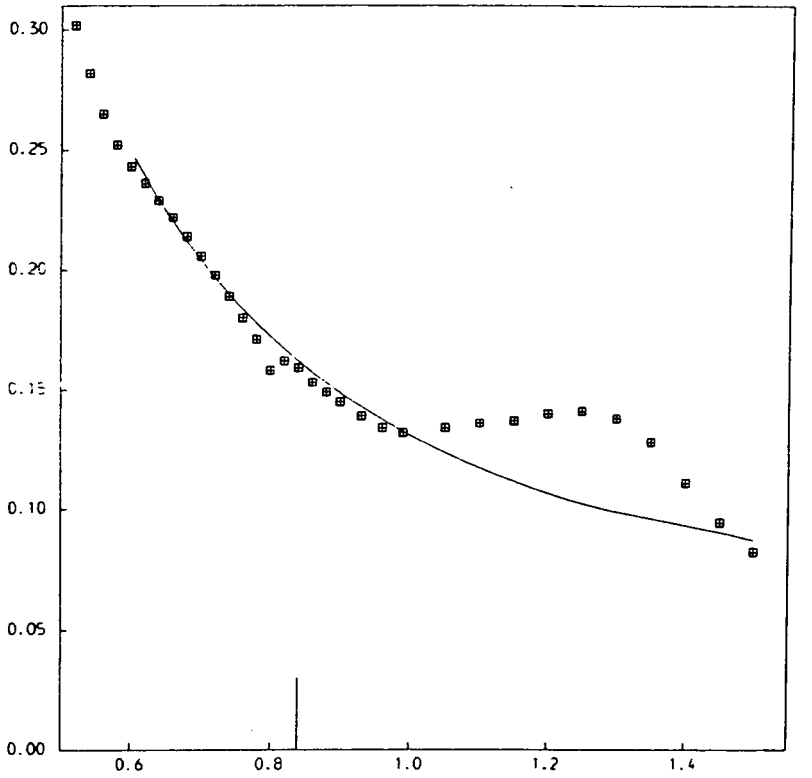

(ii) NTR = 12

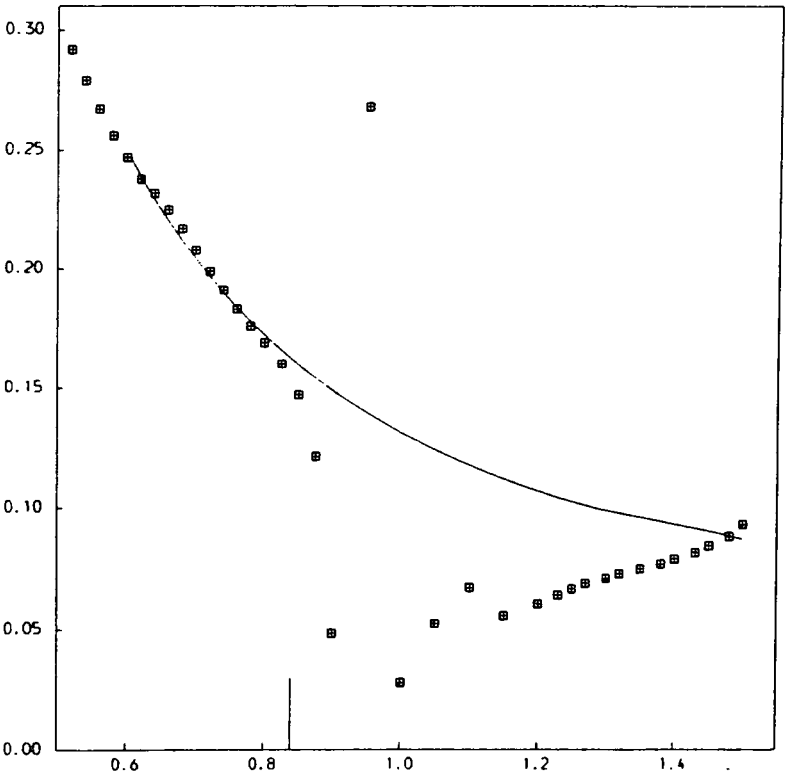

FIGURE 5.15

CROSS SECTIONS AGAINST INCIDENT ELECTRON ENERGY

Models and symbols as in the text, units as in Table 5.1.

Elastic Cross Sections: the points are results for the projection operator method, the lines are the exact results

(iii) NTR = 14

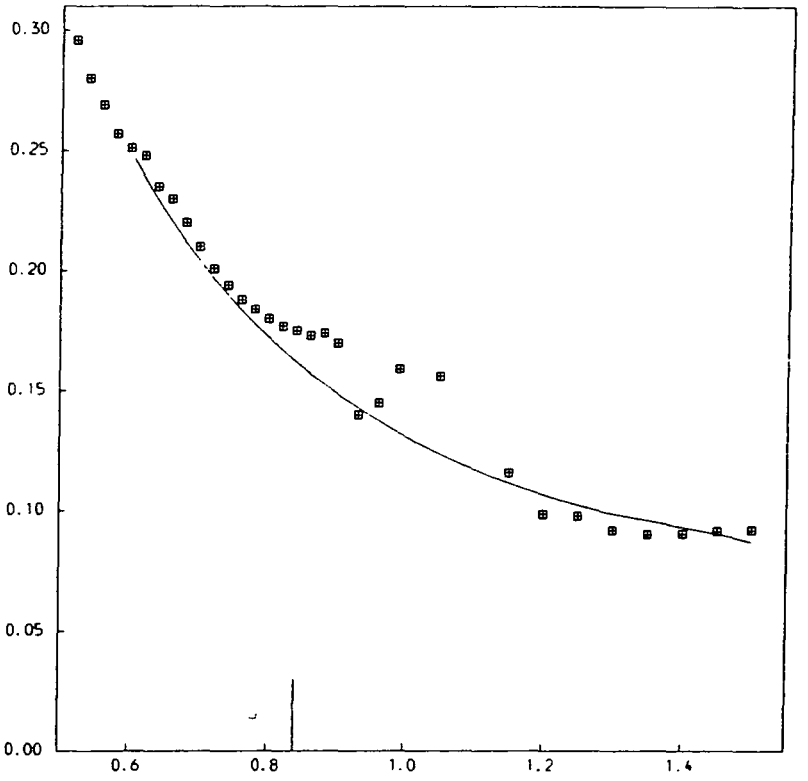

(iv) NTR = 16

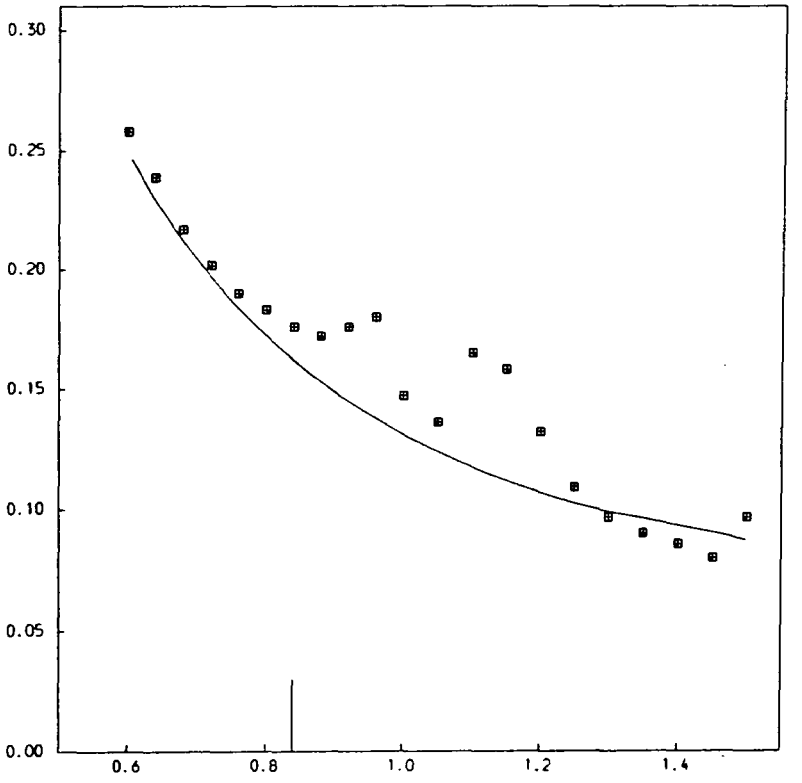

CHAPTER SIX

FUTURE WORK

Notation in sections 6.1 and 6.2 is as in chapters three and five respectively.

6.1 The L-Squared Optical Potential

The perturbation approach used in section 3.3 in the three channel problem gives stable results for the elastic channel, for which the optical potential only contributes to a small proportion of the cross section. However, for inelastic scattering the equivalent quadrature is numerically unstable, with respect to varying input parameters, as a representation of open Q space channels, although a fortuitious choice can give reasonable results, as exemplified in table 3.7. Some extra points to note about the wide range of tests of the method carried out are that results tended to be more stable at higher incident energies ($k^2 \gtrsim 3.2$), and that, as exemplified in table 3.8, if parameters were chosen so that a reasonable number of eigenvectors lay in the range $\Delta_1 > k_1^2 < \Delta_2$ (where there is no "splitting" of equivalent quadrature) stable inelastic results were given reasonably accurately up to the threshold where both Q space channels became open.

I mention these points at this later stage as they corroborate work by Stelbovics and Slim (1987), who, after reading the present work (Bransden and Plummer 1986), extended their (1986) separable potential model problem to two channels and compared an approximate finite basis L-squared solution with the exact infinite basis solution. They found that if the channels were coupled the equivalent quadrature gave accurate converged results for energies up to the threshold where both channels became open: above this energy, rather than the finite basis eigenvectors splitting into two sets, each eigenvector represented a weighted average of the two solutions $\underline{\phi}^n$, n = 1,2 at that energy, and not knowing these weights, they failed to get converged results. Thus, in this energy range the finite basis requires two weights at each eigenvalue to relate it to the exact solution, rather than one as we had assumed, the extra degree of freedom hopefully explaining the numerical instability. Stelbovics and Slim also found that at higher energies the coupling became less important and their finite basis results showed better convergence. Possible future work on our three channel model problem would be to verify these points more exactly and, although testing with several different routines and forms of interpolation has already been carried out, use a more sophisticated numerical differentiation and interpolation routine, such as that of De Blase et al. (1985) to try and separate numerical instability from the theoretical instability predicted by

Stelbovics and Slim. If the equivalent quadrature optical potential model is to be extended to cover several channels, more investigation of the "double equivalent quadrature" found by Stelbovics and Slim, and presumably higher order such quadratures is needed to give accurate open Q space results. However, as noted in section 3.3, the usefulness of the optical potential procedure is its relative simplicity which is lost if complicated procedures are needed to extract the equivalent weights (for example the method of moments is inappropriate for the present calculation as, for each energy, separate moment calculations would have to be performed for each discretised momentum space potential matrix element, these elements also not necessarily being positive definite). The method as it stands is, though, good enough to represent the effect of the Q space channels on P-space channels, in the present model giving reliable elastic cross sections over all the energy range.

6.2 The Schwinger Method

We have shown the Schwinger variational method to be a useful one for calculating coupled channel cross sections at incident energies up to $\sim$ 54 eV or more. The programmes as we used them take about 200 - 300 seconds of c.p.u. time for a 5 channel (e.g. basis B) calculation and up to 1000 - 1400 seconds for a 7 - 9 channel calculation on the Durham

University Amdahl 470/V8 computer, the main time consuming part being calculation of the Green's matrix elements of the type (5.2.13d). The programmes have not been fully optimised, and repeat certain operations as they assume the Green's and trial function bases to be different: with suitable modifications together with the use of the method of section 5.6 the c.p.u. time required can be reduced. For calculations with, say, nine or more channels investigation of an alternative, more stable matrix inversion routine would prove useful. Our further investigations have shown up the limitations of the extended Schwinger method: further investigation of the links between the Kohn principle and the Schwinger principle with trial functions as used here in multichannel formulations is required if "false" resonances are to be made predictable in terms of Kohn principle false resonances. The work of section 5.3 shows that smoothing unphysical structure from a pseudostate Green's function can lead to a smooth T matrix element, and although the Schwinger method is not at present a practical one to investigate this further, Hewitt, McCarthy and Bransden are, at the time of writing, adapting the momentum space formulation of the coupled channel Lippmann Schwinger equations for the T matrix to extend this work without bringing in false resonances, as mentioned earlier. In general, the T matrix averaging process remains at present the most straightforward way of removing pseudoresonant structure. This process assumes pseudostructure to be

localised and distinct so that fitting may be done away from regions where it occurs, and accuracy is basis dependent. Callaway (1985) has presented excitation cross sections for the full electron hydrogen atom scattering problem using an eleven state basis with seven pseudostates and T matrix averaging over pseudoresonances, which need experimental verification to test the procedure. T matrix averaging does not indicate how the pseudostate model gives rise to false structure. Investigations of the kind described here are important in leading to a greater understanding of the problem, and desirable because removing unphysical structure "at source" should, once perfected, give a better description of the processes occurring and also be more reliable.

APPENDIX ONE

Brief Summary of Gauss Quadrature, and Orthogonal Polynomials

The properties of orthogonal polynomials are described in detail and proved by Szegö (1967). A system of polynomials $p_n(x)$ of degree n in x is orthogonal on the interval (a,b) with respect to a positive weight function $\rho(x) > 0$ if

$$\int_a^b dx\, \rho(x)\, p_n(x)\, p_m(x) = \int_{x=a}^{x=b} d(\alpha(x))\, p_n(x)\, p_m(x) = 0 \quad ; \; m \neq n$$

$$\rho(x) = \frac{d}{dx}\alpha(x) \tag{A1.1}$$

The moments μ_j must exist:

$$\mu_j = \int_a^b dx\, \rho(x)\, x^j \quad , \; j = 0,1,2,\ldots \tag{A1.2}$$

The weight function $\rho(x)$ determines the $p_n(x)$ up to a constant factor in each polynomial. For suitably standardised polynomials as detailed by Abramowitz and Stegun (1972)

$$\int_a^b dx\, \rho(x)\, p_n^2(x) = h_n \quad ; \; p_n(x) = k_n x^n + k'_n x^{n-1} + \ldots$$

$$; \; h_n, k_n > 0 \tag{A1.3}$$

For the purposes of chapter two, the normalisation is as considered by Szegö (1967) and h_n is set to 1 for each polynomial (requiring $p_0(x) = 1$ then defines the normalisation of the weight function). The polynomials have

the "Sturm sequence property" and obey a three term recurrence relation.

$$p_{n+1}(x) = (A_n x + B_n) p_n(x) + C_n p_{n-1}(x) \quad ; \; p_{-1}(x) = 0$$

$$A_n = \frac{k_{n+1}}{k_n} \quad , \quad B_n = A_n \left(\frac{k'_{n+1}}{k_{n+1}} - \frac{k'_n}{k_n} \right) \quad , \quad C_n = \frac{k_{n+1} k_{n-1} h_n}{k_n^2 \, h_{n-1}} \qquad (A1.4)$$

The n zeros of $p_n(x)$ are in the interval (a,b). If these are denoted by $x_i^{(n)}$, i = 1, ...n and $x_1^{(n)} < x_2^{(n)} < \ldots < x_n^{(n)}$, then

$$\int_a^b dx \, \rho(x) f(x) = \sum_{i=1}^{n} w_i^{(n)} f(x_i^{(n)}) \qquad (A1.5)$$

In (A1.5), f(x) is a polynomial of degree less than or equal to 2n-1. The Christoffel weights $w_i^{(n)}$ are positive, and

$$(w_i^{(n)})^{-1} = \sum_{j=0}^{n} p_j^2 (x_i^{(n)}) \qquad (A1.6)$$

The quadrature may be used to approximate integrals when f(x) is not a polynomial.

The $p_n(x)$ may be found from the weight function $\rho(x)$ to within a constant by orthogonalising the non negative powers of x with respect to it. The weights and abscissae (zeros of $p_n(x)$) for an n point quadrature may also be found from the first 2n moments μ_j .

$$\mu_j = \int_a^b dx \, \rho(x) x^j = \sum_{i=1}^{n} w_i^{(n)} (x_i^{(n)})^j \quad ; \; j = 0, 1, \ldots, 2n-1 \qquad (A1.7)$$

The analysis in section 2.2 requires finding suitable weight functions $\rho(x)$ from the Sturm sequence recursion relations.

APPENDIX TWO

Laguerre/Slater L-Squared Treatment Of The S Wave Kinetic Hamiltonian

$$(E - H)\,\Psi_R(E,r) = 0 \qquad ; \quad \Psi_a(E,r) \xrightarrow[r\to 0]{} 0$$

$$H = -\frac{d^2}{2dr^2} \tag{A2.1}$$

We use the basis

$$\phi_n(r) = \frac{\lambda r}{(n+1)}\, e^{-\frac{\lambda r}{2}}\, L_n^{(1)}(\lambda r) \qquad ; n = 0,1,2,\ldots. \tag{A2.2}$$

$L^{(1)}_n(x)$ are standard generalised Laguerre polynomials, as described by Abramowitz and Stegun (1972).

$$L_n^{(\alpha)}(x) = \sum_{m=0}^{n} (-1)^m \binom{n+\alpha}{n-m} \frac{x^m}{m!} \tag{A2.3a}$$

$$\int_0^\infty dx\, e^{-x}\, x^\alpha\, L_n^{(\alpha)}(x)\, L_{n'}^{(\alpha)}(x) = \delta_{nn'}\, \frac{\Gamma(n+\alpha+1)}{n!} \tag{A2.3b}$$

$$(n+1)\, L_{n+1}^{(\alpha)}(x) = (2n+\alpha+1-x)\, L_n^{(\alpha)}(x) - (n+\alpha)\, L_{n-1}^{(\alpha)}(x) \tag{A2.3c}$$

$$x\, L_n^{(\alpha)\prime\prime}(x) + (\alpha+1-x)\, L_n^{(\alpha)\prime}(x) + n\, L_n^{(\alpha)}(x) = 0 \tag{A2.3d}$$

The ϕ_n have tridiagonal overlap, following from properties (A2.3bc).

$$\langle \phi_n \mid \phi_{n'} \rangle = \frac{1}{\lambda}\left(2\delta_{nn'} - \delta_{n,n'-1} - \delta_{n,n'+1}\right) \tag{A2.4}$$

We write the Schrödinger equation in the form:

$$\int_0^\infty dr\ \phi_n(r)\,(E-H)\sum_{m=0}^{\infty}\psi_m(E)\,\phi_m(r) = 0 \quad ; \quad n=0,1,2,\ldots \tag{A2.5}$$

Using (A2.3db), we have

$$\langle \phi_n \mid \frac{d^2}{2dr^2} + E \mid \phi_m \rangle = \langle \phi_n \mid \phi_m \rangle \left(\frac{\lambda^2}{8} + E\right) - \frac{\lambda^2}{2}\lambda^{-1}\delta_{nm} \tag{A2.6}$$

$$\sum_{m=0}^{\infty}\lambda^{-1}\left\{\left(E+\frac{\lambda^2}{8}\right)\left(2\delta_{nm}-\delta_{n,m-1}-\delta_{n,m+1}\right)-\frac{\lambda^2}{2}\delta_{mn}\right\}\psi_m(E) = 0 \quad ; \quad n=0,1,2,\ldots \tag{A2.7a}$$

$$\sum_{m=0}^{\infty}\lambda^{-1}\left(E+\frac{\lambda^2}{8}\right)\left(2x\,\delta_{nm}-\delta_{n,m-1}-\delta_{n,m+1}\right)\psi_m(E) = 0 \quad ; \quad n=0,1,2\ldots \tag{A2.7b}$$

$$x = \frac{\left(E-\frac{\lambda^2}{8}\right)}{\left(E+\frac{\lambda^2}{8}\right)} \quad ; \quad E = \frac{\lambda^2(1+x)}{8(1-x)}$$

$$-1 \le x \le 1 \tag{A2.8}$$

Writing $\psi_m(E)$ as $\psi_m(x)$ we have

$$2x\,\psi_n(x) - \psi_{n+1}(x) - \psi_{n-1}(x) = 0 \quad ; \quad n = 0,1,2,\ldots. \tag{A2.9a}$$

$$\psi_{-1}(x) = 0 \tag{A2.9b}$$

This is the recurrence relationship for the Gegenbauer polynomials $C^{(\alpha)}_n(x)$ with $\alpha = 1$ in this case. $C^{(1)}_n(x) = U_n(x)$, a Chebyschev polynomial of the second kind. The relationship (A2.9a) is also obeyed by Chebyschev

polynomials of the first kind but (A2.9b) is not: these are used as direct representatives of the solutions $q_n(x)$ described in section 2.2. Details of these polynomials are in Abramowitz and Stegun (1972). The standard polynomials $U_n(x)$ are:

$$U_n(x) = \frac{\sin(n+1)\theta}{\sin\theta} \quad , \quad \cos\theta = x \tag{A2.10a}$$

$$\int_{-1}^{1} dx\,(1-x^2)^{1/2}\,U_n(x)\,U_{n'}(x) = \frac{\pi}{2}\,\delta_{nn'} \tag{A2.10b}$$

The weight function $\rho(x)$ may thus be written

$$\rho(x) = \frac{2}{\pi}(1-x^2)^{1/2} \tag{A2.10c}$$

The solution $\psi_R(E,r)$ may be shown to be

$$\psi_R(E,r) = \sqrt{\frac{2}{\pi k}}\,\sin kr = \sqrt{\frac{2}{\pi k}}\sum_{n=0}^{\infty}\sin(n+1)\theta\;\phi_n(r)\;;\;\tfrac{1}{2}k^2 = E \tag{A2.11a}$$

$$= \sum_{n=0}^{\infty}\psi_0(x)\,U_n(x)\,\phi_n(r)\;;\;\psi_0(x) = \sqrt{\frac{2}{\pi k}}\,\sin\theta \tag{A2.11b}$$

From (A2.10c), we have

$$|\psi_0(x)|^2 = \rho(x)\left(\frac{dx}{dE}\right)^{1/2} \tag{A2.12}$$

The orthogonality relations are

$$\langle \psi_R(E') \mid \psi_R(E)\rangle = \delta(E-E') \tag{A2.13a}$$

$$\int_0^{\infty} dE\;\psi_R(E,r)\,\psi_R(E,r') = \sum_{m,n=0}^{\infty}\phi_n(r)\,\phi_m(r')\int_{-1}^{1}dx\,\rho(x)\left(\frac{dE}{dx}\right)^{1/2}U_n(x)\,U_m(x) = \delta(r-r') \tag{A2.13b}$$

(A2.13a) follows from the completeness relation for the

orthogonal polynomials $U_n(x)$:

$$\sum_{n=0}^{\infty} \rho^{1/2}(x)\, \rho^{1/2}(x')\, U_n(x)\, U_n(x') = \delta(x-x') \qquad (A2.14)$$

(A2.13b) may be seen to be true by multiplying by $\phi_m(r)\,\bar{\phi}_{m'}(r')$ and integrating over r and r'. ($\bar{\phi}_m(r) = (m+1)\,\phi_m(r)/r$).

We now consider the finite basis approximate solution

$$\psi_R^{(N)}(E_i^{(N)}, r) = \sum_{n=0}^{N-1} \psi_n^{(N)}(x_i^{(N)})\, \phi_n(r) \quad ; \quad \psi_n^{(N)}(x_i^{(N)}) = \psi_0^{(N)}(x_i^{(N)})\, U_n(x_i^{(N)}) \qquad (A2.15)$$

We require $U_N(x_i^{(N)}) = 0$. Thus:

$$\sin(N+1)\,\theta_i^{(N)} = 0 \quad ; \quad i = 1, 2, \ldots, N \qquad (A2.16a)$$

$$\theta_i^{(N)} = \pi\left(1 - \frac{i}{(N+1)}\right) \quad ; \quad x_i^{(N)} = -\cos\left\{\frac{i\pi}{(N+1)}\right\} \qquad (A2.16b)$$

For a normalised solution

$$\langle \psi_R^{(N)}(E_i^{(N)}) \mid \psi_R^{(N)}(E_j^{(N)}) \rangle = \delta_{ij}$$

$$= \sum_{n=0}^{N-1} \sum_{m=0}^{N-1} \langle \phi_n \mid \phi_m \rangle\, U_n(x_i^{(N)})\, U_m(x_j^{(N)})\, \psi_0^{(N)\dagger}(x_i^{(N)})\, \psi_0^{(N)}(x_j^{(N)})$$

$$= \frac{2}{\lambda}(1 - x_p^{(N)})\, \psi_0^{(N)\dagger}(x_i^{(N)})\, \psi_0^{(N)}(x_j^{(N)}) \sum_{n=0}^{N-1} U_n(x_i^{(N)})\, U_n(x_j^{(N)}) \quad ; \; p = i, j \qquad (A2.17)$$

Reference to the Christoffel Darbaux relation appropriate to the Gegenbauer/Chebyschev polynomials (Szegö 1967) shows:

$$\sum_{n=0}^{N-1} U_n(x_i^{(N)})\, U_n(x_j^{(N)}) = (w_i^{(N)})^{-1}\, \delta_{ij} \qquad (A2.18)$$

The $w_i^{(N)}$ are weights for an N point quadrature over (-1,1)

with weight function $\rho(x)$ and abscissae $x_i^{(N)}$. From (A2.18) we may write

$$\left| \psi_o^{(N)}(x_i^{(N)}) \right|^2 = w_i^{(N)} \left(\frac{dE}{dx} \right)^{1/2} \Big|_{x = x_i^{(N)}} \qquad (A2.19)$$

Multiplication by $\phi_m(r)\,\bar{\phi}_{m'}(r')$ and integration over r and r' shows that (A2.20) is the unit operator in the finite L-squared subspace:

$$\sum_{j=1}^{N} \psi_R^N(E_j^{(N)}, r)\, \psi_R^N(E_j^{(N)}, r') = \sum_{n=0}^{N-1} \sum_{n'=0}^{N-1} \phi_n(r)\, \phi_n(r') \sum_{j=1}^{N} w_j^{(N)} \left(\frac{dE}{dx} \right)^{1/2} \Big|_{x = x_j^{(N)}} U_n(x_j^{(N)}) U_{n'}(x_j^{(N)}) \qquad (A2.20)$$

Comparing exact and approximate solutions:

$$\psi_R(E_j^{(N)}, r) = \frac{\psi_o(x_i^{(N)})}{\psi_o^{(N)}(x_j^{(N)})}\, \psi_R^N(E_j^{(N)}, r) + \sum_{n=N+1}^{\infty} \psi_o(x_j^{(n)})\, U_n(x_j^{(N)})\, \phi_n(r) \qquad (A2.21)$$

For matrix elements with functions <f1 contained within the finite basis, the exact solution is proportional to the approximate solution.

$$\left| \frac{\psi_o^{(N)}(x_j^{(N)})}{\psi_o(x_j^{(N)})} \right|^2 = \frac{w_j^{(N)}}{\rho(x_j^{(N)})} \frac{dE}{dx} \Big|_{x = x_j^{(N)}}$$

$$= w_j^{(N)}(eq:x) \frac{dE}{dx} \Big|_{x = x_j^{(N)}} = w_j^{(N)}(eq:E) \qquad (A2.22)$$

We also note the following expression for the Green's function:

$$G(n, n', E) = \int_0^{\infty} dE' \frac{\psi_n(E')\, \psi_{n'}(E')}{(E + i\varepsilon - E')}$$

$$= \int_{-1}^{1} dx' \, \rho(x') \left(\frac{dE'}{dx} \right)^{1/2} \frac{U_n(x')\, U_{n'}(x')}{(E + i\varepsilon - E')}$$

$$= \int_{-1}^{1} dx' \, \rho(x') \frac{\lambda}{2} (1-x')^{-1} U_n(x') U_{n'}(x') \left\{ \frac{\lambda^2}{4} \frac{(x + i\varepsilon - x')}{(1-x')(1-x)} \right\}^{-1}$$

$$= \frac{2(1-x)}{\lambda} \int_{-1}^{1} dx' \frac{\rho(x') U_n(x') U_{n'}(x')}{(x + i\varepsilon - x')} \qquad (A2.23)$$

The unsubtracted finite basis Green's function is

$$G^N(E, r, r') = \sum_{n=0}^{N-1} \sum_{n'=0}^{N-1} \phi_n(r) \phi_{n'}(r') G^N(n, n', E)$$

$$G^N(n, n', E) = \sum_{j=1}^{N} w_j^{(N)} \left(\frac{dE}{dx} \right)^{1/2} \Big|_{x = x_j^{(N)}} \frac{U_n(x_j^{(N)}) U_{n'}(x_j^{(N)})}{(E - E_j^{(N)})}$$

$$= \frac{2(1-x)}{\lambda} \sum_{j=1}^{N} w_j^{(N)} \frac{U_n(x_j^{(N)}) U_{n'}(x_j^{(N)})}{(x - x_j^{(N)})} \qquad (A2.24)$$

Heller's principle (see section 2.3A) may be proved for the case of the s-wave radial kinetic Hamiltonian.

$$w_j^{(N)}(eq:x) = \frac{w_j^{(N)}}{\rho(x_j^{(N)})}$$

$$= \frac{\pi}{(N+1)} \sin \theta_j^{(N)} \qquad (A2.25)$$

We also have

$$x_j^{(N)} = -\cos\left(\frac{\xi^{(N)} \pi}{N+1} \right) \Big|_{\xi^{(N)} = j}$$

$$\frac{dx(\xi^{(N)})}{d\xi^{(N)}} \Big|_{\xi^{(N)} = j} = \sin\left(\frac{\xi^{(N)} \pi}{N+1} \right) \cdot \frac{\pi}{(N+1)} \Big|_{\xi^{(N)} = j} = w_j^{(N)}(eq:x) \qquad (A2.26)$$

We note

$$w_j^{(N)}(eq:E) = \frac{dE}{dx} \Big|_{x = x_j^{(N)}} w_j^{(N)}(eq:x) = \frac{dE(\xi^{(N)})}{d\xi^{(N)}} \Big|_{\xi^{(N)} = j} \qquad (A2.27)$$

The general Coulomb case including angular momentum is dealt with as referenced on table 2.1. Board (1983) treats the Coulomb Green's function.

Kinetic Hamiltonian Using Basis of Chapter Three

$$L^{(v)}_{I-1}(x) = \sum_{m=1}^{I} L^{(v-1)}_{m-1}(x) \quad ; \quad L^{(v)\prime}_{I-1}(x) = -\sum_{m=1}^{I-1} L^{(v)}_{m-1}(x) \tag{A2.28}$$

Using the basis (3.2.24a),(3.3.26) the kinetic Hamiltonian matrix elements

$$\langle U_j | -\frac{d^2}{dr^2} | U_{j'} \rangle = \left[\frac{1}{4}\delta_{jj'} - \frac{1}{6}\left(\frac{j(j+1)}{j'(j'+1)} \right)^{1/2} (2j+1) \right] (-\alpha^2) \quad ; \; j \leq j'$$

$$= \left[\frac{1}{4}\delta_{jj'} - \frac{1}{6}\left(\frac{j'(j'+1)}{j(j+1)} \right)^{1/2} (2j'+1) \right] (-\alpha^2) \quad ; \; j \geq j' \tag{A2.29}$$

APPENDIX THREE

The Generalised "t" Method

Notation is as used in section 5.4.B. This method was stated by Takatsuka and McKoy (1981) in terms of their "C" functional formulation. The method is stated here in terms of the Schwinger principle, but the analysis applies to the "C" functional methods.

A basis $|\chi_\alpha\rangle$, $|\vec{\phi}_\alpha^{(+)s}\rangle$ is formed by unitary transformation of the physical channels $|\chi_i\rangle$, $|\vec{\phi}_i^{(+)s}\rangle$. The basis diagonalises the operator $(\bar{V}-\bar{V}G_o^{(+)}\bar{V})$:

$$\langle \vec{\phi}_\alpha^{(-)s} | \bar{V} - \bar{V} G_o^{(+)} \bar{V} | \vec{\phi}_\beta^{(+)s} \rangle = \delta_{\alpha\beta} \langle \vec{\phi}_\alpha^{(-)s} | \bar{V} - \bar{V} G_o^{(+)} \bar{V} | \vec{\phi}_\alpha^{(+)s} \rangle \qquad (A3.1)$$

The Schrödinger equation for $\vec{\phi}_\alpha^{(+)s}$ then implies

$$\langle \chi_\alpha | \bar{V} | \vec{\phi}_\beta^{(+)s} \rangle = \delta_{\alpha\beta} \langle \chi_\alpha | \bar{V} | \vec{\phi}_\alpha^{(+)s} \rangle \qquad (A3.2)$$

The generalised t operator X is formed

$$t\,X = t \sum_\alpha \bar{V} |\chi_\alpha\rangle\langle\chi_\alpha| \bar{V} = t \sum_i \bar{V} |\chi_i\rangle\langle\chi_i| \bar{V} \qquad (A3.3)$$

For the exact functions,

$$\bar{V} |\vec{\phi}_\alpha^{(+)s}\rangle = \bar{V} |\chi_\alpha\rangle + \bar{V} G_o^{(+)} \bar{V} |\vec{\phi}_\alpha^{(+)s}\rangle \qquad (A3.4a)$$

$$\bar{V} |\vec{\phi}_\alpha^{(+)s}\rangle x_\alpha^t = \bar{V} |\chi_\alpha\rangle \frac{1}{(1 - t\langle\chi_\alpha|\bar{V}|\vec{\phi}_\alpha^{(+)s}\rangle)} + \bar{V} G_o^{(+)} \bar{V} |\vec{\phi}_\alpha^{(+)s}\rangle x_\alpha^t \qquad (A3.4b)$$

$$x_d^t = (1 - t\langle \chi_d | \bar{V} | \phi_d^{(+)s} \rangle)^{-1}$$

(A3.4c)

(A3.4b) is rewritten

$$\bar{V}|\phi_d^{(+)s}\rangle x_d^t = \bar{V}|\chi_d\rangle + \bar{V}G_0^{(+)}\bar{V}|\phi_d^{(+)s}\rangle x_d^t + t\bar{V}|\chi_d\rangle\langle\chi_d|\bar{V}|\phi_d^{(+)s}\rangle x_d^t$$

$$\bar{V}|\phi_d^{(+)s}(t)\rangle = \bar{V}|\chi_d\rangle + \bar{V}G_0^{+}\bar{V}|\phi_d^{(+)s}(t)\rangle + tX|\phi_d^{(+)s}(t)\rangle$$

$$(|\phi_d^{(+)s}(t)\rangle = |\phi_d^{(+)s}\rangle x_d^t)$$

(A3.5)

In forming (A3.5) property (A3.2) was used.

A diagonal functional is then formed which is stationary about $|\phi_d^{(+)s}(t)\rangle$.

$$G_{dd}^t = \sum_{ij} \langle \chi_d|\bar{V}|\psi_i\rangle (\underline{\underline{\Delta}}^t)^{-1}_{ij} \langle \psi_j|\bar{V}|\chi_d\rangle$$

$$G_{dB}^t = \delta_{dB} G_{dd}^t$$

(A3.6)

$$(\underline{\underline{\Delta}}^t)_{ij} = \langle \psi_i | -\bar{V} + \bar{V}G_0^{(+)}\bar{V} + tX|\psi_j\rangle$$

(A3.7)

G_{dd}^t is found by diagonalisation of the physical channel functional g_{ab}^t

$$g_{ab}^t = \sum_{ij} \langle \chi_a|\bar{V}|\psi_i\rangle (\underline{\underline{\Delta}}^t)^{-1}_{ij} \langle \psi_j|\bar{V}|\chi_b\rangle$$

(A3.8)

The unitary matrix transforming $|\chi_i\rangle$, $|\phi_i^{(+)s}\rangle$ into $|\chi_d\rangle$, $|\phi_d^{(+)s}\rangle$ is the matrix of eigenvectors of g_{ab}^t, and the G_{dd}^t are the eigenvalues, as described by Takatsuka and McKoy (1981). We then have as our approximation to $\langle \chi_d|\bar{V}|\phi_d^{(+)s}\rangle$

$$-\langle \chi_d|\bar{V}|\phi_d^{(+)s}\rangle \simeq Z_{dd}(t) = \frac{G_{dd}^t}{(1 - t\,G_{dd}^t)}$$

(A3.9)

The T matrix elements are found using the unitary transformation. We now show that this method is also independent of t.

$$\frac{d}{dt}\left(Z_{aa}(t)\right) = \frac{1}{(1-t\,G^t_{aa})^2}\left(\frac{d}{dt}G^t_{aa} + (G^t_{aa})^2\right) \qquad (A3.10)$$

$$\frac{d}{dt}G^t_{aa} = \frac{d}{dt}\left(\underline{R}^{0\,\dagger}_a (\underline{\underline{\Delta}}^t)^{-1}\underline{R}^0_a\right)$$

$$= \left(\underline{R}^{0\,\dagger}_a\left[\frac{d}{dt}(\underline{\underline{\Delta}}^t)^{-1}\right]\underline{R}^0_a\right)$$

$$= -\underline{R}^{0\,\dagger}_a(\underline{\underline{\Delta}}^t)^{-1}\left[\frac{d}{dt}\underline{\underline{\Delta}}^t\right](\underline{\underline{\Delta}}^t)^{-1}\underline{R}^0_a$$

$$= -\underline{R}^{0\,\dagger}(\underline{\underline{\Delta}}^t)^{-1}\sum_\gamma \underline{R}^0_\gamma \underline{R}^{0\,\dagger}_\gamma (\underline{\underline{\Delta}}^t)^{-1}\underline{R}^0_a$$

$$= -\sum_\gamma G^t_{a\gamma}G^t_{\gamma a}$$

$$= -(G^t_{aa})^2 \quad \text{since } \underline{\underline{G}}^t \text{ is diagonal.}$$

Thus Z_{aa} is independent of t.

$$\{\underline{R}^0_a\}_j = \langle \psi_j | \bar{V} | \chi_a \rangle \qquad (A3.12)$$

We assume the unitary transformation is independent of t, as the condition for the unitary transformation (A3.1) does not involve t.

Numerically, the unitary matrix is calculated by diagonalising g^t_{ab}. Although the eigenvalues G^t_{aa} will depend on t, the matrix of eigenvectors should be t independent; any t dependance is a measure of numerical inaccuracy.

$$g^t_{ab} = \langle \chi_a | f(t) | \chi_b \rangle$$

$$G^t_{\alpha\alpha} = \langle \chi_\alpha | f(t) | \chi_\alpha \rangle$$

$$|\chi_\alpha\rangle = \sum_a C_{\alpha a} |\chi_a\rangle \quad , \quad C_{\alpha a} \neq \text{function of t.}$$

(A3.13)

REFERENCES

Abdel-Raouf, M.A. Phys. Rev. A21, (1984), 2794.

Abramowitz, M., Stegun, I.A. "Handbook of Mathematical Functions", 10th printing, National Bureau of Standards, Applied Mathematics Series, U.S. Govt. Printing Office, Washington (1972).

Adhikari, S.K., Sloan, I.H. Phys. Rev. C11, (1975), 1133.

Altshuler, S. Phys. Rev. 89, (1953), 1278.

Atkinson F.V., "Discrete and Continuous Boundary Value Problems", Academic, New York, (1964)

Bardin, C., Dandeu, Y., Gauthier, L., Guillermin, J., Lena, T., Pernet, J.M., Wolter, M.H., Tanura, T. Comp. Phys. Comm. 3, (1972), 73.

Bassichis, W.H., Reading, J.F., Scheerbaum, R. Phys. Rev. C11, (1975), 316.

Bassichis, W.H., Strayer, M., Reading, J.F., Scheerbaum, R. Phys. Rev. C18, (1978), 632.

Brändas, E., Hehenberger, M., McIntosh, M.V. Int. J. Quantum. Chem. IX, (1975), 103.

Bransden, B.H. "Atomic Collision Theory", 2nd Edn. Reading, Mass., Benjamin Cummings 1983.

Bransden, B.H., Coleman, J.P. J. Phys. B5, (1972), 537.

Bransden, B.H., McDowell, M.R.C. Physics Reports 30, (1976), 207.

Bransden, B.H., Plummer, M. J. Phys. B19, (1986), 2007.

Bransden, B.H., Stelbovics, A.T. J. Phys. B17, (1984), 1877.

Brendlé, B., Gayet, R., Rocet, J.P., Wohrer, K. Phys. Rev. Lett. 54, (1985), 2007.

Broad, J.T., Reinhardt, W.P. Phys. Rev. A14, (1976), 2159; J. Phys. B9, (1976), 1491.

Broad, J.T. Phys. Rev. A18, (1978), 1012; 26, (1982), 3078; 31, (1985), 1494, in "Electron Atom and Electron Molecule Collisions" ed. J. Hinze, New York. Plenum, (1983), 91.

Burke, P.G., Berrington K.A., Sukumar C.V., J. Phys. B 14, (1981), 289

Burke, P.G., Gallagher, D.F., Geltman, S. J. Phys. B2, (1969), 1142.

Burke, P.G., Mitchell, J.F.B. J. Phys. B6, (1973), 320.

Burke, P.G., Robb, W.D. "Advances In Atomic and Molecular Physics Vol. 11", New York, Academic (1975), 143.

Burke, P.G., Seaton, M.J. Meth. in Comp. Phys. 10, (1971), 1.

Burke, P.G., Taylor, A.J. Proc. Phys. Soc. 88, (1966), 549.

Burke, P.G., Webb, T.G. J. Phys. B3, (1970), L131.

Byron, F.W., Joachain, C.J. Phys. Rev. A8, (1973), 1267, 3266; J. Phys. B7, (1974), L212; Phys. Rev. A15, (1977), 128.

Callaway, J. Phys. Repts. 45, (1978), 89; Adv. in Phys. 29, (1980), 7; Phys. Rev. A32, (1985), 775.

Callaway, J., McDowell, M.R.C., Morgan, L.A. J. Phys. B9, (1976), 2043.

Callaway, J., Oza, D.H. Phys. Rev. A27, (1983), 775; 29, (1984), 2416.

Condon, E.H., Odabasi, H. "Atomic Structure", C.U.P. (1980).

Corcoran, C.T., Langhoff, P.W. Chem. Phys. Lett. 41, (1976), 69; J. Math. Phys. 18, (1977), 651.

Crees, M.A., Seaton, M.J., Wilson, P.M.H. Comp. Phys. Comm. 15, (1978), 23.

De Blasi, C., Guercia, L., Paracelli, C., Manfredotti, C. Comp. Phys. Comm. 36, (1985), 339.

Doolen, G., McCastor, G., McDonald, F.A., Nuttall, J. Phys. Rev. A4, (1971), 108.

Eisner, W., Seaton, M.J. J. Phys. B5, (1972), 2187.

Fels, M., Hazi, A. Phys. Rev. A5, (1972), 1236.

Feshbach, H. Ann. Phys. New York 5, (1952), 357; 19, (1962), 287.

Fon, W.C., Berrington, K.A. J. Phys. B14, (1981), 323.

Fon, W.C., Berrington, K.A., Burke, P.G., Kingston, A.E. J. Phys. B14, (1981), 1041.

Fon, W.C., Berrington, K.A., Hibbert, A. J. Phys. B15, (1981), 307.

Gailitis, A. Sov. Phys. J.E.T.P. 20, (1965), 107, in "Theory of Electron Atom Collisions", ed. V. Veldré, Acad. Sci. Latvian S.S.R. Inst. Phys. trans. M.V. Kurepa M.I.T. (1966).

Geltman, S. "Topics in Atomic Collision Theory", Academic Press, London, Ltd. (1969).

Gibson, T.L., Lima, M.A.A.P., Marco, A.P., Takatsuka, K., McKoy, V. Phys. Rev. A30, (1984), 3085.

Hazi, A.U. J. Phys. B11, (1978), L259.

Jazi, A.U., Taylor, H.S. Phys. Rev. A1, (1970), 2109.

Heller, E.J. Thesis (1973), Harvard University.

Heller, E.J. Phys. Rev. A12, (1975), 122.

Heller, E.J., Reinhardt, W.P., Yamani, H.A. J. Comp. Phys. 13, (1972), 536.

Heller, E.J., Reinhardt, W.P. Phys. Rev. A7, (1973), 365.

Heller, E.J., Rescigno, T.N., Reinhardt, W.P. Phys. Rev. A8, (1973), 2946.

Heller, E.J., Yamani, H.A. Phys. Rev. A9, (1974), 1201, 1209.

Huck, R.J. Proc. Phys. Soc. (London), 70, (1957), 369.

Hulthen, L.K. Fys Salsk. Lund. Forh 14, (1944), 21.

Joachain, C.J. "Quantum Collision Theory", 3rd Edn. North Holland, Amsterdam, (1983).

Johnson, B.R., Reinhardt, W.P. Phys. Rev. A28, (1983), 1930.

Johnson, P.M., Langhoff, P.W., O'Neil, S.V., Corcoran, C.T., Reinhardt, W.P. Chem. Phys. Lett. 52, (1977), 380.

Kingston, A.E., Fon, W.C., Burke, P.G. J. Phys. B9, (1976), 605.

Kohn, W. Phys. Rev. 74, (1948), 1763.

Kolsrud, M. Phys. Rev. 112, (1958), 1436.

Langhoff, P.W. Chem. Phys. Lett. 22, (1973), 60; Int. J. Quantum Chem. 58, (1974), 347.

Langhoff, P.W., Corocoran, C.T. J. Chem. Phys. 61, (1974), 495; Chem. Phys. Lett. 40, (1976), 367.

Langhoff, P.W., Corcoran, C.T., Simms, J., Weinhold, F., Glover, R.M. Phys. Rev. A14, (1976), 1042.

Langhoff, P.W., Simms, J., Corcoran, C.T. Phys. Rev. A10, (1974), 840.

Lee, M.T., Takatsuka, K., McKoy, V. J. Phys. B14, (1981), 4115.

Lima, M.A.P., Gibson, T.L., Takatsuka, K., McKoy, V. Phys. Rev. A30, (1984), 1741.

Luchesse, R.R. Phys. Rev. A33, (1986), 1626.

Luchesse, R.R., McKoy, V. Phys. Rev. A21, (1979), 112; 21, (1980), 112; J. Phys. B14, (1979), L421.

Luchesse, R.R., Watson, D.K., McKoy, V. Phys. Rev. A22, (1980), 421.

Luchesse, R.R., Takatsuka, K., McKoy, V. Physics Reports (Review Section of Physics Letters) 131, (1986), 147.

Maleki, N. Phys. Rev. A29, (1984), 2470.

Maleki, N., Macek, J., Phys. Rev. A21, (1980), 1403.

McCarthy, I.E., Mitroy, J., Stelbovics, A.T., J. Phys. B19, (1986), 335.

McCarthy, I.E., Stelbovics, A.T. Phys. Rev. A28, (1983), 2693.

McDowell, M.R.G. in "Atomic Processes and Applications" eds. P.G. Burke and B.L. Moiseiwitsch, North Holland, Amsterdam, (1976).

McCurdy, C.W., Rescigno, T.N. Phys. Rev. A21, (1980), 1499.

McDonald, F.A., Nuttall, J. Phys. Rev. lett. 23, (1969), 361.

Mittleman, M.H. Phys. Rev. 147, (1966), 69.

Mittleman, M.H., Pu, R.T. Phys. Rev. 126, (1962), 370.

Moe, M., Saxon, O.S. Phys. Rev. 111, (1958), 950.

Moiseiwitsch, B.L. J. Phys. B15, (1982), L609; 15, (1982), L863; 16, (1983), 4015.

Nesbet, R.K. Adv. Quantum Chem. 9, (1957), 215, "Variational Methods In Electron Atom Scattering Theory", Plenum, (1980).

Oza, D.H. Phys. Rev. A30, (1984), 1101.

Percival, I.C., Seaton, M.J. Proc. Camb. Phil. Soc. 53, (1957), 654.

Peterkop, R.K. "Theory of Ionisation of Atoms by Electron Impact", University Press, Boulder, Colorado, (1977).

Poet, R. J. Phys. B11, (1978), 3081; 13, (1980), 2995; 14, (1981), 91.

Reinhardt, W.P. Phys. Rev. A8, (1973), 754; Comp. Phys. Comm. 17, (1979), 1.

Rowntree, J.P., Burnett, T., Henry, R.J.W., Weatherford, C.A. Comp. Phys. Comm. 112, (1976), 27.

Schlessinger, L. Phys. Rev. 171, (1968), 1523.

Schlessinger, L., Schwartz, C. Phys. Rev. Lett. 16, (1966), 1173.

Schneider, B.L. Phys. Rev. A31, (1985), 2188.

Stelbovics, A.T., Slim, H.A. Phys. Rev. A33, (1986), 3393; Phys. Rev. A, (1987) in press.

Szegö, G. "Orthogonal Polynomials", 3rd Edn. Am. Math. Soc. Providence, (1967).

Takatsuka, K., Fueno, T. Phys. Rev. A19, (1979), 1011, 1018.

Takatsuka, K., Luchesse, R.R., McKoy, V. Phys. Rev. A24, (1981), 1812.

Takatsuka, K., McKoy, V. Phys. Rev. A23, (1980), 2352, 2359; 30, (1984), 2799; 30, (1984b), 1734.

Watson, D.K., Luchesse, R.R., Rescigno, T.N. Phys. Rev. A21, (1980), 738.

Watson, D.K., McKoy, V. Phys. Rev. A20, (1979), 1474.

Weyl, H. Math. Ann. 68, (1910), 220.

Wilkinson, J.D. "The Algebraic Eigenvalue Problem", O.U.P., (1965).

Williams, J.F. J. Phys. B14, 1197.

Winick, J.R. Thesis (1976), Harvard University.

Winick, J.R., Reinhardt, W.P. Phys. Rev. A18, (1978), 910, 925.

Winters, K.H., Clark, C.D., Bransden, B.H., Coleman, J.P. J. Phys. B6, (1973), L247; 7, (1974), 788.

Yamani, H.A., Fishman, L. J. Math. Phys. 16, (1975), 410.

Yamani, H.A., Reinhardt, W.P. Phys. Rev. A11, (1975), 1144.